INTERNATIONAL ASTRONOMICAL UNION
SYMPOSIUM NO. 268

LIGHT ELEMENTS IN THE UNIVERSE:

Edited by: CORINNE CHARBONNEL,
MONICA TOSI, FRANCESCA PRIMAS
and CRISTINA CHIAPPINI

IAU IAU INTERNATIONAL ASTRONOMICAL UNION
Publisher: CAMBRIDGE UNIVERSITY PRESS

LIGHT ELEMENTS IN THE UNIVERSE

IAU SYMPOSIUM No. 268

COVER ILLUSTRATION: JET D'EAU de Genève

Designed by Cécile H.

INTERNATIONAL ASTRONOMICAL UNION

UNION ASTRONOMIQUE INTERNATIONALE

IAU

LIGHT ELEMENTS IN THE UNIVERSE

PROCEEDINGS OF THE 268th SYMPOSIUM OF THE INTERNATIONAL ASTRONOMICAL UNION HELD IN GENEVA, SWITZERLAND NOVEMBER 9–13, 2009

Edited by

CORINNE CHARBONNEL
GENEVA OBSERVATORY, GENEVA UNIVERSITY, SWITZERLAND & CNRS, FRANCE

MONICA TOSI
INAF-OSSERVATORIO ASTRONOMICO DI BOLOGNA, ITALY

FRANCESCA PRIMAS
EUROPEAN SOUTHERN OBSERVATORY-ESO, GARCHING, GERMANY

and

CRISTINA CHIAPPINI
GENEVA OBSERVATORY, GENEVA UNIVERSITY, SWITZERLAND & INAF-OSSERVATORIO ASTRONOMICO DI TRIESTE, ITALY

CAMBRIDGE
UNIVERSITY PRESS

CAMBRIDGE UNIVERSITY PRESS
The Edinburgh Building, Cambridge CB2 2RU, UnitedKingdom
40 West 20th Street, New York, NY 10011–4211, USA
10 Stamford Road, Oakleigh, Melbourne 3166, Australia

First published 2009

Printed in the United Kingdom at the University Press, Cambridge

Typeset in System LaTeX 2ε

A catalogue record for this book is available from the British Library

Library of Congress Cataloguing in Publication data

ISBN 0 521 57156 1 hardback
ISSN

Table of Contents

Preface

The light elements (H, He, Li, Be, B and their isotopes) deserve special attention because of their relationship with several important astrophysical domains: they provide key clues for stellar and ISM structure and evolution, galaxy formation and evolution, Big Bang nucleosynthesis and cosmology. They are one of the few bridges connecting several different astrophysical communities.

The previous IAU Symposium on the light elements was held in 1999 (in Natal, Brasil, IAU Symp. 198), and other, non-IAU supported, related meetings also took place about a decade ago. Since then, there have been many significant developments both on the observational and theoretical sides. Striking progress was achieved thanks to the accurate determination of the baryon density of the Universe by recent cosmic microwave background experiments. This allowed an unprecedented precision on the determination of the yields of Standard Big Bang Nucleosynthesis and a different perspective in the comparison with the D, ^{3}He, ^{4}He and ^{7}Li abundances measured from observations of low-metallicity environments.

In parallel, the advent of new generation ground and space based telescopes allowed the observation of light elements in objects previously unreachable, with new intriguing results on the present and past abundances of D, He (both ^{3}He and ^{4}He), Li and its isotopic ratio, Be and B and their isotopic ratios. Thanks to multi-fiber instruments, a wealth of data could be gathered in a consistent way which still await to be fully understood and interpreted. Also, realistic 3D, time-dependent, hydrodynamical model atmospheres strongly helped in providing more reliable abundance determinations.

On the theoretical side, we entered a golden age for the description of stellar interiors and evolution thanks to improved treatments of stellar rotation, magnetic fields, internal gravity waves, atomic diffusion, and thermohaline instability in new generation stellar models. Most of these improvements were achieved thanks to constraints coming from combined observations of light element abundances in various types of stars. Last but not least, a wealth of independent consistent chemical evolution models able to fit the general trends of the vast majority of Galaxy physical and chemical features were developed that must be tested with respect to the evolution of light elements.

Despite all these achievements, we are far from understanding and reproducing in detail all the light element patterns, their local, short term variations, as well as their global evolution in the Universe. The complete understanding of the evolution of the light elements in the Universe is a challenging task that requires the exchange of ideas and the collaboration of astrophysicists with observational and theoretical expertise in stellar hydrodynamics and evolution, Galactic and extra-galactic astronomy, and cosmology.

We felt that the route to this goal could be found only by gathering specialists in all the different relevant fields in an IAU Symposium. The various IAU Commissions and Divisions corresponding to these research fields have favourably received and endorsed our request, thus making this conference possible. The Symposium brought together 118 participants from 23 countries around the world to discuss the achievements as well as the problems concerning the light elements. We had 25 invited reviews, 53 oral contributions and 35 posters distributed over five sessions.

Several important issues, still highly controversial, have been tackled during the meeting thanks to the collective inputs from observers, stellar and galactic physicists, and cosmologists. To let the participants have time to discuss at length the hottest topics identified by the SOC, we also organized four discussion sessions: one on the dispersion

of the observational D abundances, one on the problems affecting the derivation of ^{4}He from HII regions, one on the problems affecting the derivation and interpretation of Li, Be and B abundances, and one on the stellar yields of ^{3}He, ^{4}He and ^{7}Li.

In addition to the scientific program, we enjoyed a public conference attended by more than 600 people at the Geneva University. Four speakers (the astrophysicists H.Reeves and J.Geiss, the physicist G.Laval, and the psychiatrist J.M.Aubry) presented to the public different aspects related to "Deuterium, helium, lithium: From the Big Bang to the contemporary civilisation".

Finally, with a 25% of the Symposium speakers being women, we considered it appropriate to organize a Women Networking Lunch, to let the participants from different countries exchange their experiences. The event turned out to be quite successful and we all enjoyed the opportunity to interact with other women astronomers coming from different environments. In addition F.Primas, who is co-chairing the IAU Working Group Women in Astronomy, gave a talk on Women Career Advancements for the PhD students and postdocs at the Geneva University. We are grateful to her for having had the idea of these activities, for her help in organizing them, and, most importantly, for always being ready to take initiatives against gender and minority discriminations.

It is a great pleasure to thank the Geneva Observatory, the University of Geneva, and the Museum of Natural History of Geneva for hospitality and support. We gratefully acknowledge the financial support of our sponsors, listed on the next page of these Proceedings, and the active contribution of the members of the SOC and the LOC. We are particularly grateful to Chantal Taçoy and Michel Grenon, who both did real miracles for the logistic organization of the Symposium, and to Bob Rood who took most of the pictures included in this volume. Finally, we warmly thank Cristina Chiappini and Francesca Primas for having co-edited these proceedings and shared with us their responsibility.

Corinne Charbonnel and Monica Tosi, co-chairs SOC,
Geneva, Bologna, February 4, 2010

THE ORGANIZING COMMITTEE

Scientific

C. Charbonnel (Switzerland/France, chair)
B. Barbuy (Brazil)
T. Kajino (Japan)
J. Lattanzio (Australia)
W. Moos (USA)
R.T. Rood (USA)
M. Tosi (Italy, co-chair)
Y. Izotov (Ukraine)
D. Lambert (USA)
P. Molaro (Italy)
F. Primas (Germany)

Local

C. Charbonnel (chair)
M. Dessauges-Zavadsky
M. Grenon
C. Taçoy
C. Chiappini
S. Ekström
N. Lagarde
G. Simond

Acknowledgements

The symposium is sponsored and supported by the IAU Divisions IV (Stars), VI (Interstellar Matter), VIII (Galaxies and the Universe); and by the IAU Commissions No. 28 (Galaxies), No. 29 (Stellar Spectra), No. 35 (Stellar Constitution), No. 36 (Theory of Stellar Atmospheres), No. 37 (Star Clusters and Associations).

The Local Organizing Committee operated under the auspices of the Geneva Observatory, University of Geneva (Switzerland).

Funding by the
International Astronomical Union,
Swiss National Science Foundation,
Swiss Academy of Sciences,
Museum of Natural History of Geneva City,
University of Geneva,
Geneva Observatory,
Faculty of Sciences of the University of Geneva,
Société de Physique et d'Histoire Naturelle,
and
Swiss Society for Astrophysics and Astronomy,
is gratefully acknowledged.

Participants

George **Angelou**, Monash University, CSPA, Australia george.angelou@sci.monash.edu.au
Martin **Asplund**, Max Planck Institute for Astrophysics, Germany asplund@mpa-garching.mpg.de
Dana **Balser**, NRAO, USA dbalser@nrao.edu
Thomas **Bania**, Department of Astronomy, Boston University, USA bania@bu.edu
Fabio **Barblan**, Geneva Observatory, Geneva University, Switzerland fabio.barblan@unige.ch
Beatriz **Barbuy** , Universidade de São Paulo , Brazil barbuy@astro.iag.usp.br
Yerra **Bharat Kumar**, Indian Institute of Astrophysics, India bharat@iiap.res.in
Marek **Biesiada**, Dept. of Astrophysics and Cosmology, University of Silesia, Poland marek.biesiada@us.edu.pl
Ann Merchant **Boesgaard**, Institute for Astronomy, University of Hawaii, USA boes@ifa.hawaii.edu
Piercarlo **Bonifacio**,GEPI, Observatoire de Paris, France Piercarlo.Bonifacio@obspm.fr
Angela **Bragaglia**, INAF - Osservatorio Astronomico di Bologna, Italy angela.bragaglia@oabo.inaf.it
Nahuel **Cabral** , Physikalisches Institut Universität Bern, Switzerland nahuel.cabral@space.unibe.ch
Elisabetta **Caffau**, GEPI, Observatoire de Paris, France Elisabetta.Caffau@obspm.fr
Luca **Casagrande**, Max Planck Institute for Astrophysics, Germany luca@MPA-Garching.MPG.DE
Oscar **Cavichia**, University of São Paulo , Brazil cavichia@astro.iag.usp.br
Corinne **Charbonnel**, Geneva Observatory , Switzerland and CNRS, France corinne.charbonnel@unige.ch
Sujit Kumar **Chatterjee**, IGNOU, New Alipore College Centre, India chat_sujit1@yahoo.com
Cristina **Chiappini**, Geneva Observatory , Switzerland and INAF/OATS, Italy Cristina.Chiappini@unige.ch
Roberto **Costa**, Universidade de São Paulo, Brazil roberto@astro.iag.usp.br
Katia **Cunha**, National Optical Astronomy Observatory, USA kcunha@noao.edu
Francesca **D'Antona**, INAF – Osservatorio di Roma, Italy dantona@mporzio.astro.it
Valentina **D'Orazi**, INAF - Osservatorio Astronomico di Padova, Italy valentina.dorazi@oapd.inaf.it
Patrick **de Laverny**, Observatoire de la Côte d'Azur, France laverny@oca.eu
Thibaut **Decressin** , Argelander-Institut für Astronomie, Germany decressin@astro.uni-bonn.de
Elisa **Delgado Mena**, Instituto de Astrofisica de Canarias, Spain edm@iac.es
Miroslava **Dessauges**, Geneva Observatory, Geneva University, Switzerland miroslava.dessauges@unige.ch
Marcella **Di Criscienzo**, INAF - Osservatorio Astronomico di Roma, Italy dicrisci@gmail.com
Adam **Dobrzycki** , European Southern Observatory, Germany adobrzyc@eso.org
Joanna **Dunkley**, Oxford University, United Kingdom j.dunkley@physics.ox.ac.uk
Patrick **Eggenberger**, Geneva Observatory, Geneva University, Switzerland patrick.eggenberger@unige.ch
Sylvia **Ekström**, Geneva Observatory, Switzerland sylvia.ekstrom@unige.ch
Lisa **Elliott**, Monash University, Australia Lisa.Elliott@sci.monash.edu.au
Gary **Ferland**, University of Kentucky, USA gary@pa.uky.edu
Patrick **François**, Paris Observatory, France patrick.francois@obspm.fr
Urs **Frischknecht**, University of Basel, Switzerland urs.frischknecht@unibas.ch
Johannes **Geiss**, International Space Science Institute, Switzerland johannes.geiss@issibern.ch
Cyril **Georgy**, Geneva Observatory, Geneva University, Switzerland cyril.georgy@unige.ch
Oscar **Gonzalez**, European Southern Observatory, Germany oagonzal@uc.cl
Jonay I. **Gonzalez Hernandez**, Universidad Complutense de Madrid, Spain jonay@astrax.fis.ucm.es
Claudia **Greco**, Geneva Observatory, Geneva University, Switzerland claudia.greco@unige.ch
Michel **Grenon**, Geneva Observatory, Geneva University, Switzerland Michel.Grenon@unige.ch
Roald **Guandalini**, University of Perugia, Italy guandalini@fisica.unipg.it
Guillaume **Hébrard**, Institut d'Astrophysique de Paris, France hebrard@iap.fr
J. Christopher **Howk**, University of Notre Dame, USA jhowk@nd.edu
Garik **Israelian**, Instituto de Astrofisica de Canarias, Spain gil@iac.es
Hiroko **Ito**, The Graduate University of Advanced Studies, NAOJ, Japan hiroko.ito@nao.ac.jp
Yuri **Izotov**, Main Astronomical Observatory, Ukraine izotov@mao.kiev.ua
Karsten **Jedamzik**, University of Montpellier II, France jedamzik@lpta.univ-montp2.fr
Colin **Jones**, Simon Fraser University, Canada colin_jones@sfu.ca
Andreas **Kaufer**, European Southern Observatory, Chile akaufer@eso.org
Andreas **Korn** , Uppsala Astronomical Observatory, Sweden andreas.korn@fysast.uu.se
Motohiko **Kusakabe** , Inst. for Cosmic Ray Research, University of Tokyo, Japan kusakabe@icrr.u-tokyo.ac.jp
Nadége **Lagarde**, Geneva Observatory, Geneva University, Switzerland Nadege.Lagarde@unige.ch
David **Lambert**, The University of Texas at Austin, McDonald Observatory, USA director@astro.as.utexas.edu
Livio **Lamia**, INFN–LNS Catania, Italy llamia@lns.infn.it
Norbert **Langer**, Argelander-Institut fuer Astronomie, Germany nlanger@astro.uni-bonn.de
John **Lattanzio**, Monash University, Australia john.lattanzio@sci.monash.edu.au
Karin **Lind**, European Southern Observatory, Germany klind@eso.org
Jeffrey **Linsky**, JILA, University of Colorado and NIST, USA jlinsky@jila.colorado.edu
Donald **Lubowich** , Hofstra University, USA Donald.Lubowich@Hofstra.edu
Walter **Maciel**, University of São Paulo, Brazil maciel@astro.iag.usp.br
André **Maeder**, Geneva Observatory, Geneva University, Switzerland andre.maeder@unige.ch
Enrico **Maiorca**, University of Perugia, Italy emaiorca@gmail.com
Sushma **Mallik**, Indian Institute of Astrophysics, India sgvmlk@iiap.res.in
Anna **Marino**, Universitá di Padova, Italy anna.marino@unipd.it
Francesca **Matteucci**, Trieste University, Italy matteucc@oats.inaf.it
Jorge **Meléndez**, Centro de Astrofisica da Universidade do Porto, Portugal jorge@astro.up.pt
Georges **Meynet**, Geneva Observatory, Geneva University, Switzerland georges.meynet@unige.ch
Antonino **Milone**, Universitá di Padova, Italy antonino.milone@unipd.it
Tamara **Mishenina**, Astronomical Observatory, Odessa National University, Ukraine tamar@deneb1.odessa.ua
Paolo **Molaro**, INAF - Osservatorio Astronomico di Trieste, Italy molaro@oats.inaf.it
Thierry **Montmerle**, Laboratoire d'Astrophysique de Grenoble , France montmerle@obs.ujf-grenoble.fr
Saumitra **Mukherjee**, Jawaharlal Nehru University, India saumitramukherjee3@gmail.com
Ko **Nakamura**, National Astronomical Observatory of Japan, Japan nakamura.ko@nao.ac.jp
Poul Erik **Nissen**, Department of Physics and Astronomy, University of Aarhus, Denmark pen@phys.au.dk
Pierre **North**, Laboratoire d'Astrophysique – EPFL, Switzerland pierre.north@epfl.ch
Giancarlo **Pace** , Centro de Astrofisica da Universidade do Porto, Portugal gpace@astro.up.pt
Ana **Palacios**, GRAAL, CNRS , France ana.palacios@univ-montp2.fr
Sara **Palmerin** , Universitá degli Studi di Perugia - - INFN, Italy sara.palmerini@fisica.unipg.it
Igor **Panov**, Alikahnov Institute for Theoretical and Experimental Physics, Russia Igor.Panov@itep.ru
Manuel **Peimbert**, Universidad Nacional Autonoma de Mexico, Mexico peimbert@astroscu.unam.mx
Antonio **Peimbert**, Universidad Nacional Autonoma de Mexico, Mexico antonio@astroscu.unam.mx
Ruth **Peterson**, Lick Observatory, University of California , USA
Marco **Pignatari**, University of Victoria , Canada mpignatari@gmail.com
Marc **Pinsonneault**, Ohio State University, USA pinsonneault.1@osu.edu
Nina **Polosukhina-Chuvaeva**, Crimean Astrophysical Observatory, Ukraine polo@crao.crimea.ua
Nikos **Prantzos**, Institut d'Astrophysique de Paris, France prantzos@iap.fr
Francesca **Primas**, European Southern Observatory, Germany fprimas@eso.org
Tijana **Prodanovic**, Department of Physics, University of Novi Sad, Serbia prodanvc@df.uns.ac.rs
Sofia **Randich**, INAF – Osservatorio Astrofisico di Arcetri, Italy randich@arcetri.astro.it
Alejandra **Recio-Blanco**, Observatoire de la Côte d'Azur, France arecio@oca.eu
Hubert **Reeves**, CNRS, France hreeves@club-internet.fr
Adam **Ritchey**, University of Toledo, USA adam.ritchey@utoledo.edu
Donatella **Romano**, Dipartimento di Astronomia, Universitá di Bologna , Italy donatella.romano@oabo.inaf.it
Robert **Rood**, University of Virginia , USA rtr@virginia.edu
Nuno **Santos**, Centro de Astrofisica, Universidade do Porto, Portugal nuno@astro.up.pt
Luca **Sbordone**, Max Planck Institute for Astrophysics, Germany lsbordone@mpa-garching.mpg.de
Daniel **Schaerer**, Geneva Observatory, Geneva University , Switzerland Daniel.Schaerer@unige.ch
Kenneth **Sembach**, Space Telescope Science Institute, USA sembach@stsci.edu
Evan **Skillman**, University of Minnesota, USA skillman@astro.umn.edu

Rodolfo **Smiljanic**, University of São Paulo, Brazil and ESO, Germany rsmiljanic@gmail.com
Verne **Smith**, National Optical Astronomy Observatory, USA vsmith@noao.edu
David **Soderblom**, Space Telescope Science Institute, USA drs@stsci.edu
Francois **Spite** , Observatoire de Paris, France francois.spite@obspm.fr
Monique **Spite** , Observatoire de Paris, France monique.spite@obspm.fr
Richard **Stancliffe**, Monash University, CSPA, Australia Richard.Stancliffe@sci.monash.edu.au
Matthias **Steffen**, Astrophysikalisches Institut Potsdam, Germany msteffen@aip.de
Gary **Steigman**, The Ohio State University, USA steigman@mps.ohio-state.edu
Suzanne **Talon**, Université de Montréal, Canada suzanne.talon@umontreal.ca
Friedel **Thielemann**, University of Basel , Switzerland f-k.thielemann@unibas.ch
Monica **Tosi**, INAF – Osservatorio Astronomico di Bologna, Italy monica.tosi@oabo.inaf.it
Takuji **Tsujimoto**, NAOJ, Japan taku.tsujimoto@nao.ac.jp
Sylvie **Vauclair**, LATT, Université de Toulouse, France sylvie.vauclair@ast.obs-mip.fr
Paolo **Ventura**, INAF – Observatory of Rome, Italy ventura@oa-roma.inaf.it
Mark **Walker**, Maw Technology Manly, Australia
George **Wallerstein**, University of Washington, USA wall@astro.washington.edu
Laimons **Zacs** , University of Latvia, Latvia zacs@latnet.lv
Jean-Paul **Zahn** , Observatoire de Paris, France jean-paul.zahn@obspm.fr

Opening Session

David Lambert

Gary Steigman

Light elements in the Universe
Proceedings IAU Symposium No. 268, 2010
C. Charbonnel, M. Tosi, F. Primas & C. Chiappini, eds.

DOI: 00.0000/X000000000000000X

Light elements - one observer's historical perspective

David L. Lambert

The W.J. McDonald Observatory,
The University of Texas at Austin
1 University Station, C1400, Austin, Texas, USA, 78712-0259
email: dll@astro.as.utexas.edu

Abstract.
This essay attempts to provide a historical perspective on some of the key questions that engaged the attention of participants at the symposium. In particular, the writer offers and comments on a personal list of milestones in the literature published between 1957 and 1982.

Keywords. nuclear reactions, nucleosynthesis, abundances

1. Introduction

In today's rush to publish new results, one may overlook and even dismiss as unimportant the context in which new observational and theoretical findings should be placed. This essay is an imperfect attempt to provide one individual's perspective on the historical development of the roles played by the light elements in contemporary astrophysics. A warning to the reader: the perspective is biassed towards observations and, perhaps more importantly, is surely incomplete with respect to even the central events. Nonetheless, I hope I achieve my primary goal which is to identify when the seeds were planted that blossomed into the flowers whose scents we are chasing and trying to interpret at this symposium.

Here, this symposium considers the class of light elements to encompass just the first five elements: H, He, Li, Be, and B. In this quintet, the stable nuclides are ^{1}H, ^{2}H, ^{3}He, ^{4}He, ^{6}Li, ^{7}Li, ^{9}Be, ^{10}B, and ^{11}B. Each one of these will feature in talks at this symposium. Certain unstable light nuclides – ^{7}Be, ^{10}Be, and ^{8}B – also play a role in observational astrophysics and deserve a mention. ^{7}Be is important because of its role in the synthesis of ^{7}Li in stars, a topic of several presentations here. Electron capture on ^{7}Be results not only in ^{7}Li but also in a γ-ray and a neutrino. In stable stars, the γ-rays are locally absorbed deep in the interior and so lost to observers; searches for ^{7}Be γ-rays emitted by novae have been attempted but proven unsuccessful. The neutrinos are freed to roam the Universe; ^{7}Be neutrinos account for a fraction of the Sun's neutrino output. ^{10}Be with a half-life of 1.5 Myr is present in cosmic rays where it serves as a clock, a subject notably not aired at this meeting. ^{8}B's notoriety arises from a contribution to the solar neutrino problem with its ultimate resolution ending in the discovery of neutrino oscillations.

A crucial tool from the perspective of an observer is the inventory of spectral lines providing evidence for the light elements. Detection of these lines in absorption or emission is the first step in a determination of the abundance of a light element or of an isotopic ratio. Hydrogen and helium, when detectable, offer several series of lines. On the other hand, Li, Be, and B present - except in very rare circumstances - in trace amounts are detectable almost always only through the resonance lines of neutral atoms or ions. Lithium atoms are detectable in cool gas via the well known resonance doublet at 6707Å and, if Li

is abundant, excited lines at 6104Å and 8126Å are also detectable. The He-like Li^{+} ion and H-like Li^{++} ions are not providers of detectable lines at the abundances expected for Li. Perhaps, a great disappointment is that Be atoms are not detectable; the Be I resonance line at 2348.6Å has to my knowledge not been detected in a stellar spectrum. Beryllium abundances are based exclusively on the Be II resonance doublet at 3130Å. Higher Be ions of the H-like and He-like isoelectronic sequences are not on an observer's list for detection. With one more electron, the species of boron potentially accessible to the observer are the neutral atom and the ions B^{+} and B^{++} with the He-like ion B^{3+} and the H-like ion B^{4+} far beyond accessibility. Indeed, resonance lines of B I at 2496.8Å, B II at 1362.4Å, and B III at 2065.8Å have featured prominently in discussions of the boron abundance in, as appropriate, cool and hot stars and the interstellar medium. In addition to providing estimates of the elemental abundance of a light element, this array of lines for the light elements has under appropriate circumstances provided isotopic abundances for stellar atmospheres, interstellar and extragalactic gas: D/H, $^{3}He/^{4}He$, $^{6}Li/^{7}Li$, and $^{10}B/^{11}B$.

2. Hydrogen's title role

To stellar spectroscopists, measurements of absorption lines of element X in the spectrum of a normal (i.e. H-rich) star yield the abundance of the element X with respect to H, i.e., the ratio X/H. As shown by years of oral examinations of students, there may not always be a clear understanding of how the ratio X/H is the *natural* outcome of measurements of lines of element X. This lack of clarity reflects, in part, a failure of the student's teachers to explain a fundamental piece of stellar atmospheric physics and, in part, a lack of curiosity by the student who, nonetheless, may be adept at running the appropriate computer programmes. The crucial link between the observation of (say) X I lines and the abundance X/H is, of course, that the strength of the line is set not by the line opacity alone but by both the line and the continuous opacity.

Hydrogen's dominant role was first suggested by Cecilia Payne in her Harvard dissertation published as *Stellar Atmospheres* (Payne 1925). Not only did the dissertation show that similar compositions account for the diverse spectra of stars – spectroscopic variations are primarily due to differences in atmospheric temperature and pressure – but also that hydrogen and helium are the two most abundant elements by far in stellar atmospheres. However, as Longair (2006) reminds us in his majesterial *The Cosmic Century*, Payne qualified her conclusion by writing 'Although hydrogen and helium are manifestly very abundant in stellar atmospheres, the actual values derived from estimates of their marginal appearances are regarded as spurious', Longair adds judiciously 'The conclusion simply reflected the prevailing prejudice' but notes that the dominant role of H was proven a little later by Unsöld (1928) from an analysis of solar absorption lines and by McCrea (1929) from an analysis of the solar chromospheric (flash) spectrum.

Gaseous nebulae to invoke an old term – H II regions, planetary nebulae, for example – are also a major source of information on the abundances of the elements. In the context of the light elements, information is obtainable on H and He and their minor isotopes D and ^{3}He. Inspection of the optical emission line spectrum of a nebula shows H I, He I, and [O III] (say) lines to be of comparable intensity. Yet, the H and He are much more abundant than O. This seeming paradox is today readily understood as arising from the different excitation mechanisms for the permitted H and He lines and the forbidden O and heavy element lines. An early understanding of the paradox's resolution - perhaps, the first - was provided by Bowen (1935), the identifier of the forbidden lines (Bowen 1927, 1928). In his abstract, Bowen wrote 'A study of nebular line intensities in light

of the foregoing processes indicates that H is the most abundant element and He is the second, N, O, Ne, S – and possibly C and A – are present but are very much rarer. The lines of these heavier elements are strong, not because the elements are very abundant but because they are able to make use of large sources of energy that are not available to the predominent [*sic*] H and He lines'. Bowen's attempt to provide quantitative abundance estimates for – say – O/H was frustrated, in part, by his inability to detect recombination lines of oxygen that might be compared simply and directly with the recombination lines of hydrogen. Amusingly, this comparison may now be made and, as I recall, provides an oxygen abundance at odds with that derived from oxygen forbidden lines. The first paper to provide quantitative abundance estimates may be that by Aller & Menzel (1945).

3. Helium's dark role

Every astronomical spectroscopist has surely experienced the frustration over an inability to determine the abundance of a trace element of distinctive astrophysical significance – say, Li, Be or B – but just as frustrating but more rarely expressed must be the inability to determine the He abundance of a cool star. The He abundance of the Sun, for example, is one of the least securely established elemental abundances. This important quantity is not determinable from solar absorption lines but from measurements (e.g., sampling the solar wind) that are impossible to secure on other stars.

Fortunately, all normal Galactic stars are anticipated to have a similar He abundance. The floor is set by the primordial abundance and the likely ceiling by the He abundance of local H II regions and B stars. The error affecting derived elemental abundances resulting from adopting a 'standard' He/H ratio between the floor and the ceiling is almost certainly less than that incurred from the multiplicity of other sources of error, recognized and unrecognized. Yet, there are reasons to wish to ferret out bounds on the atmospheric He/H ratio.

One recalls at once that the dredge-ups experienced by giants on the first ascent and particularly on the asymptotic giant branch are predicted to change the He content of the atmosphere along with the changes to the light elements, C, N, and O as well as the *s*-process in the case of AGB stars. A recent discovery has been that of multiple sequences in the colour-magnitude diagrams of globular clusters. These sequences have generally beeen attributed to differences in He abundance. A lack of spectroscopic confirmation of such differences may be inevitable but is certainly frustrating and, therefore, stands as a challenge for observers.

Helium-rich and hydrogen-poor stars are known, if rare. The prototypes might be said to be (the warm) R Coronae Borealis and (the hot) Popper's star HD124448, the latter discovered at the McDonald Observatory (Popper 1942). These stars are obviously very H-poor because at their effective temperatures the Balmer lines are either absent or very weakly present. At lower temperatures, the H-deficiency may be judged by the weak or absent CH bands.

In light of the impossibility of direct detection of He lines in photospheric spectra of cool stars, one is led to wonder if mildly He-rich cool stars exist, how they might be detected, and how they might arise (diffusion, internal nucleosynthesis and mixing, binary interactions, etc.?).

4. Milestones - a personal selection

Writing the definitive history of the light elements requires talents beyond those at my command. Here, I offer a personal selection of papers that occurred to me as I prepared

my talk and which I consider to be milestones marking the road from 1957 to 1982 and, in particular, those that anticipated the hot topics featured at this symposium, and, in particular, the issues and questions providing the four discussion sessions. My selection begins in 1957, a date recognized by all (I hope!) as marking the publication of 'Nucleosynthesis of elements in stars' by Burbidge, Burbidge, Fowler & Hoyle (1957, here B^2FH, of course) and 'Nuclear reactions in stars and nucleogenesis' by Cameron (1957). The final milestone from 1982a is the seminal paper 'Lithium abundance at the formation of the Galaxy' (Spite & Spite 1982) marking the beginning of continuing studies of the Li abundances in halo stars and their relation to the primordial Li yield from the Big Bang.

4.1. *Light elements in 1957*

Hydrogen was considered the basic raw material for all element synthesis by B^2FH and Cameron. The former wrote 'It seems probable that the elements all evolved from hydrogen, since the proton is stable while the neutron is not'. Fair comment but this suppresses the issue of baryogenesis, a subject oddly not raised at this meeting.

Helium was presumed to originate from H-burning in stars. For example, Cameron in his summary table listed He along with C, N, O, Fe, and Ne as products of 'hydrogen and helium thermonuclear reactions in orderly evolution of stellar interiors.

Trace light nuclides of Li, Be, and B (and D) were noted by both B^2FH and Cameron as 'not formed in stellar interiors'. B^2FH were (reluctantly, I conjecture) forced to admit 'We have made some attempt to explain possible modes of production of deuterium, lithium, beryllium, and boron, but at present must conclude that these are little more than qualitative suggestions'. The label x-process was introduced by B^2FH to cover the 'possible modes'. This use of x presumably sprang from the authors' initiation into the symbolic language of algebra in their early schooling in different counties and countries. Cameron's says of D, Li, Be, and B 'possibly made by nuclear reactions in stellar atmospheres after the acceleration of charged particles in changing magnetic fields', a component of B^2FH's x-process.

4.2. *Cosmic He puzzle*

In my tally of milestones, the earliest recognition that He was likely not the product of H-burning in the course of orderly stellar evolution came from Hoyle & Tayler (1964) with observational evidence assembled and theoretical arguments marshalled in a short article in *Nature* with the title 'The mystery of the cosmic helium abundance'. Genesis of this milestone in a lecture course by Hoyle is described by Longair (2006) and in a delightful reminiscence by Faulkner (2009) who recalls lectures, Hoyle the man, and helium the element. Four decades after attending Hoyle's lectures as a first-year research student at Cambridge, Longair would write 'Fred Hoyle gave a course of lectures on the problems of extragalactic research. He would arrive with, at best, a scrap of paper with some notes and expound an area of current research. One week the topic was the problem of the cosmic helium abundance.' The problem and its resolution are succinctly set out in the concluding paragraph of the *Nature* article: 'There has been difficulty in explaining the high helium content of cosmic material in terms of ordinary stellar processes. The mean luminosity of galaxies come out appreciably too high on such a hypothesis. The arguments presented here make it clear, we believe, that the helium was produced in a far more dramatic way. Either the Universe has had at least one high-temperature, high-density phase, or massive objects must play (or have played) a larger part in astrophysical evolution than has hitherto been supposed.' Calculations involving He synthesis in a high-temperature high-density phase were, as Faulkner engagingly

retells, very quickly completed by him with the principal result relayed to Hoyle on the Sunday morning following the key lecture. As Longair notes 'the audience had the privilege of being present as a key piece of modern astrophysics was created in real time in a graduate lecture course.'

4.3. *Stellar evolution - dredge-ups*

In the 1960s, papers first appeared describing computer calculations of low mass stars from the main sequence through the first giant branch and then the asymptotic giant branch. Dilution of the surface abundances of the light elements Li, Be, and B (with emphasis sensibly on Li) was noted early in the series of papers. Perhaps, the first paper pointing out how observations might provide quantitative verification of the calculations is Iben's 'The surface ratio of N^{14} to C^{12} during helium burning' (Iben 1964). Iben's purpose was to draw attention to a prediction that 'the ratio of N^{14} to C^{12} at the surface of a star undergoes a significant increase during the rise into the red giant region immediately preceding the phase of helium burning in the core' and to call for spectroscopic verification of this prediction. Of course, N surface enrichment implies reduction of Li, Be, and B surface abundances. Iben was one of the prime movers in this endeavour to model stellar evolution and his reviews 'Stellar evolution: Comparison of theory with observation' and 'Stellar within and off the main sequence' remain valuable reading for the student (Iben 1967a, b). Discovery of the He-shell flashes (thermal pulses) in theoretical models of post-He core burning low mass (i.e., AGB) stars by Schwarzschild & Härm (1965) marked the birth of a vigourous area still of theoretical and observational study. Subsequent and continuing observational and theoretical work on surface abundance changes arising from the first and second dredge-ups in early red giants and the third dredge-up in asymptotic giant branch stars spring from these exploratory calculations.

4.4. *Discovery of the Cosmic Microwave Background*

Discovery of the cosmic microwave background radiation has had fundamental implications for our understanding of the origins of the light elements, as is evidenced here by several papers discussing contemporary strains between prediction and observation. Perhaps, *the* discovery of the CMB was announced by Penzias & Wilson (1965) in a short note with the title 'A measurement of excess antennna temperature at 4080 Mc/s' whose abstract noted the excess temperature was 3.5K higher than expected and 'isotropic, unpolarized, and free from seasonal variations' with a 'possible explanation' being relic radiation from the Big Bang.

This discovery quickly focussed theoretical attention anew on possible observable consequences of the Big Bang, with areas of particular relevance for the light elements being related issues of the primordial nucleosynthesis and the power spectrum of the CMB's very small anisotropy which is fundamental to determining the baryon density, the value of which sets the yields from the nucleosynthesis. First theoretical explorations of the acoustic oscillations in this regard were reported by Zel'dovich & Sunyaev (1969) and Peebles & Yu (1970).

4.5. *Pioneering calculations of Big Bang nucleosynthesis*

Faulkner's calculations inspired by Hoyle's 1964 lecture course were expanded thoroughly by Wagoner, Fowler, & Hoyle (1967) in their paper 'On the synthesis of elements at very high temperatures'. Their study which went beyond the synthesis of He discussed by Faulkner and also by Peebles (1966a,b) provided 'a detailed calculation of element production in the early stages of a homogeneous and isotropic expanding universe as well as within imploding-exploding supermassive stas' with a conclusion 'if the recently

measured microwave background radiation is due to primeval photons, then significant quantities of only D, He^3, He^4, and Li^7 can be produced in the universal fireball.' The insertion of 'if' presumably reflected not only natural professional caution about the reality of the microwave radiation background but also possibly tension among the authors over acceptance of a hot Big Bang. Hoyle, of course, never accepted the idea of the Big Bang, a term coined long before by him in a prestigious series of broadcasts on the BBC (Kynaston 2007).

4.6. *Back to the x-process*

Recognition that 'significant quantities' of D and ^{7}Li could be produced in the Big Bang did not address fully the identity of the x-process. What were the origins of ^{6}Li, ^{9}Be, ^{10}B and ^{11}B? This question was very largely answered when the role of Galactic cosmic rays in the spallation of abundant C, N, and O nuclei was appreciated. Reeves (1993) has provided a fascinating account of how this appreciation occurred when he caught Hoyle 'talking in class': 'In 1969, I presented these ideas in a seminar at the former IOTA (Institute of Theoretical Astronomy) in Cambridge (UK). During my seminar, Fred Hoyle kept on talking to Willie Fowler. I could overhear some of his words "I have been repeating that to you for many years. You should have listened to me." Later on, he told me that he had considered this scenario for a long time. We published a paper together on this subject.'

The paper was 'Galactic cosmic ray origins of Li, Be, and B in stars' (Reeves, Hoyle, & Fowler 1970). This and subsequent work with Reeves as an active player showed that spallation by (high energy) Galactic cosmic rays could account satisfactorily for ^{6}Li, ^{9}Be, and ^{10}B as the products of collisions between protons and α particles on the one hand and C, N, and O nuclei on the other hand; the solar system ratios ^{6}Li/^{9}Be and ^{10}B/^{9}Be were well reproduced by the calculations. But the ratios ^{7}Li/^{9}Be and ^{11}B/^{9}Be were greater than could be accounted for by high-energy spallation. ^{9}Be is taken to be a benchmark because no process of stellar Be nucleosynthesis has been identified. Spallation by low energy cosmic rays may account for some of the required extra ^{7}Li and ^{11}B, as first suggested by Meneguzzi, Audouze, & Reeves (1971). In low metallicity gas, collisions between cosmic ray and interstellar He nuclei – α on α collisions – will produce ^{6}Li and ^{7}Li but not Be and B. Neutrino-induced spallation in Type II supernovae may produce ^{7}Li and ^{11}B - the so-called ν-process (Woosley 1977; Woosley et al. 1990). Of course, a major contributor to ^{7}Li is the Big Bang.

4.7. *A role for diffusion?*

Discussion of diffusive separation of elements, even isotopes, in a modern form is traceable to Georges Michaud (1970) and the paper 'Diffusion processes in peculiar A stars'. Proposals generally by Michaud and his disciples concerning observable effects of diffusion – principally describing a competition between gravitational settling and radiative levitation – have since 1970 encompassed many kinds on stars across the H-R diagram.

Of relevance here, the principal appearance of diffusion is surely the role attributed by some to it in accounting for the disagreement between the Li abundance of the Spite plateau and the several times higher abundance predicted from Big Bang nucleosynthesis according the baryon density required by the fit to the cosmic microwace background fluctuations.

4.8. *Li synthesis in stars*

Speculations about the x-process included Li (and Be, B) synthesis by spallation on a stellar surface. The stellar interior was known to be highly unfavourable to Li survival;

the very low solar Li abundance (relative to that in chondritic meteorites) was early attributed to convection resulting in Li destruction. Seemingly, the first proposal for Li production in stellar interiors with a consequence for high atmospheric abundances of Li was by Cameron (1955), a proposal further developed by Cameron & Fowler (1971). Today, this idea is widely referred to as the 'Cameron-Fowler mechanism'.

In 1971, the mechanism was presented as an explanation for the high Li abundances seen in a few cool carbon and S stars. The prototype of the group is WZ Cas (McKellar 1940). 'It is tempting to believe that the lithium has been produced by some internal process. However, since the majority of the carbon and S giants do not possess nearly so much lithium, it is necessary to postulate that the production process involves some unusual events' (Cameron & Fowler 1971). The 'unusual events' were suggested by Cameron & Fowler to be the He-burning shell flashes predicted by Schwarzschild & Härm (1965) to occur in stars on the asymptotic giant branch. These flashes had already been suggested by others to be a site for operation of a *s*-process and thus to account for the heavy element enrichment in carbon and S stars and notably the presence of Tc in selected S stars. The paper proposed that the neutron source was the now familiar $^{13}C(\alpha, n)^{16}O$ with fresh ^{13}C provided by the mixing of protons into the He-shell.

Lithium synthesis involved the sequence $^{3}He(\alpha, \gamma)^{7}Be(e^{-}\nu)^{7}Li$ (Cameron 1955). To achieve efficient conversion of ^{3}He to ^{7}Li, the ^{7}Be must be swept out of the hot layers where it is produced to cooler layers where it and ^{7}Li are immune to destruction by protons. Cameron & Fowler sited initiation of the sequence at the base of the H-rich convective envelope with ^{7}Be and ^{7}Li convected outward to safety. Today, we would refer to the situation as a hot-bottomed convective envelope. In addition to its applicability to AGB stars with such an envelope, the Cameron-Fowler conversion of ^{3}He to ^{7}Li has been applied to account for Li-rich first ascent red giants, stars with internal structures very different from that of an AGB star, as several papers at this symposium discuss,

A star's internal reservoir of ^{3}He is built up from two sources. First, there is the ^{3}He and ^{2}H present at its birth. The ^{2}H, surviving Big Bang deuterium, is burnt to ^{3}He in the pre-main sequence phase. The initial ^{3}He is a consequence of Galactic chemical evolution but likely dominated by the Big Bang's ^{3}He, and any ^{3}He synthesised by stars during the Galaxy's evolution. A contribution from stellar nucleosynthesis, apart from the D to ^{3}He conversion, is significant only in low mass stars where their long main sequence life allows the initial reaction of the *pp*-chain with its very small cross-section governed by the weak interaction to provide ^{3}He exterior to the energy-energy generating core. A corollary of the last point is that ^{3}He is *not* synthesised by stars once they have evolved off the main sequence. Initiation of the Cameron-Fowler mechanism may begin by increasing the Li abundance in the stellar atmosphere but extended operation will eventually lead to a reduction of the Li abundance as the ^{7}Li is recycled to high temperatures and destroyed and the ^{3}He supply is run to exhaustion.

4.9. *Helium is primarily primordial*

In their 1964 paper, Hoyle & Tayler presented a convicing theoretical argument that the reported He/H ratio of about 0.1 in several Galactic and extragalactic objects could not be accounted for by stellar nucleosynthesis but had been produced 'in a far more dramatic way'. Apart from a measurement of the He/H ratio in a planetary nebula belonging to a globular cluster (O'Dell, Peimbert, & Kinman 1964), observational evidence that He might have a primordial origin with a minor supplement from stellar nucleosynthesis was scant in the extreme. Furthermore, the stellar ejecta comprising a planetary nebula may have been enriched in He in the course of stellar evolution.

Spectroscopy of halo stars (i.e., old and expected to be He-poor if stellar nucleosynthesis

is the dominant origin of He) sufficiently hot to show He lines had displayed a tendency to present low He/H ratios but with compositions that 'are quite exotic and hard to accept as being primordial ' (Searle & Sargent 1972). Now, we identify 'exotic' as consequences of diffusion that has distorted the 'true' composition of the stars.

Definitive observational spectroscopic evidence of the primarily primordial origin of He was first provided by Searle & Sargent (1972) in their paper 'Inferences from the composition of two dwarf blue galaxies'. Emission lines in the galaxies I Zw 18 and II Zw 40 showed that O/H and Ne/H were lower than local Galactic values ([O/H] $\simeq -1$ in the case of I Zw 18) but He has a normal abundance. 'These galaxies are the first metal-poor systems of Population I to be discovered: the normal helium abundance is taken as evidence that this abundance is primordial' (Searle & Sargent). I Zw 18 remains one of a handful of O-poor galaxies anchoring the low O/H end of the relation between He/H and O/H that provides our estimates of the Big Bang's He yield (see papers at this symposium).

4.10. *Deuterium as a baryometer*

The realization that the deuterium abundance - D/H - in appropriate locales might serve as a baryometer for the Big Bang was boosted with Reeves et al.'s (1973) paper 'On the origin of the light elements'. While the paper offered a comprehensive survey of the origins of all the light nuclides, perhaps its most telling and lasting point were the assertions that 'The deuterium can *only* be produced pregalactically either by the big bang or in some pregalactic event' [emphasis added] and 'the most plausible origin of D is big-bang nucleosynthesis'. Another way to express this result is to say that all modes of stellar nucleosynthesis destroy ('astrate') D and possible production paths involving energetic particles in diverse places (interstellar medium, stellar atmospheres, for example) cannot produce D without overproducing other light elements. The primordial origin of D was amplified by Epstein, Lattimer, & Schramm (1976) with the caveat that 'other, more speculative, sources are not ruled out'. Todate, no such 'other' sources have been ruled in.

Detection of D in the interstellar medium was first reported by Rogerson & York (1973) from *Copernicus* spectra of the hot star β Cen showing Lyman lines of H I and D I - the isotopic wavelength shift of 81 km s^{-1} provided well resolved lines. Measurements of the D/H ratio along several lines of sight followed this pioneering determination for β Cen.

Of course, the D/H measurement might reasonably be taken to be a lower limit to the Big Bang D/H ratio; cycling of gas through stars astrates D. Various attempts were made (and continue to be made) to devise the correction for the cumulative astration. Substantial additions to the library of interstellar D/H measurements, especially from *FUSE* spectra, have added challenges to modelling of GCE of D.

Adams (1976) proposed that the difficulties of correcting the interstellar D/H ratios for astration in order to obtain the pregalactic/primordial ratio could be alleviated, if not avoided, by detecting the Lyman D I lines in absorption from intergalactic clouds along the lines of sight to distant quasars. Such clouds representing almost pristine primordial gas should have essentially their primordial D abundance. The degree to which the clouds have been contaminated by products of stellar nucleosynthesis is assessable from absorption lines of ions of C, O, Si etc. Adams' proposal was ahead of its time. It took 8-meter class telescopes with high-resolution spectrographs to obtain suitable spectra. Even today, as discussed at this symposium, useful D/H ratios have been published for just a handful of quasars; many quasars turn out to have ill-suited spectra; the D I lines of a strong cloud are blended with H I lines of a weaker cloud at a different velocity. A definitive set of D/H determinations continues to elude us.

4.11. *The hyperfine line 8.7 GHz line of $^3He^+$*

The ground state of the ion $^3He^+$ with a nuclear spin of 1/2 has a hyperfine line at 8.7 GHz, the analogue of the H atom's 21 cm line. Rood, Wilson, & Steigman (1979) reported on 'The probable detection of interstellar $^3He^+$ and its significance'. The 'tentative detection' referred to a giant H II region. Since 1979, Rood and colleagues have doggedly pursued the 8.7 GHZ line in Galactic H II regions and planetary nebulae, as described by Bania at this symposium. Abundances of $^3He^+$ in these sources have led to what has been dubbed 'the ^{3}He problem' (Galli et al. 1997).

The isotope ^{3}He with D and ^{7}Li is a minor product of the standard Big Bang. Additionally, main sequence stars are predicted to synthesise ^{3}He as part of the *pp*-chain and from D-burning (as outlined above in Section 4.8). If one assumes that the synthesised ^{3}He is not subsequently destroyed (astrated) and returned to the interstellar medium, the ^{3}He abundance in the interstellar medium might be expected to increase with time, i.e., the abundance in local H II regions might be higher than the protosolar value, as apparently first pointed out by Rood, Steigman, & Tinsley (1976). This possibility and the lure of pinning down the Big Bang's ^{3}He yield prompted the now 30-year old pursuit of the 8.7 GHz line.

In the 1979 paper, the single probable detection of ^{3}He in an H II region led to the determination of a ^{3}He/H ratio 'comparable to the protosolar number' and the conclusion that there is 'no evidence for the production of ^{3}He predicted for low mass stars'. Knowing the ingenuity of students of Galactic chemical evolution, the conclusion may not necessarily follow from the determination of the similar ^{3}He/H abundances. However, the '^{3}He problem' was starkly evident after the 8.6 GHz line was detected from Galactic planetary nebulae. Balser et al. (1997) report the first successful observations of the line with the result that the ^{3}He/H abundances 'are more than an order of magnitude larger than those found in any H II region, the local interstellar medium, or the proto-solar system'. Clearly, 'there is *some* stellar production of ^{3}He' [emphasis in the 1979 abstract]. The ^{3}He problem is the subject of several papers here.

4.12. *The Spite plateau*

My final milestone in this chronological listing is the pair of 1982 papers by Spite & Spite: The *Nature* Letter 'Lithium abundance at the formation of the Galaxy' (Spite & Spite 1982a) and the *A&A* article 'Abundance of lithium in unevolved halo stars and old disk stars: interpretation and consequences' (Spite & Spite 1982b).

The landscape in which this milestone was uncovered may be appreciated by recalling the summary of Li observations assembled by Reeves et al. (1973). The local Li abundance was put at $\log \epsilon \simeq 3$ with Li-richer stars (e.g., WZ Cas) attributed to internal Li synthesis and Li-poorer stars (e.g., Sun) attributed to internal Li astration. In their presentation of the possible Galactic evolution of the ^{7}Li abundance (Fig. 6 of Reeves et al.), two extremes were presented: (i) the assumption that ^{7}Li was a Big Bang product led to the suggestion of a factor of several *increase* in the Li/H ratio from the present ratio back to the formation of the Galaxy; (ii) an assumption that ^{7}Li came only from enrichment of the interstellar medium by Li-rich gas from red giants led, of course, to Li-poor gas at early times. A third possibility was that the local Li abundance seen in stars with ages spanning at least 5 Gyr represents the pre-Galactic abundance.

Spite & Spite exploiting the spectroscopic capabilities of the (then) new CFHT telescope observed a small sample of halo dwarfs, stars recognized as very old and known to be very metal-poor, i.e., the gas from which these stars had formed should be a fair approximation to pre-Galactic gas. To their (I presume) surprise and delight, the Li

abundance of the warmest of these stars was uniform (hence, the Spite plateau) and at $\log \epsilon(\mathrm{Li}) = 2.05$ much lower than the local value. 'After discussion, it is suggested that the abundance in halo dwarfs is therefore representative of the interstellar matter which formed the stars and also this matter itself retains the lithium abundance of the Big Bang, hardly altered' (Spite & Spite 1982b).

The existence of a plateau, the Li abundance of the plateau, and the relation between the Li abundance and the abundance provided by the Big Bang have been debated from 1982 to this day, and, indeed, these questions were among the reasons advanced for holding this symposium.

5. Final thoughts

The four discussion sessions at the symposium were intended to focus on the 'hot' questions involving light elements in contemporary astrophysics. My contribution sheds light on the historical perspective behind most of these questions. Omissions will be excused, I hope, on the grounds of lack of time and space.

In closing, I offer two rather different historical thoughts: the first on the publication of symposium proceedings and the second on the sophistication of our scientific endeavours.

As a research student, I recall the particular joy I experienced in reading the extended discussions that were reported at length in the two IAU symposia (#12 and #28) on 'Aerodynamic Phenomena in Stellar Atmospheres' edited by R.N. Thomas (1960, 1965). These were not meetings I had attended but the discussions almost brought me into the meeting room as an engaged listener, if one too shy and ignorant to participate. Why do organisers of meetings not aspire to emulate these two volumes?

Astronomical spectra are beautiful objects, especially when a striking conclusion may be drawn by inspection. In Geneva, I drew attention once again to Spite & Spite's (1982b) Figure 1 showing spectra around the Li I 6707Å doublet for four metal-poor dwarfs. Inspection shows Ca I and Fe I lines of differing strength but Li I lines of similar strength in all but the coolest dwarf HD 103095 (alias Groombridge 1830). Thus, the Spite plateau is there in front of ones eyes. (Li is strongly depleted in HD 103095.)

Of course, conversion of spectra to a quantitative abundance estimate cannot be done by visual inspection alone. Tools for the conversion have certainly become more sophisticated and refined over the years spanned by milestones and certainly since 1982. Had I not concentrated on results exclusively, I would have entertained including milestones relating to telescopes, instruments, and analytical tools. Currently, the apex of analytical sophistication surely involves the application of 3D or hydrodynamical model atmospheres with the selective addition of non-LTE considerations in certain cases.

In the area of light elements, 3D atmospheres are being applied in particular to analyses of the Li I 6707Å line in metal-poor dwarf stars to address key questions from cosmology, early Galactic evolution, and stellar physics. If I were to limit the questions to two, my choices would be 'Is the Li abundance of Spite plateau stars reconcilable with that predicted from the Big Bang with the baryon density set by the CMB fluctuations? and 'Is there ^{6}Li mixed in with the ^{7}Li in these stars?

To the first question, there appear to be two diametrically different answers to account for the result obtained (even with 3D atmospheres) that the stellar Li abundance is a factor of several less than the Big Bang prediction. One, diffusion is invoked to reduce the atmospheric abundance but to account for the plateau's observed height and shape over several dex in metallicity turbulent diffusion is introduced without thorough detailed physical understanding. Two, the standard model of the Big Bang is modified by intro-

ducing new physics including modifications to the standard model of particle physics. One or two? Or both?

Obviously, observational tests are sought. In the case of one, there is now evidence that diffusion whose effects should be partially undone in evolution off the main sequence has occurred - see the beautiful work reported here on the composition of globular cluster stars. In the case of two, an indicator of some failures of the standard Big Bang model is the presence of ^{6}Li in significant amounts. Measurements of small amounts of ^{6}Li in the presence of ^{7}Li demand a sophistication of line profile analysis rarely required, and possibly not yet achievable.

One looks forward to the next workshop, conference, or symposium on light elements in the Universe. Perhaps, no other set of five elements brings together in such an interlocked fashion matters of cosmology, galaxy formation and evolution, and an array of matters in stellar astrophysics.

In preparing this essay for publication, I took the occasion to explore the literature somewhat more thoroughly than I did prior to the oral presentation in Geneva. This led to some modification of the presentation but, more fundamentally, I was humbled afresh by how much of the history I had forgotten or had never ever appreciated. Thus, I apologise to those whose contributions I have still overlooked or underappreciated. I thank my Austin friends who answered several questions at short notice, especially Volker Bromm and Paul Shapiro. As has been the case for more than 30 years, I are indebted to the Robert A. Welch Foundation of Houston, Texas for grant F-634 which has supported my research into the chemical compositions of stars.

References

Adams, T.F. 1976, *A&A*, 50, 461
Aller, L.H., Menzel, D.H. (1945), *ApJ*, 102, 239
Balser, D.S., Bania, T.M., Rood, R.T., & Wilson, T.L. 1997, *ApJ*, 483,320
Bowen, I.S. (1927), *PASP*, 39, 295
Bowen, I.S. (1928), *ApJ*, 67, 1
Bowen, I.S. 1935, *ApJ*, 81, 1
Burbidge, E.M., Burbidge, G.R., Fowler, W.A., & Hoyle, F. 1957, *Rev. Mod. Phys.*, 29, 547
Cameron, A.G.W. 1955, *ApJ*, 121, 144
Cameron, A.G.W. 1957, *PASP*, 69, 201
Cameron, A.G.W., & Fowler, W.A. 1971, *ApJ*, 164, 111
Epstein, R.I., Lattimer, J.M., & Schramm, D.N. 1976, *Nature*, 263, 198
Faulkner, J., 2009, in *Finding the Big Bang*, ed. P.J.E. Peebles, L.A. Page, Jr., & R.B. Partridge, Cambridge:Cambridge University Press, p. 244
Hoyle, F., & Tayler, R.J., 1964, *Nature*, 203, 1108
Galli, D., Stanghellini, L., Tosi, M., & Palla, F. 1997, *ApJ*, 477, 218
Iben, I., Jr., 1964, *ApJ*, 140, 163
Iben, I., Jr., 1967a, *Science*, 155, 785
Iben, I., Jr., 1967b, *ARAA*, 5, 571
Kynaston, D. 2007, *Austerity Britain 1945-51*, London:Bloomsbury Publishing plc, p. 387
Longair, M.S. 2006, *The Cosmic Century:A History of Astrophysics and Cosmology*, Cambridge: Cambridge University Press
McCrea, W.H. 1929, *MNRAS*, 89, 483
McKellar, A. 1940, *PASP*, 52, 407
Meneguzzi, M., Audouze, J., & Reeves, H. 1971, *A&A*, 15, 337
Michaud, G. 1970, *ApJ*, 160, 641
O'Dell, C.R., Peimbert, M., & Kinman, T.D. 1964, *ApJ*, 140, 119

Payne, C.H. 1925, *Stellar Atmospheres:Harvard College Observatory Monographs, No. 1*, Cambridge, MA:Harvard University Press
Peebles, P.J.E. 1966a, *Phys. Rev. Lett.*, 16, 410
Peebles, P.J.E. 1966b, *ApJ*, 146, 542
Peebles, P.J.E., & Yu, J.T. 1970, *ApJ*, 162, 815
Penzias, A.A., & Wilson, R.W. 1965, *ApJ*, 142, 419
Popper, D.M. (1942), *PASP*, 54, 160
Reeves, H. 1993, in *Origin and Evolution of the Elements*, ed. N. Prantzos, E. Vangioni-Flam, & M. Cassé, Cambridge:Cambridge University Press
Reeves, H., Fowler, W.A., & Hoyle, F. 1970, *Nature*, 226, 727
Reeves, H., Audouze, J, Fowler, W.A., & Schramm, D.N. 1973, *ApJ*, 179, 909
Rogerson, J.B., & York, D.G. 1973, *ApJ*, 186, L95
Rood, R.T., Steigman, G., & Tinsley, B.M. 1976, *ApJ*, 207, L57
Rood, R.T., Wilson, T.L., & Steigman, G. 1979, *ApJ*, 227, L97
Schwarzschild, M., & Härm, R. 1965, *ApJ*, 142, 855
Searle, L., & Sargent, W.L.W. 1972, *ApJ*, 173, 25
Spite, M., & Spite, F. 1982a, *Nature*, 297, 483
Spite, F., & Spite, M. 1982b, *A&A*, 115, 357
Thomas, R.N. 1960, editor of *Aerodynamic Phenomena in Stellar Atmospheres*, Proc. IAU Symposium No. 12, Nuovo Cimento Suppl., 22
Thomas, R.N. 1965, editor of *Aerodynamic Phenomena in Stellar Atmospheres*, Proc. IAU Symposium No. 28, London & New York:Academic Press
Unsöld, A. 1928, *Z. f. Phys.*, 46, 765
Wagoner, R.V., Fowler, W.A., & Hoyle, F. 1967, *ApJ*, 148, 3
Woosley, S.E. 1977, *Nature*, 269, 42
Woosley, S.E., Hartmann, D.H., Hoffman, R.D., & Haxton, W.C. 1990, *ApJ*, 356, 272
Zel'dovich, Ya.B., & Sunyaev, R.A. 1969, *ApSS*, 4, 301

Session I

Production of the light elements

in the first minutes of the Universe

Monica Tosi, Bob Rood, Tom Bania

Richard Stancliffe, Sara Palmerini, Thibaut Decressin

Light elements in the Universe
Proceedings IAU Symposium No. 268, 2010
C. Charbonnel, M. Tosi, F. Primas & C. Chiappini, eds.

DOI: 00.0000/X000000000000000X

Constraints from the cosmic microwave background experiments

Joanna Dunkley[1]

[1]Oxford University - United Kingdom
email: j.dunkley@physics.ox.ac.uk

Abstract. I will give a review of the current constrains on light element abundances from cosmic microwave background experiments, focusing on results from WMAP and discussing prospects from upcoming data from Planck and ground-based experiments. I will describe how the production of light elements affects the CMB anisotropies, and how we use the data to extract cosmological information that includes constraints on the baryon density, and primordial abundances.

Keywords. Cosmology: cosmic microwave background

A couple of months after the Symposium, Joanna Dunkley informed the editors of these proceedings that *"The WMAP collaboration's policy is not to write conference proceedings if they contain results published in WMAP papers. Since this review has been almost entirely focused on results from the 5-year WMAP analysis it cannot be reported here. The results can be found in Komatsu et al. (2009) and Dunkley et al. (2009)."*

Given the relevance of her review to the discussions and the results of the whole Symposium we felt it would not be appropriate to simply skip her contribution. We thus report here the abstract that she originally sent and the references where the reader can find the WMAP results that she presented to the audience.

The responsibility of this decision is fully of the editors and should not be ascribed to Dr. Dunkley.

References

Dunkley, J., Komatsu, E., Nolta, M.R., Spergel, D.N., Larson, D., et al. 2009, *ApJS*, 180, 306
Komatsu, E., Dunkley, J., Nolta, M.R., Bennett, C.L., Gold, B., et al. 2009, *ApJS*, 180, 330

Michel Grenon & Sushma Mallik

Chantal Taçoy & Nadège Lagarde

Light elements in the Universe
Proceedings IAU Symposium No. 268, 2010
C. Charbonnel, M. Tosi, F. Primas & C. Chiappini, eds.

DOI: 00.0000/X000000000000000X

Primordial nucleosynthesis: A cosmological probe

Gary Steigman

Departments of Physics and Astronomy
Center for Cosmology and Astro-Particle Physics
The Ohio State University
192 West Woodruff Avenue
Columbus, OH 43210 USA
email: steigman@mps.ohio-state.edu

Abstract.
During its early evolution the Universe provided a laboratory to probe fundamental physics at high energies. Relics from those early epochs, such as the light elements synthesized during primordial nucleosynthesis when the Universe was only a few minutes old, and the cosmic background photons, last scattered when the protons (and alphas) and electrons (re)combined some 400 thousand years later, may be used to probe the standard models of cosmology and of particle physics. The internal consistency of primordial nucleosynthesis is tested by comparing the predicted and observed abundances of the light elements, and the consistency of the standard models is explored by comparing the values of the cosmological parameters inferred from primordial nucleosynthesis with those determined by studying the cosmic background radiation.

Keywords. cosmology: early universe, nucleosynthesis, cosmological parameters

1. Introduction

Primordial nucleosynthesis provides a key probe of the physics and early evolution of the Universe. Big Bang Nucleosynthesis (BBN; ~ 20 minutes) and the cosmic microwave background (CMB) photons, last scattered at recombination (~ 400 kyr), provide complementary probes of the physics of the early evolution of the Universe.

For a brief period during its early evolution the hot, dense Universe is a cosmic nuclear reactor. Since the Universe is expanding and cooling rapidly, there is only time to synthesize in astrophysically interesting abundances the very lightest nuclides (D, ^{3}He, ^{4}He, and ^{7}Li). In the standard models of cosmology and particle physics described by General Relativity, the universal expansion rate, the Hubble parameter, H, is determined by the total mass/energy density: $H^2 \propto G\rho$, where $H = H(z)$, z is the redshift, G is the gravitational constant, and ρ is the energy density. During such early epochs, the Universe, which is filled with relativistic particles including three flavors of light neutrinos ($N_\nu = 3$), is "radiation dominated", and the abundances of the nuclides synthesized during BBN depend on only one cosmological parameter, η_B, which provides a measure of the universal density of baryons.

$$\eta_B \equiv n_B/n_\gamma \equiv 10^{-10}\eta_{10}. \tag{1.1}$$

In eq. 1.1, n_B is the number density of baryons and n_γ is the number density of cosmic background photons. The only baryons present at BBN are nucleons, *i.e.*, protons and neutrons. In contrast to the standard model of cosmology, there is a class of non-standard cosmological (and/or particle physics) models in which the expansion rate may differ from

its standard model value, $H' \neq H$. In these non-standard models the expansion rate can be parameterized by an "expansion rate parameter", S, or equivalently, by an "effective number of neutrinos", $N_\nu \neq 3$, where

$$S^2 \equiv (H'/H)^2 \equiv G'\rho'/G\rho \equiv 1 + 7\Delta N_\nu/43. \quad (1.2)$$

More generally, the effective number of "extra" neutrinos, $\Delta N_\nu \equiv N_\nu - 3$, parameterizes any non-standard energy density ($\rho' \neq \rho$), normalized to the contribution from one standard model neutrino by,

$$\Delta N_\nu \equiv (\rho' - \rho)/\rho_\nu. \quad (1.3)$$

However, even if $\rho' = \rho$, it could be that $N_\nu \neq 3$ ($\Delta N_\nu \neq 0$) if the early-Universe gravitational constant differs from its current value, $G' \neq G$,

$$G'/G = S^2 = 1 + 7\Delta N_\nu/43. \quad (1.4)$$

As will be seen below, in this class of non-standard models the BBN-predicted (nSBBN) primordial abundance of deuterium depends largely on the baryon density parameter, η_B (deuterium is a cosmological baryometer), while that of helium-4 is sensitive to the early Universe expansion rate, S (^{4}He is an early universe chronometer).

In order to test the standard models of cosmology and particle physics, two key questions are addressed:

1. Do the light element abundances predicted by BBN agree with the primordial abundances inferred from observations?

2. Do the BBN values of η_B and S (N_ν) agree with those inferred from independent, non-BBN observations (e.g., from the CMB)?

2. Standard Big Bang Nucleosynthesis (SBBN)

For SBBN ($N_\nu = 3$), the light element relic abundances are only a function of the baryon density parameter, η_B. Among the light nuclides, deuterium is the baryometer of choice. There are several reasons why D occupies this special place. One is that the post-BBN evolution of deuterium is simple and monotonic: as gas is cycled through stars (producing the heavy elements), D is only destroyed (Reeves *et al.* 1973, Epstein, Lattimer, & Schramm 1976). As a result, if deuterium is observed anywhere in the Universe, at any time in its evolution, the observed abundance will be no larger than the primordial value: $(D/H)_{OBS} \leqslant (D/H)_P$. In addition, for systems of low metallicity, a sign that very little of their gas has been cycled through stars which destroy deuterium, the observed D abundance should approach the primordial value: $(D/H)_{OBS} \rightarrow (D/H)_P$ (the "Deuterium Plateau"). Another reason to prefer D is that its predicted primordial abundance is sensitive to the baryon density parameter; since $(D/H)_P \propto \eta_B^{-1.6}$, a $\sim 10\%$ determination of $(D/H)_P$ results in a $\sim 6\%$ determination of η_B.

The deuterium abundance is determined by comparing the H I and D I column densities inferred from observations of absorption of radiation from background UV sources by intervening gas. In searching for the Deuterium Plateau the relelvant data is provided by observations of high-redshift, low-metallicity, QSO Absorption Line Systems (QSOALS). Unfortunately, at present there are only seven, relatively reliable D abundance determinations (Pettini et al. 2008), which are shown in Figure 1.

The weighted mean of the seven D abundances is $\log(y_{DP}) = 0.45$. However, as may be seen from the Figure 1, only three of the seven abundances lie within 1σ of the mean. Indeed, the fit to the weighted mean of these seven data points has a $\chi^2 = 18$ ($\chi^2/dof = 3$). Either the quoted errors are too small or, one (or more) of the determinations is

wrong, perhaps contaminated by unidentified (and, therefore, uncorrected) systematic errors. In the absence of evidence identifying the reason(s) for such a large dispersion, the best that can be done at present is to adopt the mean D abundance and to inflate the error in the mean in an attempt to account for the unexpectedly large dispersion among the D abundances (Steigman 2007).

$$\log(y_{\rm DP}) \equiv 0.45 \pm 0.03. \tag{2.1}$$

For this relic D abundance, SBBN predicts that the baryon density parameter is

$$\eta_{10}({\rm SBBN}) = 5.80 \pm 0.28, \tag{2.2}$$

corresponding to a baryon mass density $\Omega_{\rm B}h^2 = 0.0212 \pm 0.0010$.

For η_{10}(SBBN), the SBBN-predicted abundances of the remaining light nuclides are

$$y_{\rm 3P} \equiv 10^5({}^3{\rm He/H})_{\rm P} = 1.07 \pm 0.04, \tag{2.3}$$

$$Y_{\rm P} = 0.2482 \pm 0.0007, \tag{2.4}$$

$$[{\rm Li}]_{\rm P} \equiv 12 + \log({\rm Li/H})_{\rm P} = 2.67^{+0.06}_{-0.07}. \tag{2.5}$$

2.1. *Consistency of SBBN?*

Having used the deuterium observations along with the predictions of SBBN to determine the baryon density parameter, we may now ask if the observed abundances of ^{3}He, ^{4}He, and ^{7}Li are consistent with their SBBN-predicted primordial values.

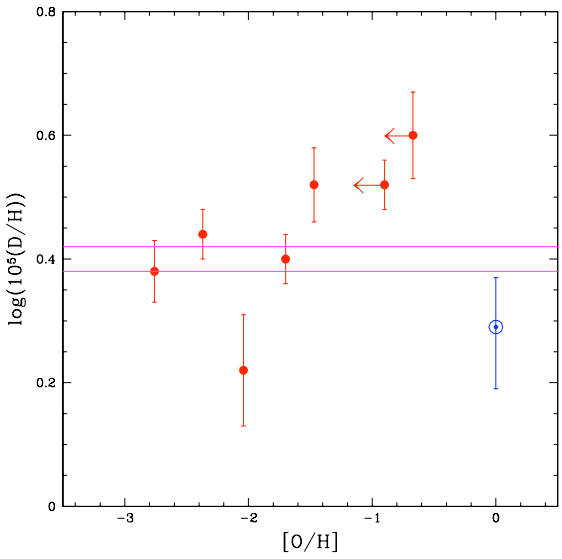

Figure 1. The logs of the deuterium abundances, $y_{\rm D} \equiv 10^5({\rm D/H})$, observed in high-$z$, low-Z QSO Absorption Line Systems (Pettini et al. 2008), as a function of the corresponding oxygen abundances. For comparison, the solar deuterium and oxygen abundances are shown (Geiss & Gloeckler 1998). The band indicated by the solid lines is the 68% range of the SBBN-predicted primordial D abundance using the CMB-determined baryon density parameter (see §3).

Helium - 3.

The post-BBN evolution of ^{3}He is model dependent and, considerably more complicated than that of D. Overall, the ^{3}He abundance is expected to increase during Galactic chemical evolution (see, *e.g.*, Rood 1972, Rood, Steigman & Tinsey 1976). Observations of ^{3}He are limited to the relatively evolved H II regions in the Galaxy (Bania, Rood, & Balser 2002). The data are shown in Figure 2, where the observed ^{3}He abundances are plotted versus the corresponding H II region oxygen abundances. The data reveal a *minimum* (primordial?) ^{3}He abundance which is consistent with the SBBN prediction. While the higher observed abundances support the expectation of net post-BBN production of ^{3}He, the absence of a correlation with the oxygen abundances is puzzling.

Helium - 4.

The primordial abundance (mass fraction) of ^{4}He is inferred from observations helium and hydrogen recombination lines from metal-poor, extragalactic H II regions (Blue Compact Galaxies: BCDs). In using these data to determine the primordial helium abundance, the systematic errors (underlying stellar absorption, temperature and density inhomogeneities, ionization corrections, atomic emissivities, etc.) dominate over the statistical errors and the uncertain extrapolation to zero metallicity. In my opinion, the uncertainty in Y_P is $sigma(Y_P) \approx 0.006$ and **not** $\sigma(Y_P) < 0.001$, as claimed in some published papers. Therefore, rather than show the helium abundances inferred from observations of hundreds of BCDs, in Figure 3 are shown the handful of helium abundances determined from careful observations of a few H II regions where attention has been paid to some but, even here, not all, sources of systematic uncertainties (Olive & Skillman 2004, Pe-

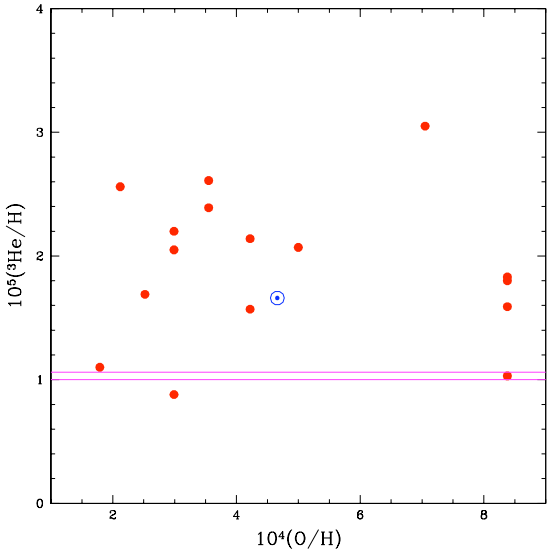

Figure 2. The ^{3}He abundances, $y_3 \equiv 10^5(^3\mathrm{He/H})$, observed in Galactic H II regions from Bania, Rood, & Balser (2002) are shown as a function of the corresponding oxygen abundances. For comparison, the solar helium-3 and oxygen abundances are shown. The band indicated by the solid lines is the 68% range of the SBBN prediction for the primordial ^{3}He abundance using the CMB-determined baryon density parameter (see §3).

imbert, Luridiana & Peimbert 2007). The seven Olive & Skillman (2004) H II regions are consistent with **no** correlation between the helium and oxygen abundances, leading to a weighted mean, $Y_{OS} = 0.2500 \pm 0.0030$. The same is true for the five H II regions studied by Peimbert, Luridiana, & Peimbert (2007), with $Y_{PLP} = 0.2517 \pm 0.0043$, where the PLP statistical and systematic errors have been added linearly. The independent analyses of OS and PLP agree. The surprising absence of evidence for statistically significant slopes in their Y versus O/H relations prevents an extrapolation to zero metallicity in order to find Y_P. However, the weighted means do provide *upper bounds* to Y_P: $Y_P < \langle Y \rangle$. As may be seen by comparison with eq. 2.4, these data are consistent with the SBBN prediction.

Lithium - 7.

Like deuterium, lithium (^{6}Li and ^{7}Li) is fragile. In contrast to deuterium, post-BBN lithium is produced via Cosmic Ray Nucleosynthesis and by some stars (see these Proceedings). This is confirmed by Galactic observations of lithium as a function of metallicity. It is therefore expected that in the limit of low metallicity the lithium abundance should approach a plateau, the "Spite Plateau". However, while the primordial abundances of ^{3}He and ^{4}He inferred from the observational data are consistent with the SBBN predicted abundances based on the deuterium abundance, ^{7}Li poses a severe problem. As may be seen from Figure 4, the lithium abundances derived from observations of the most metal-poor halo and globular cluster stars in the Galaxy lie well below the SBBN-predicted value (see eq. 2.5). The discrepancy between the prediction and the ob-

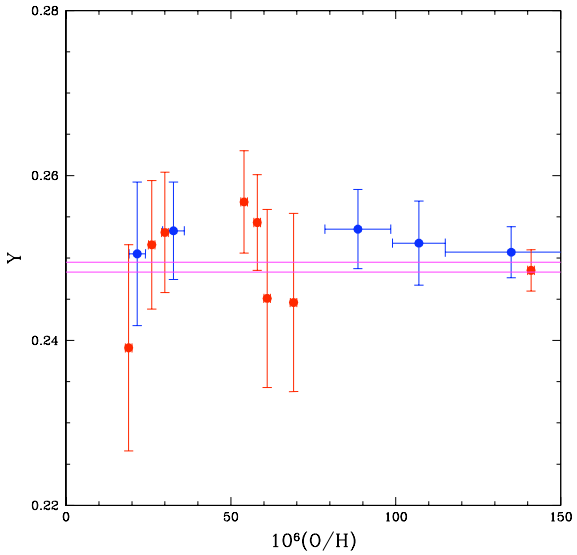

Figure 3. The ^{4}He mass fractions, Y, derived from a selected sample (see the text) of low metallicity, extragalactic H II regions, as a function of the corresponding H II region oxygen abundances. The blue filled circles are from Peimbert, Luridiana, & Peimbert (2007) and the red filled squares are from Olive & Skillman (2004). The band indicated by the solid lines is the 68% range of the SBBN prediction for the primordial ^{4}He mass fraction using the CMB-determined baryon density parameter (see §3).

servations is a factor of $\sim 3-5$. In addition, at the lowest iron abundances, the lithium abundances appear to be decreasing with metallicity. Where is the Spite Plateau? What is the value of $[\mathrm{Li}]_{\mathrm{P}}$?

Thus, although the predictions and observations of D, ^{3}He, and ^{4}He are consistent with SBBN, lithium is a problem. Setting lithium aside, we may ask if SBBN is consistent with the CMB?

3. SBBN with the CMB-inferred baryon density parameter

The CMB temperature anisotropy spectrum depends on the baryon density parameter η_{B} (see the contribution by Dunkley). From the WMAP data Dunkley *et al.* (2009) find $\Omega_{\mathrm{B}}h^2 = 0.02273 \pm 0.00062$, which corresponds to (Steigman 2006)

$$\eta_{10}(\mathrm{CMB}) = 6.226 \pm 0.170. \tag{3.1}$$

The baryon density parameters inferred from deuterium and SBBN, when the Universe was ~ 20 minutes old, and from the CMB, last scattered some 400 thousand years later, agree within $\sim 1.5\sigma$ (the glass is half full). SBBN and the CMB are consistent (modulo the lithium problem).

It is interesting to check the consistency of SBBN and the CMB by comparing the SBBN-predicted primordial light nuclide abundances determined using the CMB value of baryon density parameter to the observations. These comparisons are shown by the

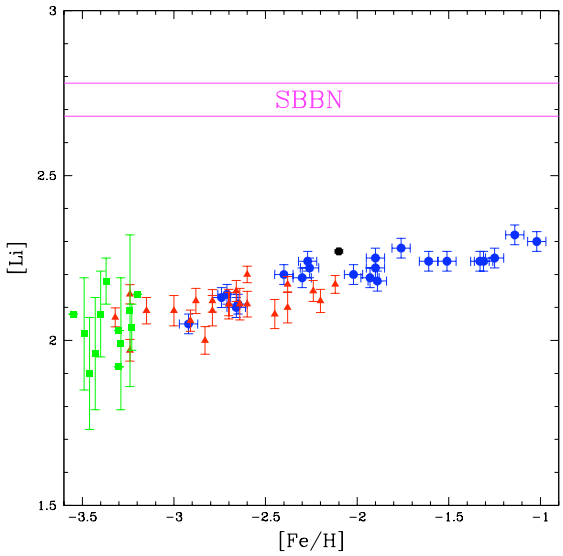

Figure 4. The lithium abundances, [Li] ≡ 12+log(Li/H), derived from observations of low metallicity Galactic halo and globular cluster stars as a function of the iron abundance (relative to solar). Blue filled circles (Asplund et al. 2006), red, filled triangles (Boesgard et al. 2005), green filled squares (Aoki et al. 2009). The black filled circle (Lind et al. 2009) is for the globular cluster NGC6397. The band indicated by the solid lines is the 68% range of the SBBN prediction for the primordial ^{7}Li abundance using the CMB-determined baryon density parameter (see §3).

horizontal bands in Figures 1-4. For SBBN with $\eta_{\rm B}$(CMB),

$$\log(y_{\rm DP}) = 0.40 \pm 0.02 \quad (y_{\rm DP} = 2.52 \pm 0.13), \tag{3.2}$$

$$y_{\rm 3P} = 1.03 \pm 0.03, \tag{3.3}$$

$$\rm Y_P = 0.2489 \pm 0.0006, \tag{3.4}$$

$$[\rm Li]_P = 2.74 \pm 0.05. \tag{3.5}$$

The SBBN/CMB-predicted abundances of D, ^{3}He, and ^{4}He are consistent with their observationally-inferred primordial values, but the lithium discrepancy is exacerbated. SBBN ($\rm N_\nu = 3$) and the CMB are consistent (but lithium is a problem!).

4. Non-Standard Big Bang Nucleosynthesis (nSBBN): $\rm N_\nu \neq 3$

For non-standard BBN (nSBBN) with $\rm N_\nu \neq 3$, the relic abundances of the light nuclides are functions of two parameters, $\eta_{\rm B}$ and $\rm N_\nu$. First, consider deuterium. The nSBBN primordial abundance is predicted to vary as $y_{\rm DP} \propto \eta_{\rm D}^{-1.6}$, where $\eta_{\rm D} = \eta_{\rm D}(\eta_{10},{\rm N_\nu})$ (see, *e.g.*, Kneller & Steigman 2004, Steigman 2007). It is interesting to explore the consequences of using the CMB (Dunkley et al. 2009) to fix η_{10} and the observed primordial D abundance to determine $\eta_{\rm D}$. This leads to a combined BBN and CMB prediction for $\rm N_\nu$. For $\log(y_{\rm D}) = 0.45 \pm 0.03$ and η_{10}(CMB) $= 6.23 \pm 0.17$, $\rm N_\nu = 4.0 \pm 0.7$. Here, the relative insensitivity of $y_{\rm DP}$ to $\rm N_\nu$ has amplified the small difference between η_{10} and $\eta_{\rm D}$ into a relatively large value (and uncertainty) of $\Delta \rm N_\nu = 1.0 \pm 0.7$. Although the central value of the effective number of neutrinos determined this way is $\rm N_\nu \neq 3$, this result is consistent with $\rm N_\nu = 3$ at $\sim 1.4\sigma$. Using this value of $\rm N_\nu$ along with η_{10}(CMB), how do the predicted BBN abundances of the remaining light nuclides compare with their observationally inferred primordial values? Here, I concentrate on the two key elements, ^{4}He and ^{7}Li (by construction, D is de facto consistent).

For this combination of η_{10} and $\rm N_\nu$, the primordial ^{4}He mass fraction is $\rm Y_P = 0.261 \pm 0.009$. Here, the sensitivity of $\rm Y_P$ to $\rm N_\nu$ has amplified the small difference between η_{10} and $\eta_{\rm D}$ into a relatively large value (and uncertainty) of $\rm Y_P$. As may be seen from Figure 3, within the large uncertainty of this prediction, the very high central value is consistent with the data.

The BBN-predicted abundances of D and ^{7}Li are very tightly correlated, both for $\rm N_\nu = 3$ and $\rm N_\nu \neq 3$ (Kneller & Steigman 2004, Steigman 2007). As a result, even for this example of nSBBN, the predicted primordial lithium abundance is very similar to its SBBN value, $[\rm Li]_P = 2.70^{+0.05}_{-0.06}$, in conflict with the observational data in Figure 4.

Thus, although this variant of nSBBN is consistent with D, ^{3}He, and ^{4}He, the lithium problem persists! Nonetheless, this example illustrates the potential value of combining BBN and the CMB to constrain and test non-standard models of particle physics and cosmology. A slightly different variant of this approach is presented in the next section.

5. Using ^{4}He and the CMB to constrain $\rm N_\nu$

Of the light nuclides synthesized during BBN, the ^{4}He mass fraction is most sensitive to non-standard physics ($\rm N_\nu \neq 3$). Indeed, for $|\Delta \rm N_\nu| \lesssim 1$, $\Delta \rm Y_P \approx 0.013 \Delta N_\nu$, so that a good bound (small uncertainty) to $\rm Y_P$ would result in a tight constraint on $\rm N_\nu$. According to Kneller & Steigman (2004) and Steigman (2007), using η_{10}(CMB)$= 6.23 \pm 0.17$, a very good fit to $\rm Y_P$, is

$$\rm Y_P \approx 0.2486 \pm 0.0007 + 0.013 \Delta N_\nu. \tag{5.1}$$

As mentioned earlier, the present uncertainty in the observationally inferred value of Y_P is dominated by systematic errors. To illustrate the potential value of an accurate determination of Y_P, let's adopt the weighted mean of the Olive & Skillman (2004) helium abundances as an *upper bound* to the primordial ^{4}He mass fraction: $Y_P < \langle Y \rangle_{OS} = 0.2500 \pm 0.0030$. Comparing this BBN prediction of Y_P with the upper bound inferred from the data leads to an *upper bound* on the effective number of neutrinos,

$$\Delta N_\nu < 0.11 \pm 0.24 \quad (N_\nu < 3.11 \pm 0.24). \tag{5.2}$$

If, instead, we had adopted the weighted mean of the Peimbert, Luridiana, & Peimbert (2007) helium abundances, we would have found $\Delta N_\nu < 0.24 \pm 0.33$ ($N_\nu = 3.24 \pm 0.33$). Just a few good H II region ^{4}He abundances are all that is needed to obtain a very strong constraint on N_ν. For these combinations of η_{10}(CMB) and N_ν, the bounds to the D and ^{3}He abundances are consistent with the data, while lithium remains a problem.

6. Challenges

In answer to the first question posed in §1, yes, SBBN ($N_\nu = 3$) is consistent with the observationally-inferred primordial abundances of D, ^{3}He, and ^{4}He, but ^{7}Li poses a problem. The answer to the second question posed in §1 is also yes, the CMB and the BBN values of η_B and S agree. SBBN and the CMB in combination allow, but also constrain, some models of non-standard physics. The challenges facing BBN, largely observational, makes the timing of this meeting ideal. Having had the luxury of being one of the first speakers, I will end by presenting my list of challenges to those who follow.

1. Why is the spread in the observed deuterium abundances so large?
2. Why are the observed ^{3}He abundances uncorrelated with either the oxygen abundances or with the distance from the center of the Galaxy?
3. What are the sources (and the magnitudes) of the systematic errors in Y_P and, are there observing strategies to reduce them?
4. What is the primordial abundance of ^{7}Li (and of ^{6}Li)?

References

Aoki, W. *et al.* (2009), *ApJ*, 698, 1803.
Asplund, M., *et al.* 2006, *ApJ*, 644, 229.
Bania, T.M., Rood, R.T., & Balser, D.S. 2002, *Nature*, 415, 54.
Boesgaard, A.M., Stephens, A., & Deliyannis, C.P. 2005, *ApJ*, 633, 398.
Dunkley, J., *et al.* 2009, *ApJS*, 180, 306.
Epstein, R. I., Lattimer, J. M., & Schramm, D. N. 1976, *Nature*, 265, 219.
Geiss, J. & Gloeckler, J.G. 1998, *Space Sci. Rev.* 84, 239.
Kneller, J.P. & Steigman, G. 2004, *New J. Phys.*, 6, 117.
Lind, K., *et al.* 2009, *A&A*,503, 545.
Olive, K. A. & Skillman, E. D. 2004, *ApJ*, 617, 29
Peimbert, M., Luridiana, V. & Peimbert, A. 2007, *ApJ*, 666, 634
Pettini, M., Zych, B.J., Murphy, M.T., Lewis, A., & Steidel, C.C. 2008, *MNRAS*, 391, 1499.
Reeves, H., Audouze, J., Fowler, W. A., & Schramm, D. N. 1973, *ApJ*, 179, 909.
Rood, R.T. 1972, *ApJ*, 177, 681.
Rood, R.T., Steigman, G., & Tinsley, B.M. 1976, *ApJL*, 207, L57.
Steigman, G. 2006, *JCAP*, 10, 016.
Steigman, G. 2007, *Ann. Rev. Nucl. Part. Sci.*, 57, 463.

Light elements in the Universe
Proceedings IAU Symposium No. 268, 2010
C. Charbonnel, M. Tosi, F. Primas & C. Chiappini, eds.

DOI: 00.0000/X000000000000000X

The cosmic lithium problem and physics beyond the Standard Model

Karsten Jedamzik

Laboratoire de Physique Théorique et Astroparticules, Université Montpellier II, place Eugne Bataillon 34095 Montpellier, FRANCE
email: jedamzik@lpta.univ-montp2.fr

Abstract. In this proceeding I briefly discuss the possibility of relic decaying or annihilating particles to explain the cosmological ^{7}Li anomaly and/or to be the source of significant amounts of pre-galactic ^{6}Li. The effect of relic massive charged particles through catalysis of nuclear reactions is also discussed. The possibility of a connection of the ^{7}Li problem to the cosmic dark matter and physics beyond the standard model of particle physics, such as supersymmetry, is noted.

Keywords. Cosmology: theory, early universe, cosmological parameters

---

The standard scenario of Big Bang nucleosynthesis (BBN), with its minimalistic assumptions about the composition and state of the Universe at around one second, predicts light-element abundances generally in approximate agreement with those observed. However, after an independent precise observational determination of the baryon density through observations of the cosmic microwave background radiation by the WMAP satellite, a significant discrepancy between the predicted and observationally inferred ^{7}Li/H ratio has emerged (Cyburt et al. 2008). This discrepancy may not be due to seriously underestimated stellar surface temperatures and only very unlikely due to nuclear reaction rate uncertainties (Cyburt & Pospelov 2009). The mismatch may, however, be due to ^{7}Li depletion in low-metallicity halo stars (Richard et al. 2005, Korn et al. 2006), though the

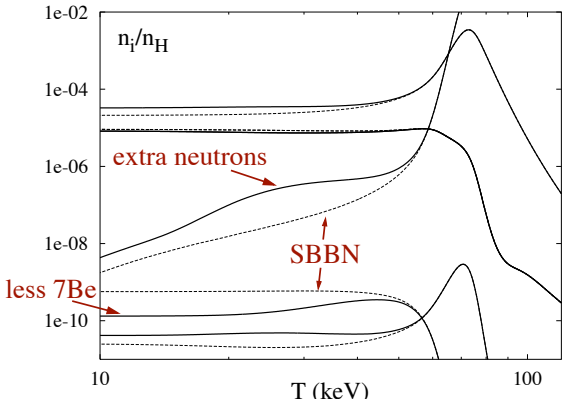

Figure 1. Evolution of light element abundances during BBN in a standard BBN scenario (solid) and in a BBN scenario with $\sim 10^{-5}$ additional neutrons/baryon injected at time $\tau \approx 1000$ sec (dashed). From top to bottom (at low temperatures), the lines show ^{2}H/H, ^{3}He/H, n/p, ^{7}Be/H, and ^{7}Li/H, respectively. Figure taken from **?**.

details of such depletion remain uncertain. Alternatively, the discrepancy may be due to physics operating during the BBN epoch itself. Such non-standard BBN scenarios also often lead to the production of considerable amounts of ^{6}Li. Interestingly, the existence of substantial ^{6}Li in low-metallicity stars has been claimed (Asplund et al. 2006), though due to the difficulty of these observations is currently controversial (Cayrel et al. 2007). A brief summary of BBN scenarios leading to a reduction of ^{7}Li and the production of ^{6}Li will be the main subject of this note.

^{7}Li is only produced in trace amounts during BBN the main reason being that its synthesis requires the presence of ^{4}He and by the time that neutrons are incorporated into ^{4}He the Coulomb barriers for the two main ^{7}Li producing reactions, i.e ^{3}H $+^4$He $\rightarrow^7$Li$+\gamma$ and ^{3}He $+^4$He$\rightarrow^7$Be$+\gamma$ are already substantial. Production of ^{6}Li in standard BBN is even further supressed compared to ^{7}Li by an additional factor $\sim 10^{-4}$ due to the weakness of the quadrupole reaction ^{2}H $+^4$He $\rightarrow^6$Li$+\gamma$. Most alternative BBN scenarios, such as inhomogeneous or with antimatter domains or with lepton chemical potentials, etc., do not lead to a reduction of the ^{7}Li abundance, rather usually the opposite happens. Attempting to reduce the ^{7}Li by later photodisintegration is highly problematic (Ellis et al. 2005) due to the concommitant ^{2}H photo-disintegration or ^{3}He/^{2}H overproduction due to ^{4}He photodisintegration. One known way of reducing ^{7}Li is by the assumption of varying fundamental constants, since ^{7}Li production is very sensitive to the ^{2}H and ^{7}Be binding energies (Dmitriev et al. 2004). It is nevertheless very difficult to test for such a hypothesis by other means.

There exists, however, a very simple way of reducing the ^{7}Li yield (Jedamzik 2004a). At a baryon-to-photon ratio of $\eta \approx 6.2 \times 10^{-10}$ around 90% of all ^{7}Li is synthesized in form of ^{7}Be which after BBN electron captures to form ^{7}Li. In case this ^{7}Be is converted prematurely, already during BBN, to ^{7}Li, the resultant ^{7}Li will be destroyed by the reaction ^{7}Li$+p \rightarrow^4$He $+ ^4$He. The main reaction which converts ^{7}Be to ^{7}Li is ^{7}Be$+n \rightarrow^7$Li$+p$. The efficiency of such conversion depends on the ambient neutron density. Due to the large cross section for this reaction already a minute amount of extra neutrons $n/p \sim 10^{-5}$ injected at temperature $T \approx 30\,$keV may severely deplete the ^{7}Li. This is seen in Fig.1

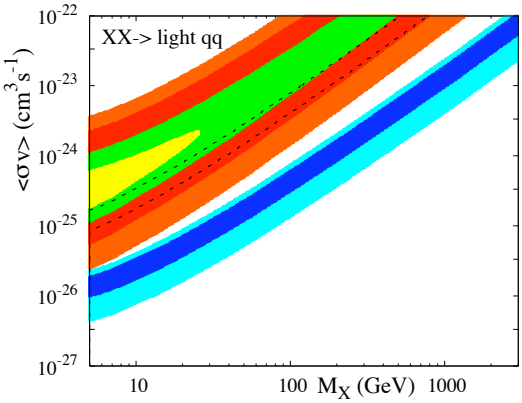

Figure 2. Dark matter annihilation rate versus dark matter mass. The blue band shows parameters where ^{6}Li due to residual dark matter annihilation may account for the ^{6}Li abundance as inferred in HD84937 (^{6}Li/^{7}Li$\approx 0.014 - 0.09$ at 2-σ), whereas the orange-red-green-yellow region shows where ^{7}Li is efficiently destroyed (e.g. green band - ^{7}Li/H$< 2 \times 10^{-10}$). From **?**.

where the evolution of abundance yields of such a model with extra neutron injection is compared to standard BBN. Such neutron injection also leads to some additional ^{2}H.

^{6}Li is a sensitive probe of non-standard BBN scenarios and the evolution of the early Universe (Jedamzik 2000), since in a large number of non-standard scenarios, already small deviations from standard BBN (SBBN) lead to ^{6}Li synthesis beyond that in SBBN. All scenarios which include the injection of energetic hadrons or photons into the plasma, lead to either photodisintegration of ^{4}He or nuclear spallation of ^{4}He. The resultant energetic ^{3}H and ^{3}He nuclei may participate in the non-thermal nuclear reaction ^{3}H (^{3}He) + ^{4}He$\rightarrow$ ^{6}Li + n (p) (Dimopulos et al. 1988) to form ^{6}Li. Note that these reactions are not available to thermal BBN, due to the existence of energy thresholds.

When searching for scenarios which may lead to an injection of extra neutrons during BBN to solve the ^{7}Li problem, one immediate idea is the possibility of residual annihilation of cosmological particle dark matter during BBN (Jedamzik 2004b). It is well know that the correct cosmological dark matter density results when assuming a thermal freeze-out from equilibrium of a self-annihilating stable particle (e.g. a supersymmetric neutralino) with annihilation rate $< \sigma v > \approx 3 \times 10^{-26}$cm^{3}s^{-1}. Since such annihilation rates are typical for weak mass scale particles, an attractive possibility for the cosmological dark matter is a new stable particle of mass $m_\chi \sim 100\,$GeV, potentially to be discovered at the LHC. Such particles would also be present during BBN with residual annihilations taking place. Since in many extensions of the standard model their annihilation products are quarks, the concommitant formation of baryons and anti-baryons would lead to the injection of extra neutrons. In Fig.2 the parameter space in the annihilation rate $< \sigma v >$ and particle mass m_χ is shown where annihilations significantly affect the ^{6}Li and ^{7}Li abundances. It is seen, however, that residual dark matter annihilation can only solve the ^{7}Li problem (the orange-red-green band) at the expense of overproducing ^{6}Li (the blue band). Annihilations are therefore most likely not at the heart of the ^{7}Li problem. However, it is intruiging that a dark matter particle of $m_\chi \sim 20 - 80\,$GeV annihilating into quarks at the required rate for the dark matter density may produce *all* the ^{6}Li as claimed to exist in the star HD84937. Note, that this already includes a

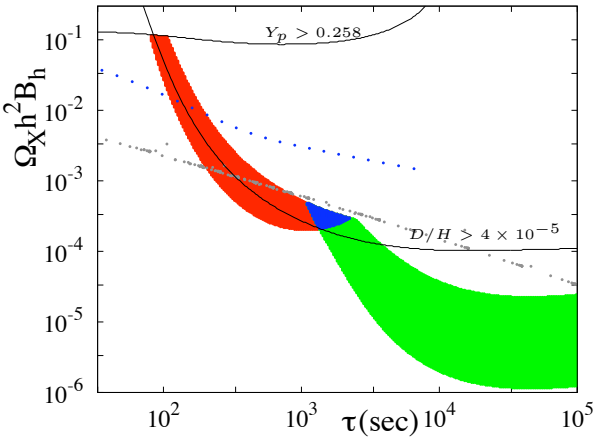

Figure 3. Parameter space in the relic decaying particle abundance times hadronic branching ratio B_h, i.e. $\Omega_X h^2 B_h$, and life time τ_X plane, where ^{7}Li is significantly reduced (red and blue) and ^{6}Li is efficiently produced (green and blue). See text for further details. From **?**.

factor ~ 3 stellar depletion of ^{7}Li (and ^{6}Li) to solve the ^{7}Li problem. Here it has been assumed that both isotopes are depleted by the same amount.

Whereas dark matter annihilation can not solve the ^{7}Li problem, the decay of metastable particles during BBN can. This may be seen in Fig.3, which shows the parameter space in the $\Omega_X B_h$ and τ_X plane for which the ^{7}Li problem may be solved and/or significant ^{6}Li is synthesized. Here Ω_X would be the contribution of the X-particle to the present critical density if it wouldn't have decayed. It is seen that for decay times $\tau_X \sim 100 - 2000\,$sec the ^{7}Li abundance may be significantly reduced due to the injection of extra neutrons from the decay. For larger $\tau_X \gtrsim 10^3$sec large amounts, i.e. ^{6}Li/^{7}Li$\approx 0.015 - 0.3$, of ^{6}Li are synthesized. At $\tau_X \approx 10^3$, both, ^{7}Li and ^{6}Li, are in agreement with observations. In this area, additional ^{2}H production results as well.

It has been recently realized that significant amounts of ^{6}Li may also result simply due to the presence of negatively charged weak mass scale particles during BBN (Pospelov 2007). This is due to such particles entering into bound states with nuclei and thereby leading to catalysis of nuclear reactions. The most important of these reactions is (^{4}He-X^-)+^{2}H$\rightarrow^6$Li + X^-. Nevertheless, though interesting in its physics, and having received wide-spread attention, concerning ^{6}Li production, catalysis is only more important that the ^{6}Li production due to hadronic decay products, when the particle has a hadronic branching ratio smaller than $B_h \lesssim 10^{-2}$. Though this may occur (e.g. the supersymmetric partner of the stau lepton) it is often not the case. Catalysis may not present the solution to the ^{7}Li problem (Bird et al. 2007, Kanimura et al. 2009), unless the hadronic branching ratio of the charged weak mass scale particles is very small $B_h \lesssim 10^{-5}$ and its abundance is very large, i.e. $\Omega_X \gtrsim 10$. However, though currently not certain, catalysis could lead to the formation of ^{9}Be in BBN (Pospelov 2008), something impossible to achieve with neutral decaying particles.

In summary, the decay of metastable relic particles during BBN may easily reduce the standard BBN predicted ^{7}Li/H$\sim 5 \times 10^{-10}$ to its observationally inferred value ^{7}Li/H$\sim 1 - 2 \times 10^{-10}$. When such decays occur around $\gtrsim 10^3$ seconds they are also associated with considerable ^{6}Li production. In contrast, residual annihilation of dark matter during BBN may account for all the ^{6}Li as claimed to exist in the star HD84937, but not solve the ^{7}Li problem without significant ^{6}Li overproduction. Catalysis of nuclear reactions due to electrically charged weak scale particles may lead to additional ^{6}Li, potentially produce ^{9}Be, but only very unlikely has impact on the cosmological ^{7}Li problem. It is the hope that many of these scenarios are testable at the LHC accelerator, either in form of production of light dark matter particles (e.g. a supersymmetric neutralinos) or metastable particles being stopped and decaying in the detector (e.g. a supersymmetric staus or gluinos). However, some particularly attractive scenarios are unfortunately not reachable in energy at the LHC (**?**).

References

Asplund, M., Lambert, D. L.,Nissen, P. E., Primas, F., and Smith, V. V., 2006, *ApJ*, 644, 229
Bailly, S., Jedamzik , K., and Moultaka, G., 2009, *Phys. Rev. D*, 80, 63509
Bird, C., Koopmans, K., and Pospelov, M., 2008, *Phys. Rev. D*, 78, 83010
Cayrel, R. *et al.*, 2007, arXiv:0708.3819
Cyburt, R. H., Fields, B. D., and Olive, K. A., 2008 *JCAP*, 811, 12
Cyburt, R. H. and Pospelov, M., 2009, arXiv:0906.4373
Dimopoulos, S., Esmailzadeh, R., Hall, L. J., and G. D. Starkman, G. D., 1988, *ApJ*, 330, 545
Dmitriev, V. F., Flambaum, V. V., and Webb, J. K., 2004 *Phys. Rev. D*, 69, 63506
Ellis, J. R., Olive, K. A., and Vangioni, E., 2005 *Phys.Lett. B*, 619, 30

Jedamzik, K., 2000, *Phys.Rev. Lett.*, 84, 3248
Jedamzik, K., 2004, *Phys.Rev. D*, 70, 63524
Jedamzik, K., 2004, *Phys.Rev. D*, 70, 83510
Jedamzik, K., Choi, K. Y., Roszkowski. L., and Ruiz de Austri, R., 2006, *JCAP*, 607, 7
Jedamzik, K. and Pospelov, M., 2009 *New J. Phys.*, 11, 105028
Kamimura, M., Kino, Y., and Hiyama, E., 2009, *Prog. Theor. Phys.*, 121, 1059
Korn , A. J. et al., 2006, *Nature* 442, 657
Pospelov, M., 2007, *Phys. Rev. Lett.*, 98, 231301
Pospelov, M., 2007, arXiv:0712.0647
Richard, O., Michaud, G., and Richer, J., 2005 *ApJ*, 619, 538

Guillaume Hébrard

Motohiko Kusakabe

Light elements in the Universe
Proceedings IAU Symposium No. 268, 2010
C. Charbonnel, M. Tosi, F. Primas & C. Chiappini, eds.

DOI: 00.0000/X000000000000000X

Big Bang nucleosynthesis with long-lived strongly interacting relic particles

Motohiko Kusakabe[1]†, Toshitaka Kajino[2,3,4], Takashi Yoshida[2] and Grant J. Mathews[5]

[1]Institute for Cosmic Ray Research, University of Tokyo, Kashiwa, Chiba 277-8582, Japan
email: kusakabe@icrr.u-tokyo.ac.jp

[2]Department of Astronomy, Graduate School of Science, University of Tokyo, Bunkyo-ku, Tokyo 113-0033, Japan

[3]Division of Theoretical Astronomy, National Astronomical Observatory of Japan, Mitaka, Tokyo 181-8588, Japan

[4]Department of Astronomical Science, The Graduate University for Advanced Studies, Mitaka, Tokyo 181-8588, Japan

[5]Department of Physics, Center for Astrophysics, University of Notre Dame, Notre Dame, IN 46556, USA

Abstract. We study effects of relic long-lived strongly interacting massive particles (X particles) on big bang nucleosynthesis (BBN). The X particle is assumed to have existed during the BBN epoch, but decayed long before detected. The interaction strength between an X and a nucleon is assumed to be similar to that between nucleons. Rates of nuclear reactions and beta decay of X-nuclei are calculated, and the BBN in the presence of neutral charged X^0 particles is calculated taking account of captures of X^0 by nuclei. As a result, the X^0 particles form bound states with normal nuclei during a relatively early epoch of BBN leading to the production of heavy elements. Constraints on the abundance of X^0 are derived from observations of primordial light element abundances. Particle models which predict long-lived colored particles with lifetimes longer than ~ 200 s are rejected. This scenario prefers the production of ^{9}Be and ^{10}B. There might, therefore, remain a signature of the X particle on primordial abundances of those elements. Possible signatures left on light element abundances expected in four different models are summarized.

Keywords. elementary particles; nuclear reactions; nucleosynthesis; abundances; stars: abundances; cosmology: early universe

1. Introduction

Primordial lithium abundances are inferred from measurements in metal-poor stars (MPSs). Observed abundances are roughly constant as a function of metallicity (Spite & Spite 1982, Ryan et al. 2000, Meléndez & Ramírez 2004, Asplund et al. 2006, Bonifacio et al. 2007, Shi et al. 2007, Aoki et al. 2009) at ^{7}Li/H$= (1-2)\times 10^{-10}$. The theoretical prediction by the standard big bang nucleosynthesis (BBN) model, however, is a factor of $2-4$ higher when its parameter, the baryon-to-photon ratio, is fixed to the value deduced from the observation with Wilkinson Microwave Anisotropy Probe of the cosmic microwave background (CMB) radiation (Dunkley et al. 2009). A recent study including a reevaluation of nuclear reaction rate of ^{3}He$(\alpha,\gamma)^7$Be shows the standard BBN (SBBN) prediction of ^{7}Li/H$=(5.24^{+0.71}_{-0.67})\times 10^{-10}$ (Cyburt et al. 2008). The discrepancy indicates some mechanism of ^{7}Li reduction having operated in some epoch from the BBN to this day. One possible astrophysical process to reduce ^{7}Li abundances in stellar surfaces is the combination of the atomic and turbulent diffusion (Richard et al. 2005, Korn et al. 2006,

† Research Fellow of the Japan Society for the Promotion of Science (JSPS).

2007). The precise trend of Li abundance as a function of effective temperature found in the metal-poor globular cluster NGC 6397 is, however, not reproduced yet (Lind et al. 2009).

^{6}Li/^{7}Li isotopic ratios of MPSs have also been measured spectroscopically. A ^{6}Li abundance as high as $^6\mathrm{Li/H}\sim 6\times10^{-12}$ was suggested (Asplund et al. 2006), which is about 1000 times higher than the SBBN prediction. Convective motions in the atmospheres of MPSs could cause systematic asymmetries in the observed line profiles and mimic the presence of ^{6}Li (Cayrel et al. 2007). Nevertheless, there still remain a few or several MPSs with certain detections of high ^{6}Li abundances after estimations of convection-triggered line asymmetries (García Pérez et al. 2009, Steffen et al. 2009). This high ^{6}Li abundance is a problem since the standard Galactic cosmic ray (CR) nucleosynthesis models predict negligible amounts of ^{6}Li yields compared to the observed level in the epoch corresponding to the metallicity of $[\mathrm{Fe/H}] < -2$ (Prantzos 2006).

Be and B abundances are also observed in MPSs. ^{9}Be abundances increase linearly as iron abundance when the Galaxy evolves chemically (Boesgaard et al. 1999, Primas et al. 2000a, Tan et al. 2009, Smiljanic et al. 2009, Ito et al. 2009, Rich & Boesgaard 2009). In a region of very low metallicities of $[\mathrm{Fe/H}]< -3$, a dispersion in Be abundances is indicated (Primas et al. 2000b, Boesgaard & Novicki 2006). B abundances increase linearly as iron abundance (Duncan et al. 1997, Garcia Lopez et al. 1998, Primas et al. 1999, Cunha et al. 2000). So far no primordial plateau abundances of Be and B are found.

As a cosmological solution to the Li problems, BBN models including exotic decaying particles have been studied (see contribution by Jedamzik, this volume). Nonthermal nuclear reactions triggered by the radiative decay of long-lived particles can produce ^{6}Li nuclides in amounts greater than observed in MPSs and at most ~ 10 times as much as the level without causing discrepancies in abundances of other light elements or the CMB energy spectrum (Kusakabe et al. 2006, 2009a). If negatively-charged leptonic X^- particles exist in the BBN epoch, they affect the nucleosynthesis (see contribution by Jedamzik, this volume). The X^- particles get bound to positively charged nuclides with binding energies of $\sim O(0.1-1)$ MeV. Since the binding energies are low, the bound states between the X^- and nuclides form late in BBN epoch. Nuclear reactions at this temperature are no longer efficient so that the effect of negatively-charged particles is rather small. Interestingly the X^- particle can catalyze a preferential production of ^{6}Li (Pospelov 2007) and weak destruction of ^{7}Be (Bird et al. 2008, Kusakabe et al. 2007). Non-equilibrium nuclear network calculation of this model (Kusakabe et al. 2008) with realistic cross sections derived from a quantum mechanical calculation (Kamimura et al. 2009) shows that ^{6}Li production and ^{7}Li reduction can simultaneously occur and that there are no likely signatures in primordial abundances of Be and heavier nuclei.

As an astrophysical solution to the ^{6}Li problem, the cosmological CR nucleosynthesis associated with a possible activity of supernova explosions in the early epoch of structure formation has been suggested (Rollinde et al. 2005, 2006). This ^{6}Li production mechanism is likely realized with coproduction of ^{9}Be and ^{10,11}B nuclides in abundances probably within reach of future observations of MPSs (Kusakabe 2008, Rollinde et al. 2008). The ^{6}Li production is, however, not a certain possibility since a calculation in a similar scenario but using a different star formation and chemical evolution history fails to reproduce the ^{6}Li plateau level (Evoli et al. 2008).

In this paper we show a new BBN scenario which includes long-lived strongly interacting relic particles which appear in some particle models beyond the standard. Constraints on their abundance and lifetime is derived. Signatures of such relic particles are found to be possibly left on the primordial abundances of Be and B. A theoretical prediction of primordial light element abundances are given in the limit of long lifetime.

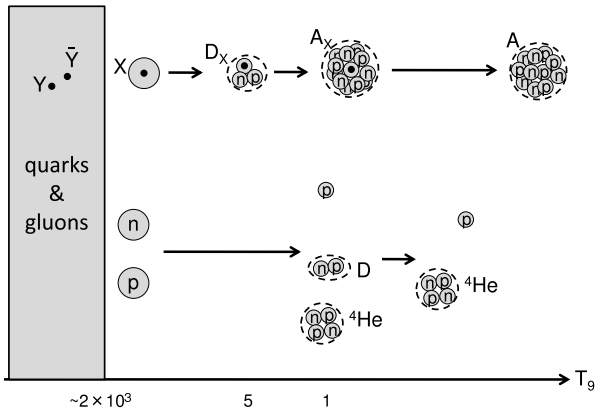

Figure 1. Nucleosynthesis in the presence of the long-lived strongly interacting X particle.

2. Model

Some particle models include long-lived heavy colored particles, denoted by Y (Kang et al. 2008). If the hypothetical colored particle Y exists, they would have experienced production and annihilation in the early universe. When the temperature of the universe decreases to $T < 180$ MeV, Y gets confined in exotic hadrons, which we call X (see Fig.1). Two X particles can form bound states and the bound states decay into lower energy states gradually. Y particles in X particles could annihilate eventually when two X particles approach. Taking account of this process, Kang et al.(2008) estimated the relic abundance of X to be $n_X \sim 10^{-8} n_b$, where n_X and n_b are number densities of X and baryon, respectively. If the strongly interacting X particle had existed in BBN epoch, it would have affected the nucleosynthesis. We study effects of X on BBN. The X particle is assumed to be of spin 0, charge 0 and mass much larger than nuclear mass of $O(1$ GeV). The strength of interaction between an X^0 particle and nuclei is supposed to be similar to that between a nucleon and the nuclei as a rough approximation.

Binding energies between nuclides and an X^0 are calculated. The adopted nuclear potential between a nucleon and an X is well reproducing the binding energy of n+p system when used for the n+p system. The Woods-Saxon potential is adopted for systems of nuclides and an X. Two-body Shrödinger equations are solved by a variational calculation, and binding energies are derived. The binding energies are of $O(10$ MeV), and this strong binding leads to bound state formations early in the BBN epoch.

Thermonuclear reaction rates and β-decay rates of X-bound nuclei (i.e., X-nuclei or A_X) are, then, calculated. Reaction Q-values are derived taking account of binding energies of X-nuclei. The rates associated with X-nuclei are estimated using available cross sections for normal nuclei by correcting for Q-values and mass numbers of reactants.

We have put radiative X capture reactions by nuclides, nuclear reactions and β-decay of X-nuclides and all inverse reactions into the SBBN network code (Kawano 1992) and solved a set of rate equations. See Kusakabe et al.(2009b) for details on this study.

3. Result

Figure 1 shows a schematic view of nucleosynthesis as a function of $T_9 \equiv T/(10^9$ K) with temperature T. The relic abundance of X would be rather small ($Y_X = n_X/n_b \sim 10^{-8}$) although it depends on the mass and interaction strength of the exotic colored

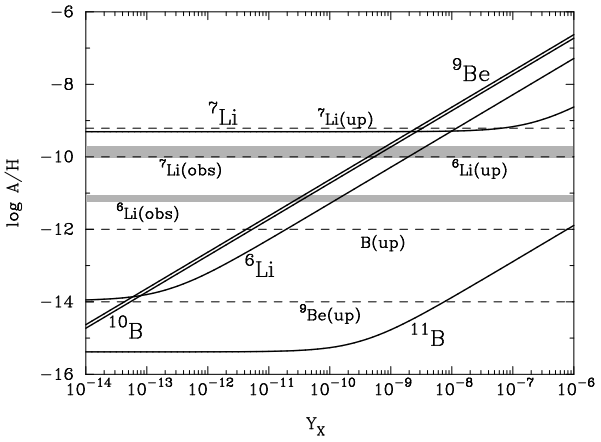

Figure 2. Calculated abundances of ^{6,7}Li, ^{9}Be and ^{10,11}B (solid lines) as a function of the X abundance Y_X. The grey bands correspond to the observed mean values of ^{7}Li abundances and ^{6}Li abundances of MPSs with detection of the isotope. The dashed lines indicate the adopted upper limits on the primordial abundances (see text).

Y particle. The main story of BBN, therefore, does not change even if the strongly interacting X particle exists. Effects on abundant light elements, i.e., H and He are small, while those on minor elements, i.e., Li, Be and B are significant. At high temperature of $T_9 > 5$, the X particles exist in the free state. When the temperature decreases to $T_9 \sim 5$, X particles radiatively capture neutrons and protons to form bound states. n_X and H_X thus formed are processed to $^{2}\mathrm{H}_X$ and $^{3}\mathrm{He}_X$. At $T_9 \sim 5$, the normal D abundance temporarily increases during the ^{4}He production. An efficient nuclear process of X-nuclei then occurs through consecutive nonradiative strong D-capture reactions, i.e., (d,p) and (d,n). Finally the X particles decay and heavy nuclides are left. From the fact that all X particles form X-nuclei before their decay, it can be seen that strongly interacting exotic particles have a great impact on BBN (Kusakabe et al. 2009b). One reason is that binding energies between an X and nuclides are large, and cross sections of captures of nucleons by X are large, leading to early formation of bound states between nucleons and an X. Another reason is that ^{5}He, ^{5}Li and ^{8}Be which are unstable to particle decays can be stabilized against the decays when they are bound to X particles, so that heavy X-nuclides can form through those stabilized states.

Figure 2 shows calculated abundances of ^{6,7}Li, ^{9}Be and ^{10,11}B (solid lines) as a function of the initial X abundance Y_X in the case of very long lifetime, τ_X, compared to the BBN time scale. Resulting yields through the X-catalyzed nucleosynthesis are all proportional to Y_X. The prediction of primordial abundances in this scenario is as follows:

$$^{6}\mathrm{Li/H} \sim^{9} \mathrm{Be/H} \sim^{10} \mathrm{B/H} \sim 10^{-9} \left(Y_X/10^{-8}\right). \tag{3.1}$$

$$^{7}\mathrm{Li/H} \sim 10^{-11} \left(Y_X/10^{-8}\right). \tag{3.2}$$

$$^{11}\mathrm{B/H} \sim 10^{-14} \left(Y_X/10^{-8}\right). \tag{3.3}$$

The grey bands correspond to the observed mean values of ^{7}Li abundances (Ryan et al. 2000) and ^{6}Li abundances of MPSs with detection of the isotope (Asplund et al. 2006). The dashed lines show the adopted upper limits on the primordial abundances from observations: $^{7}\mathrm{Li/H} < 5 \times 1.23 \times 10^{-10}$ allowing for large depletion factors of up to five, $^{6}\mathrm{Li/H} < 5 \times 10^{-10}$ allowing for depletion factors up to ~ 10, $^{9}\mathrm{Be/H} < 10^{-14}$ (Ito et al.

Table 1. Possibility to solve the Li problems and expected signatures in elemental abundances.

Model	^{6}Li Problem solved ?	^{7}Li Problem solved ?	Possible Signatures on Other Nuclides
radiative decay	**YES**	NO	NO
leptonic X^-	**YES**	**YES**	**NO**
strongly interacting X^0	**NO**	**NO**	**^{9}Be and/or ^{10}B**
early cosmic ray	**YES**	NO	**^{9}Be and ^{10,11}B**

2009) and B/H$< 10^{-12}$ (Garcia Lopez et al. 1998). Y_X values leading to overproductions of light nuclides in abundances above the observational upper limits should be ruled out. The upper limits on the primordial Be abundance is found to give the most stringent constraint on X abundance, i.e., $Y_X < 10^{-13}$ in the case of long lifetime.

When the lifetime τ_X is not much longer than the BBN time scale, the decay of X should be considered in the numerical calculation. A constraint on the initial abundance Y_X and the lifetime τ_X is derived (Kusakabe et al. 2009b). A solution to the ^{6}Li or ^{7}Li problems was not found in this paradigm. As seen in Fig.2, the light element abundances monotonically increase by the existence of X. A reduction of ^{7}Li abundance is thus NOT possible. The ^{6}Li production is realized with overproduction of ^{9}Be and ^{10}B, which is excluded from observations of Be and B. A ^{6}Li production is then NOT possible.

Constraints on the Y_X and τ_X are derived from limits on Li, Be, B abundances depending on lifetime ranges. Two important predictions of this scenario are found. First, ^{9}Be and B can be produced in amounts more than SBBN predictions. Future observations of Be and B abundances in MPSs might show plateaus suggesting a primordial origin. Second, ^{10}B tends to be produced much more than ^{11}B, i.e., a resulting isotopic ratio ^{10}B/^{11}B is very high (see Fig.2). This preferential production of ^{10}B has never been predicted in other models of Be production like the Galactic or cosmological CR nucleosynthesis (^{10}B/^{11}B$\sim$ 0.4: e.g., Ramaty et al. 1997, Kusakabe 2008) or the supernova neutrino process (^{10}B/^{11}B$\ll$ 1: e.g., Woosley & Weaver 1995, Yoshida et al. 2005).

A constraint on τ_X is derived from this result and estimations of initial abundance of X. If $Y_X \sim 10^{-8}$ (Kang et al. 2008) is adopted, its lifetime should be $\tau_X < 200$ s.

4. Summary

The BBN scenario in the presence of long-lived strongly interacting relic particle X is described. Particles which interact with nuclei as a nucleon do capture nucleons to form X-nuclei in an early stage of BBN. The X-nuclei capture deuterons and increase their mass numbers. This nuclear catalysis of X activates new reaction paths to heavy nuclei. Constraints on the lifetime and abundance of X are derived. The lifetime should be less than 200 s.

Table 1 summarizes possibilities for four models to be solutions to the ^{6}Li or ^{7}Li problems and expected signatures in abundances of other light nuclides. In light of all available observational data, nonstandard BBN processes (first two models) possibly operate to produce ^{6}Li and/or reduce ^{7}Li. The existence of long-lived relic particles should be ascertained with future astronomical observations and collider experiments. The cosmological CR nucleosynthesis might also have produced light elements in an early epoch of the structure formation. Observations of primordial abundances of Li, Be and B are very important to constrain the possible processes in the early universe.

Acknowledgements

This work was supported by the Mitsubishi Foundation, the MEXT KAKENHI (20105004, 20244035), the JSPS Core-to-Core Program EFES, and the Grant-in-Aid for JSPS Fellows (21.6817). Work at the University of Notre Dame was supported by the U.S. Department of Energy under Nuclear Theory Grant DE-FG02-95-ER40934.

References

Aoki, W., et al. 2009, *ApJ*, 698, 1803
Asplund, M., et al. 2006, *ApJ*, 644, 229
Bird, C., Koopmans, K., & Pospelov, M. 2008, *Phys. Rev. D*, 78, 083010
Boesgaard, A. M., et al. 1999, *AJ*, 117, 1549
Boesgaard, A. M., & Novicki, M. C. 2006, *ApJ*, 641, 1122
Bonifacio, P., et al. 2007, *A&A*, 462, 851
Cayrel, R., et al. 2007, *A&A*, 473, L37
Cunha, K., Smith, V. V., Boesgaard, A. M., Lambert, D. L. 2000, *ApJ*, 530, 939
Cyburt, R. H., Fields, B. D., & Olive, K. A. 2008, *J. Cosmol. Astropart. Phys.*, 11, 12
Duncan, D. K., et al. 1997, *ApJ*, 488, 338
Dunkley, J., et al. 2009, *ApJS*, 180, 306
Evoli, C., Salvadori, S., & Ferrara, A. 2008, *MNRAS*, 390, L14
Garcia Lopez, R. J., et al. 1998, *ApJ*, 500, 241
García Pérez, A. E., et al. 2009, *A&A*, 504, 213
Ito, H., Aoki, W., Honda, S., Beers, T. C. 2009, *ApJ* (Letters), 698, L37
Kamimura, M., Kino, Y., & Hiyama, E. 2009, *Progress of Theoretical Physics*, 121, 1059
Kang, J., Luty, M. A., & Nasri, S. 2008, *J. High Energy Phys.*, 9, 86
Kawano, L. 1992, *NASA STI/Recon Technical Report N*, 92, 25163
Korn, A. J., et al. 2006, *Nature*, 442, 657; 2007, *ApJ*, 671, 402
Kusakabe, M., Kajino, T., & Mathews, G. J. 2006, *Phys. Rev. D*, 74, 023526
Kusakabe, M., et al. 2007, *Phys. Rev. D*, 76, 121302
Kusakabe, M., et al. 2008, *ApJ*, 680, 846
Kusakabe, M. 2008, *ApJ*, 681, 18
Kusakabe, M., et al. 2009a, *Phys. Rev. D*, 79, 123513
Kusakabe, M., Kajino, T., Yoshida, T., Mathews, G. J. 2009b, *Phys. Rev. D*, 80, 103501
Lind, K., et al. 2009, *A&A*, 503, 545
Meléndez, J., & Ramírez, I. 2004, *ApJ* (Letters), 615, L33
Pospelov, M. 2007, *Phys. Rev. Lett.*, 98, 231301
Prantzos, N. 2006, *A&A*, 448, 665
Primas, F., Duncan, D. K., Peterson, R. C., Thorburn, J. A. 1999, *A&A*, 343, 545
Primas, F., Molaro, P., Bonifacio, P., Hill, V. 2000, *A&A*, 362, 666
Primas, F., Asplund, M., Nissen, P. E., Hill, V. 2000, *A&A*, 364, L42
Ramaty, R., Kozlovsky, B., Lingenfelter, R. E., Reeves, H. 1997, *ApJ*, 488, 730
Rich, J. A., & Boesgaard, A. M. 2009, *ApJ*, 701, 1519
Richard, O., Michaud, G., & Richer, J. 2005, *ApJ*, 619, 538
Rollinde, E., Vangioni, E., & Olive, K. 2005, *ApJ*, 627, 666; 2006, *ApJ*, 651, 658
Rollinde, E., et al. 2008, *ApJ*, 673, 676
Ryan, S. G., et al. 2000, *ApJ* (Letters), 530, L57
Shi, J. R., et al. 2007, *A&A*, 465, 587
Smiljanic, R., et al. 2009, *A&A*, 499, 103
Spite, F., & Spite, M. 1982, *A&A*, 115, 357
Steffen, M., et al. 2009, arXiv:0910.5917
Tan, K. F., Shi, J. R., & Zhao, G. 2009, *MNRAS*, 392, 205
Woosley, S. E., & Weaver, T. A. 1995, *ApJS*, 101, 181
Yoshida, T., Kajino, T., & Hartmann, D. H. 2005, *Phys. Rev. Lett.*, 94, 231101

Light elements in the Universe
Proceedings IAU Symposium No. 268, 2010
C. Charbonnel, M. Tosi, F. Primas & C. Chiappini, eds.

DOI: 00.0000/X000000000000000X

Primordial nucleosynthesis in higher dimensional cosmology

S. Chatterjee

Relativity and Cosmology Research Centre, Jadavpur University, Kolkata - 700032, India, and also at IGNOU, New Alipore College, Kolkata 700053 email: chat_ sujit1@yahoo.com

Abstract. We investigate nucleosynthesis and element formation in the early universe in the framework of higher dimensional cosmology. We find that temperature decays less rapidly in higher dimensional cosmology, which we believe may have nontrivial consequences *vis-a-vis* primordial physics.

Keywords. Cosmology: theory, cosmological parameters, early universe

1. The element formation

The work is primarily motivated by the consideration that both light element formation and higher dimensional cosmology are particularly relevant in the context of early universe.

From Einstein's field equations generalised to $(n+2)$dim. (Chatterjee & Bhui 1990) we get the following equations as

$$\frac{n(n+1)}{2}\frac{\dot{R}^2+k}{R^2}=\rho \tag{1.1}$$

$$-\frac{n\ddot{R}}{R}-\frac{n(n-1)}{2}\frac{\dot{R}^2+k}{R^2}=p \tag{1.2}$$

where ρ and p are the homogeneous mass density and pressure respectively. In the early universe one takes the radiation dominated case as our equation of state such that for a (n+2) dim. universe, $p=\frac{\rho}{n-1}$. One of the phenomenal successes favoring big bang cosmology is the almost correct prediction of the primeval nucleosynthesis, particularly the observed abundances of the light nuclei in the current universe.Now it can be shown via the field equations(1) and (2) that for the radiation dominated case we get

$$\rho=\frac{2n(n+1)}{(n+2)^2}(\frac{1}{t^2}) \tag{1.3}$$

Assuming absence of any dissipative mechanisms (for example, viscosity, friction etc.) and also that the laws of thermodynamics are valid in the early universe also with such huge temperature one gets from elementary thermodynamical considerations (Alvarez & Gavela 1983) that

$$\rho=\sigma T_{rad}^{n+2} \tag{1.4}$$

where σ is the higher dimensional Steffan's constant, hence it follows that

$$T_{rad}=\frac{2n(n+1}{(n+2)^2\sigma}t^{-\frac{2}{n+2}} \tag{1.5}$$

where T_{rad} is the temperature of radiation and 't' is the age of the universe. For the usual

4D spacetime it reduces to the well known relation $T_{kelvin} = 1.52 \times 10^{10} t^{-1/2}$ s. Equation (5) is the key equation for our attempt to investigate the effect of extra dimensions on the process of nucleosynthesis in early universe. We here study the situation when elementary particles have already materialized allowing us to take the low temperature approximation, $T << m_\mu c^2 = T_\mu$ for their distribution function. Here m_μ is the mass of a particular species. We here try to study the equilibrium condition for neutrinos with other species. As the reactions involving the neutrinos fall within the category of weak interactions and $T < T_\mu$ the cross section of a typical reaction is of the order of

$$A = f^2 h^{-4} (kT) \tag{1.6}$$

where f is the weak coupling constant. For simplicity it is further assumed that the constant A does not depend on the number of spatial dimensions. Moreover the number densities of the participating particles (say, muons) are, for (n+1) spatial dimensions, of the order of $(T/ch)^{n+1}$ and for reactions involving muons at low temperatures an exponential damping factor of $exp(-T/T_\mu)$ should also be considered. In the cosmological context one should also consider the rate of expansion of the background, which from equations (1) and (2) give

$$H^2 = \frac{\dot{R}^2}{R^2} \sim t^{-2} = T^{n+2} \tag{1.7}$$

Thus the ratio of the reaction rate to the expansion rate now becomes

$$\frac{Q}{H} \sim (\frac{T}{10^{10} K})^{\frac{n+4}{2}} exp(\frac{10^{12} K}{T}) \tag{1.8}$$

One recovers the familiar 4D form when $n = 2$. As the temperature falls below the critical level of $10^{10} K$, the exponential decays rapidly. One can at this stage call attention to a significant quantitative difference from the 4D case. From equations (5) and (8) it is tempting to suggest that as the temperature falls less rapidly in higher dimensional cosmology than the analogous 4D situation it takes relatively more time for the elementary particles to cool below the threshold temperature. More importantly the quotient $\frac{Q}{H}$ is more sensitive to temperature fluctuations in multidimensional universe. Thus Q is larger than H for $T > 10^{12}$ depending on the number of extra dimensions and in these temperature ranges the neutrinos would be in thermal equilibrium with the rest of the other species. As the temperature falls further below $10^{10} K$ both the terms in the rhs of equation(8) drop rapidly, which means that the reactions involving neutrinos run at a slower rate than compared to the expansion of the universe. This triggers the so called decoupling of the neutrinos from the rest of the other constituents of matter and as pointed earlier in the higher dimensional universe it takes relatively more time for this decoupling phase of the neutrinos to occur. However, the theoretical and observational consequences of this supposed time lag for the initiation of the decoupling era need to be worked out in more detail before any definite inferences could be drawn.

2. Acknowledgments

The financial support of UGC, New Delhi in the form of a MRP award is acknowledged.

References

Chatterjee, S., & Bhui B., 1990 *MNRAS*, 247, 57
Alvarez, E., & Gavela, M., 1983 *Phys.Rev.Lett.* 51, 931

Session II

Abundances of D, ^{3}He and ^{4}He:

Observations

Paolo Ventura

Gary Ferland

Light elements in the Universe
Proceedings IAU Symposium No. 268, 2010
C. Charbonnel, M. Tosi, F. Primas & C. Chiappini, eds.

DOI: 00.0000/X000000000000000X

Measurements of deuterium in the Milky Way

Kenneth Sembach[1]

[1]Space Telescope Science Institute
3700 San Martin Dr., Baltimore, Maryland, USA
email: sembach@stsci.edu

Abstract. In this article I review measurements of deuterium in the Milky Way.

Keywords. ISM: abundances, Galaxy: abundances, Galaxy: solar neighborhood

1. Introduction

The abundance of deuterium in galactic environments depends upon both the primordial abundance created during Big Bang nucleosynthesis and the subsequent chemical evolution of the gas as a function of time. The primordial abundance is inferred from measurements of the angular power spectrum of the cosmic microwave background with the *Wilkinson Microwave Anisotropy Probe* (Spergel et al. 2007; Dunkley et al. 2009) and from ground-based measurements of D I absorption in a small number of quasar absorption systems at redshifts $z > 2$ (see Kirkman et al. 2003; O'Meara et al. 2006; Pettini et al. 2008; and references therein). A review of the extragalactic measurements and theory is given by Steigman (2007), who adopts $(\mathrm{D/H})_p = (2.68 \pm^{0.27}_{0.25}) \times 10^{-5}$.

The deuterium nucleus has a binding energy of only ~ 2.2 MeV, and thus is easily destroyed in the following step of the proton-proton chain reaction occurring in the interiors of stars:

$$^{2}_{1}\mathrm{D} + \mathrm{p} \rightarrow {}^{3}_{2}\mathrm{He} + \gamma + 5.49 \text{ MeV}$$

This astration of deuterium leads to a net decrease in its abundance with time. Galactic chemical evolution models typically predict astration factors $f_D \sim 1.4 - 1.8$, leading to expected present-day values of $\mathrm{D/H} \sim (1.4 - 1.9) \times 10^{-5}$ (see Tosi et al. 1998; Steigman, Romano, & Tosi 2007; and references therein). These models incorporate estimates of the production of heavier elements (C, N, O, Fe, etc.), as well as varying degrees of interstellar mixing and infall of unprocessed material from outside the Galaxy. Most models assume the interstellar material is chemically homogeneous, a reasonable assumption for regions of 100-200 parsecs in size but perhaps less certain for larger volumes (see the discussion in Moos et al. 2002). In conjunction with such models, measurements of deuterium in the Milky Way can provide valuable insights into the efficiency of mixing and the role of infalling gas in the evolving interstellar medium. They can also provide some guidance on the possible explanations for the large scatter in D/H values observed at higher redshifts.

There are two primary means by which the deuterium abundance in the neutral interstellar medium can be estimated. The most common is measurement of the D I Lyman series absorption in the ultraviolet spectra of stars, which began with pioneering observations by the *Copernicus* satellite in the 1970s (Rogerson & York 1973; York & Rogerson 1976; Vidal-Madjar et al. 1977), followed by extensive work with the *Hubble Space Telescope (HST)* and the *Far Ultraviolet Spectroscopic Explorer (FUSE)* (see Linsky et al. 2006 for a relatively recent review). Observations with these latter facilities

have been particularly important in making precise measurements for nearby gas, increasing the number of sight lines examined, and extending the path length over which the absorption is probed. D I Lyman series observations were a key science driver for the design and operation of the *FUSE* mission (Moos et al. 2002). Although limited in number, important observations have also been made with experiments on the Shuttle-based *ASTRO-SPAS* platform; these include high resolution measurements with the Princeton *IMAPS* experiment (Jenkins et al. 1999; Sonneborn et al. 2000) and echelle spectroscopy with the *ORFEUS* telescope (Bluhm et al. 1999).

The other primary means for estimating the deuterium abundance is measuring the emission of the D I hyperfine transition at 91.6 cm (327 MHz). Work to detect this radio line began with Weinreb (1962) and has continued sporadically to the present day (Anantharamaiah & Radhakrishnan 1979; Blitz & Heiles 1987; Lubowich, Anantharamaiah, & Pasachoff 1989; Heiles, McCullough, & Glassgold 1993; Chengalur, Braun, & Burton 1997), albeit with limited success until recently (Rogers et al. 2005, 2007). The main limitation here is one of sensitivity, and as these latter two studies have shown this can be overcome with appropriate instrumentation tailored to detect the weak D I signal. Sadly, Tom Bania reported at this conference that the antenna array used for these observations at Haystack Observatory has been moth-balled and is unlikely to be resurrected anytime soon.

A secondary means for estimating the deuterium abundance is radio emission observations of deuterated molecules in the molecular component of the interstellar medium. However, even simple deuterium chemistry networks in molecular clouds become complicated quickly (Watson 1976; Dalgarno & Lepp 1984). Chemical fractionation makes it very difficult to determine D/H from molecular observations in most dark cloud environments because of the large number of molecular species and transitions that must be observed to account for each element (see, for example, Parise et al. 2009). This is a topic worthy of review, but too extensive to do so here.

Work on determining D/H in the Milky Way has slowed in the past few years since *FUSE* is no longer operating, but the debate over what the results mean continues. Figure 1 shows the value of D/H measured for sight lines in the local interstellar medium, the solar neighborhood, and the Galactic disk. These regions are delineated with dashed vertical lines. As can be seen in this figure, there is considerable variation in the D/H ratio from sight line to sight line, particularly at higher column densities. The measurements shown are estimates of the D/H ratio in the gas and do not account for any deuterium that may be locked into dust grains, a topic to which I will return briefly later. In the sections that follow, I summarize the measurements of atomic deuterium in the Milky Way that have been made to date and discuss some of their implications. I refer the reader to other articles in this proceedings by Linsky, Hébrard, Pradanović, and others for specific details on some of the topics discussed below.

2. The Local Bubble [$d \lesssim 100\ pc$]

The local interstellar medium within about 100 pc of the Sun is often referred to as the Local Bubble. Within this cavity the properties of the interstellar medium are relatively homogeneous. The boundary of the Local Bubble appears to occur at hydrogen column densities of log N(H) $\sim 19.2 - 19.3$ (Sfeir et al. 1999). Within the Local Bubble D/H $\approx (1.5 - 1.6) \times 10^{-5}$ (Wood et al. 2004; Linsky et al. 2006), with some variation seen. Most of the Local Bubble measurements shown in Figure 1 are for sight lines to nearby, hot white dwarf stars with strong UV continua (e.g., Hébrard et al. 2002; Kruk et al. 2002; Lehner et al. 2002) or for later-type stars for which it is possible to measure

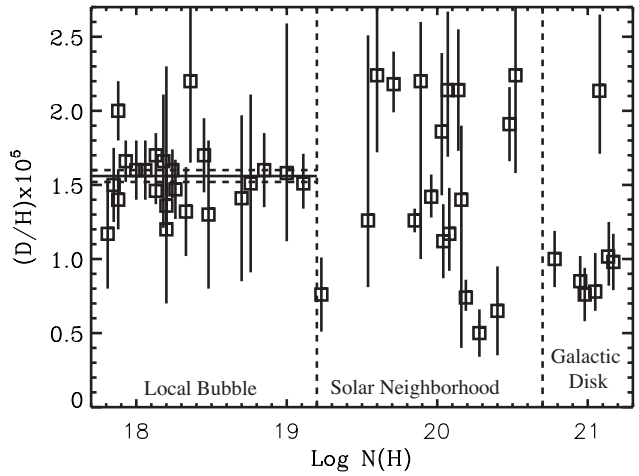

Figure 1. D/H as a function of hydrogen column density for sight lines observed with *Copernicus*, *IMAPS*, *HST*, and *FUSE* (adapted from Linsky et al. 2006 and Oliveira & Hébrard 2006). The vertical dashed lines denote the approximate column densities [N(H) = N(H I)+2N(H_2)] distinguishing the Local Bubble and Solar Neighborhood from more distant gas.

the H I and D I absorption against chromospheric emission lines (see, e.g., Linsky et al. 1995).

Vidal-Madjar et al. (1998) first suggested the possible detection of spatial variations in the D/H ratio within the Local Bubble. For many years debate raged over whether such variations were real or simply due to measurement error. Today, it seems reasonable to conclude that there are sight line to sight line variations of D/H in the Local Bubble, but for the most part such variations are small, especially when compared to those of more extended sight lines (see Figure 1). At this conference, Hébrard raised the interesting point that both the D/O and O/H ratios for Local Bubble sight lines tend to show less scatter than D/H, suggesting that there may be some systematic effects that could give rise to the (albeit small) variations seen in D/H.

3. The solar neighborhood [$100 \lesssim d(pc) \lesssim 500$]

There are now approximately 20 estimates of D/H for sight lines extending beyond the Local Bubble out to a few hundred parsecs. Most of the background sources are either white dwarf stars near the edge of the Local Bubble (e.g., Sonneborn et al. 2002), sub dwarfs (Friedman et al. 2002), or more distant OB stars (e.g., Jenkins et al. 1999; Sonneborn et al. 2000). These sight lines show a much stronger variation in D/H than the nearby stars, with roughly half showing larger values and half showing lower values than the Local Bubble average. There are no obvious correlations of D/H with Galactic longitude or latitude, nor with any known large interstellar structures. It is interesting that the mean value of D/H = 1.5×10^{-5} is indistinguishable from that of the Local Bubble.

On these scales, one would expect some variations around the Local Bubble value as a result of different gas mixing histories and deuterium astration. Several of these sight lines pass into known star-forming regions for which the chemical history of the gas is likely to be different than for the intervening interstellar medium along the sight lines. However, the magnitude of the variations seen, a factor of 2.5–3 for some sight line

combinations, has led several authors to suggest that they might be due to deuteration of polycyclic aromatic hydrocarbons (PAHs → PADs; see Draine 2006; Linsky et al. 2006). Since astration and differential depletion into grains both serve to lower the gas-phase abundance of deuterium, this suggestion raises the obvious question: Why are some values of D/H so much higher than the Local Bubble values?

4. The Galactic disk [$d \gtrsim 500$ *pc*]

Deuterium absorption has been measured in the Galactic disk beyond the solar neighborhood along only seven sight lines for which the hydrogen column density exceeds log N = 20.7. Of these, only four (HD 41161, HD 53975, HD 90087, HD 191877) extend beyond 1 kpc (Hoopes et al. 2003; Hébrard et al. 2005; Oliveira & Hébrard 2006), and all lie within 3 kpc of the Sun. Several hundred extended sight lines have been observed with *FUSE* for a variety of purposes (see, e.g., Bowen et al. 2008), but few have proven useful for studies of D/H. The complex velocity structure arising from the superposition of gas clouds makes it difficult to disentangle the D I absorption from the very strong H I Lyman series absorption. Contamination of the D I lines by molecular hydrogen absorption is also problematic in many cases. We are fortunate to have seven cases for which N(D I) can be measured, but it is important to note that both the D I and H I measures are averages integrated over each sight line. The modest spectral resolution of *FUSE* and the great breadth of the H I absorption do not allow component by component analyses.

The D/H ratios for 6 of the 7 sight lines in this region of Figure 1 lie well below the Local Bubble average and are quite consistent with the average of the low D/H subset for the solar neighborhood. The single high D/H value (HD 41161) is similarly offset from the Local Bubble average and is consistent with the average of the high D/H subset for the solar neighborhood. This suggests that whatever processes serve to introduce variations in the solar neighborhood sample likely operate at larger distances as well. To first order, the variation in absorption beyond ~ 1 kpc does not seem dramatically larger (or smaller) than in the $100 \lesssim d(pc) \lesssim 500$ gas. Unfortunately, it isn't possible with the present data to separate out the foreground solar neighborhood contributions from the more distant cloud contributions for these sight lines.

A separate estimate for the D/H ratio in the Galactic plane has been made by Rogers et al. (2005, 2007), who report measurements of the 92 cm line emission in the Galactic plane at longitudes $l = 171^o$, 183^o, and 195^o. Using an array of 24 small radio telescopes equipped with low-noise amplifiers to conduct these observations, they found values of D/H = $(2.4\pm0.3, 1.9\pm0.2,$ and $1.8\pm0.5)\times10^{-5}$ in the three directions, with a final estimate of $(2.1 \pm 0.7) \times 10^{-5}$ (3σ) after accounting for uncertainties in the spin temperature of the gas. This value is very similar to that for the average of the high solar neighborhood and Galactic disk values inferred from the absorption-line measurements.

Rodgers et al. estimate that the deuterium emission is spread over approximately 5 kpc, which would make this the longest integrated path for which deuterium has been measured in the Galaxy. It may also well be the best average value for any region beyond the Local Bubble since the beam width of 14^o samples a much larger volume of gas than the absorption-line observations. The fact that the value of D/H found is high does not rule out the possibility that some of the gas has low D/H, but it does suggest that the average value for the Galactic disk and low halo in the Galactic anti-center is higher than the local value and has a relatively low astration factor, $f_D \lesssim 1.3$. Similar measures for other directions, particularly those for extended directions observed by *FUSE* would be highly desirable but do not appear to be feasible at this time.

5. The Galactic halo [$|z| \gtrsim 200$ *pc*]

High latitude sight lines with measurable D I absorption have been observed, but most of these are very nearby and do not extend far enough to probe the warm neutral medium of the Galactic halo, which has a different history than warm gas in the Galactic disk. In particular, the neutral Galactic halo gas has higher gas-phase abundances of refractory elements, due in large part to grain destruction caused by the passage of shocks that transport material from the disk into the halo (Sembach & Savage 1996).

Savage et al. (2007) report the detection of D I in the Galactic halo gas toward the high latitude QSO HE 0226-4110 observed with *FUSE*. Absorption is present in several lines of the Lyman series. They find D/H = $(2.1\pm^{0.8}_{0.6}) \times 10^{-5}$ for the warm neutral medium of the Galactic halo, after correcting for absorption by foreground gas in the Local Bubble. The quoted value for the halo clouds is a weighted average over all clouds more distant than the Local Bubble. In these clouds, the gas-phase oxygen abundance is approximately solar and the gas-phase iron abundance is 1/10 solar; these differential depletion results are typical of halo clouds and are less severe than the depletions seen for the average warm neutral medium in the Galactic disk (Savage & Sembach 1996).

The value of D/H toward HE 0226-4110 is consistent with the higher values of D/H found in the Galactic disk, again suggesting a low astration factor that pushes up against the limits of predictions of galactic chemical evolution models. The past dynamical history of the gas does not help alleviate this problem since the transport time for disk gas into the low halo ($|z| \lesssim 3$ kpc) is on the order of a few hundred Myr. The high value of D/H also leaves little, if any, room for depletion of deuterium into dust grains, which is consistent with the expectation that the grain mantles in such clouds should be highly processed. An extremely low abundance of molecular hydrogen along the sight line also implies that there is little molecular material in which to incorporate deuterium.

6. The high velocity cloud Complex C [$d = 10 \pm 2$ *kpc*]

Sembach et al. (2004) report the detection of D I absorption in high velocity cloud Complex C, a large parcel of gas in the northern Galactic sky at a distance of 10 ± 2 kpc and an altitude of ~ 8 kpc (Thom et al. 2008). Complex C has a metallicity of 0.1-0.25 solar, exhibits no evidence of dust, and has a low nitrogen abundance thereby implying that it is chemically young. It is composed of gas falling onto the Milky Way and is unlikely to be Galactic disk or halo gas ejected to large distances. The mass of Complex C is on the order of 10^7 M_o.

The velocity separation between Complex C and the Galaxy in the *FUSE* spectrum of QSO PG 1259+593 allows for an analysis of D/H in the high velocity gas. Sembach et al. (2004) find a value of D/H = $(2.2 \pm 0.7) \times 10^{-5}$, similar to that obtained for the warm halo clouds toward HE 0226-4110. Complex C contains metals and has therefore undergone some chemical evolution. Therefore, the similarity of its D/H value to some of the values found for the disk and halo of the Milky Way is somewhat perplexing since the oxygen abundances in Complex C and these other regions differ by roughly a factor of 5-10.

7. The outer planets

Several estimates of D/H have been made for Jupiter and Saturn, with the most reliable being those for Jupiter. There have been three different techniques used to measure D/H on Jupiter: weak optical H_2 and HD absorption lines (Trauger et al. 1973), in-situ *Galileo*

Table 1. D/H Summary

Site	D/H [ppm]	Possible Importance of Dust Depletion	No. of Meas.	Reference or Compilation
Primordial gas	$26.8\pm^{2.7}_{2.5}$	Not important	...	Steigman 2007
IGM	28.5 ± 7.6 (SD)	Not important	7	Pettini et al. 2008
Complex C	22 ± 7 (1σ)	Not important	1	Sembach et al. 2004
Galactic halo	$22\pm^{8}_{6}$ (1σ)	Not important	1	Savage et al. 2007
Galactic disk (92cm)	21.0 ± 2.3 (1σ)	Probably not important	3	Rodgers et al. 2007
Galactic disk (high)	$21.4\pm^{5.1}_{4.3}$ (1σ)	Probably not important	1	Oliveira & Hébrard 2006
Galactic disk (low)	9.0 ± 1.2 (SD)	Perhaps important	6	Oliveira & Hébrard (2006)
Solar neighborhood (high)	21.1 ± 1.5 (SD)	Probably not important	8	Oliveira et al. 2006 Oliveira & Hébrard 2006
Solar neighborhood (low)	10.3 ± 3.3 (SD)	Perhaps important	10	Oliveira et al. 2006 Oliveira & Hébrard 2006
Local Bubble	15.8 ± 2.1 (SD)	Perhaps important	22	Linsky et al. 2006
Jupiter	23.0 ± 2.6 (1σ)	Unknown	3	see Section 7

Note: This table is an update of a similar table that first appeared in Savage et al. (2007). "SD" indicates that the simple standard deviation of the mean was adopted in computing the error.

mass spectrometer measurements (Mahaffy et al. 1998), and *Infrared Space Observatory* observations of H_2 and HD emission (Lellouch et al. 2001). Following Savage et al. (2007), I adopt here an error-weighted average of these values: $D/H = (2.30 \pm 0.26) \times 10^{-5}$.

8. D/H summary

Table 1 and Figure 2 summarize the results for D/H in various Galactic environments, together with the values available for QSO absorption-line systems at high redshift. Data for each of these points comes from the references cited in Table 1 and references therein. For regions for which multiple measurements exist, the values shown are straight averages of the measurements, and the error quoted is the standard deviation about the mean value. Otherwise, the 1σ error on the mean value is quoted from the original source.

9. Variations in D/H and the role of dust

Variations in D/H and D/O have been discussed extensively elsewhere (see Linsky et al. 2006; Oliveira & Hébrard 2006; Oliveira et al. 2006), so I will not delve into the details here. Suffice it to say that variations in D/H, O/H, and D/O exist to differing degrees for the sight lines measured, and that one possible explanation for some of these variations is extreme deuteration of hydrocarbon molecule chains (Draine 2006). It is tempting to jump on the "dust bandwagon" to explain all of these variations, but it seems equally plausible that differing levels of astration and incomplete mixing play important roles as well. It is probably fair to say that what we presently (don't) know about these sight lines leaves room for all of these possibilities. Indeed, in the one region we expect to have a reasonably uniform chemical history and be well mixed, the Local Bubble, the variations in D/H and D/O are small.

Table 1 contains a subjective assessment of whether or not depletion of deuterium onto dust is likely to be important for the regions represented. Some regions with high D/H values, such as the QSO absorbers and Complex C, should contain very little dust

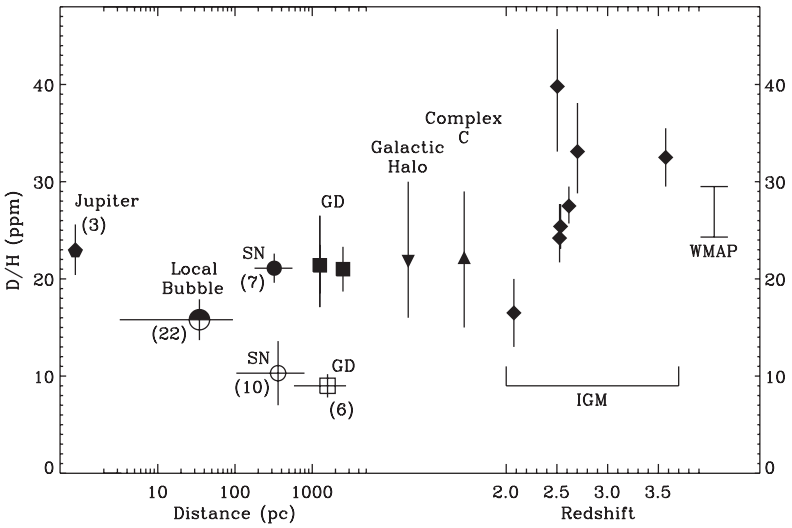

Figure 2. D/H measurements for a variety of environments. Values for the data points shown are given in Table 1, with symbol coding corresponding to the types of regions considered ("SN" = solar neighborhood. "GD" = Galactic disk). Numbers in parentheses indicate the number of measurements included for each data point if greater than one. Filled symbols indicate those measurements for which depletion of deuterium into dust is unlikely to be important.

and are unlikely to harbor PAHs or PADs. But what about the regions with lower D/H values? Oliveira et al. (2006) find an anti-correlation between D/H and n(H), the sight line averaged density of H, as one typically sees for elements incorporated into dust (see Jenkins, Savage, & Spitzer 1986), but this result depends strongly on the measurements for a few sight lines.

It has been proposed that a positive correlation of D/H with the gas-phase abundances of highly refractory elements would indicate that deuterium is subject to inclusion in dust grains, as the gas-phase abundance of the refractories is highly dependent on the presence and processing of dust. Higher observed abundances of elements such as Si, Fe, and Ti would imply less dust and should be associated with higher values of D/H. Similarly, the more refractory elements are depleted from the gas phase, the better the chance that deuterium is also depleted. Linsky et al. (2006) checked this hypothesis using measures of Fe II and Si II along 38 of the Galactic disk sight lines with D/H measures (see their Figures 3 and 4) and found a positive correlation, as expected, with considerable scatter. The correlation between $(\mathrm{Si/H})_{gas}$ and D/H is strongly dependent on a few data points, but the correlation with $(\mathrm{Fe/H})_{gas}$ appears to be more secure.

Follow-up observations of the abundance of Ti from the ground have provided preliminary evidence for a correlation with D/H. Early results for 7 sight lines by Prochaska, Tripp, & Howk (2005) showed a strong correlation between $(\mathrm{Ti/H})_{gas}$ and D/H, providing further support to the idea that the scatter in D/H is linked to differential depletion. More extensive studies (Ellison, Prochaska, & Lopez 2007; Lallement, Hébrard, & Welsh 2008) confirm a correlation, but indicate that it is weaker than originally found and that the gradient observed for Ti/D is less than for Fe/D, contrary to expectations. It is possible that the results are subject to sight line selection effects (see below).

10. Some things to consider

It is tempting to take the existing deuterium results and generalize them to the Galaxy as a whole. However, that would surely be a dangerous thing to do, as the existing samples are subject to a variety of selection effects. The majority of deuterium measurements are obtained through observations of D I Ly-series absorption at far-ultraviolet wavelengths. Some possible caveats and concerns to keep in mind when considering the broader applicability of these results include:

(*a*) *Volume probed*: The volume of the Galaxy probed by the absorption-line measurements is very small, even with *FUSE*. Most of the sight lines are confined to within a few hundred parsecs of the Sun, a region which is not necessarily typical of the rest of the Galaxy. Only a few sight lines extend outside the local spiral arm, and only 1 or two sight lines extend as far as the nearest (Sagittarius) spiral arm.

(*b*) *Sight line conditions*: The types of regions probed are *not* conducive to the formation of molecules or dust grains. The sight lines observed have average densities typical of very diffuse clouds and were chosen for their simple velocity structure. The molecular content of the sight lines is orders of magnitude smaller than the atomic content. As a result, there is a strong selection against dark cloud environments where grain growth and molecular chemistry occurs.

(*c*) *Biased line strength*: There is probably a bias to report results for which the D I absorption is strong enough to detect, but not so strong as to be overwhelmed by H I absorption in close spectral proximity. This may limit the range of D/H probed, and sight line to sight line variations larger than those reported may exist. I am unaware of any systematic search through the existing archives for sight lines for which D I absorption should have, and could have, been seen but isn't.

(*d*) *Line saturation and unresolved velocity structure*: At the velocity resolution of *FUSE*, about 20 km s^{-1}, it is not possible to distinguish one absorbing region from another along most sight lines. Therefore, the values of N(D I) and N(O I) are necessarily averages for the sight line, weighted by the gas content of the individual clouds encountered. Similarly, only the total sight line column density of H I can be measured from the Ly-series lines. Narrow velocity structure resulting in line saturation could depress the values of N(D I) and N(O I) below their true values, even for cases for which multiple transitions can be observed. This effect can be quantified but depends strongly on the actual velocity structure encountered.

(*e*) *Not all grains are the same*: PADs and "normal" silicate or carbonaceous grains may have very different histories. Comparisons of D/H or D/O to the gas-phase abundances of refractory elements to infer the depletion of D are most meaningful if the deuterium and refractories are incorporated into the same grains. The relatively small variation in refractory element abundance with changes in D/H is somewhat surprising. Take Ti as an example. For diffuse clouds like those observed toward ζ Oph, this element has 999 of 1000 atoms locked into dust grains, with only 0.1% of the atoms in the gas phase (see Savage & Sembach 1996). To change the gas-phase depletion of Ti by two requires only 1 more of those 1000 atoms to be liberated into the gas, whereas for deuterium which has a depletion no more than a factor of a few, roughly half of the D atoms would have to be liberated to change the gas-phase abundance of D by a factor of two. Why isn't there more variation in the abundances of the refractory elements along these sight lines if dust content and the processing of dust are responsible for the variations in D/H? I suspect it is because the grains are already highly processed, and I remain

somewhat skeptical that the observed variations are due mainly to differential depletion.

(*f*) *Local sources of deuterium*: All methods of deuterium production require either extreme environments or special conditions, with Big Bang nucleosynthesis being the only viable source for cosmological quantities (see Epstein, Lattimer, & Schramm 1976; Jedamzik 2002). However, localized sources could potentially account for some variability of D/H within the Galaxy. Possible sites of production include stellar flares (Mullan & Linsky 1999; Prodanović & Fields 2003) or supernova shock waves (see above references). Unfortunately, independent confirmation of deuterium production in such sources is notoriously difficult to come by, so for now it is difficult to quantify their importance.

(*g*) *Unknown unknowns*: There may be unknown systematic measurement effects leading to the apparent bifurcation of D/H into high and low branches beyond the Local Bubble. The absence of many points near the mean value for the Local Bubble, which is also the mean for all of the solar neighborhood points, is surely telling us something important about either the nature of the absorption or our ability to measure it.

11. Concluding remarks

Over the years, the focus of D/H determinations has evolved from trying to determine the primordial abundance of deuterium to trying to understand chemical evolution and the detailed physics of the sight lines along which deuterium can be measured. Despite their limitations, observations of deuterium in the Galaxy have proven to be extremely interesting and thought provoking. The lively discussion at this conference was direct proof of that!

The prospects for obtaining further D I absorption-line measurements within the Milky Way in the near future are not very bright. However, with the installation of the Cosmic Origins Spectrograph in *HST* in May 2009, there is again a chance that it will be possible to measure D/H in the low-redshift intergalactic medium along one or more of the many QSO sight lines that will be observed in the coming years. The key to doing this will be to find a strong enough Lyman-limit system at $z \lesssim 0.5$ in which to measure the D I Lyα absorption. The COS Team is also investigating whether it might be possible to use COS to observe at wavelengths below 1100 Å. Initial results using the low resolution grating (G140L) demonstrate that the *HST* optics transmit light at these wavelengths (McCandliss et al. 2010). Further tests using the G130M medium resolution grating, which could potentially reopen the possibility of measuring deuterium absorption in the Galaxy, may be undertaken.

I thank the organizers of this conference for the invitation to participate in this conference and to share my thoughts in this article. I acknowledge travel support from grant COS GTO grant NNX08AC14G.

References

Anantharamaiah, K.R., & Radhakrishnan, V. 1979, *A&A*, 79, L9
Blitz, L., & Heiles, C. 1987, *ApJ*, 313, L95
Bluhm, H., Marggraf, O., de Boer, K.S., Richter, P., & Heber, U. 1999, *A&A*, 352, 287
Bowen, D.V., et al. 2008, *ApJS*, 176, 59
Chengalur, J.N., Braun, R., & Burton, W.B. 1997, *A&A*, 318, L35
Dalgarno, A., & Lepp, S. 1984, *ApJ*, 287, L47

Draine, B.T. 2006, in *Astrophysics in the Far Ultraviolet: Five Years of Discovery with FUSE*, ASP Conf. Ser. 48, eds., G. Sonneborn, H.W. Moos, & B.-G. Andersson (San Francisco: ASP), 58
Dunkley, J., et al. 2009, *ApJS*, 180, 360
Ellison, S.L., Prochaska, J.X., & Lopez, S. 2007, *MNRAS*, 380, 1245
Epstein, R.I., Lattimer, J.M., & Schramm, D.N. 1976, *Nature*, 263, 198
Friedman, S.D., et al. 2002, *ApJS*, 140, 37
Hébrard et al. 2002, *ApJS*, 140, 103
Hébrard et al. 2005, *ApJ*, 635, 1136
Heiles, C., McCullough, P.R., & Glassgold, A.E. 1993, *ApJS*, 89, 271
Hoopes, C.G., Sembach, K.R., Hébrard, G., Moos, H.W., Knauth, D.C. 2003, *ApJ*, 586, 1094
Jedamzik, K. 2002, *Planetary & Space Sci.*, 50, 1239
Jenkins, E.B., Savage, B.D., & Spitzer 1986, *ApJ*, 301, 355
Jenkins, E.B., Tripp, T.M., Woźniak, P.R., Sofia, U.J., & Sonneborn, G. 1999, *ApJ*, 520, 182
Kirkman, D., Tytler, D., Suzuki, N., O'Meara, J., & Lubin, D. 2003, *ApJS*, 149, 1
Kruk, J.W. et al. 2002, *ApJS*, 140, 19
Lallement, R., Hébrard, G., & Welsh, B.Y. 2008, *A&A*, 481, 381
Lehner, N., et al. 2002 *ApJS*, 140, 81
Linsky, J.L., et al. 1995, *ApJ*, 451, 335
Linsky, J.L., et al. 2006, *ApJ*, 647, 1106
Lubowich, D.A., Anantharamaiah, K.R., & Pasachoff, J.M. 1989, *ApJ*, 345, 770
Lellouch, E., et al. 2001, *A&A*, 370, 610
Mahaffy, P.R., et al. 1998, *Space Sci. Rev.*, 84, 251
McCandliss, S.R., et al. 2010, *ApJ*, 709, L183
Moos, H.W., et al. 2002, *ApJS*, 140, 3
Mullan, D.J., & Linsky, J.L. 1999, *ApJ*, 511, 502
Oliveira, C., & Hébrard, G. 2006, *ApJ*, 653, 345
O'Meara, J., et al. 2006, *ApJ*, 649, L61
Parise, B., Leurini, S., Schilke, P., Roueff, E., Thorwirth, S., & Lis, D.C. 2009, *A&A*, 508, 737
Pettini, M., Zych, B.J., Murphy, M.T., Lewis, A., & Steidel, C.C. 2008, *MNRAS*, 391, 1499
Prochaska, J.X., Tripp, T.M., & Howk, J.C. 2005, *ApJ*, 620, L39
Prodanović, T., & Fields, B.D. 2003, *ApJ*, 597, 48
Rogers, A.E.E., et al. 2005, *ApJ*, 630, L41
Rogers, A.E.E., Dudevoir, K.A., & Bania, T.M. 2007, *AJ*, 133, 1625
Rogerson, J.B., & York, D.G. 1973, *ApJ*, 186, L95
Savage, B.D., Lehner, N., Fox, A., Wakker, B., and & Sembach, K.R. 2007, *ApJ*, 659, 1222
Savage, B.D., & Sembach, K.R. 1996, *ARA&A*, 34, 279
Sembach, K.R., & Savage, B.D. 1996, *ApJ*, 457, 211
Sembach, K.R., et al. 2004, *ApJS*, 150, 387
Sfeir, D.M., Lallement, R., Crifo, F., & Welsh, B.Y. 1999, *A&A*, 346, 785
Sonneborn, G., et al. 2000, *ApJ*, 545, 277
Sonneborn, G., et al. 2002, *ApJS*, 140, 51
Spergel, D.N., et al. 2007, *ApJS*, 170, 377
Steigman, G. 2007, *Ann. Rev. Nucl. Part. Sci.*, 57, 463
Steigman, G., Romano, D., & Tosi, M. 2007, *MNRAS*, 378, 576
Thom, C., et al. 2008, *ApJ*, 684, 364
Tosi, M., Steigman, G., Matteucci, F., & Chiappini, C. 1998, *ApJ*, 498, 226
Trauger, J.T, Roessler, F.L, Carelton, N.P., & Traub, W.A. 1973, *ApJ*, 184, L137
Vidal-Madjar, A., Laurent, C., Bonnet, R.M., & York, D.G. 1977, *ApJ*, 211, 91
Vidal-Madjar, A., et al. 1998, *A&A*, 338, 694
Watson, W.D. 1976, *Rev. Mod. Phys.*, 48, 513
Weinreb, S. 1962, *Nature*, 195, 367
Wood, B.E., et al. 2004, *ApJ*, 609, 838
York, D.G., & Rogerson, J.B. 1976, *ApJ*, 203, 378

Light elements in the Universe
Proceedings IAU Symposium No. 268, 2010
C. Charbonnel, M. Tosi, F. Primas & C. Chiappini, eds.

DOI: 00.0000/X000000000000000X

The total deuterium abundance in the local Galactic disk: decisions and implications

Jeffrey L. Linsky[1]

[1]JILA, University of Colorado and NIST,
Campus Box 440, Boulder, CO 80309-0440, USA
email: jlinsky@jilau1.colorado.edu

Abstract.
Analyses of FUSE spacecraft spectra have provided measurements of D/H in the gas phase of the interstellar medium for many lines of sight extending to several kpc from the Sun. These measurements, together with the earlier Copernicus, HST, and IMAPS data, show a wide range of D/H values that have challenged both observers and chemical evolution modellers. I believe that the best explanation for the diverse D/H measurements is that deuterium can be sequestered on to carbonaceous grains and PAH molecules and thereby removed from the interstellar gas. Grain destruction can raise the gas phase D/H value to approximately the total D/H value. Supernovae and stellar winds, however, can decrease the total D/H value along lines of sight on time scales less than mixing time scales. I will summarize the theoretical and observational arguments for this model and estimate the most likely range for the total D/H in the local Galactic disk. This range in total D/H presents a constraint on realistic Galactic chemical evolution models or the primordial value of D/H or both.

Keywords. ISM: abundances; cosmology: cosmological parameters; ultraviolet: ISM

1. Introduction

It has long been recognized that accurate measurements of the primordial abundance of deuterium provides the best constraint on the properties of the early universe (100–1000 seconds after the Big Bang) and, in particular, the ratio of baryons to photons (η_{10}). Deuterium plays this critical role because it is an ideal relic; since its initial creation there has been no known process for creation of a significant amount of deuterium, but only destruction by nuclear reactions in stars. Analysis of quasar absorption lines (QAL) in seven lines of sight led Pettini et al. (2008) to infer $(\mathrm{D/H})_{\mathrm{QAL}} = 28.2^{+2.0}_{-1.8}$ parts per million (ppm). Analysis of the cosmic microwave background signal leads to a measurement of η_{10} and thus inference of the primordial D/H ratio. In the most recent analysis of the 5-year WMAP data set, Dunkley et al. (2009) obtain the parameter $100\ \Omega_{b,0} = 2.273 \pm 0.062$, which corresponds to $\eta_{10} = 6.225 \pm 0.0170$ and $(\mathrm{D/H})_{\mathrm{WMAP}} = 25.2 \pm 1.1$. While the two values for the primordial or near-primordial D/H ratio, $(\mathrm{D/H})_{\mathrm{QAL}}$ and $(\mathrm{D/H})_{\mathrm{WMAP}}$, are consistent, they are sufficiently different and likely to be subject to different systematic errors that they should not be averaged to obtain a more "robust" value of $(\mathrm{D/H})_{\mathrm{prim}}$.

Since the first measurements of the interstellar deuterium Lyman lines by the Copernicus satellite, there have been many attempts to measure accurate deuterium abundances in the interstellar medium of our Galaxy. These have included measurements of the deuterium and hydrogen Lyman-α line with IUE and HST, as well as measurements of the higher Lyman lines with the Interstellar Medium Absorption Profile Spectrograph (IMAPS). More recently, the Far Ultraviolet Spectrograph Explorer (FUSE) has provided many new deuterium measurements along lines of sight extending to nearly 3pc.

Until recently, the factor of four range in measured D/H values for different lines of sight (Fig. 1) extending to stars beyond the Local Bubble posed a severe problem as no chemical evolution model of the Galaxy could explain this wide range. A solution to the problem proposed by Jura (1982) and developed by Draine (2003) and Draine (2006) is that deuterium is more tightly bound to carbonacious grains and PAH molecules than hydrogen because the C-D bond is slightly larger than the C-H bond. This is important because interstellar grains are cold ($T \sim 20$ K) and can thus sequester significant amounts of deuterium from the gas phase. Linsky et al. (2006) provided support for this explanation with three lines of evidence: (1) very high D/H ratios measured in interstellar carbonaceous dust grains embedded in interplanetary dust particles (a proof of concept), (2) correlation of high D/H values in interstellar gas with large depletions of refractory metals (Fig. 2), implying that deuterium and metals both deplete onto and evaporate from dust grains although the story is more complex, and (3) D/H abundances increase with interstellar gas temperature as inferred from excitation of H_2. Thus the total D/H ratio in the interstellar medium $(D/H)_{total}$ can be significantly larger than the gas phase measurements $(D/H)_{gas}$. Since even in recently shocked gas, some of the grains containing deuterium may still be present, one must conclude that $(D/H)_{total} \geqslant (D/H)_{gas}$. This statement is strengthened by recognizing that lines of sight likely include both recently shocked and unshocked gas containing grains with deuterium.

Many authors have now accepted the deuterium-depleted dust hypothesis as the explanation for the measured low values of $(D/H)_{gas}$. In this talk I would like to address

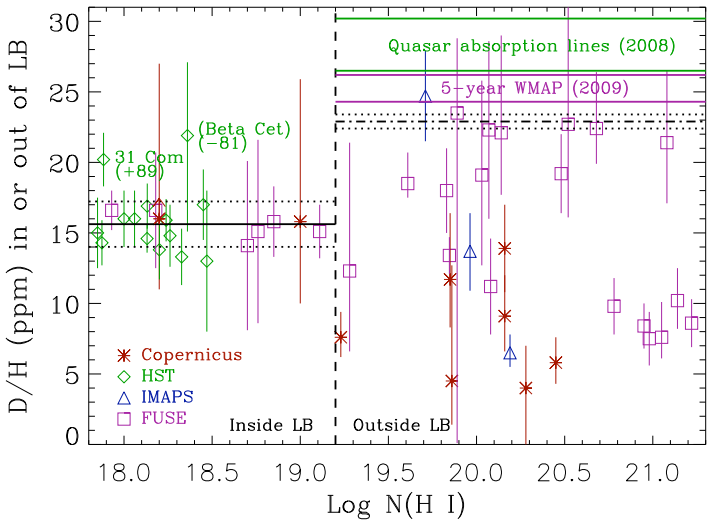

Figure 1. Measurements of the $(D/H)_{gas}$ for the 24 lines of sight located entirely inside of the Local Bubble (to the left of the vertical dashed line) and the gas located outside of the Local Bubble, $(D/H)_{gas-LB}$, (to the right of the vertical dashed line). The error bars are 1σ, and the horizontal axis is the hydrogen column density to the star at the end of the line of sight. The symbols are coded by the spacecraft that obtained the Lyman line spectra. The range of $(D/H)_{prim}$ values obtained from quasar absorption lines (Pettini et al. 2008) and from WMAP (Dunkley et al. 2009) are shown in the upper right. Just below is the range of the total deuterium abundance in the local Galactic disk, $(D/H)_{high} = 22.9 \pm 0.5$ ppm.

the high values of $(D/H)_{gas}$ including recent measurements, infer a sensible value for $(D/H)_{total}$ in the Galactic disk, and relate this high value of $(D/H)_{total}$ to the measurements of primordial D/H.

2. Analysis of the high values of $(D/H)_{gas}$

Linsky et al. (2006) assembled all of the then-available published values of $(D/H)_{gas}$ obtained with Copernicus, IUE, HST, IMAPS, and FUSE for lines of sight toward 47 stars. Since that paper was published, $(D/H)_{gas}$ measurements for five additional lines of sight observed by FUSE have became available (Table 1) and are included in the following analysis. I consider only the direct measurements of N(HI) and N(DI) for which the hydrogen and deuterium components of the molecules H_2 and HD are added when measured. There are alternative methods for evaluating D/H, in particular from the product (D/O)x(O/H). As described by Hébrard (2010), this method minimizes errors in N(HI) due to the high opacity of the Lyman lines. However, this method introduces additional uncertainties associated with measurements of the oxygen lines, including depletion of oxygen on interstellar dust grains.

Linsky et al. (2006) separated the $(D/H)_{gas}$ measurements into two groups depending upon whether the target star is located inside of or beyond the Local Bubble. The Local Bubble has been described as a superbubble of 10^6 K gas produced by recent supernovae in the Scorpio-Centaurus Association of young stars, although Welsh & Shelton (2009) argue that most of the volume of the gas is highly ionized but far cooler than 10^6 K. The N(HI) and N(DI) measurements toward stars inside of the Local Bubble refer to warm gas (4,000–10,000 K) located in clouds near the Sun (Redfield & Linsky 2008). The Local Bubble is mostly surrounded by cold gas detected in NaI beginning at about log

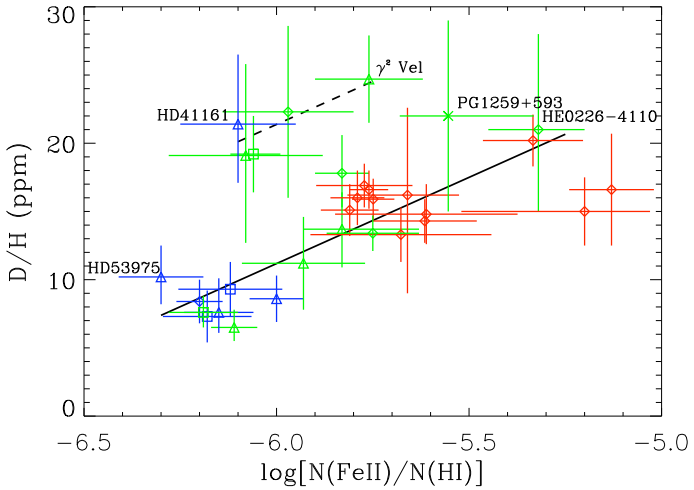

Figure 2. Plot of $(D/H)_{gas}$ vs. depletion of iron for the lines of sight observed by HST, IMAPS, and FUSE. The coding symbols are the same as in Fig. 1. The solid line is the best fit to all of the data, and the dashed line is a displacement of this line upward by 8.5 ppm to be consistent with the five data points that lie well above the mean fit line. The five high points may be lines of sight where weak shocks have removed deuterium, but not iron, from the grains.

Table 1. Recent measurements of $(D/H)^1_{gas}$.

Target	l	b	$d(pc)$	log N(HI)[2]	log N(DI)[3]	$(D/H)_{gas}$	$(D/H)_{gas-LB}$
REJ 1738+665	97	+32	243	19.83 ± 0.05	15.08 ± 0.04	$17.8^{+2.8}_{-2.5}$	18 ± 3
HD 41161	165	+13	1253	21.08 ± 0.08	16.41 ± 0.05	$21.4^{+5.1}_{-4.3}$	$21.4^{+5.1}_{-4.3}$
HD 53975	226	-02	1318	21.14 ± 0.06	16.15 ± 0.07	$10.2^{+2.3}_{-2.0}$	$10.2^{+2.3}_{-2.0}$
HD 93521[4]	183	+62		19.61 ± 0.055	$14.85^{+0.05}_{-0.02}$	$17.4^{+2.0}_{-0.8}$	$18.5^{+2.2}_{-1.0}$
LSE 234	329	-21	460 ± 120	$20.68^{+0.025}_{-0.05}$	16.02 ± 0.045	$22.0^{+4}_{-2.5}$	$22.4^{+4}_{-2.5}$

Notes:
[1]All errors are $\pm 1\sigma$. References: Dupuis et al. (2009) for REJ 1738+665, Oliveira & Hébrard (2006) for HD 41161 and HD 53975, Kruk et al. (2006) for HD 93521, and Lecavelier des Etangs et al. (2006) for LSE 234.
[2]N(HI) includes $2N(H_2)$ and N(HD).
[3]N(DI) includes N(HD).
[4]HD 93521 is located in the Galactic halo at z = 1.5 kpc.

N(HI)=19.2, but there is no cold gas near the Galactic poles (Fig. 3) allowing the Local Bubble gas to interact with the halo. Most lines of sight to the 24 stars located inside of the Local Bubble show $(D/H)_{gas}$ ratios consistent with the mean value of 15.6 ± 0.4 ppm, but the two highest points toward 31 Com and β Cet are for stars located at high Galactic latitudes (+89° and −81°). I include the line of sight to 31 Com in the Local Bubble measurements as the N(HI) and N(DI) gas in this line of sight has a velocity consistent with the North Galactic Pole cloud of warm gas located within 8.5 pc of the Sun (Redfield & Linsky 2008). I also include the line of sight to β Cet in the Local Bubble measurements as the velocities of the H(I) and D(I) gas are consistent with the Microscopium and Ceti clouds located within 5.1 and 15.5 pc of the Sun.

Since the inner boundary of the Local Bubble lies at log N(HI) ≈ 19.2 (Sfeir et al. 1999, Lallement et al. 2003) in nearly all directions, it is sensible to subtract the Local Bubble foreground from the column densities toward stars that lie beyond the Local Bubble to infer $(D/H)_{gas}$ ratios for the ISM not modified by deuterium-depleted gas from the Local Bubble supernovae. Assuming $(D/H)_{gas} = 15.6 \pm 0.4$ ppm, the Local Bubble foreground is log $N(HI)_{LB} = 19.20$ and log $N(DI)_{LB} = 14.39$. The ratios $(D/H)_{gas-LB}$ in Table 1 and

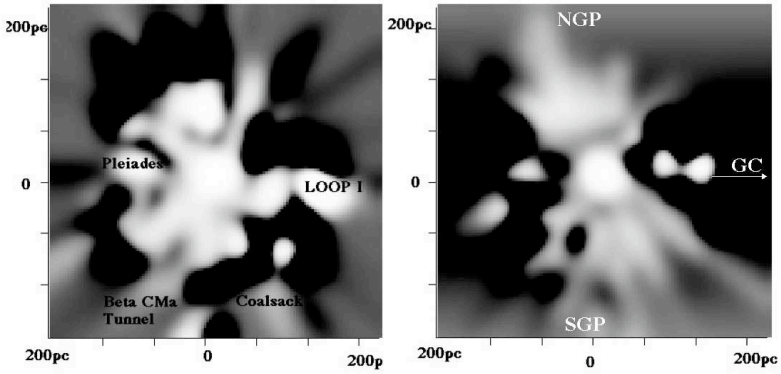

Figure 3. Two views of the Local Bubble from Welsh (2009) and Lallement et al. (2003). Dark indicates cold gas seen in the NaI, and white indicates no cold gas. Left: view of the Galactic plane from the North Galactic pole. Right: view from Galactic longitude 270° and latitude 0°.

in Table 3 of Linsky et al. (2006) include this correction. The effect of subtracting the Local Bubble foreground is to produce somewhat higher or lower values of $(D/H)_{gas-LB}$ for lines of sight toward stars just beyond the Local Bubble when $(D/H)_{gas}$ is greater or less than 15.6 ppm. The correction is small for stars with log N(HI)> 20.5.

In Fig. 1, ten lines of sight have $(D/H)_{gas-LB} > 15.6$, and six lie above 20.0. If the deuterium-depletion hypothesis is the major cause of low values of $(D/H)_{gas-LB}$, then the highest credible value or values of $(D/H)_{gas-LB}$ should be the best approximation to a lower limit to $(D/H)_{total}$. Given that the data have errors, one can only estimate the highest credible value of $(D/H)_{gas-LB}$ statistically. At this symposium, Steigman (2010), has proposed another statistical method for estimating $(D/H)_{total}$. In Fig. 4, I plot the value of $(D/H)_{high}$ estimated as the mean of the $(D/H)_{gas-LB}$ values starting with the highest value and sequentially including lower values and weighting each data point by the inverse errors. Also plotted is σ, the error of the mean for each number of lines of sight included. The value of σ goes through a minimum at seven lines of sight **and** increases thereafter. For these seven lines of sight, $(D/H)_{high} = 22.9 \pm 0.5$ ppm. I therefore propose that the total D/H ratio (gas plus dust) in the Galactic disk near the Sun is $(D/H)_{total} \geqslant 22.9 \pm 0.5$ ppm.

3. Decisions and implications

Comparison of our estimate of the total D/H ratio in the nearby Galactic disk outside of the Local Bubble with estimates of the primordial D/H ratio places constraints on the evolution of deuterium over the lifetime of the Galaxy. Models of the chemical evolution of the Galaxy (e.g., Romano et al. 2006) include both the destruction of deuterium by nuclear reactions in stars and estimates of the infall of gas from captured galaxies and the intergalactic medium containing near primordial D/H. For different assumptions, these models compute the deuterium astration factor, $f_D = (D/H)_{prim}/(D/H)_{high}$. In Table 2,

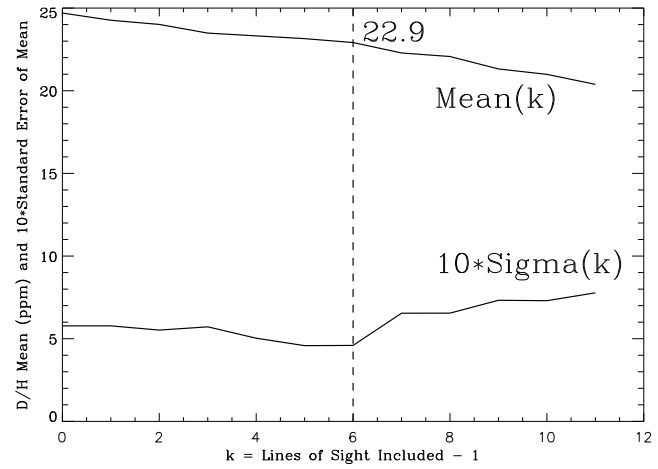

Figure 4. Mean values of $(D/H)_{high}$ obtained as a weighted average of $(D/H)_{gas-LB}$ values starting with the highest and including next lower values in sequence. The error in the mean, σ, increases above seven lines of sight, implying that the best value of the total D/H ratio in the local Galactic disk is $(D/H)_{high} \geqslant 22.9 \pm 0.5$ ppm.

Table 2. Is Concordance Possible?

Method	**D/H (ppm)**	$100\Omega_{b,0}h^2$	η_{10}	$f_{\rm D}$	**Fraction**
ISM (high 7)	$\geqslant 22.9 \pm 0.5$	$\leqslant 2.411 \pm 0.33$	$\leqslant 6.604 \pm 0.090$		
QAL (7 LOS)	$28.2^{+2.0}_{-1.8}$	2.13 ± 0.09	5.84 ± 0.27	$\leqslant 1.23 \pm 0.09$	$\geqslant 81 \pm 7$ %
WMAP (5 years)	25.2 ± 1.1	2.273 ± 0.062	6.225 ± 0.170	$\leqslant 1.10 \pm 0.07$	$\geqslant 91 \pm 6$ %

I list $f_{\rm D}$ computed from the QAL and WMAP values for $({\rm D/H})_{\rm prim}$. Also, given are the corresponding fractions of deuterium atoms today in the nearby Galactic disk that have not been processed through stars.

The values of $f_{\rm D}$ listed in the table computed from the QAL value of $({\rm D/H})_{\rm prim}$ and especially the WMAP value challenge recent Galactic chemical evolution models for the galactocentric distance of the Sun. The models of Chiappini et al. (2002), for example, predict that $f_{\rm D} \approx 1.5$ for a wide range of assumptions. The more recent models of Romano et al. (2006) can accommodate values of $f_{\rm D}$ as low as ~ 1.3. While there may not be an inconsistency with the QAL data, the WMAP value for $f_{\rm D}$ severely challenges even the Romano et al. (2006) models. At this point, it is not clear to me which are the major causes for the inconsistency, but important unknowns are the accretion rate of near primordial gas and the time scale for mixing of this gas with the ISM. Prodanović & Fields (2008) argue that an accretion rate of $\sim 1 M_\odot$ yr^{-1} could explain the high percentage of unprocessed deuterium. This topic is becoming increasingly interesting.

References

Chiappini, C., Renda, A., & Matteucci, F. 2002, *A&A*, 395, 789

Draine, B.T. 2003, *ARAA*, 41, 241

Draine, B.T. 2006, in A. McWilliam & M. Rauch (eds.), *Origin and Evolution of the Elements*, (Cambridge Univ. Press), p. 317

Dunkley, J. et al. 2009, *ApJS*, 180, 306

Dupuis, J., Oliveira, C.M., Hébrard, G.H., Moos, H.W., & Sonnentrucker, P. 2009, *ApJ*, 690, 1045

Hébrard, G. 2010, in C. Charbonnel, M. Tosi, F. Primas, & C. Chiappini (eds), *Light Elements in the Universe* (Cambridge Univ. Press), this volume

Jura, M. 1982, in Y. Kondo, J.M. Meade, & R.D. Chapman (eds), *Advances in UV Astronomy: 4 Years of IUE Research*, (NASA CP 2238), p. 54

Kruk, J.W., Oliveira, C., Sembach, K.R., & Savage, B.D. 2006, in G. Sonneborn, H.W. Moos, & B.-G. Andersson (eds), *Astrophysics in the Far Ultraviolet, Five Years of Discovery with FUSE*, *ASP-CS*, 348, p. 85

Lallement, R., Welsh, B., Vergeley, J.L., Crifo, F., & Sfeir, D. 2003, *A&A*, 411, 447

Lecavelier des Etangs, A., Hébrard, G., & Williger, G.M. in G. Sonneborn, H.W. Moos, & B.-G. Andersson (eds), *Astrophysics in the Far Ultraviolet, Five Years of Discovery with FUSE*, *ASP-CS*, 348, p. 88

Linsky, J.L. *et al.* 2006, *ApJ*, 647, 1106

Oliveira, C.M., & Hébrard, G. 2006, *ApJ*, 653, 345

Pettini, M., Zych, B.J., Murphy, M.T., Lewis, A., & Steidel, C.C. 2008, *MNRAS*, 391, 1499

Redfield, S., & Linsky, J.L. 2008, *ApJ*, 673, 283

Prodanović, T., & Fields, B.D. 2008, *J. Cosmology & Astroparticle Physics*, 09, 003

Romano, D., Tosi, M., Chiappini, C., & Matteucci, F. 2006, *MNRAS*, 369, 295

Sfeir, D.M., Lallement, R., Crifo, F., & Welsh, B.Y. 1999, *A&A*, 346, 785

Steigman, G. 2010, in C. Charbonnel, M. Tosi, F. Primas, & C. Chiappini (eds), *Light Elements in the Universe* (Cambridge Univ. Press), this volume

Welsh, B.Y., & Shelton, R.L. 2009, *AP&SS*, 323, 1

Light elements in the Universe
Proceedings IAU Symposium No. 268, 2010
C. Charbonnel, M. Tosi, F. Primas & C. Chiappini, eds.

DOI: 00.0000/X000000000000000X

What the D/O ratio tells us about the interstellar abundance of deuterium?

Guillaume Hébrard

Institut d'Astrophysique de Paris, UMR7095 CNRS, Université Pierre & Marie Curie,
98bis boulevard Arago, 75014 Paris, France
email: hebrard@iap.fr

Abstract. The ionization balances for HI, OI and DI being locked together by charge exchange, the deuterium-to-oxygen ratio is considered to be a good proxy for the deuterium-to-hydrogen ratio, in particular within the interstellar medium. As the DI and OI column densities are of similar orders of magnitude for a given sight line, comparisons of the two values are generally less subject to systematic errors than comparisons of DI and HI. Moreover, D/O is additionally sensitive to astration, because as stars destroy deuterium, they should produce oxygen. D/O measurements are now available for tens of lines of sight in the interstellar medium, most of them from *FUSE* observations. The D/H and D/O ratios show different pictures, D/H being clearly more dispersed than D/O. The low, homogeneous D/O ratio measured on distant lines of sight suggests a deuterium abundance representative of the present epoch that is about two times lower than this measured within the local interstellar medium.

Keywords. ISM: abundances; Galaxy: abundances; cosmology: cosmological parameters; ultraviolet: ISM

1. Introduction

In the Big Bang standard model, deuterium is produced in significant amounts only during the Big Bang nucleosynthesis. Among the elements created in BBN, the abundance of deuterium is the most sensitive to the baryonic density of the Universe. As deuterium is destroyed in stellar interiors, its abundance D/H is expected to continuously decrease, from its primordial value $(D/H)_{prim}$ to the value characteristic of the present epoch, $(D/H)_{PE}$. This $(D/H)_{PE}$ ratio is measured within the interstellar medium and should be characteristic of cosmic material after ~ 14 Gyrs of Galactic evolution.

$(D/H)_{PE}$ is a key ratio. It serves as a reference baseline for $(D/H)_{prim}$, providing a lower limit for $(D/H)_{prim}$. It also yields important constraints for chemical evolution models of the Galaxy. The depletion factor due to astration, $f_{ev} = (D/H)_{prim}/\ (D/H)_{PE}$, depends on the star formation and infall rates, and possibly other processes such as early Galactic wind. Models predict values around $f_{ev} \simeq 1.5$ (e.g. Chiappini et al. 2002). In addition, $(D/H)_{PE}$ can be studied more thoroughly than the other deuterium abundances, because it is measured in the interstellar medium. Several tens of sight lines suitable for high quality deuterium abundance measurements are available, and potentially, small sample size should not be an issue.

The determination of the canonical value of $(D/H)_{PE}$ has been the subject of considerable debate over the years. Numerous measurements have been performed through Lyman absorption-line observations in the far-ultraviolet spectral range. By observing hydrogen and deuterium directly in their atomic form, they provide accurate column density determinations that are not dependent on ionization or chemical fractionation. Among them, the ratio $D/H = 1.6 \times 10^{-5}$ measured toward Capella (Linsky et al. 1995) has often been used as a benchmark of $(D/H)_{ISM}$. Although it has been performed in

a particular cloud, namely the Local Interstellar Cloud (Lallement & Bertin 1992), it has been taken as the canonical $(D/H)_{PE}$ value by numerous theoretical studies of the chemical evolution of the Galaxy. However, several lines of sight observed with *Copernicus* revealed values outside this range (see, e.g., Laurent et al. 1979; York 1983). It was uncertain whether the dispersion was the signature of spatial variations in $(D/H)_{ISM}$, or due to unknown systematic errors. The *FUSE* mission has brought significant progress on these issues. Tens of targets observed with *FUSE* have allowed D/H and D/O ratios to be measured in the the interstellar medium.

2. D/O as a proxy for D/H

One of the challenges of D/H measurements is to evaluate for the same line of sight the HI and DI column densities, N(HI) and N(DI), which differ by about five orders of magnitude. Such a large difference is a potential source of systematic errors. For example, all lines from the same species may lie on the non-linear part of the curve of growth, or HI column densities may be detectable in clouds for which DI are below the detection limit (see, e.g., Linsky & Wood 1996, Lemoine et al. 2002, or Vidal-Madjar & Ferlet 2002).

Many of the difficulties associated with obtaining accurate D/H ratios may be avoided by measuring the deuterium-to-oxygen ratio, D/O (Timmes et al. 1997, Hébrard & Moos 2003). First of all, the D/O ratio is of order of a few percent rather than $\sim 10^{-5}$ as for D/H. Many OI and DI transitions with different oscillator strengths are present in the *FUSE* bandpass, allowing measurement of N(OI) and N(DI) over a wide range of values. OI is believed to be a good tracer of HI in the nearby Galactic disk (Meyer et al. 2001; André et al. 2003; Cartledge et al. 2004). The neutral forms of oxygen and hydrogen likely dominate over their ions for many sight lines in the diffuse interstellar medium. In any case, because both species have nearly the same ionization potential, their ionization balances are strongly coupled to each other by charge exchange reactions (Jenkins et al. 2000). Thus, no corrections from ionization models are required, and we can use $N(DI)/N(OI)$ for D/O. Finally, D/O is particularly sensitive to stellar activity, because of both deuterium destruction (deuterium is burned in stellar interiors at temperatures as low as 6×10^6 K) and oxygen production (oxygen is mainly produced by type II supernovae). Hence, spatial variations of the deuterium abundance due to different astration rates at different locations would translate in even higher D/O spatial variations.

3. Deuterium within the Local Bubble

The first published *FUSE* $(D/H)_{ISM}$ results focussed on the local interstellar medium (e.g. Moos et al. 2002; Friedman et al. 2002; Hébrard et al. 2002; Lemoine et al. 2002; Sonneborn et al. 2002). These early studies have shown that $(D/H)_{ISM}$ likely presents a single value in the Local Bubble. Oliveira et al. (2003) reported $(D/H)_{LB} = (1.52 \pm 0.07) \times 10^{-5}$ from *FUSE* data only. Wood et al. (2004) included previous LB measurements, and reported $(D/H)_{LB} = (1.56 \pm 0.04) \times 10^{-5}$. The Local Bubble is a ~ 100 pc-size low-density cavity which includes the LIC in which the Solar System is embedded, and other interstellar clouds (e.g. Snowden et al. 1998). The spectral resolution of *FUSE* is too low to distinguish these different individual clouds. However, as the $(D/H)_{ISM}$ integrated along the studied sight lines show no variations, it seems secure to conclude that the different clouds probed within the LB present an homogeneous $(D/H)_{ISM}$ ratio.

The homogeneity of the deuterium abundance in the different interstellar clouds within the LB was also shown from *FUSE* D/O measurements (Hébrard & Moos 2003). D/O was found to be constant within the Local Bubble, with the averaged value $(D/O)_{LB} =$

$(3.84\pm0.16)\times10^{-2}$ (see Figure 1, left panel). This homogeneity of $(\mathrm{D/O})_{\mathrm{LB}}$ argues against variations of D/H in the LB. Indeed, the only possible way for a stable D/O together with a varying D/H would be for D/H and O/H to be correlated. Moreover, they would have to precisely vary in such a way that D/O remains constant. That seems unlikely for two different reasons: (i) O/H appears to be uniform in the interstellar medium over paths of several hundred parsecs (Meyer et al. 2001; André et al. 2003; Cartledge et al. 2004), and (ii) astration processes should lead to an anti-correlation of DI and OI abundances.

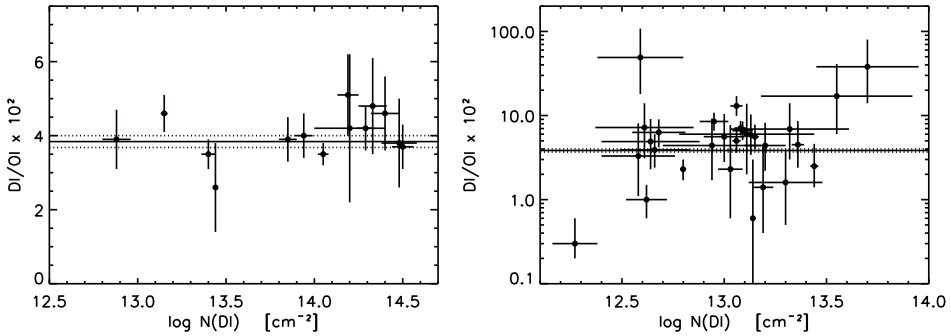

Figure 1. D/O in the Local Bubble from *FUSE* (left) and HST (right) measurements.

Using the interstellar O/H ratio from Meyer (2001), the $(\mathrm{D/O})_{\mathrm{LB}}$ ratio translates into $(\mathrm{D/H})_{\mathrm{LB}} = (1.32\pm0.08)\times10^{-5}$. According to the error bars, this result is $2.5\,\sigma$ lower than the direct $(\mathrm{D/H})_{\mathrm{LB}}$ measurement reported above, which is significant. The explantion is unlikely to be due to the O/H used to translate D/O into D/H, as Oliveira et al. (2005) found a $(\mathrm{O/H})_{\mathrm{LB}}$ ratio in good agreement with the O/H ratio measured in more distant interstellar medium by Meyer (2001). Whatever is the explanation, the homogeneity of the local D/O measurements implies that the spatial variations of D/H in the Local Bubble must be extremely small, if any (Hébrard & Moos 2003).

It seems now that the homogeneity of the deuterium abundance within the Local Bubble has reached consensus. One can note however the N(DI) and N(OI) measurements reported within 100 pc by Redfield & Linsky (2004), using HST data. The corresponding D/O ratios are plotted in Figure 1 (right panel). A wide dispersion appears of about 2 orders of magnitude. Apparently, the *FUSE* and HST studies produce opposite conclusions. It is unlikely that a malicious systematic effect disturbs the *FUSE* measurements in a way that erases actual variations. More probably, the HST measurements are perturbed in a random way by uncontroled systematics. The probable cause is the N(OI) measurements, performed with the λ1302Å saturated transition in the HST spectra, whereas N(OI) is measured from unsaturated lines in the *FUSE* bandpass. Hébrard et al. (2005) and Friedman et al. (2006) have shown examples of systematic effects on column densities due to saturated lines.

4. Deuterium in the distant interstellar medium

Whatever the true $(\mathrm{D/H})_{\mathrm{LB}}$ is, 1.32×10^{-5} or 1.56×10^{-5}, it now appears clear that this ratio should not be considered as a canonical value for $(\mathrm{D/H})_{\mathrm{ISM}}$. $(\mathrm{D/H})_{\mathrm{LB}}$ is not representative of the cosmic material at the present epoch. Indeed, in addition to the

early *Copernicus* results reported above, *FUSE* has provided extra clues for a significant dispersion in $(D/H)_{ISM}$ beyond the Local Bubble (Friedman et al. 2002; Hoopes et al. 2003; Wood et al. 2004; Williger et al. 2005; Hébrard et al. 2005; Friedman et al. 2006; Oliveira & Hébrard 2006; Oliveira et al. 2006; Dupuis et al. 2009). It is difficult to decide which one of the different values is representative of the present epoch, and even if a canonical value for $(D/H)_{ISM}$ does exist. There is certainly no reason to preferentially adopt $(D/H)_{LB}$.

If a $(D/H)_{ISM}$ canonical value exists, the best way to determine it might be to measure deuterium along the long lines of sight with high column densities. More material is probed, and thus localized anomalies are likely to be averaged out. Following that approach, Hébrard & Moos (2003) reported a trend mainly based on D/O: the deuterium abundance is lower for the most distant lines of sight and the highest column densities. This trend was reinforced since then by the additional *FUSE* results, as shown on the left panel of Figure 2. This figure plots the lines of sight from Hébrard & Moos (2003) and all the subsequent *FUSE* measurement published after and quoted above. It does not include the HST measurements presented in Redfield & Linsky (2004). On this plot, the local D/O is homogeneous; the distant D/O is also homogeneous, but with a value about two times lower. There are just two lines of sight with high D/O (Oliveira et al. 2006), but the OI column density is here possibly affected by saturation, as shown in the cases discussed in Hébrard et al. (2005) and Friedmand et al. (2006).

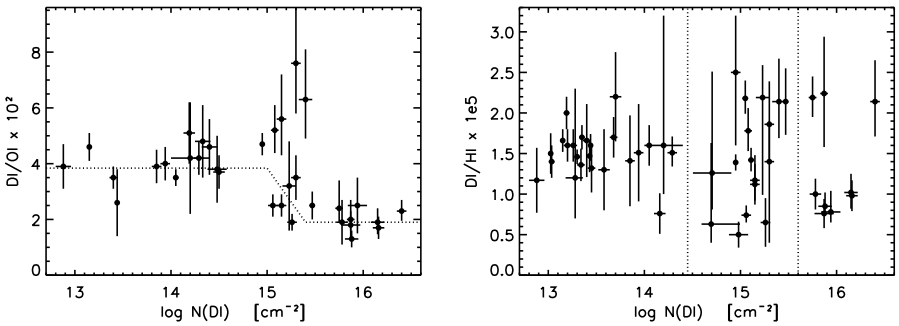

Figure 2. D/O and D/H as a function of DI column density.

This trend could suggest that the local deuterium abundance might be abnormally high, whereas the actual value of $(D/H)_{PE}$ may be significantly below 1×10^{-5} (Hébrard & Moos 2003). On the other hand, following an idea proposed by Jura (1982) and updated by Draine (2004; 2005), Wood et al. (2004) argued that deuterium can be preferentially depleted onto dust grains. This would imply total $(D/H)_{ISM}$ ratios larger than those measured in the gas phase, and a $(D/H)_{PE}$ value significantly larger than 2×10^{-5}. Thus, presently, two possibilities are proposed for the present-epoch deuterium abundance.

5. Two scenarios for $(D/H)_{PE}$

If deuterium is significantly depleted onto dust grains, $(D/H)_{PE}$ can only be measured in interstellar clouds in which all deuterium has been released in the gas phase by recent shocks. Assuming this is the case for the few high $(D/H)_{ISM}$ values measured to date,

Linsky & Wood (2004) claimed $(\mathrm{D/H})_{\mathrm{PE}} = (2.3 \pm 0.4) \times 10^{-5}$. Following this idea, this value was updated to $(\mathrm{D/H})_{\mathrm{PE}} \geqslant (2.3 \pm 0.2) \times 10^{-5}$ by Linsky et al. (2006), and to a similar vaue $(\mathrm{D/H})_{\mathrm{PE}} \geqslant (2.0 \pm 0.1) \times 10^{-5}$ using a Bayesian approach by Prodanovic et al. (2009). According to this scenario, lower D/H ratios are found for the sight lines which probe primarily interstellar clouds that have not been recently shocked. That may explain the three D/H regimes apparently seen by Linsky et al. (2006). Locally, the D/H is homogeneous but lower than $(\mathrm{D/H})_{\mathrm{PE}}$ because the Local Bubble has been shocked recently, but not recently enough, so that part of the deuterium has been incorporated in the solid phase. At intermediate column densities, D/H shows variations, depending on the nature of the clouds, which may or may not have been shocked. Thirdly, at the largest column densities, deuterium is on average significantly depleted in the interstellar clouds probed, except for a few recently shocked clouds.

However, this third regime presenting an homogeneous, low D/H was not confirmed by subsequent *FUSE* measurements. This is shown in right panel of Figure 2, which includes all the measurements available now. The two vertical lines show the limits of the three regimes, as presented in Linsky et al. (2006). Rather than a 3-regime picture, this plot shows an homogeneous D/H ratio locally, and an increasing dispersion together with the increasing column density.

Moreover, the D/O measurements are difficult to fit with the depletion scenario. Indeed, D/H and D/O measurements are presently available for 9 distant targets (i.e. clearly outside the Local Bubble): HD 195965 and HD 191877 (Hoopes et al. 2003), LSS 1274 (Hébrard & Moos 2003; Wood et al. 2004), JL 9 (Wood et al. 2004), PG 0038+199 (Williger et al. 2005), HD 90087 (Hébrard et al. 2005), LSE 44 (Friedman et al. 2006), HD 41161 and HD 53975 (Oliveira & Hébrard 2006). The χ^2 are 35.8 for D/H and 5.9 for D/O, for 8 degrees of freedom. Thus, D/O measurements show less dispersion than D/H. Here again, it is difficult to guess a malicious effect able to erase actual variations in the deuterium abundance. In fact, the D/O measurements suggest a different scenario than the "depletion" hypothesis. In Figure 2 (left panel), D/O is homogeneous, with values near 3.8×10^{-2} for $\log N(\mathrm{DI}) \leqslant 15$, i.e. in the Local Bubble, and is homogeneous with about two times lower value for $\log N(\mathrm{DI}) \geqslant 15.5$. The intermediate region ($15 \leqslant \log N(\mathrm{DI}) \leqslant 15.5$) appears more as a transition between these two different plateaus than a particular regime in itself. The lines of sight showing high D/H show low D/O (Williger et al. 2005; Friedman et al. 2006; Oliveira & Hébrard 2006).

The values of D/O for sight lines to distant targets are homogeneous, around $(2.0 \pm 0.5) \times 10^{-2}$. Because these lines of sight probe large amounts of material, this ratio may be characteristic of the present epoch. If so, it would imply $(\mathrm{D/H})_{\mathrm{PE}} = (7 \pm 2) \times 10^{-6}$. Then, the reason for a high local D/H value is uncertain; the possibility of unknown deuterium enrichment process(es) or local infall of less evolved material must be considered. One can note that Cartledge et al. (2004) invoked local infall to possibly explain their O/H measurements.

6. Conclusions

The "depletion argument" and the "D/O argument" lead to two different values for $(\mathrm{D/H})_{\mathrm{PE}}$: $\sim 2.3 \times 10^{-5}$ and $\sim 7 \times 10^{-6}$, respectively. As shown in Figure 3, the high $(\mathrm{D/H})_{\mathrm{PE}}$ would imply a low deuterium destruction through astration, even possibly no destruction at all. Conversely, the low $(\mathrm{D/H})_{\mathrm{PE}}$ would imply larger depletion factors f_{ev}, especially in the latest stages of the Universe evolution.

It appears clearly that the local value 1.5×10^{-5} should no longer be considered as a canonical value for $(\mathrm{D/H})_{\mathrm{PE}}$. Up to now, neither the "depletion" nor the "D/O"

hypothesis (or both of them) can be firmly ruled out. Their is no hope of extra deuterium measurements in the distant interstellar medium, as *FUSE* now stopped operations. In addition, it won't be possible to probe deuterium on column densities larger than those detected with *FUSE*, as the denser ones are at the limit where unsaturated deuterium lines are detectable. Additional deuterium measurements are thus unlikely to provide new constraints on this issue for a while.

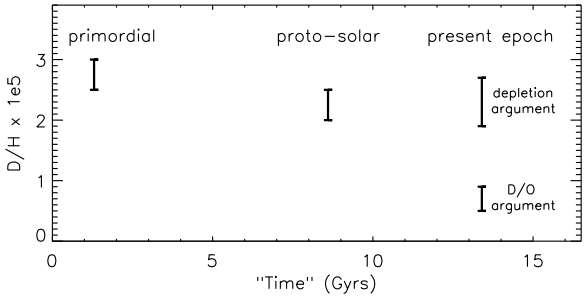

Figure 3. Deuterium abundance as a function of time after BBN.

References

André, M. K., Oliveira, C. M., Howk, J. C., et al. 2003, ApJ, 591, 1000
Cartledge, S., Lauroesch, J. , Meyer, D., Sofia U. 2004, ApJ, 613, 1037
Chiappini, C., Renda, A., & Matteucci, F. 2002, A&A, 395, 789
Dupuis, J., Hébrard, G., Oliveira, C., Moos, H. W., Sonnentrucker, P., 2009, ApJ, 690, 1045
Friedman, S. D., Howk, J. C., Chayer, P., et al. 2002, ApJS, 140, 37
Friedman, S. D., Hébrard, G., Tripp, T. M., et al. 2006, ApJ, 638, 847
Hébrard, G., Lemoine, M., Vidal-Madjar, A., et al. 2002, ApJS, 140, 103
Hébrard, G., & Moos, H. W. 2003, ApJ, 599, 297
Hébrard, G., Tripp, T. M., Chayer, P., et al. 2005, ApJ, 635, 1136
Hoopes, C. G., Sembach, K. R., Hébrard, G., et al. 2003, ApJ, 586, 1094
Lallement, R., & Bertin, P. 1992, A&A, 266, 479
Laurent, C., Vidal-Madjar, A., & York, D. G. 1979, ApJ, 229, 923
Lemoine, M., Vidal-Madjar, A., Hébrard, G., et al. 2002, ApJS, 140, 67
Linsky, J. L., Diplas, A., Wood, B. E., et al. 1995, ApJ, 451, 335
Linsky, J. L. & Wood, B. E. 1996, ApJ, 463, 254
Linsky, J. L., Draine, B. T., Moos, H. W., et al., 2006, ApJ, 647, 1106
Meyer, D. M. 2001, XVIIth IAP Colloquium, Paris, Edited by R. Ferlet et al., p. 135
Moos, H. W., Sembach, K. R., Vidal-Madjar, A., et al. 2002, ApJS, 140, 3
Oliveira, C. M., Hébrard, G., Howk, J. C., et al. 2003, ApJ, 587, 235
Oliveira, C. M., Hébrard, G., 2006, ApJ, 653, 345
Oliveira, C. M., Moos, H. W., Chayer, P., Kruk, J. W., 2006, ApJ, 642, 283
Prodanovic, T., Steigman, G., Fields, B. D., 2009, arXiv:0910.4961
Redfield, S., & Linsky, J. L. 2004, ApJ, 602, 776
Snowden, S. L., Egger, R., Finkbeiner, D. P., et al. 1998, ApJ, 493, 715
Sonneborn, G., André, M., Oliveira, C., et al. 2002, ApJS, 140, 51
Timmes, F. X., Truran, J. W., Lauroesch, J. T., & York, D. G. 1997, ApJ, 476, 464
Vidal-Madjar, A. & Ferlet, R. 2002, ApJ, 571, L169
Williger, G. , Oliveira, C., Hébrard, G., Dupuis, J., Dreizler, S., Moos, H. W., 2005, ApJ 625, 210
Wood, B. E., Linsky, J. L., Hébrard, G., et al. 2004, ApJ, 609, 838
York, D. G. 1983, ApJ, 264, 172

Light elements in the Universe
Proceedings IAU Symposium No. 268, 2010
C. Charbonnel, M. Tosi, F. Primas & C. Chiappini, eds.

DOI: 00.0000/X000000000000000X

(Un)true deuterium abundance in the Galactic disk

Tijana Prodanović[1], Gary Steigman[2] and Brian D. Fields[3]

[1]Department of Physics, University of Novi Sad,
Trg Dositeja Obradovića 4, 21000 Novi Sad, Serbia
email: prodanvc@df.uns.ac.rs

[2]Department of Physics and Astronomy, Ohio State University,
191 W. Woodruff Ave., Columbus OH 43210-1117, USA
email: steigman@mps.ohio-state.edu

[3]Department of Astronomy, University of Illinois,
1002 W. Green St., Urbana IL 61801, USA
email: bdfields@illinois.edu

Abstract. Deuterium has a special place in cosmology, nuclear astrophysics, and galactic chemical evolution, because of its unique property that it is only created in the big bang nucleosynthesis while all other processes result in its net destruction. For this reason, among other things, deuterium abundance measurements in the interstellar medium (ISM) allow us to determine the fraction of interstellar gas that has been cycled through stars, and set constraints and learn about different Galactic chemical evolution (GCE) models. However, recent indications that deuterium might be preferentially depleted onto dust grains complicate our understanding about the meaning of measured ISM deuterium abundances. For this reason, recent estimates by Linsky et al. (2006) have yielded a lower bound to the "true", undepleted, ISM deuterium abundance that is very close to the primordial abundance, indicating a small deuterium astration factor contrary to the demands of many GCE models. To avoid any prejudice about deuterium dust depletion along different lines of sight that are used to determine the "true" D abundance, we propose a model-independent, statistical Bayesian method to address this issue and determine in a model-independent manner the undepleted ISM D abundance. We find the best estimate for the *gas-phase* ISM deuterium abundance to be $(\mathrm{D/H})_{\mathrm{ISM}} \geqslant (2.0 \pm 0.1) \times 10^{-5}$. Presented are the results of Prodanović et al. (2009).

Keywords. ISM: abundances, ISM: dust, Galaxy: abundances, Galaxy: evolution

1. Introduction

Deuterium is only created in significant amounts during the big bang nucleosynthesis (BBN) while all other processes destroy it (Epstein et al. 1976, Prodanović & Fields 2003, Steigman 2007). Consequently, the deuterium abundance should monotonically decrease after the Big Bang, where the main destruction channel is the stellar processing. Because of this unique property deuterium can be used as a cosmic baryometer but also to discriminate between different Galactic chemical evolution (GCE) models (see eg. Steigman et al. 2007, Prodanović & Fields 2008, Vangioni-Flam et al. 1994). Specifically, given that deuterium is mostly destroyed in stars, its abundance ($y_{\mathrm{D}} \equiv 10^5(\mathrm{D/H})$) can be used to probe the fraction of the interstellar gas that has never been processed through stars (Steigman & Tosi 1992, 1995), which is often quantified with the astration factor $f_{\mathrm{D}} \equiv y_{\mathrm{DP}}/y_{\mathrm{D,ISM}}$, the ratio of the primordial D abundance (the D to H ratio by number) to the ISM D abundance.

The primordial D abundance, y_{DP}, predicted by the BBN model (Cyburt et al. 2003,

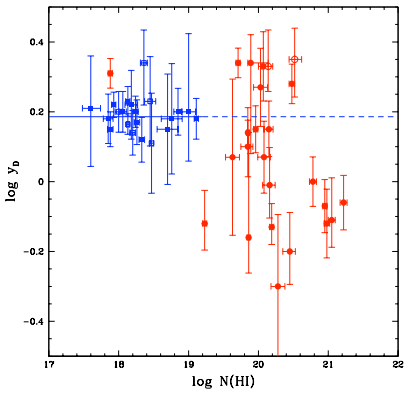

Figure 1. The logs of the deuterium abundances versus the logs of the H I column densities [cm^{-2}] for the 46 LOS from Table 2 of Linsky et al.(2006). The filled symbols are for the 38 LOS which have iron abundance data, while the open symbols are for the 8 LOS which lack iron abundances. The squares (blue) are for the LOS within the Local Bubble (LB) and the circles (red) are for the non-LB (nLB) LOS. The solid line is at the mean D abundance for the LB LOS ($\log y_{\mathrm{D,LB}} = 0.19$); the dashed line is its extension to the nLB LOS.

Steigman 2007) based on the cosmic microwave background observations (Spergel et al. 2007), is in excellent agreement with D abundance observations at high-redshift systems (Pettini et al. 2008). However, observations of the *gas-phase* deuterium abundance in the interstellar medium (ISM) have revealed large variations over different lines of sight (LOS) by factors of ~ 4 ($0.5 \lesssim y_{\mathrm{D,ISM}} \equiv 10^5(\mathrm{D/H})_{\mathrm{ISM}} \lesssim 2.2$; Jenkins et al. 1999, Hébrard et al. 2002, Sonneborn et al. 2000, Hoopes et al. 2003). The range of these variations is best seen on Figure 1, where we have plotted the logs of the gas-phase D/H ($\log y_{\mathrm{D}} \equiv 5 + \log\mathrm{N(D\,I)} - \log\mathrm{N(H\,I)}$) as a function of the logs of the H I column densities toward 46 different LOS inside and outside of the Local Bubble (LB) where the data has been taken from Linsky et al.(2006). Blue squares represent 21 LB LOS, while red circles represent 25 LOS from outside of the LB. Filled symbols represent those LOS for which iron abundance has also been measured. As an explanation for the observed scatter, it has been proposed that the gas-phase deuterium is depleted onto dust grains preferential to hydrogen (Jura 1982, Draine 2006). This hypothesis is in agreement with findings that the gas phase D/H correlates positively with refractory elements (Prochaska et al. 2005, Linsky et al. 2006, Steigman et al. 2007).

Arguing that deuterium is severely depleted onto dust grains, Linsky et al.(2006) have used the five *highest* D/H ratios to determine the *lower bound* to the true, gas-phase ISM deuterium abundance $y_{\mathrm{D,ISM}} \geqslant 2.31 \pm 0.24$, which is at the level of $\sim 80\%$ of the primordial deuterium abundance $y_{\mathrm{DP}} = 2.82^{+0.20}_{-0.19}$ (Pettini et al. 2008). Adopting this new estimate of the ISM D abundance, and the primordial abundance of Pettini et al.(2008), one finds the upper bound to the astration factor $f_{\mathrm{D}} \leqslant 1.22 \pm 0.15$, which is inconsistent with many GCE models that require $1.4 \lesssim f_{\mathrm{D}} \lesssim 1.8$ (Steigman et al. 2007). In order to account for such high ISM deuterium abundance and a low astration factor, most GCE models would require large infall rates of close to pristine material (Romano et al. 2006, Prodanović & Fields 2008).

Because the observed variations and a possibly severe dust-depletion complicate determination of the true, gas-phase, deuterium abundance in the ISM, we have proposed a

Bayesian statistical approach (§2) in analyzing the deuterium data which yields the maximum likelihood estimate of the true, undepleted, *gas-phase* ISM deuterium abundance $y_{\rm D,max}$(Prodanović et al. 2009). The underlying assumption of this analysis is that the observed spread in abundance measurements is the result of incompletely homogenized dust depletion. Our results are presented in §3, and conclusions in §4.

2. Bayesian analysis

To limit ourself to fewest assumptions possible, we have analyzed the FUSE ISM gas-phase deuterium abundance measurements (46 LOS from Table 2. of Linsky et al. 2006) by using a statistical Bayesian approach, which was first developed by Hogan et al.(1997) for the purpose of determining the primordial helium abundance that best fits the observations. The main assumption of this approach is that, in our case, depletion of gas-phase deuterium abundance is present at some level, but where there is no further assumption about the nature, level or spatial distribution of this depletion. In this sense, the Bayesian statistical approach is model independent. Thus, the available data are analyzed in an unbiased, statistical manner, which as a result determines the two parameters – the undepleted (or a lower bound to it), gas-phase ISM D abundance $y_{\rm D,ISM} \gtrsim y_{\rm D,max}$, and the depletion parameter $w \equiv y_{\rm D,max} - y_{\rm D,min}$.

The values of the two parameters, $y_{\rm D,max}$ and w, that best fit the set of measurements $y_{{\rm D},i}$, with errors δ_i, are found by determining the maximum value of the likelihood function

$$\mathscr{L}(y_{\rm D,max}; w) = \prod_i P(y_{{\rm D},i}|y_{\rm D,max}; w) \tag{2.1}$$

$$= \prod_i \int dy_{{\rm D},i,{\rm T}} P(y_{{\rm D},i}|y_{{\rm D},i,{\rm T}}) P(y_{{\rm D},i,{\rm T}}|y_{\rm D,max}; w) \tag{2.2}$$

The probability distribution $P(y_{{\rm D},i}|y_{{\rm D},i,{\rm T}})$ represents the probability of measuring the abundance $y_{{\rm D},i}$ along the ith LOS , given the true, error-free (but possibly depleted!) abundance $y_{{\rm D},i,{\rm T}}$ along that LOS. This distribution reflects the fact that real observed data have errors, and thus we assume that the shape of this distribution is a Gaussian of width σ_i. We treat the data with asymmetrical errors by assuming that σ_{i+} corresponds to $y_{{\rm D},i} > y_{{\rm D},i,{\rm T}}$ and σ_{i-} to $y_{{\rm D},i} < y_{{\rm D},i,{\rm T}}$. The probability distribution $P(y_{{\rm D},i,{\rm T}}|y_{\rm D,max}; w)$ is the probability of finding the true, depleted, LOS deuterium abundance $y_{{\rm D},i,{\rm T}}$, given the values of the maximum and minimum gas phase ISM deuterium abundances, $y_{\rm D,max}$ and $y_{\rm D,min} = y_{\rm D,max} - w$ respectively. If we assume that depletion is due to dust, then $P(y_{{\rm D},i,{\rm T}}|y_{\rm D,max}; w)$ represents the distribution of dust depletion along different LOS w_i. Given that we know very little about this distribution, and to limit ourselves to the fewest assumptions possible, we adopt three simplest forms of this depletion distribution: a top-hat (all levels of depletion are equally probable), a positive-bias (favors low depletion) and a negative-bias (favors large depletion) function. Functional forms of the three depletion distributions for $y_{\rm D,min} \leqslant y_{{\rm D},i,{\rm T}} \leqslant y_{\rm D,max}$ are given in Eq. (2.3), while outside of this range $P(y_{{\rm D},i,{\rm T}}|y_{\rm D,max}; w) = 0$. All depletion distributions are normalized to unity when integrated over $y_{{\rm D},i,{\rm T}}$.

$$P_t(y_{{\rm D},i,{\rm T}}|y_{\rm D,max}; w) = \begin{cases} 1/w\ , & \text{Top-hat} \\ 2(y_{{\rm D},i,{\rm T}} - y_{\rm D,min})/w^2, & \text{Positive-bias} \\ 2(y_{\rm D,max} - y_{{\rm D},i,{\rm T}})/w^2, & \text{Negative-bias} \end{cases} \tag{2.3}$$

With a choice of depletion distribution and a set of deuterium abundance measurements

with errors $y_{\mathrm{D},i}, \delta_i$, from Equation (2.2) one can numerically calculate the likelihood function $\mathscr{L}(y_{\mathrm{D,max}}; w)$ for a choice of parameter $(y_{\mathrm{D,max}}; w)$ values. Likelihood is then calculated for a range of parameter values, where the combination of values that results in the maximum likelihood determines the most likely value of undepleted, gas-phase ISM deuterium abundance $y_{\mathrm{D,max}}$ and the corresponding depletion parameter w, that best fit the observed abundances (with their errors) with a spread that results from depletion of deuterium onto dust (Prodanović et al. 2009).

3. Results

Because the spread between the observed abundances is very different for only LB and only non-LB LOS (Fig. 1), we have first analyzed the two subsets of data separately. The analyzed data have been taken from Table 2 of Linsky et al.(2006), and there are 21 LB LOS and 25 non-LB LOS (about LB and non-LB LOS assignment see Linsky et al. 2006, Prodanović et al. 2009).

Measured LB deuterium abundances show very little scatter, and thus it is not surprising that all three shapes of depletion distribution given in Eq. (2.3) yield almost the same maximum likelihood udepleted, gas-phase deuterium abundance $y_{\mathrm{D,max}} \approx 1.5$ which is consistent with no depletion $w \approx 0$. The likelihood contours for the top-hat case and for the LB data are shown on the top panel of Fig. 2. This deuterium abundance that best fits the LB observations results in the astration factor $f_{\mathrm{D}} \leqslant 1.8$ (Prodanović et al. 2009) which is consistent with a range of successful GCE models presented in Steigman et al.(2007). In terms of the GCE models presented in Prodanović & Fields (2008) where the infall rate of the pristine material is taken to be proportional to the star formation rate with the proportionality constant α, our new ISM deuterium abundance for this

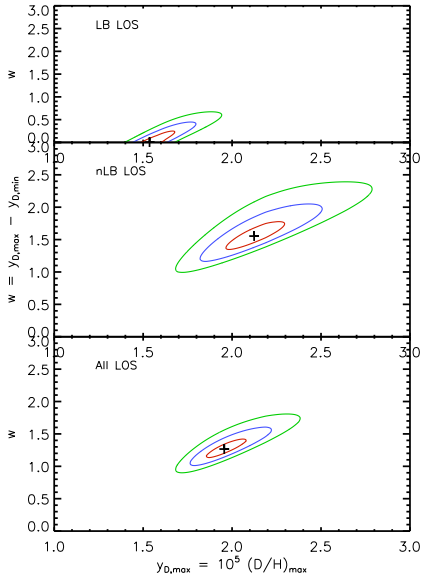

Figure 2. Likelihood contours (68%, 95%, 99%) in the w – $y_{\mathrm{D,max}}$ plane for the 21 LB LOS (top panel), the 25 nLB LOS (middle panel), and all 46 LOS (bottom panel), using the top-hat prior.

case, is consistent with low infall rates $\alpha \lesssim 0.1$ and return fractions of $R \lesssim 0.5$ (fraction of the stellar mass that is returned to the ISM), which can now accommodate even the more recent initial mass functions.

On the other hand, observations of the gas-phase D abundances along different LOS outside of the LB, show significant scatter which can be seen from Fig. 1. The maximum likelihood values for the non-LB data set and the top-hat depletion distribution are $y_{\rm D,max} = 2.1$ and $w = 1.6$. This result is presented on the middle panel of Figure 2 (Prodanović et al. 2009). The resulting astration factor $f_{\rm D,LB} \leqslant 1.3$ is within the errors consistent with some GCE models discussed in Steigman et al.(2007). Within our new ISM D abundance in this case, a wide range of infall rates required by the GCE models of Prodanović & Fields (2008) is now allowed with the infall parameter $0 \lesssim \alpha \lesssim 1$ where the corresponding return fractions can be found in the range are $0.2 \lesssim R \lesssim 0.4$, which can again accommodate even the modern initial mass functions.

Finally, when the full data set with all 46 LOS deuterium observations is considered with a choice of a top-hat depletion distribution, the maximum likelihood value of the undepleted, gas-phase deuterium abundance that best fits the observed data is found to be $y_{\rm D,max} = 2.0$ with a non-zero depletion of $w = 1.3$. This result is presented on the bottom panel of Figure 2 (Prodanović et al. 2009). The corresponding astration factor is found to be $f_{\rm D} \leqslant 1.4$ which is consistent with some but not all GCE models adopted Steigman et al.(2007). Similarly to the non-LB case, a wide range of the GCE models presented in Prodanović & Fields (2008) is allowed with our new estimate of the undepleted, gas-phase D abundance.

The two subsets of data, only LB and only non-LB, as well as the complete set of all 46 LOS measurements, have all been analyzed with all three depletion probability distributions from Eq. (2.3). In all cases, it was found that the top-hat distribution results in the largest maximum likelihood value, i.e. that it fits the spread observed in the data the best (Prodanović et al. 2009).

4. Conclusion

Observations of deuterium in the ISM have revealed large variations (Jenkins et al. 1999, Hébrard et al. 2002, Sonneborn et al. 2000, Hoopes et al. 2003) which complicates the determination of the unique, ISM deuterium abundance (see Figure 1). It was proposed that the observed variations originate from inhomogeneous depletion of deuterium onto dust grains preferential to hydrogen (Jura 1982, Draine 2006). In the light of this hypothesis, Linsky et al.(2006) have proposed that most of the deuterium in the ISM has been depleted and that the true, undepleted D abundance is $y_{\rm D,ISM} \geqslant 2.31 \pm 0.24$ which is at the $\sim 80\%$ level of the primordial D abundance (Pettini et al. 2008). If the ISM D abundance is indeed so high this in turn creates tension with otherwise successful GCE modes (see eg. Romano et al. 2006, Prodanović & Fields 2008).

Because of the importance of knowing the undepleted, gas-phase ISM D abundance, we have employed a model-independent Bayesian statistical analysis first used by Hogan et al.(1997) to determine the primordial helium abundance. By determining the maximum likelihood value of the likelihood function for the assumed depletion distribution function, this approach yields the values of two parameters, undepleted, gas-phase deuterium abundance $y_{\rm D,max}$ and the depletion parameter w, that best fit the observed data and scatter which is assumed to be due to different, in our case dust, depletion levels. We have investigated three different depletion distribution functions: a top-hat that equally favors both high and low depletion levels, a positive-bias that favors low-depletion and a negative-bias function that favors large depletion. Of the three depletion distributions

the uniform top-hat distribution results in the largest maximum likelihood and thus fits the data best.

We have applied the Bayesian statistical analysis to the data set of deuterium abundance measurements along 46 different LOS, where the data has been adopted from Linsky et al.(2006). Figure 2 shows likelihood contours for the top-hat depletion distribution and for Bayesian analysis applied to 3 data subsets: LB only, non-LB only and the full data set. We found that the LB deuterium abundance measurements are consistent with having zero depletion $w = 0$ and D abundance of $y_{\rm D,LB} = 1.5(1 \pm 0.03)$. Unlike the LB, the non-LB data require significant depletion. Because it is still unclear whether the LB D is undepleted while some or all non-LB LOS have been enriched by unmixed infall, or if LB is uniformly depleted, we find that the best estimate of the undepleted, gas-phase ISM deuterium abundance is that which follows from analyzing the full 46 LOS data set, with a top-hat depletion distribution function, and is $y_{\rm D,ISM} \geqslant y_{\rm D,max} = 2.0 \pm 0.1 = 2.0(1 \pm 0.05)$ (Prodanović et al. 2009). With the primordial deuterium abundance adopted from Pettini et al.(2008), we find that our new ISM D abundance corresponds to the astration factor $f_{\rm D} \leqslant 1.4 \pm 0.1$ that is consistent with some successful GCE models (Steigman et al. 2007, Prodanović & Fields 2009), which releases some tension with GCE models that is created when a high ISM deuterium abundance, such as that of Linsky et al.(2006), is required.

Acknowledgements

The work of TP is supported in part by the Provincial Secretariat for Science and Technological Development, and by the Ministry of Science of the Republic of Serbia under project number 141002B.

References

Cyburt, R.H., Fields, B.D. & Olive, K.A. 2003, *Phys. Lett. B*, 567, 227
Draine, B.T. 2006, *Astrophysics in the Far Ultraviolet: Five Years of Discovery with FUSE*, 348, 58
Epstein, R.I., Lattimer, J.M. & Schramm, D.N. 1976, *Nature*, 263, 198
Hébrard, G., et al. 2002, *ApJS,* , 140, 103
Hogan, C.J., Olive, K.A. & Scully, S.T. 1997, *ApJL,* , 489, L119
Hoopes, C.G., Sembach, K.R., Hébrard, G., Moos, H.W. & Knauth D.C. 2003, *ApJ,* , 586, 1094
Jenkins, E.B., Tripp, T.M., Woźniak, P.R., Sofia, U.J. & Sonneborn, G. 1999, *ApJ,* , 520, 182
Jura, M. 1982, *Advances in Ultraviolet Astronomy*, Kondo, Y., Mead, J., Chapman, R.D., eds., NASA, Washington, p. 54
Linsky, J.L., et al. 2006, *ApJ,* , 647, 1106
Pettini, M., Zych, B.J., Murphy, M.T., Lewis, A. & Steidel, C.C. 2008, *MNRAS*, 391, 1499
Prochaska, J.X., Tripp, T.M. & Howk, J.C. 2005, *ApJ,* , 620, L39
Prodanović, T. & Fields, B.D. 2003, *ApJ,* , 597, 48
Prodanović, T. & Fields, B.D. 2008, *JCAP*, 9, 3
Prodanović, T., Steigman, G., & Fields, B.D. 2009, *submitted to MNRAS*, arXiv:0910.4961
Romano, D., Tosi, M., Chiappini, C. & Matteucci, F. 2006, *MNRAS*, 369, 295
Sonneborn, G., Tripp, T.M., Ferlet, R., Jenkins, E.B., Sofia, U.J., Vidal-Madjar, A. & Woźniak, P.R. 2000, *ApJ,* , 545, 277
Spergel, D.N., et al. 2007, *ApJS,* , 170, 377
Steigman, G. & Tosi, M. 1992, *ApJ,* , 401, 150
Steigman, G. & Tosi, M. 1995, *ApJ,* , 453, 173
Steigman, G., Romano, D. & Tosi, M. 2007, *MNRAS*, 378, 576
Steigman, G. 2007, *Ann. Rev. Nucl. Part. Sci*, 57, 463
Vangioni-Flam, E., Olive, K.A. & Prantzos, N. 1994, *ApJ,* , 427, 618

Light elements in the Universe
Proceedings IAU Symposium No. 268, 2010
C. Charbonnel, M. Tosi, F. Primas & C. Chiappini, eds.

DOI: 00.0000/X000000000000000X

Abundances of hydrogen and helium isotopes in the Protosolar Cloud

Johannes Geiss[1] and George Gloeckler[2]

[1]International Space Science Institute, Hallerstrasse 6, CH-3012 Bern, Switzerland,
email: geiss@issibern.ch

[2]Department of Atmospheric, Oceanic and Space Sciences, University of Michigan
2455 Hayward St., Ann Arbor, MI 48109, USA
email: gglo@umich.edu

Abstract. For our understanding of the origin and evolution of baryonic matter in the Universe, the Protosolar Cloud (PSC) is of unique importance in two ways: 1) Up to now, many of the naturally occurring nuclides have only been detected in the solar system. 2) Since the time of solar system formation, the Sun and planets have been virtually isolated from the galactic nuclear evolution, and thus the PSC is a galactic sample with a degree of evolution intermediate between the Big Bang and the present.

The abundances of the isotopes of hydrogen and helium in the Protosolar Cloud are primarily derived from composition measurements in the solar wind, the Jovian atmosphere and "planetary noble gases" in meteorites, and also from observations of density profiles inside the Sun. After applying the changes in isotopic and elemental composition resulting from processes in the solar wind, the Sun and Jupiter, PSC abundances of the four lightest stable nuclides are given.

Keywords. Sun: solar wind, corona, abundances

1. Introduction

Our concepts of nucleosynthesis were originally derived from solar system abundances, and even to this day, our knowledge of the production of most stable and long-lived nuclei is based on elemental and isotopic composition measurements in solar system material. Without isotopic abundances in meteorites and terrestrial samples, could we clearly distinguish the s- and r-processes, recognize the p-nuclei or establish a nuclear chronology for the Galaxy? For most nuclear species, Galactic evolution models are really models for the evolution of the matter that made up the PSC some 4.6 Gyr ago. Extensions to the present for most nuclei would be mere extrapolations, if we had not reliable Galactic *and* solar system data for several elements and a few isotopic ratios. Among these are, most importantly, the isotopes of hydrogen and helium. Composition measurements in the solar wind, the Jovian atmosphere and to a lesser extend - the "planetary gas" in meteorites provide the main evidence from which the protosolar abundances of these nuclides are derived (Table 1).

2. Protosolar (D+^{3}He)/H derived from ^{3}He/^{4}He in the solar wind

In the early Sun, deuterium was converted into ^{3}He by the reaction

$$\mathrm{D} + \mathrm{H} = {}^3\mathrm{He} + \gamma. \tag{2.1}$$

The short D-burning phase, involving the whole Sun, preceded the H-burning epoch (Ezer & Cameron, 1965; Mazzitelli & Moretti, 1980). In the material of the Outer Convective Zone (OCZ) of the present Sun, ^{3}He has not been further processed, as can be surmised

Table 1. Measurements primarily used in this paper for deriving Solar and Protosolar Abundances.

SOLAR WIND ^{3}He/^{4}He measurements with SWICS/Ulysses, SWC/Apollo, old solar wind in lunar material → Extrapolation to ^{3}He/^{4}He in the OCZ (Outer Convective Zone of the Sun) →Protosolar (D + ^{3}He)/H → Protosolar D/H
METEORITES ^{3}He/^{4}He measurement in the "Planetary Gas" Component of Meteorites → Protosolar ^{3}He/^{4}He
SUN Density Profile from SOHO Seismology → Protosolar He/H
JUPITER ^{3}He/^{4}He, He/H measurement with Galileo Entry-Probe D/H measurement with ISO → Protosolar D/H, ^{3}He/^{4}He, (D + ^{3}He)/H

from the abundance there of beryllium (Geiss & Reeves, 1972). At any temperature ^{9}Be is destroyed much faster by thermonuclear reactions than ^{3}He (Figure 1). Thus, ^{3}He in the OCZ represents not only protosolar ^{3}He, but the sum of protosolar D and ^{3}He (see Geiss, Eberhardt & Signer, 1966).

Systematic investigations of ^{3}He/^{4}He in the solar wind have been carried out using various space experiments: SWC/Apollo, ICI/ISEE-3, SWICS/Ulysses, SWICS/ACE and

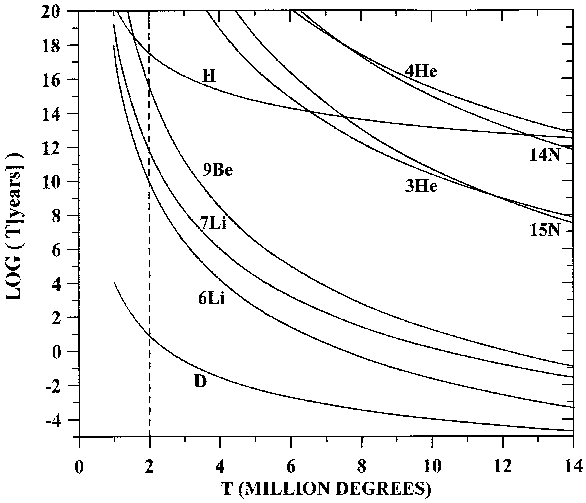

Figure 1. Life-time of light nuclides as a function of temperature. Given are the life-times due to thermonuclear reactions with density and composition normalized to the present conditions at the bottom of the Outer Convective Zone (OCZ) of the Sun. The dashed line marks the present temperature at the bottom of the OCZ. Note: D-burning proceeds well before H-burning commences due to the temperature difference at which the two hydrogen isotopes are fusing (Ezer & Cameron,1965; Mazzitelli & Moretti, 1980). ^{9}Be is destroyed much faster than ^{3}He at all temperatures that could have occurred during the life of the Sun. Thus the presence of Beryllium (^{9}Be) in the OCZ at protosolar abundance precludes the loss there of ^{3}He by nuclear reactions (Geiss & Reeves, 1972).

Table 2. Protosolar (D+^{3}He)/^{4}He from ^{3}He/^{4}He in the solar wind.

Solar Wind (SWICS/Ulysses)	^{3}He/^{4}He	Figure 1
Solar Wind (SWC/Apollo)	^{3}He/^{4}He	Figure 1
Sun, Outer Convective Zone	^{3}He/^{4}He	$(3.83 \pm 0.25) \times 10^{-4}$
Protosolar Cloud	**(D +^{3}He)/^{4}He**	$\mathbf{(3.68 \pm 0.25) \times 10^{-4}}$

recently Genesis. The results have revealed significant variations in solar wind composition. Theoretical studies have shown that the variations are caused by separation processes in the corona (Geiss, Hirt & Leutwyler, 1970; Bürgi & Geiss, 1986; Isenberg & Hollweg, 1983) as well as ion-neutral separation processes in or near the chromosphere (Geiss, 1982; von Steiger & Geiss, 1989). Several physical processes were identified that cause or control charging, separation and transport of major and minor ion species from the chromosphere to the corona and into the supersonic solar wind. Their varying influence produces the observed variations in space and time. Theory alone cannot exactly predict the changes in composition caused by different solar and solar wind conditions, but theory can predict which pairs of ion species should causally correlate and could be used to obtain OCZ abundances from solar wind data by extrapolation.

So far empirical extrapolations from abundances in the slow solar wind and the high-speed streams coming out of the polar coronal holes give the best results. We follow here the method introduced by Gloeckler & Geiss (2000). Figures 2a and 2b show, respectively, the correlations of ^{3}He/^{4}He with Si/O and with H/He measured by SWICS/Ulysses in several periods each of in-ecliptic solar wind and high speed streams. Extrapolating by linear regression to Si/O observed in the photosphere and to H/He = 11.9 determined for the OCZ (Pérez Hernández & Christensen-Dalsgaard, 1994) gives $(^3\mathrm{He}/^4\mathrm{He})_{\mathrm{OCZ}} = (3.78 \pm 0.18) \times 10^{-4}$ and $(^3\mathrm{He}/^4\mathrm{He})_{\mathrm{OCZ}} = (3.88 \pm 0.14) \times 10^{-4}$ respectively (Figure 2). The 1-σ errors include statistical uncertainties as well as the spread due to solar wind variability. The systematic instrumental uncertainties are estimated to be 0.2×10^{-4} (Gloeckler & Geiss, 2000). The two extrapolation methods give essentially the same result, leading to an average of $(^3\mathrm{He}/^4\mathrm{He})_{\mathrm{OCZ}} = (3.83 \pm 0.25) \times 10^{-4}$ (Table 2), which is in remarkable agreement with earlier values of $(^3\mathrm{He}/^4\mathrm{He})_{\mathrm{OCZ}}$ obtained by other methods (see Geiss & Gloeckler, 1998).

During the in-ecliptic periods, steady low-speed solar wind prevailed, free of CME events. Winds related to CMEs would compromise the correlation between ^{3}He/^{4}He and H/He, because they combine low H/He ratios with relatively high ^{3}He/^{4}He ratios, i.e. opposite to the correlation in Figure 2b.

We have plotted in Figure 2 also the average ^{3}He/^{4}He ratio of the SWC/Apollo experiments that collected the solar wind during five periods in 1969-1972 (Geiss et al., 2004, see also Geiss et al. 1970). These were slow wind periods (320-510 km/s), and there are no indications of a CME influence. The H/He and Si/O ratios for the SWC exposure periods are estimates. Solar wind composition data were rudimentary during the Apollo epoch (1969-1972). Thus the corresponding estimates of H/He and Si/O are crude by necessity.

Recently Heber et al. (2009) published precise isotopic abundances of noble gases including the ^{3}He/^{4}He ratio obtained from the DOS Genesis target. The Genesis value is 9 % higher then the SWC/Apollo average i.e. well within the known variability of in-ecliptic ^{3}He/^{4}He ratios. The collection period of the DOS target lasted 2.3 years and included slow solar wind, high speed streams and some CME events. Therefore, their results are not directly applicable to our extrapolation method.

The ^{3}He/^{4}He value derived from the extrapolations shown in Figure 2 refers to the

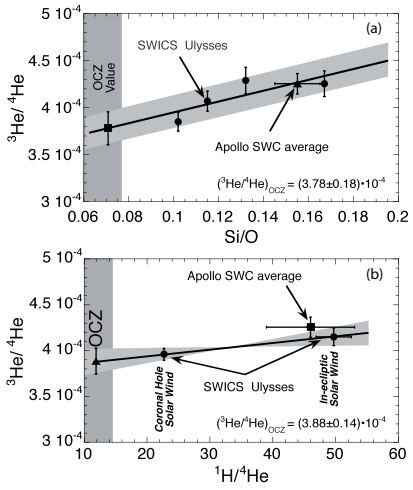

Figure 2. ^{3}He/^{4}He versus Si/O (2a) and ^{1}H/^{4}He (2b)) measured in the Solar Wind with SWICS/Ulysses and extrapolated to the corresponding values in the Outer Convective Zone (OCZ) of the Sun (adapted from Gloeckler & Geiss, 2000). The OCZ value for H/He was given by Pérez Hernández & Christensen-Dalsgaard (1994), the Si/O value by Grevesse & Sauval (1998). Combining these methods of extrapolation gives $^3\mathrm{He}/^4\mathrm{He} = (3.83 \pm 0.25) \times 10^{-4}$ for the OCZ (Table 2). The ^{3}He/^{4}He ratio measured in 1969-1972 with Apollo SWC is identical to the "in-ecliptic" ^{3}He/^{4}He ratio measured with SWICS/Ulysses during quiet slow solar wind conditions.

present-day OCZ. Two processes, however, could have changed this ratio during the life of the Sun.

Solar models show that He/H in the OCZ is 16% lower than it was in the PSC (e.g. Bahcall, Pinsonneault & Wasserburg, 1995). The difference is interpreted as being due to settling of helium out of the OCZ into deeper layers of the Sun. ^{3}He settles more slowly than ^{4}He, resulting in an increase in the present-day $(^3\mathrm{He}/^4\mathrm{He})_{\mathrm{OCZ}}$ ratio of 2 to 3% (Gautier & Morel, 1997).

The second possible change of $(^3\mathrm{He}/^4\mathrm{He})_{\mathrm{OCZ}}$ over solar history is due to solar mixing. During the lifetime of the Sun, the pp-reaction produces additional ^{3}He outside the solar core at intermediate depth in the Sun (Figure 3). H-burning at low temperature is controlled by the weak interaction reaction

$$^1\mathrm{H} + {}^1\mathrm{H} \rightarrow {}^2\mathrm{H} + e^+ + \nu. \qquad (2.2)$$

Deuterium (D or ^{2}H) is immediately converted into ^{3}He (Eq. 2.1). Further fusion of ^{3}He becomes effective only at substantially higher temperature (see Figure 1).

A significant increase of ^{3}He in the OCZ could have been caused by mixing of pp-produced ^{3}He into the OCZ. Theoretical studies show this increase to be small, dependent on solar models and solar rotation (Vauclair, 1998; Turck-Chièze et al., 2001). Recent changes in solar abundances imply changes in opacity. Whether this has a significant effect on solar mixing is under investigation.

Addition of pp-produced ^{3}He to the OCZ has also been investigated by comparing solar wind helium trapped in very old and more recent lunar surface material. Using this method, Wieler & Heber (2003) concluded, that the increase of ^{3}He/^{4}He in the OCZ by

Table 3. Protosolar ^{3}He/^{4}He from ^{3}He/^{4}He in Jupiter and the Meteoritic "Planetary Gas".

	^{3}He/^{4}He $\times 10^{-4}$
Planetary Component in Meteorites[1,2]	$\sim 1.5 \pm 0.2$
Q-Phase of Carbonaceous Chrondite Isna[3]	1.23 ± 0.02
Jupiter Entry-Probe[4]	1.66 ± 0.06
Protosolar Cloud[5]	$\mathbf{1.66^{+0.06}_{-0.10}}$

Notes: [1]Eberhardt (1974); [2]Frick & Moniot (1977); [3]Busemann, Baur & Wieler (2000); [4] Mahaffy et al (1998); [5]see text.

solar mixing is at most 5%. Combining the two effects, settling of helium out of the OCZ and solar mixing, we thus adopt a correction of $-(4 \pm 2)\%$ for $(^3\mathrm{He}/^4\mathrm{He})_{\mathrm{OCZ}}$ and obtain $[(\mathrm{D} + ^3\mathrm{He})/^4\mathrm{He}]_{\mathrm{PSC}} = (3.68 \pm 0.25) \times 10^{-4}$ (Table 2).

3. Protosolar ^{3}He/^{4}He

Before data of the Galileo Entry Probe were available, the ^{3}He/^{4}He ratio in the "planetary gas" of meteorites (e.g. Eberhardt, 1974; Frick and Moniot, 1977) served as a proxy for the isotopic abundance of helium in the PSC. More recently, it was realized that this planetary component is a mixture of components differing somewhat in composition. In Table 3 we have included the ^{3}He/^{4}He ratio in the "Q-phase" of the carbonaceous chondrite Isna (e.g., Busemann et al., 2000). The situation changed when the ^{3}He/^{4}He ratio in the Jovian atmosphere was measured by the Galileo Probe Mass Spectrometer (GPMS), (see Niemann et al., 1996). The ratio of $(1.66 \pm 0.06) \times 10^{-4}$ obtained by Mahaffy et al. (1998) given in Table 3 is presently considered to be the best value for estimating the protosolar value.

In the atmosphere of Jupiter helium is depleted by $\sim 18\%$ relative to the protosolar cloud (von Zahn, Hunten & Lehmacher, 1998). The degree, of helium depletion in the OCZ of the Sun is similar, but the causes could be quite different: diffusive separation in the case of the Sun, and probably descent of helium-rich droplets in the case of Jupiter (Stevenson & Salpeter, 1976; von Zahn, Hunten & Lehmacher, 1998). If the droplet hypothesis is correct, the Jovian process should fractionate isotopes much less than the solar process, and ^{3}He/^{4}He fractionation in the Jovian atmosphere would be less than the $\sim$2% fractionation that has occurred in the OCZ of the Sun (Gautier & Morel, 1997; Vauclair, 1998). Thus, we adopt here the Jovian ^{3}He/^{4}He ratio obtained by Mahaffy et al. (1998) as the protosolar value, giving it, however, an asymmetric error.

The ^{3}He/^{4}He ratios in the "planetary gas" of meteorites are typically lower by (10-20)% than the Jovian ratio (Table 3). If ^{3}He/^{4}He in the Jovian atmosphere is identical to the OCZ value, a depletion of ^{3}He/^{4}He by (10-20)% in the planetary component in meteorites is certainly not high, considering the large mass difference of the two helium isotopes (cf. Geiss & Gloeckler, 2003).

4. Protosolar deuterium abundance

The deuterium abundance in the PSC has been derived in two ways: One method is based on a direct deuterium abundance measurement in Jupiter, either by remote spectroscopy (e.g. Beer & Taylor, 1973; Drossart et al., 1982; Encrenaz et al., 1996; Lellouch et al., 2001) or by in-situ mass spectrometry (Niemann et al., 1996; Mahaffy et al., 1998). The values obtained by infrared spectroscopy have been given lower errors than those obtained by the Galileo Probe Mass Spectrometer (cf. Table 4). Lellouch

Table 4. Protosolar D/H from D/H in the Jovian Atmosphere.

	D/H $\times 10^{-5}$
Galileo Probe 1	2.6 ± 0.7
ISO 2	
H2	2.4 ± 0.4
CH4	2.2 ± 0.7
H2, CH4 Combined	2.25 ± 0.35
Corrected for D-Excess in Ice-Phase	2.1 ± 0.4
Protosolar D/H from Jovian D/H Data	$\mathbf{2.1 \pm 0.4}$

et al. (2001) measured D/H = $(2.40 \pm 0.4) \times 10^{-5}$ in molecular hydrogen and D/H = $(2.2 \pm 0.7) \times 10^{-5}$ in methane. Recently, Bézard (2002) obtained a D/H ratio in the methane below $< 2 \times 10^{-5}$. We adopt here the results of Lellouch et al. (2001) who combined their two determinations and obtained D/H = $(2.25 \pm 0.35) \times 10^{-5}$ as representative for Jupiter.

For the other method, the relation

$$(\mathrm{D/H})_{\mathrm{Protosolar}} = \{[(\mathrm{D} + {}^3\mathrm{He})/{}^4\mathrm{He}]_{\mathrm{Protosolar}} - ({}^3\mathrm{He}/{}^4\mathrm{He})_{\mathrm{Protosolar}}\} \times (\mathrm{He/H})_{\mathrm{Protosolar}} \quad (4.1)$$

is used. With protosolar (D + ^{3}He)/^{4}He = $(3.68 \pm 0.25) \times 10^{-5}$, protosolar ^{3}He/^{4}He = $(1.66^{+0.06}_{-0.10}) \times 10^{-4}$ (cf. Table 3) and protosolar H/He = 10.28 (Bahcall, Pinsonneault & Wasserburg (1995)) we obtain $(\mathrm{D/H})_{\mathrm{Protosolar}} = (1.97 \pm 0.3) \times 10^{-5}$ (Table 5).

Jupiters D/H ratio is probably enriched above the protosolar value by the admixture of deuterium-rich ices to the nebular gas during the planets formation (cf. Owen, 2003). According to Guillot (1999) the enrichment is about (5-10)%. Lellouch et al. (2001) have corrected their ISO value for this effect and obtain $(\mathrm{D/H})_{\mathrm{Protosolar}} = (2.1 \pm 0.4) \times 10^{-5}$. The agreement between the D/H ratio determined using the solar wind value and that based on Jupiter measurements is excellent. We adopt $(2.0 \pm 0.3) \times 10^{-5}$ as the protosolar D/H ratio (Table 5).

5. Remarks and Conclusions

The protosolar abundances of hydrogen and helium isotopes are summarized in Table 5. We give "recommended abundances" whenever there are two independent values for the same abundance ratio. Our results are not very different from those in our earlier publications (Gloeckler & Geiss, 2000; Geiss & Gloeckler, 2003).

Deriving OCZ abundances from solar wind measurements could be improved, if data from experiments with different capabilities can be sensibly combined. Using Figure 2b, we present here an example. The SWC/Apollo ^{3}He/^{4}He ratio is 2.9% above the SWICS/Ulysses correlation line. There are two extremes we could consider: (1) Assuming that the 2.9% difference is due to a systematic error of the ^{3}He/^{4}He ratios determined with SWICS Ulysses and the difference of 2.9% was the same for all solar wind conditions covered in Figure 2b, the Apollo data would extrapolate to $({}^3\mathrm{He}/{}^4\mathrm{He})_{\mathrm{OCZ}} = 3.99 \times 10^{-4}$. This value lies well within the systematic error limit assumed for the $({}^3\mathrm{He}/{}^4\mathrm{He})_{\mathrm{OCZ}}$ ratio in Table 2. (2) As Figure 2a suggests, we assume that there are no systematic deviations between the ^{3}He/^{4}He values measured by the two instruments. In this case we correlate the SWC/Apollo slow wind data point with the high speed data point measured by SWICS/Ulysses and obtain $({}^3\mathrm{He}/{}^4\mathrm{He})_{\mathrm{OCZ}} = 3.83 \times 10^{-4}$, about 1.3 % below the value

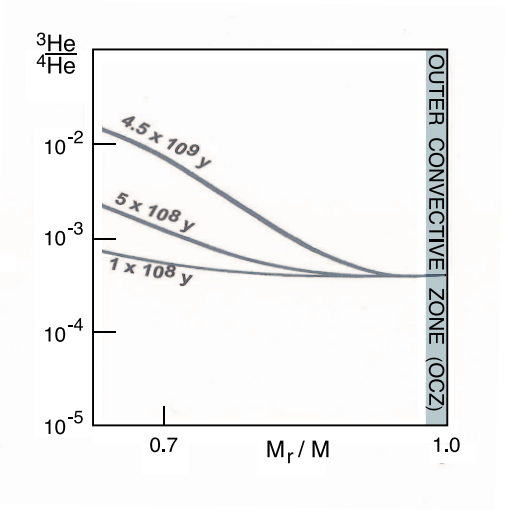

Figure 3. The secular buildup of ^{3}He at intermediate depth in the Sun as a function of M_r, (where M_r is the mass radius), calculated for a non-mixing Sun (Bochsler & Geiss, 1973) The buildup does not get close to the OCZ, but thorough experimental and theoretical investigations are needed to exclude contamination by ^{3}He produced at intermediate depth of the Sun.

Table 5. Protosolar Abundances.

From Solar Wind (SW) Data	$[(D+^3He)/H]_{Protosolar}$	$(3.58 \pm 0.25) \times 10^{-5}$
From Jupiter Data	$[(D+^3He)/H]_{Protosolar}$	$(3.72 \pm 0.42) \times 10^{-5}$
Recommended	$\mathbf{[(D+^3He)/H]_{Protosolar}}$	$\mathbf{(3.65 \pm 0.30) \times 10^{-5}}$
From Jupiter Data	$\mathbf{[^3He/H]_{Protosolar}}$	$\mathbf{(1.66^{+0.06}_{-0.10}) \times 10^{-4}}$
From Jupiter D/H	$[D/H]_{Protosolar}$	$(2.1 \pm 0.4) \times 10^{-5}$
From $(^3He/^4He)_{SW}$ and $(^3He/^4He)_{Jup}$	$[D/H]_{Protosolar}$	$(1.97 \pm 0.3) \times 10^{-5}$
Recommended	$\mathbf{[D/H]_{Protosolar}}$	$\mathbf{(2.0 \pm 0.3) \times 10^{-5}}$

given in Table 2. These examples demonstrate the potential of combining the composition data of two experiments.

Presently, the uncertainties in the protosolar abundances are not so much due to measurement errors, but they result mainly from uncertainties in the transformation of solar wind or Jupiter data to protosolar values.

The systematic difference in H/He between OCZ and high-speed streams is caused mainly by ion-atom separation in or near the chromosphere (Geiss, 1982). Therefore, models applicable to corona ion fractionation cannot be applied to extend the (^{3}He/^{4}He) versus H/He correlation from the high-speed wind data to the OCZ abundance. Theories for ion-atom separation depending on photo-ionization time predict only very minor fractionation for ^{3}He/^{4}He (von Steiger & Geiss, 1989). Since the difference between ^{3}He/^{4}He in the High-Speed Streams and the OCZ is only 2% (see Figure 2), the error introduced by the extrapolation ought to be small.

The contamination of the OCZ with pp-produced ^{3}He from below is one of the more serious uncertainties, but what could be done about this problem? The ^{9}Be abundance gives us a solid argument against loss of ^{3}He in the OCZ due to nuclear reactions. There is no comparable argument against a raise of ^{3}He/^{4}He in the OCZ by admixture of pp-

produced ^{3}He. It is the other way around: a raise in time of ^{3}He in the OCZ or the solar wind is the most sensitive indicator for admixture of material to the OCZ from below, as was recognized long ago (Schatzman, Maeder, Angrand & Glowinski, 1981). Only by further theoretical studies and analyses of solar wind particles trapped in ancient dust and breccias could we further reduce the uncertainty of the protosolar (D+^{3}He)/H ratio.

If we accept $^3\mathrm{He}/^4\mathrm{He} = 1.66 \times 10^{-4}$ as measured in the Jovian atmosphere by Mahaffy et al. (1998) as the protosolar value, then ^{3}He/^{4}He in the "planetary gas" of meteorites would have been reduced by 10%. This seems to be a small reduction, considering that in the "planetary gas" ^{20}Ne/^{22}Ne is reduced relative to the solar abundance by (25-30)% (Geiss et al. 2004) and ^{36}Ar/^{38}Ar by 2% (Heber et al., 2009).

Considering that the age of the Sun is about 35% of the age of the Galaxy, the chemical evolution during this 35% time interval is small, and for many nuclear species, evolution in time disappears in the noise of local differences. The levelling of evolution is attributed to infall (Tosi, 1998), but there is no consensus on the nature of this infall. Studying the evolution of dwarf galaxies should help to clarify this point.

The principal effect of stellar processing is the conversion of D into ^{3}He with the sum (D + ^{3}He) remaining nearly constant (e.g. Geiss & Gloeckler, 2003). This was recognized when ^{3}He and D were determined in both the Protosolar Cloud and the Local Interstellar Cloud (Gloeckler & Geiss, 1996; Linsky, 1998). At the same time, theoretical studies showed (Charbonnel, 1998; Tosi, 1998) that ^{3}He from incomplete hydrogen burning could not have a large effect on the chemical evolution in the Galaxy. Since then, progress in understanding late Galactic evolution has slowed. Determining abundances of a larger number of nuclides in one and the same Galactic sample could correct this impasse better than further collecting scattered composition data. This could be accomplished with a mission similar to Ulysses but with the primary objective of measuring the composition of the Local Interstellar Cloud by determining abundances of elements and isotopes in the gas and dust that is entering the heliosphere. A study to identify the nuclear species in the Local Interstellar Cloud that could be determined in this way would be most worthwhile. Advanced solar wind composition measurement would be a second objective of such a mission. Moreover, comparing the differing paths of the physical and the chemical evolution of our Galaxy and dwarf galaxies would lead to identifying the nature and origin of the infall into the Milky Way.

Acknowledgements

The authors thank Rudolf von Steiger and Rudolf Treumann for discussions. J.G. is grateful to the ISSI directors and staff for their support. The work of G.G. was supported in part by NASA's Ulysses Heliophysics Investigation NNX09AH726 and the ACE Data Analysis Contract, 44A-1080828.

References

Bahcall, J.N., Pinsonneault, M.H. & Wasserburg, G.J. 1995, *Rev. Mod. Phys.*, 67, 781
Beer, R. & Taylor, F.W. 1973, *ApJ*, 179, 309
Bézard, B. 2002, in: *Highlights in Astronomy* (Astron. Soc. Pacific: San Francisco) Vol. 12, pp. 607
Bochsler, P. & Geiss, J. 1973, *Solar Phys.*, 32, 3
Bürgi, A. & Geiss, J. 1986, *Solar Phys.*, 103, 347
Busemann, H., Baur, H. & Wieler, R. 2000, *Meteorites & Planetary Sci.*, 35, 949
Charbonnel, C. 1998, in: *Space Science Series of ISSI*, SSSI-4, and *Space Sci. Rev.*, 84, 199
Drossart, P., Encrenaz, T., Combes, M., Kunde, V. & Hanel, R. 1982, *Icarus*, 49, 416-426
Eberhardt, P. 1974, *Earth Planet. Sci. Lett.*, 24, 182

Encrenaz, Th., de Graauw, Th., Schaeidt, S., Lellouch, E., Feuchtgruber, H., Beintema, D. A., Bézard, B., Drossart, P., Griffin, M., Heras, A., Kessler, M., Leech, K., Morris, P., Roelfsema, P. R., Roos-Serote, M., Salama, A., Vandenbussche, B., Valentijn, E. A., Davis, G. R.,& Naylor, D. A. 1996, *A&A*, 315, L397

Ezer, D. & Cameron, A.G.W. 1965, in *Solar Wind Three* (University of California Press: Los Angeles), pp. 58

Frick, U. & Moniot, R.K. 1977, in *Eighth Lunar Science Conference* (Pergamon Press: New York), Vol. 1, pp. 229

Gautier, D. & Morel, P. 1997, *A&A*, 323, L9

Geiss, J. 1982, *Space Sci. Rev.*, 33, 201

Geiss, J. & Gloeckler, G. 1998, in *Space Science Series of ISSI*, SSSI-4, and *Space Sci. Rev.*, 84, 239

Geiss, J. & Gloeckler, G. 2003, in *Space Science Series of ISSI*, SSSI-16, and *Space Sci. Rev.*, 106, 3

Geiss, J. & Reeves, H. 1972, *A&A*, 18, 126

Geiss, J., Eberhardt, P. & Signer, P. 1966, *Proposal to NASA for Apollo experiment S-080*, (NASA archive, Record Number 14759)

Geiss, J., Eberhardt, P., Bühler, F., Meister, J. & Signer, P. 1970, *J. Geophys. Res.*, 75, 5972

Geiss, J., Hirt, P. & Leutwyler, H. 1970, *Solar Phys.*, 12, 458

Geiss, J., Bühler, F., Cerutti, H., Eberhardt, P., Filleux, Ch., Meister, J. & Signer, P. 2004, *Space Sci. Rev.*, 110, 307

Gloeckler, G. & Geiss, J. 1996, *Nature*, 381, 210

Gloeckler, G. & Geiss, J. 2000, in *The Light Elements and their Evolution*, Proc. IAU-Symp. Vol. 198, (IAU: Natal, Brazil) pp. 224

Grevesse, N. & Sauval, A.J. 1998, in *Space Science Series of ISSI*, SSSI-5, and *Space Sci. Rev.*, 85, 161

Guillot, T. 1999, *Planet. Space Sci.*, 47, 1183

Heber, V.S. Wieler, R., Baur, H., Olinger, C., Friedmann, T.A. & Burnett, D.S. 2009, *Geochimica et Cosmochimica Acta*, 73, 7414

Isenberg, P.A. & Hollweg, J.V. 1983, *J. Geophys. Res.*, 88, 3923

Lellouch, E., Bézard, B., Fouchet, T., Feuchtgruber, H., Encrenaz, T. & de Graauw, T. 2001, *A&A*, 370, 610

Linsky, J.L. 1998, in *Space Science Series of ISSI*, SSSI-4, and *Space Sci. Rev.*, 84, 285

Mahaffy, P.R., Donahue, T.M., Atreya, S.K., Owen, T.C. & Niemann, H.B. 1998, in *Space Science Series of ISSI*, SSSI-4, and *Space Sci. Rev.*, 84, 251

Mazzitelli, I. & Moretti, M. 1980, *ApJ*, 235, 955

Niemann, H.B., Atreya, S.K., Carignan, G.R., Donahue, T.M., Haberman, J.A., Harpold, D.N., Hartle, R.E., Hunten, D.M., Kasprzak, W.T., Mahaffy, P.R., Owen, T.C., Spencer, N.W. & Way, S.H. 1998, *Science*, 272, 846

Owen, T. 2003, in *Space Science Series of ISSI*, SSSI-28, and *Space Sci. Rev.*, 138, 301

Pérez Hernández, F. & Christensen-Dalsgaard, J. 1994, *MNRAS*, 269, 475

Schatzman, E., Maeder, A., Angrand, F. & Glowinski, R. 1981, *A&A*, 96, 1

von Steiger, R. & Geiss, J. 1989, *A&A*, 225, 222

Stevenson, D.J. & Salpeter, E.E. 1976, in *Jupiter* (University of Arizona Press: Tucson), pp. 85

Tosi, M. 1998, in *Space Science Series of ISSI*, SSSI-4, and *Space Sci. Rev.*, 84, 207

Turck-Chièze, S., Nghiem, P., Couvidat, S. & Turcotte, S. 2001, *Solar Phys.*, 200, 323

Vauclair, S. 1998, in *Space Science Series of ISSI*, SSSI-4, and *Space Sci. Rev.*, 84, 256

Wieler, R. & Heber, V.S. 2003, in *Space Science Series of ISSI*, SSSI-16, and *Space Sci. Rev.*, 106, 197

von Zahn, U., Hunten, D.M. & Lehmacher, G. 1998, *J. Geophys. Res.*, 103, 22815

Johannes Geiss, Corinne Charbonnel, Hubert Reeves

Manuel Peimbert & Tom Bania

Light elements in the Universe
Proceedings IAU Symposium No. 268, 2010
C. Charbonnel, M. Tosi, F. Primas & C. Chiappini, eds.

DOI: 00.0000/X000000000000000X

Measurements of ^{3}He in Galactic H II regions and planetary nebulae

T. M. Bania[1], R. T. Rood[2] and D. S. Balser[3]

[1]Department of Astronomy, Boston University
725 Commonwealth Ave., Boston, MA 02215, USA
email: bania@bu.edu

[2]Astronomy Department, University of Virginia
P.O. Box 400325, Charlottesville, VA 22904, USA
email: rtr@virginia.edu

[3]National Radio Astronomy Observatory,
520 Edgemont Rd., Charlottesville, VA 22903
email: dbalser@nrao.edu

Abstract. The cosmic abundance of the ^{3}He isotope has important implications for many fields of astrophysics. We are using the 8.665 GHz hyperfine transition of ^{3}He$^+$ to determine the ^{3}He/H abundance in Milky Way H II regions and planetary nebulae. Here we review the 30 year history of our ^{3}He program, report on its current status, and describe our future plans.

Keywords. Cosmology: cosmological parameters; The Galaxy: abundances, evolution; ISM: abundances, evolution, H II regions; Stars: AGB, post-AGB

1. The ^{3}He Problem

The ^{3}He abundance in Milky Way sources impacts stellar evolution, chemical evolution, and cosmology. The abundance of ^{3}He is derived from measurements of the hyperfine transition of ^{3}He$^+$ which has a rest wavelength of 3.46 cm (8.665 GHz). As with all the light elements, the present interstellar ^{3}He abundance results from a combination of Big Bang Nucleosynthesis (BBN) and stellar nucleosynthesis (Wilson & Rood 1994). We are measuring the ^{3}He abundance in Milky Way H II regions and planetary nebulae (PNe). H II regions are examples of zero-age objects that are young relative to the age of the Galaxy. Their ^{3}He abundances chronicle the results of billions of years of Galactic chemical evolution (GCE). PNe ^{3}He abundances arise from material that has been ejected from low-mass ($M \leqslant 2\,M_\odot$) and intermediate-mass ($M \sim 2$–$5\,M_\odot$) stars. Because the Milky Way ISM is optically thin at centimeter wavelengths, our source sample probes a larger volume of the Galactic disk than does any other light element tracer of GCE. The sample is currently comprised of 60 H II regions and 12 PNe.

The present ^{3}He abundance is an important GCE diagnostic. H II regions sample the result of the chemical evolution of the Milky Way since its formation. The ^{3}He/H abundance ratio is expected to grow with time and to be higher in those parts of the Galaxy where there has been substantial stellar processing. If the ^{3}He yields predicted by standard models of stellar nucleosynthesis (SSN) had been correct then we should have detected extremely strong ^{3}He$^+$ emission in Galactic H II regions (RST: Rood, Steigman, & Tinsley 1976). Our ^{3}He$^+$ experiment would then have taken about two weeks. After 30 years of effort (Rood, Wilson, & Steigman 1979; Bania et al. 2007) our observations still yield ^{3}He abundances for H II regions that are inconsistent with these expectations, leading to "The ^{3}He Problem" (Galli et al. 1995).

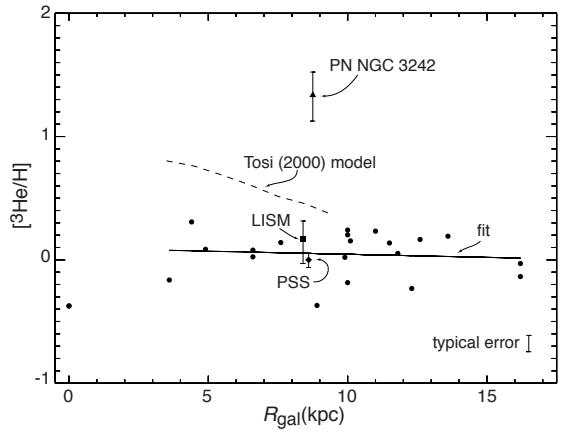

Figure 1. "The ^{3}He Problem" ^{3}He/H abundances as a function of Galactic radius. The [^{3}He/H] abundances by number for the BRB H II region sample are given with respect to the solar ratio. Shown also are the abundances for the planetary nebula NGC 3242 (triangle), the local interstellar medium (LISM—square), and protosolar material (PSS—diamond). There is no gradient in the ^{3}He/H abundance with Galactic position.

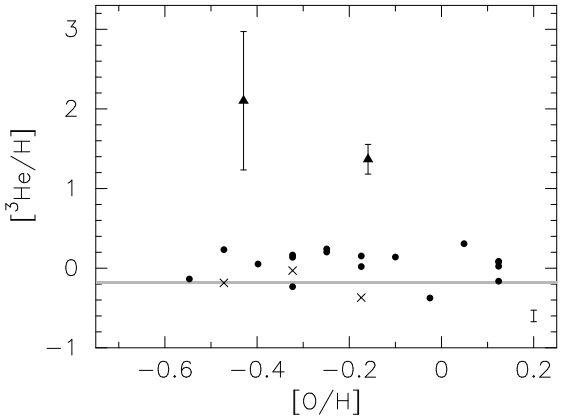

Figure 2. "The ^{3}He Plateau" [^{3}He/H] abundances as a function of source metallicity for the "simple" H II region sample. The gray line is the WMAP result. The ~ 0.15 dex typical error is shown in the right hand corner. The triangles denote abundances for the PNe J 320 (left) and NGC 3242. There is no trend in the ^{3}He/H abundance with source metallicity.

2. H II region abundances

Until its decommissioning in 1999 we used the NRAO 140-Foot telescope to observe $^3He^+$ in a sample of 60 Galactic H II regions (Rood, Bania, & Wilson 1984; Bania, Rood, & Wilson 1987; Balser et al. 1994; Rood et al. 1995; Bania et al. 1997; Balser et al. 1999a; Bania, Rood, & Balser 2002; Bania et al. 2007). The $\sim 200''$ resolution (FWHM "beam") of the 140-Foot at the $^3He^+$ frequency is comparable to the angular size of typical Galactic H II regions, making this the instrument of choice at the time.

Besides detecting $^3He^+$ emission from an H II region and accurately determining the line intensity and line width, in order to derive the $^3He^+/H^+$ abundance ratio we also need to measure the intensity of the continuum emission produced by thermal free-free

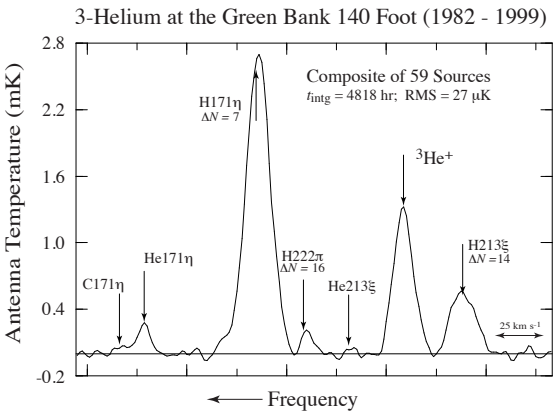

Figure 3. NRAO 140-Foot H II region composite ^{3}He spectrum. This 200 day integration is the most sensitive cm-wavelength spectrum ever taken. Besides the $^3He^+$ emission, a variety of recombination lines from H, ^{4}He, and C are seen. Many of these arise from transitions resulting from large changes in principle quantum number, e.g. H 171 η, Δ N = 7, and H 213 ξ, Δ N = 14.

brehmstrahlung in the nebular plasma. A nebula's $^3He^+/H^+$ abundance thus depends on its $^3He^+$ line to thermal continuum intensity ratio. For typical Galactic H II regions the observed line-to-continuum ratio is $\sim 10^{-4}$ to $\sim 10^{-5}$. The 140-Foot's conventional on-axis optics are, moreover, a very poor design for the ^{3}He experiment. Typically, the ^{3}He emission lines have intensities of a few mK and line widths of $\sim$ 1 MHz and this weak, wide line emission must be measured in the presence of the far stronger continuum emission. For conventional blocked aperture optics such as those of the 140-Foot, this strong continuum emission is reflected and scattered by the secondary mirror, its support legs, the receiver cabin, etc., causing direct and multipath standing waves that lead to frequency structure in the observed spectra. This instrumental spectral baseline frequency structure is extremely complex and impossible to model a priori because these standing waves are not pure tones and they vary on short time scales as a source is tracked. Some of the baseline frequency structure can be removed by purposefully defocussing by $\pm\lambda/8$, but much structure remains and needs to be modeled empirically. Baseline modeling errors contribute to the uncertainty in the $^3He^+$ line parameters that we can measure. For H II regions, such errors are too small to compromise our $^3He^+$ detections.

Deriving an accurate ^{3}He/H abundance ratio also requires modeling the nebular density and ionization structure. In doing so we identified a special class of "simple" H II regions for which accurate ^{3}He/H abundances can be determined (Balser et al. 1999a). This source sample provides a strong constraint on GCE models. Standard evolution models predict that: (1) the protosolar ^{3}He/H value should be less than that found in the present ISM; (2) the ^{3}He/H abundance should grow with source metallicity; and (3) there should be a ^{3}He/H abundance gradient in the Galactic disk with the highest abundances occurring in the highly-processed inner Galaxy. None of these predictions is confirmed by observations.

Specifically, measurements of ^{3}He/H in protosolar material (Geiss 1993), the local solar neighborhood (Gloecker & Geiss 1996), and Galactic H II regions (Rood et al. 1995) all indicate a value of $^3\mathrm{He/H} \sim 2 \times 10^{-5}$ by number. Thus the H II regions show no evidence for stellar ^{3}He enrichment during the last 4.5 Gyr. There is no significant ^{3}He abundance gradient across the Milky Way (Fig. 1). And, finally, there is no trend of

^{3}He abundance with source metallicity (Fig. 2). To be compatible with this result GCE models require that $\sim 90\%$ of solar analog stars are non-producers of ^{3}He (Tosi 2000). Finally, BRB argued that the "The ^{3}He Plateau" ^{3}He/H abundance is an upper limit for the cosmological production of ^{3}He. They derived $\eta_{10} = 5.4$ $(+2.2/-1.2)$, a year before and in complete concordance with the WMAP value (Spergel et al. 2003; Romano et al. 2003).

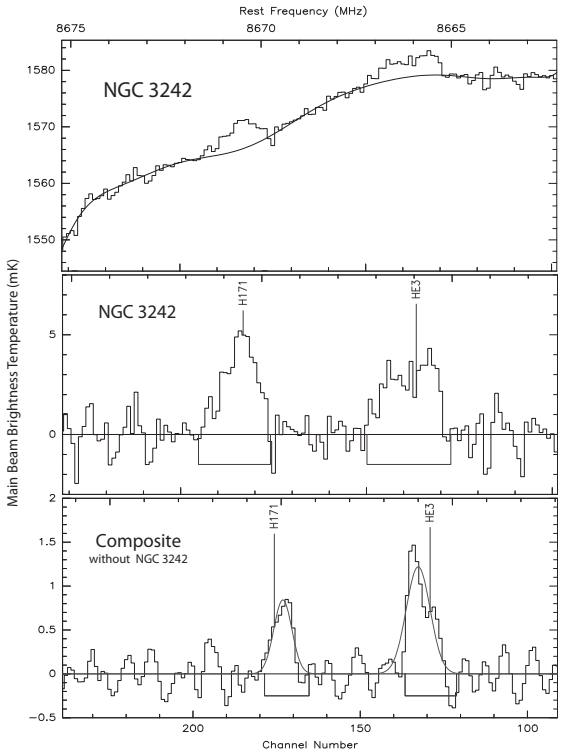

Figure 4. MPIfR 100-m ^{3}He$^+$ spectra for Galactic PNe. **TOP:** The NGC 3242 average spectrum (106 hr integration) with the baseline model superimposed. The H 171 η and ^{3}He$^+$ features are clearly seen. **MIDDLE:** The NGC 3242 spectrum after the baseline model is subtracted. **BOTTOM:** Composite ^{3}He$^+$ average spectrum (443 hr integration) for 6 PNe (NGC 6543, NGC 6720, NGC 7009, NGC 7662, & IC 289).

3. Planetary nebula abundances

Standard stellar evolution theory predicts not only that common solar-type stars produce ^{3}He but also that the mass lost from winds generated at advanced stages of their evolution and the final planetary nebulae should be substantially enriched in ^{3}He. Planetary nebula ^{3}He abundances are therefore important tests of stellar evolution theory since these low-mass, evolved objects are expected to be significant sources of ^{3}He. It is thus crucial to see if stars actually do produce ^{3}He. Detecting ^{3}He$^+$ in the nebulae surrounding PNe is an even more challenging experimental problem than that for H II regions. Finding ^{3}He in PNe challenges the sensitivity limits of all existing radio telescopes.

PNe nebulae contain $\sim$1 $M_\odot$ of gas whereas H II region plasmas have masses $\sim$ 100's to $\sim$ 1000's $M_\odot$. The detection of ^{3}He in *any* PN, however, will require ^{3}He/H $\sim 10^{-4}$, which is the abundance predicted by standard stellar models.

We are observing a sample of 12 PNe that is purposefully biased to maximize the likelihood of finding ^{3}He. Between 1987 and 1997 we used the 100-m telescope of the Max Planck Institut für Radioastronomie (MPIfR) to observe ^{3}He$^+$ in a sample of 6 PNe (Rood, Bania, & Wilson 1992; Balser et al. 1997). The $\sim 85''$ 100-m beam is a good match to the angular extent of typical Galactic PNe. We reported a ^{3}He$^+$ detection for NGC 3242 and found significant ^{3}He$^+$ emission in a composite spectrum resulting from the average of 6 PNe (Fig. 4). Even though the continuum emission from PNe is significantly weaker than that from H II regions, the MPIfR optics, which have 22% geometric blockage, produce extremely complex instrumental baseline frequency structure as can be seen in Fig. 4 (top). It was important to verify our ^{3}He$^+$ detection with another telescope. Despite the fact that PNe with their small angular sizes were not good NRAO 140-Foot targets we were able to verify our NGC 3242 result at the $\sim 4\,\sigma$ level (Fig. 5). The MPIfR and NRAO NGC 3242 line shapes were consistent and they suggested that much of the emission ^{3}He$^+$ emission comes from a large, diffuse halo. Subsequently we detected ^{3}He$^+$ emission at the $\sim 4\,\sigma$ level from the PN J 320 with the NRAO Very Large Array (VLA) (Balser et al. 2006). It seems that at least *some* (i.e., > 2) PNe produce significant amounts of ^{3}He that survives the PN stage and enriches the ISM.

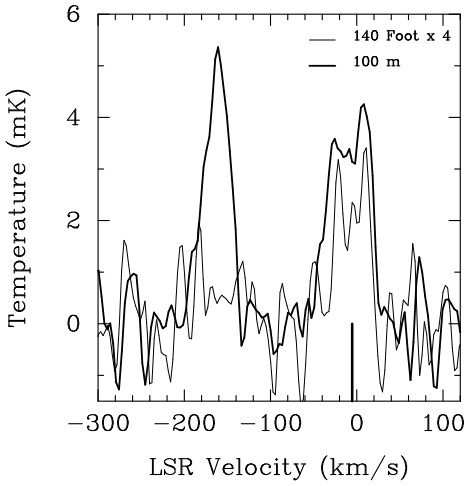

Figure 5. NRAO 140-Foot ^{3}He$^+$ spectrum for NGC 3242 compared with the MPIfR result. The ^{3}He$^+$ emission is flagged at $-5.3\,\mathrm{km\,sec^{-1}}$. This 270 hr integration is one of the longest cm-wavelength spectra ever made toward a single source.

4. Current status of the ^{3}He experiment

The ^{3}He$^+$ experiment challenges the sensitivity limits of all exisiting radio telescope spectrometers. We are now studying ^{3}He with the NRAO Green Bank Telescope (GBT) and NAIC's Arecibo Observatory. We are soon to begin using the NRAO Expanded VLA (EVLA) and ATNF's Parkes 64-m telescope. The EVLA will be a factor of 10 better than the VLA in all relevant experimental parameters. It will be a powerful new

tool for studying ^{3}He in PNe. With Parkes it is feasible to detect $^3He^+$ in the 30 Doradus H II region in the Large Magellanic Cloud. Doing so would extend the metallicity range of the ^{3}He plateau ^{3}He/H abundances.

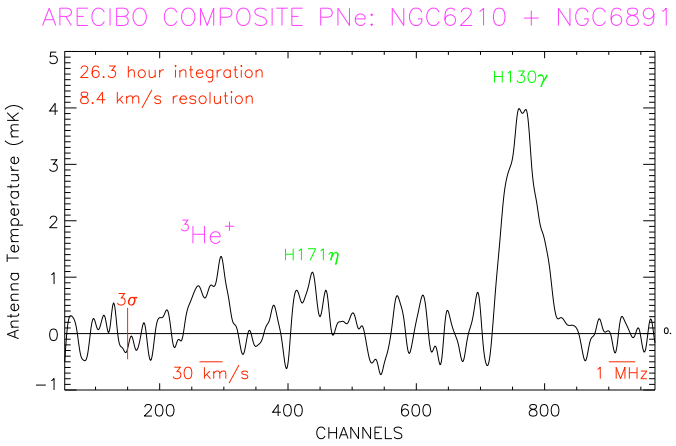

Figure 6. Arecibo $^3He^+$ spectrum for a composite average of 2 Galactic PNe, NGC 6210 & NGC 6891, aligned to a common LSR velocity. A baseline model was removed and the spectrum smoothed to 8.4 km sec^{-1} resolution. The H130γ recombination and $^3He^+$ spin-flip transitions are clearly seen.

We are using the 305-m Arecibo telescope to study $^3He^+$ in PNe. Fig. 6 shows a composite $^3He^+$ spectrum for two PNe. We choose targets to match the properties of the particular telescope we are using. For the most part our Arecibo target PNe were chosen to have angular sizes well matched to its $\sim 45''$ beam. Even though not on our initial Arecibo target list, our VLA results suggested that J 320 was also a plausible target. Thus, to confirm our VLA detection we began observing J 320 in January 2009. At Arecibo we are observing at the high frequency limit set by the surface accuracy of the primary mirror. The primary is fixed in place, which makes Arecibo a semi-transit instrument, so as a source is tracked across the sky different areas of the primary mirror are illuminated. Because of this the telescope gain varies significantly as a source is tracked, which makes intensity calibration difficult. The semi-transit nature of Arecibo also means that progress will be slow. We need significant integration times for our sources, $\sim$ 50–100 hrs, but a full week of observing, 7 sidereal passes of a source, yields 14 hrs of source integration time.

We were part of the 100-m GBT project from its inception through commissioning and are now using it to study $^3He^+$ in H II regions and PNe. Our $^3He^+$ program thus far has focussed on the S 209 H II region and the NGC 3242 PN. Located in the outer Galactic disk at $R_{\rm gal} \sim 16.9$ kpc, S 209 provides an important constraint on BBN and GCE. Confirming the NGC 3242 ^{3}He abundance has important consequences for SSN and GCE. We are also observing the W 3 H II region and the PNe NGC 6543, NGC 6826, and NGC 7009.

The GBT's clear aperture, unblocked optics are unique; it has the potential to be much more sensitive than any cm-wavelength spectrometer ever built. This increased sensitivity

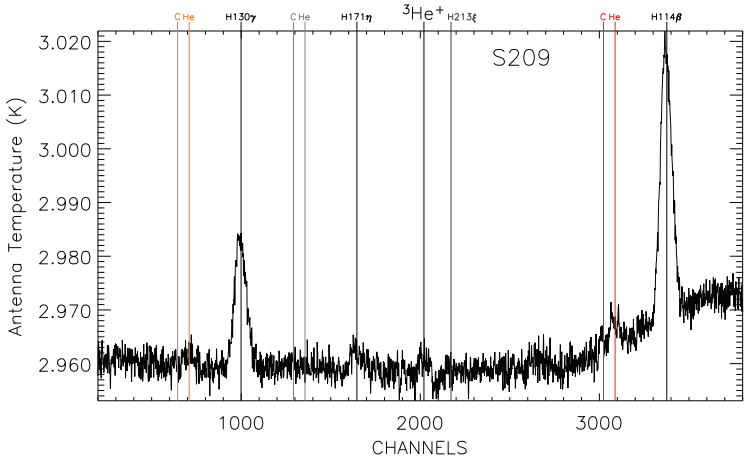

Figure 7. First epoch GBT ^{3}He$^+$ spectrum for H II region S 209. This calibrated, but otherwise unprocessed spectrum, shows that the GBT's unblocked optics have eliminated instrumental standing waves. There is a clear ^{3}He$^+$ signal in this 14.5 hr spectrum. Numerous recombination line transitions of H, and ^{4}He can be seen, including a clear detection of the H 213 ξ line.

results from the 100-m aperture, the unblocked optics, which allow for unprecedented dynamic range, and the unique capabilities of the 3 cm receiver and autocorrelation spectrometer (ACS). For the ^{3}He$^+$ experiment we simultaneously measure 8 different frequency bands at two orthogonal polarizations (RR and LL). Each band is 50 MHz wide and is sampled by 4096 channels. We tune two bands to ^{3}He$^+$ in order to assess the GBT's electronics by sampling the identical signal through two independent paths. We thus measure a source's emission over 350 MHz of spectrum (7×50 MHz). The different bands are tuned to a host of radio recombination lines (RRLs) of H, ^{4}He, and C. Our targets' fully ionized plasmas will emit all possible RRL transitions, but at a vast range of intensities. We analyze more than 50 RRL transitions, spanning principal quantum number, N, from 90 through 224 and order, ΔN, from 1 through 16.

As we have done for all the ^{3}He$^+$ experiment telescopes, we use this plethora of RRL measurments to assess the performance of the GBT spectrometer. For example, the RRL line intensities should not vary with time, the ^{4}He/H intensity ratio should not be a function of principle quantum number, and the lines should only be seen in emission. RRL theory predicts line intensities for all these transitions, which can then be used to assess spectrometer performance. For example, in the ^{3}He$^+$ band, LTE models for diffuse H II regions predict that the H 213 ξ intensity should be $\sim 25\%$ the H 171 η intensity (see, e.g., Fig. 3, Fig. 4, & Fig. 5). For any given nebula the entire ensemble of RRLs should give an astrophysically self-consistent set of measured line parameters. Any deviations or inconsistencies are caused by instrumental effects which, experience shows, inevitably appear at some point as one attains ever increasing sensitivity levels. At the sensitivity required by the ^{3}He experiment, characterizing the spectrometer's performance is a on-going, evolving process. We are just now in a position, for example, to begin exploring possible diurnal and seasonal effects on the GBT's instrumental baseline frequency structure.

The current status of the GBT ^{3}He$^+$ experiment for S 209 and NGC 3242 is shown in Fig. 8 (25.8 receiver-hr integration) and Fig. 9 (91.6 receiver-hr integration), respectively.

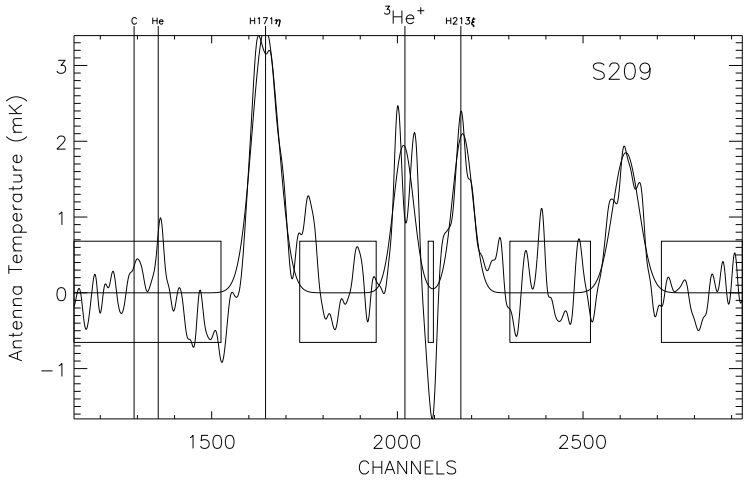

Figure 8. GBT $^3He^+$ average spectrum for H II region S 209 as of November 2009.

Our GBT $^3He^+$ result for S 209 is completely consistent with our 140-Foot measurement, confirming the $^3He/H$ abundance of "The ^3He Plateau."

Extensive analysis of the RRLs from S 209 shows that at our current sensitivity level all spectral features with $\gtrsim 1$ mK intensities are reliably detected. Below this intensity, however, the observed line parameters become uncertain and we begin to see evidence for instrumental baseline frequency structure (BFS). In the entire 350 MHz spectral range that we measure, we find only a few cases of instrumental BFS that mimic the weak, ~ 1 mK, wide, ~ 1 MHz, lines characteristic of $^3He^+$ emission. Alas, we are very, very unlucky in that the two strongest such instrumental features not only occur within the $^3He^+$ band, but also lie atop the H 213 ξ and H 203 μ RRLs! These instrumental BFS components make the observed H 213 ξ and H 203 μ intensities much too strong (Fig. 8 & Fig. 9). We currently estimate that instrumental BFS enhances these transition intensities by $\sim 20\%$ up to a factor of a few, increasing with source continuum intensity.

Our GBT $^3He^+$ measurements for the PN NGC 3242 (Fig. 9) do not confirm our MPIfR result: the GBT intensities for $^3He^+$ and H 171 η are both lower by a factor of ~ 4. Interestingly, our 140-Foot observations, Fig. 3, also suggested the MPIfR intensities were too high. At the time we attributed the differences between the 100 m and 140-Foot to be due to the different beam sizes: the observed spectra sampled very different volumes surrounding the PN. Density structure, in particular a large, low density, expanding halo could plausibly account for the intensity differences. This can no longer be the case since the GBT and MPIfR beams sizes are essentially identical.

Nonetheless, NGC 3242 *does* have a large, low density, expanding halo which produces a large, ~ 50 km sec^{-1} wide $^3He^+$ line. As can be seen in Fig. 9 this wide $^3He^+$ line blends with the H 213 ξ emission. Moreover, the proximity of H 203 μ, together with the instrumental BFS associated with these RRL transitions makes the $^3He^+$ line parameters uncertain.

We explored a range of baseline models for the NGC 3242 $^3He^+$ emission. Currently, at best, the GBT data are consistent with a $^3He^+$ abundance ratio of $\sim 10^{-4}$ by number, with an uncertainty of $\sim 50\%$. We also studied a variety of composite $^3He^+$ spectra for our GBT PNe sources. The best such cases are consistent with the composite PNe

spectra obtained at the MPIfR and Arecibo. Again, these composites are consistent with a $^3He^+$ abundance ratio of $\sim 10^{-4}$ by number.

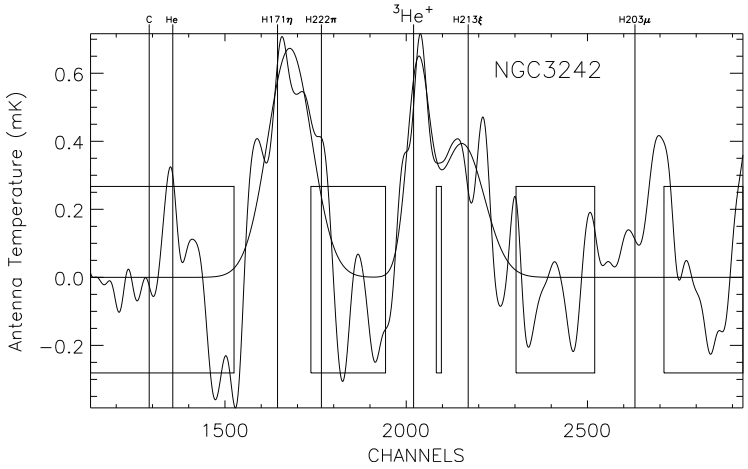

Figure 9. GBT $^3He^+$ average spectrum for NGC 3242 as of November 2009.

5. Solving "The ^{3}Helium Problem"

Rood, Bania, & Wilson (RBW: 1984) suggested that the ^{3}He problem could be related to striking chemical anomalies in red giant stars. Much accumulated observational evidence shows that low-mass RGB stars undergo an extra-mixing event. This extra-mixing adds to the standard first dredge-up to modify the surface abundances. Efforts by many groups during the past 25 years have confirmed that RBW were on the right track. Significantly, all the relevant data indicate that the extra-mixing occurs in $\sim$ 90 to 95% of the low-mass stars. Thermohaline instability and rotation-induced mixing now seem to be able to account for the drastically reduced ^{3}He yields produced by low-mass red giants (Charbonnel & Zahn 2007a,b; Charbonnel & Lagarde 2010; Eggleton, Dearborn, & Lattanzio 2006).

6. Summary

The NRAO GBT result for S 209 is consistent with *all* previous Galactic H II region ^{3}He/H abundance determinations. Thus "The 3-Helium Plateau" ^{3}He/H abundance, important for primordial nucleosynthesis and Galactic chemical evolution, stands. The ^{3}He/H abundance by number, which is not seen to be a function of either source metallicity or Galactic position, is $\sim 2 \times 10^{-5}$.

Attempting to detect ^{3}He in PNe challenges the capabilities of all existing radio spectrometer systems. We reported ^{3}He detections in NGC 3242 with the MPIfR 100 m and NRAO 140-Foot telescopes. Our NRAO GBT observations are, however, inconsistent with the MPIfR 100 m result, implying a ^{3}He/H abundance that is $\sim$ 25% of that we previously reported. We find ^{3}He in J 320 at the $4\,\sigma$ level with the NRAO VLA. Confirmation observations are underway using the NAIC Arecibo telescope. Composite PNe $^3He^+$ spectra, made from MPIfR, Arecibo, and GBT observations, consistently show

$^3He^+$ emission at the ~ 1 mK level. As a class our sources imply a ^{3}He/H abundance by number of $\sim 10^{-4}$, which suggests that some PNe produce ^{3}He.

Resolving "The ^{3}He Problem" requires that the vast majority of low-mass stars fail to enrich the ISM with ^{3}He due to extra-mixing in the RGB stage. GCE models can account for "The ^{3}He Plateau" only if $\gtrsim 90\%$ of solar analog stars are non-producers of ^{3}He. Thermohaline instability and rotation-induced mixing are able to account for the drastically reduced ^{3}He yields produced by these stars. Our PNe target sample is purposefully biased to contain objects whose progenitor stars underwent no extra-mixing, which has been suppressed by some yet to be determined mechanism (but see the conjecture by Charbonnel & Zahn 2007b; Charbonnel & Lagarde 2010). These rare PNe seem to be returning ^{3}He to the ISM.

Acknowledgements

We thank the international light element abundances community for their collegiality and support over the years.

References

Balser, D.S., Bania, T.M., Brockway, C.J., Rood, R.T. & Wilson, T.L. 1994, *ApJ*, 430, 667
Balser, D.S., Bania, T.M., Rood, R.T. & Wilson, T.L. 1997, *ApJ*, 483, 320
Balser, D.S., Bania, T.M., Rood, & T. W. Wilson 1999, *ApJ*, 510, 759
Balser, D.S., Rood, R.T., & Bania, T.M. 1999, *ApJ*, 522, L73 [N3242]
Balser, D.S., Goss, W.M., Bania, T.M., & Rood:, R.T. 2005, *ApJ*, 640, 360 [J320]
Bania, T.M., Balser, D.S., Rood, R.T., Wilson, T.L, & Wilson, T.J. 1997, *ApJS*, 415, 54
Bania, T.M., Balser, D.S., Rood, R.T., Wilson, T.L., & LaRocque, J.M. 2007, *ApJ*, 664, 915
Bania, T.M., Rood, R.T., & Wilson, T.L. 1987, *ApJ*, 323, 30
Bania, T.M., Rood, R.T., & Balser, D.S. 2002, *Nature*, 415, 54
Charbonnel, C., & Zahn, J.P. 2007a, *A&A*, 467, L15
Charbonnel, C., & Zahn, J.P. 2007b, *A&A*, 476, L29
Charbonnel, C., & Lagarde, N. 2010, in: C. Charbonnel, M. Tosi, F. Primas, & C. Chiappini (eds.), *Light Elements in the Universe*. Proc. IAU Symposium No. 268, (Cambridge: CUP), p. XX
Eggleton, P.P., Dearborn, D.S.P., & Lattanzio, J.C. 2006, *Science*, 314, 1580
Galli, D., Palla, F., Ferrini, F., & Penco, U. 1995, *ApJ*, 443, 536
Galli, D., Stanghellini, L., Tosi, M., & Palla, F. 1997, *ApJ*, 456, 478
Geiss, J. 1993, in: N. Prantzos, E. Vangioni-Flam, & M. Casse (eds.), *Origin and Evolution of Elements*. (Cambridge: CUP), p. 89
Gloecker, G., & Geiss, J. 1996, *Nature*, 381, 210
Palla, F., Galli, D., Marconi, A., Stanghellini, L., & Tosi, M. 2002, *ApJ*, 568, L57
Romano, D., Tosi, M., Matteucci, F., & Chiappini, C. 2003, *MNRAS*, 346, 295
Rood, R.T., Bania, T.M., & Wilson, T.L. 1984, *ApJ*, 280, 629
Rood, R.T., Bania, T.M., & Wilson, T.L. 1992, *Nature*, 355, 618
Rood, R.T., Bania, T.M., Wilson, T.L., & Balser, D.S. 1995, in: P. Crane (ed.), *ESO/EIPC Workshop on the Light Elements*. (Heidelberg: Springer), p. 201
Rood, R.T., Steigman, G., & Tinsley, B.M., 1976, *ApJ*, 207, L57 [RST]
Rood, R.T., Wilson, T.L., & Steigman, G., 1979, *ApJ*, 227, L97
Spergel, D.N. et al., 2003 *ApJS*, 148, 175
Tosi, M. 2000, in: L. da Silva, M. Spite, & J.R. de Medeiros (eds.), *The Light Elements and Their Evolution*, Proc. IAU Symposium No. 198, (San Francisco: ASP), p. 525
Wilson, T.L., & Rood, R.T., 1994, *ARAA*, 32, 191

Light elements in the Universe
Proceedings IAU Symposium No. 268, 2010
C. Charbonnel, M. Tosi, F. Primas, & C. Chiappini, eds.

DOI: 00.0000/X000000000000000X

Measurements of ^{4}He in metal-poor extragalactic H II regions: the primordial Helium abundance and the $\Delta Y/\Delta O$ ratio

Manuel Peimbert[1], A. Peimbert[1], L. Carigi[1], and V. Luridiana[2]

[1]Instituto de Astronomía, Universidad Nacional Autónoma de México, Apdo. postal 70-264, México D.F. 04510, Mexico
email: peimbert@astroscu.unam.mx

[2]Instituto de Astrofísica de Canarias, c/ Vía Láctea s/n, 38205 La Laguna, Spain

Abstract.
We present a review on the determination of the primordial helium abundance Y_p, based on the study of hydrogen and helium recombination lines in extragalactic H II regions. We also discuss the observational determinations of the increase of helium to the increase of oxygen by mass $\Delta Y/\Delta O$, and compare them with predictions based on models of galactic chemical evolution.

Keywords. ISM: abundances – H II regions – galaxies: abundances, evolution, irregular – Galaxy: disk – early universe

1. Overview

The determinations of the helium abundance by mass, Y, from metal-poor extragalactic H II regions provide the best method to obtain the primordial helium abundance. During their evolution galaxies produce a certain amount of helium and oxygen per unit mass that we will call ΔY and ΔO. The galaxies less affected by chemical evolution are those that present a large fraction of their baryonic mass in gaseous form and a small fraction of their baryonic mass in stellar form. These galaxies when experiencing bursts of star formation present bright metal poor H II regions that have been used to determine their chemical composition.

From a set of Y and O values and assuming a linear relationship it is possible to obtain Y_p and $\Delta Y/\Delta O$ from the following equation:

$$Y_p = Y - O\frac{\Delta Y}{\Delta O}. \tag{1.1}$$

The determinations of Y_p and $\Delta Y/\Delta O$ are important for at least the following reasons: (a) Y_p is one of the pillars of Big Bang cosmology and an accurate determination of Y_p permits to test the Standard Big Bang Nucleosynthesis (SBBN), (b) the models of stellar evolution require an accurate initial Y value; this is given by Y_p plus the additional ΔY produced by galactic chemical evolution, which can be estimated based on the observationally determined $\Delta Y/\Delta O$ ratio, (c) the combination of Y_p and $\Delta Y/\Delta O$ is needed to test models of galactic chemical evolution.

Recent reviews on primordial nucleosynthesis have been presented by Steigman (2007), Olive (2008), Weinberg (2008), and Pagel (2009). A review on the primordial helium abundance has been presented by Peimbert (2008) and a historical note on the primordial helium abundance has been presented by Peimbert & Torres-Peimbert (1999).

2. Recent Y_p determinations

The best Y_p determinations are those by Izotov, Thuan, & Stasińska (2007) that amount to 0.2516 ± 0.0011 and Peimbert, Luridiana, & Peimbert (2007a) that amounts to 0.2477 ± 0.0029. The procedures used by both groups to determine Y_p are very different and it is not easy to make a detailed comparison of all the steps carried out by each of them. We consider that the error presented by Izotov et al. is a lower limit to the total error because it does not include estimates of some systematic errors. The difference between the central Y_p values derived by both groups is mainly due to the treatment of the temperature structure of the H II regions. Izotov et al. adopt temperature variations that are smaller than those derived by Peimbert et al.

To be more specific we can define the temperature structure of the H II regions by means of an average temperature, T_0, and a mean square temperature fluctuation, t^2 (Peimbert 1967). The value of t^2 derived by Izotov et al. (2007) for their sample is about 0.01; while Peimbert et al. (2007a) obtain a t^2 of about 0.026. From the observations adopted by Peimbert et al. and assuming $t^2 = 0.000$ we obtain $Y_p = 0.2523 \pm 0.0027$, and for $t^2 = 0.01$ we obtain $Y_p = 0.2505$.

The small value of t^2 derived by Izotov et al. (2007) is due to the parameter space used in their Monte Carlo computation where they permitted T(He I) to vary from 0.95 to 1.0 times the $T(4363/5007)$ value, which yields a t^2 of about 0.01. By allowing their T(He II) to vary from 0.80 to 1.0 times the $T(4363/5007)$ value their t^2 result would have become higher. This can be seen from their Table 5 where 71 of the 93 spectra corresponded to the lowest T(He I) allowed by the permitted parameter space of the Monte Carlo computation. A higher t^2 value for the Izotov et al. (2007) sample produces a lower Y_p, reducing the difference with the Peimbert et al. (2007a) Y_p value.

Two other systematic problems with the Izotov et al. (2007) determination related with the temperature structure are: (a) that to compute the $N(O^{++})$ abundance they adopted the $T(4363/5007)$ value which is equivalent to adopt $t^2 = 0.00$, and (b) to compute the once ionized oxygen and nitrogen abundances, $N(O^+)$ and $N(N^+)$, they adopted the $T(4363/5007)$ value, but according to photoionization models and observations of O-poor objects, the temperature in the O^+ regions, $T(O^+)$, is considerably smaller than in the O^{++} regions, typically by about 2000 K for objects with $T(O^{++}) = 16000$ K, and reaching 4000 K for the metal poorest H II regions (*e. g.* Peimbert, Peimbert, & Luridiana 2002; Stasińska 1990).

2.1. *Recombination coefficients of the helium I lines*

There are two recent line emissivity estimates to derive the He abundance from recombination lines: one due to Benjamin, Skillman, & Smits (1999, 2002), and another by Bauman et al. (2005) and Porter et al. (2007, 2009). The difference in the Y values derived from both sets of data amount to about 0.0040, the emissivities by the first group yielding values smaller than those of the second group. According to Porter, Ferland, & MacAdam (2007), the error introduced in their emissivities by interpolating in temperature the equations provided by them is smaller than 0.03%, which translates into an error in Y_p considerably smaller than 0.0001. Moreover according to Porter et al. (2009) the expected error in their line emissivities amounts to about 0.0010 in the Y derived values. In this review we are adopting the Bauman et al. and Porter et al. emissivities in the presented Y_p values.

2.2. *Beyond case B*

There are at least four processes that modify the level populations of H and He atoms relative to case B and consequently the Y_p determination: the optical depth of the He I

Table 1. Cosmological predictions based on SBBN and observations for $\tau_n = 885.7 \pm 0.8$ s

Method	Y_p	D_p	η_{10}	$\Omega_b h^2$
Y_p	0.2477 ± 0.0029^a	$2.93 + 2.53 - 1.06^b$	5.625 ± 1.81^b	0.02054 ± 0.00661^b
D_p	0.2479 ± 0.0007^b	2.82 ± 0.28^a	5.764 ± 0.360^b	0.02104 ± 0.00132^b
$WMAP$	0.2487 ± 0.0006^b	2.49 ± 0.13^b	6.226 ± 0.170^b	0.02273 ± 0.00062^a

[a]Observed value. [b]Predicted value. References: τ_n Arzumanov et al. (2000); Y_p Peimbert et al. (2007a); D_p O'Meara *etal.*(2006); $WMAP$ Dunkley et al. (2009).

Table 2. Cosmological predictions based on SBBN and observations for $\tau_n = 878.5 \pm 0.8$ s

Method	Y_p	D_p	η_{10}	$\Omega_b h^2$
Y_p	0.2477 ± 0.0029^a	$2.22 + 1.46 - 0.71^b$	6.688 ± 1.81^b	0.02442 ± 0.00661^b
D_p	0.2462 ± 0.0007^b	2.82 ± 0.28^a	5.764 ± 0.360^b	0.02104 ± 0.00132^b
$WMAP$	0.2470 ± 0.0006^b	2.49 ± 0.13^b	6.226 ± 0.170^b	0.02273 ± 0.00062^a

[a]Observed value. [b]Predicted value. References: same as in Table 1 with the exception of τ_n that comes from Serebrov et al. (2005, 2008).

lines, the collisional excitation from the He $2\,^3S$ metastable level, the collisional excitations from the H ground level, and the fluorescent excitation of the H I and the He I lines (case D of Luridiana et al. 2009). The last two processes are the least studied of the four.

Luridiana et al. (2009) have introduced case D into the study of gaseous nebulae. Case D increases slightly the emissivities of the H I and He I lines affecting the accuracy of the Y_p determination. There are no published estimates of the importance of this effect but it depends on the spectra of the ionizing stars, particularly in the region of the H I and He I lines, the spatial distribution of the ionizing stars, the gaseous electron density distribution, the fraction of ionizing photons that escape the nebula, the radial velocity of the gas relative to that of the stars, the nebular turbulence, and the region of the nebula observed. Therefore it requires tailor-made models for each observed object. Peimbert et al. (2007a) presented a list of thirteen sources of error in the Y_p determination, each of them with systematic and statistical components but dominated by one or the other. The systematic error produced by not having considered Case D should be added to that list.

3. Comparison of the directly determined Y_p with the Y_p values computed under the assumption of the SBBN and the observations of D_p and WMAP

To compare the Y_p value with the primordial deuterium abundance D_p (usually expressed as $10^5(D/H)_p$) and with the WMAP results, we will use the framework of the SBBN. The ratio of baryons to photons multiplied by $10^{10}, \eta_{10}$, is given by (Steigman 2006, 2007):

$$\eta_{10} = (273.9 \pm 0.3)\Omega_b h^2, \tag{3.1}$$

where Ω_b is the baryon closure parameter, and h is the Hubble parameter. In the range $4 < \eta_{10} < 8$ (corresponding to $0.2448 < Y_p < 0.2512$), Y_p is related to η_{10} by (Steigman 2006, 2007):

$$Y_p = 0.2483 \pm 0.0005 + 0.0016(\eta_{10} - 6). \tag{3.2}$$

In the same η_{10} range, the primordial deuterium abundance is given by (Steigman

2006, 2007):

$$10^5(D/H)_p = D_p = 46.5(1 \pm 0.03)(\eta_{10})^{-1.6}. \quad (3.3)$$

From the Y_p value by Peimbert et al. (2007a), the D_p value by O'Meara et al. (2006), the $\Omega_b h^2$ value by Dunkley et al. (2009), and the previous equations we have produced Table 1. From this table, it follows that within the errors Y_p, D_p, and the WMAP observations are in very good agreement with the predicted SBBN values.

Equations (2), (3), and (4) were derived under the assumption of a neutron lifetime, τ_n , of 885.7 ± 0.8 s (Arzumanov et al. 2000). A recent result by Serebrov et al. (2005, 2008) yielded a τ_n of $878.5 \pm 0.7 \pm 0.3$ s. This result would lead to a SBBN Y_p value of 0.2470 for the WMAP $\Omega_b h^2$ determined value (Steigman 2007, Mathews et al. 2005). Mathews et al. obtain for $\tau_n = 881.9 \pm 1.6$ s, mainly the average of the results by Arzumanov et al. (2000) and Serebrov et al. (2005, 2008), a Y_p value 0.0009 smaller than for $\tau_n = 885.7 \pm 0.8$.

The 9σ difference between both τ_n determinations probably indicates that at least one of them includes systematic errors that have not yet been sorted out.

From the Y_p by Peimbert et al. (2007a), the D_p by O'Meara et al. (2006), and SBBN it is found that for $\tau_n = 881.9 \pm 1.6$ the number of effective neutrino families, N_{eff}, is equal to 3.12 ± 0.23. Based on the production of the Z particle by electron-positron collisions in the laboratory and taking into account the partial heating of neutrinos produced by electron-positron annihilations during SBBN Mangano et al. (2002) find that $N_{eff} = 3.04$. The N_{eff} value derived from Y_p, D_p, and SBBN is in excellent agreement with the value derived by Mangano et al. (2002).

The Y_p derived from WMAP is based on the very strong assumption of SBBN. It is also possible to derive Y_p from the study of the microwave radiation without assuming SBBN: from the cosmic microwave background radiation (*i.e.* WMAP + ACBAR + CBI + BOOMERANG), Ichikawa, Sekiguchi and Takahashi (2008a,b) obtain that $Y_p < 0.44$, when they also include the information obtained from BAO + SN + HST (baryon acoustic oscillations in the distribution of galaxies, the distance measurements from type Ia supernovae, and the HST value for H_0) the constrain improves to $Y_p = 0.25^{+0.10}_{-0.07}$. Including the expected data from the Planck satellite they predict a reduction on the Y_p error of about a factor of four to seven, an error still about four to six times higher than the one estimated from the best Y_p determinations based on metal poor H II region observations.

4. The $\Delta Y/\Delta O$ ratio

To determine the Y_p value from a set of metal poor H II regions it is necessary to estimate the fraction of helium, present in the interstellar medium of the galaxy where each H II region is located, produced by galactic chemical evolution. From observations of metal poor extragalactic H II regions it has been found that the Y versus O observations can be fitted with a straight line given by $\Delta Y/\Delta O$ and equation (1) has been used often to derive Y_p. A straight line is predicted by chemical evolution models of metal poor galaxies with the same initial mass function, a given set of stellar yields, and different star formation rates. To obtain different $\Delta Y/\Delta O$ from the models it is necessary to change the initial mass function (for example the maximum mass allowed or the slope at high masses), or the adopted yields.

The observational Y_p, ΔY, and ΔO are affected by different amounts in the presence of temperature variations, while Y_p diminishes by 0.0046 due to temperature variations in the sample of Peimbert et al. (2007a), ΔY is slightly affected and ΔO is strongly affected

by temperature variations (*e. g.* Carigi & Peimbert 2008, Table 3). In addition a fraction of O is embedded in dust grains, fraction that needs to be estimated to compare with models of galactic chemical evolution.

The importance of $\Delta Y/\Delta O$ is two fold: it permits us to obtain a more accurate Y_p value, and permits us to test for the presence of large temperature variations in gaseous nebulae when comparing nebular values with stellar ones.

4.1. *The gaseous O/H determination*

There are two methods to derive the gaseous O/H ratio, from the $I(4363)/I(5007)$ ratio together with the $I(3727)/I(\mathrm{H}\beta)$ and the $I(5007)/I(\mathrm{H}\beta)$ line ratios, the so called $T(4363)$ method, and from the intensity ratio of O II recombination lines to H I recombination lines that has been called the O II$_{RL}$ method by Peimbert et al. (2007b). The O II$_{RL}$ method usually provides higher O/H ratios by 0.15 to about 0.3 dex, this difference is due to temperature variations inside the observed volume and is smaller for metal poor H II regions and higher for metal rich H II regions. The $T(4363)$ method in the presence of temperature variations produces a systematic effect that lowers the O/H abundances relative to the real ones. On the other hand the O II$_{RL}$ method is independent of the temperature structure.

4.2. *The total O/H determination*

Another factor that has to be taken into account to obtain the total O/H ratio is the fraction of O atoms trapped in dust grains. Esteban et al. (1998), based on the depletion of Fe, Mg and Si in the Orion nebula, estimated that the fraction of oxygen atoms trapped in dust grains amounts to 0.08 dex. Mesa-Delgado et al. (2009) have estimated that the fraction of O atoms trapped in dust grains in the Orion nebula amounts to 0.12 ± 0.03 dex; this result is based on three different methods: a) by comparing the O abundances of the B stars of the Orion association with the O abundance of the Orion nebula, b) from the depletion of Fe, Mg and Si in the nebula and assuming that these atoms are combined with molecules containing O, and c) by comparing the shock and nebular abundances of the material associated with the Herbig-Haro object 202.

Rodríguez & Rubin (2005) have estimated the fraction of Fe atoms in galactic and extragalactic H II regions in the gaseous phase, the depletions derived for the different objects define a trend of increasing depletion at higher metallicities; while the Galactic H II regions show less than than 5% of their Fe atoms in the gas phase, the extragalactic ones (LMC 30 Doradus, SMC N88A, and SBS 0335-052) have somewhat lower depletions. Izotov et al. (2006) find a slight increase of Ne/O with increasing metallicity, which they interpret as due to a moderate depletion of O onto grains in the most metal-rich galaxies, they conclude that this O/Ne depletion corresponds to $\sim 20\%$ of oxygen locked in the dust grains in the highest-metallicity H II regions of their sample, while no significant depletion would be present in the H II regions with lower metallicity. Peimbert & Peimbert (2010) based on the Fe/O abundances of Galactic and extragalactic H II regions estimate that for objects in the $8.3 < 12 + \log \mathrm{O/H} < 8.9$ range the fraction of O atoms trapped by dust grains amounts to 0.12 ± 0.03 dex, for objects in the $7.7 < 12 + \log \mathrm{O/H} < 8.3$ range amounts to 0.09 ± 0.03 dex, and for objects in the $7.3 < 12 + \log \mathrm{O/H} < 7.7$ range amounts to 0.06 ± 0.03 dex.

4.3. *Extrapolation of the Y determinations to the value of Y_p, or the O ($\Delta Y/\Delta O$) correction*

From chemical evolution models of different galaxies it is found that $\Delta Y/\Delta O$ depends on the initial mass function (IMF), the star formation rate, the age, and the O value of

the galaxy in question. Peimbert et al. (2007b) have found that $\Delta Y/\Delta O$ is well fitted by a constant value for objects with the same IMF, the same age, and an O abundance smaller than 4×10^{-3}. This result is consistent with the custom of using a constant value for $\Delta Y/\Delta O$ to fit observational data.

To obtain an accurate Y_p value, a reliable determination of $\Delta Y/\Delta O$ for O-poor objects is needed. The $\Delta Y/\Delta O$ value derived by Peimbert, Peimbert, & Ruiz (2000) from observational results and models of chemical evolution of galaxies amounts to 3.5 ± 0.9. More recent results are those by Peimbert (2003) who finds 2.93 ± 0.85 from observations of 30 Dor and NGC 346, and by Izotov & Thuan (2004) who, from the observations of 82 H II regions, find $\Delta Y/\Delta O = 4.3 \pm 0.7$. Peimbert et al. (2007a) have recomputed this value by taking into account two systematic effects not considered by Izotov & Thuan: the fraction of oxygen trapped in dust grains, and the increase in the O abundances due to the presence of temperature variations. From these considerations they obtained for the Izotov & Thuan sample that $\Delta Y/\Delta O = 3.2 \pm 0.7$.

On the other hand Peimbert et al. (2007b) from chemical evolution models with different histories of galactic inflows and outflows for objects with $O < 4 \times 10^{-3}$ find that $2.4 < \Delta Y/\Delta O < 4.0$. From the theoretical and observational results Peimbert et al. (2007a) adopted a value of $\Delta Y/\Delta O = 3.3 \pm 0.7$, that they used with the Y and O determinations from each object to obtain the Y_p value.

4.4. *Comparison of the oxygen abundances of the ISM of the solar vicinity with those of the Sun and F and G stars of the solar vicinity*

In addition to the evidence presented in section 2 in favor of large t^2 values, and consequently in favor of the O II$_{RL}$ method, there is another independent test that can be used to discriminate between the $T(4363)$ method and the O II$_{RL}$ method that consists in the comparison of stellar and H II region abundances of the solar vicinity.

Esteban et al. (2005) determined that the gaseous O/H value derived from H II regions of the solar vicinity amounts to 12 + log (O/H) = 8.69, and including the fraction of O atoms tied up in dust grains it is obtained that 12 + log (O/H) = 8.81 ± 0.04 for the O/H value of the ISM of the solar vicinity. Alternatively from the protosolar value by Asplund et al. (2009), that amounts to 12 + log(O/H) = 8.71, and taking into account the increase of the O/H ratio due to galactic chemical evolution since the Sun was formed, that according to the chemical evolution model of the Galaxy by Carigi et al. (2005) amounts to 0.13 dex, we obtain an O/H value of 8.84 ± 0.04 dex, in excellent agreement with the value based on the O II$_{RL}$ method. In this comparison we are assuming that the solar abundances are representative of the abundances of the solar vicinity ISM when the Sun was formed.

There are two other estimates of the O/H value in the ISM that can be made from observations of F and G stars of the solar vicinity. According to Allende-Prieto et al. (2004) the Sun appears deficient by roughly 0.1 dex in O, Si, Ca, Sc, Ti, Y, Ce, Nd, and Eu, compared with its immediate neighbors with similar iron abundances; by assuming that the O abundances of the solar immediate neighbors are more representative of the local ISM than the solar one, and by adding this 0.1 dex difference to the solar value by Asplund et al. (2009) we obtain that the present value of the ISM has to be higher than 12 + log O/H = 8.81. A similar result is obtained from the data by Bensby & Feltzing (2005) who obtain for the six most O-rich thin-disk F and G dwarfs of the solar vicinity an average [O/H] = 0.16; by assuming their value as representative of the present day ISM of the solar vicinity we find 12 + log O/H = 8.87. Both results are in good agreement with the O/H value derived from the O II$_{RL}$ method.

4.5. *Comparison of $\Delta Y/\Delta Z$ values of the Galactic H* II *region M17 with K dwarfs of the solar vicinity*

The best Galactic H II region to determine the He/H ratio is M17 because it contains a very small fraction of neutral helium and the error introduced by correcting for its presence is very small. Carigi & Peimbert (2008) obtained from observations for M17 (and adopting a Y_p value) a value of $\Delta Y/\Delta Z = 1.97 \pm 0.41$ for $t^2 = 0.036 \pm 0.013$, where Y and Z are the helium and heavy elements by unit mass; by correcting this value considering that the fraction of O trapped in dust amounts to 0.12 dex instead of 0.08 dex (Mesa-Delgado et al. 2009) we obtain $\Delta Y/\Delta Z = 1.77 \pm 0.37$. This $\Delta Y/\Delta Z$ value is in agreement with two independent $\Delta Y/\Delta Z$ determinations derived from K dwarf stars of the solar vicinity that amount to 2.1 ± 0.4 (Jiménez et al. 2003) and to 2.1 ± 0.9 (Casagrande et al. 2007).

On the other hand the value $\Delta Y/\Delta Z = 3.6 \pm 0.68$ derived from collisionally excited lines of M17 under the assumption of $t^2 = 0.00$ by Carigi and Peimbert (2008) (value corrected for a fraction of O trapped by dust grains of 0.12 dex) is not in agreement with the values derived from K dwarf stars of the solar neighborhood.

4.6. *Comparison of Y_p and $\Delta Y/\Delta O$ with models of chemical evolution for the disk of the Galaxy*

To compare Galactic chemical evolution models of Y and O with observations we need to use the best determinations available of the abundances of these elements. We consider that the two most accurate Galactic Y and O determinations are the presolar values (Asplund et al. 2009) and the M17 H II region values (Carigi & Peimbert 2008).

Carigi et al. (2005) presented chemical evolution models for the disk of the Galaxy that

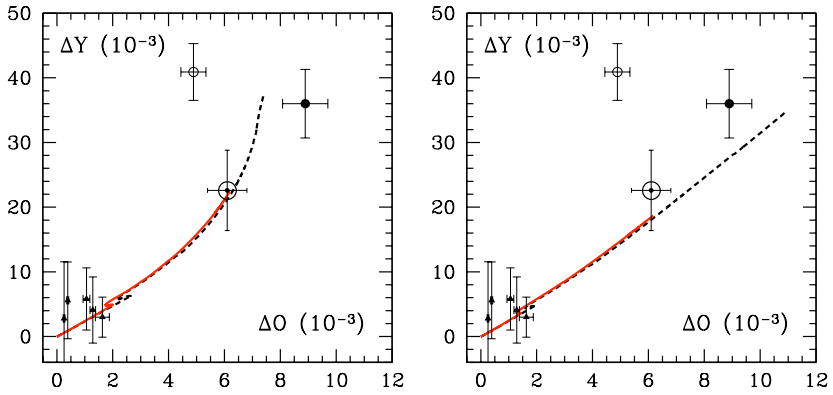

Figure 1. In the two panels the origin corresponds to $Y_p = 0.2477$, the triangles represent the Y and O values derived by Peimbert et al. (2007a) for five metal poor extragalactic H II regions, the open and filled circles represent the M17 values for $t^2 = 0.00$, and $t^2 = 0.036$ respectively from Carigi & Peimbert (2008), the large open circle with a dot in the center corresponds to the presolar values by Asplund et al. (2009). The left panel presents two chemical evolution models by Carigi & Peimbert (2010), the solid line is a model for the Galactic disk with a time span from the formation of the Galaxy to the formation of the Sun at a galactocentric distance of 8 kpc, while the dashed line corresponds to a model for the Galactic disk with a time span from the formation of the Galaxy to the present at a galactocentric distance of 6.75 kpc, the distance of M17 to the galactic center; the stellar yields for the two panels are different, see subsection 4.6 for further details.

fit the slope and the absolute value of the O/H gradient, these models are also successful in reproducing the C/O gradient derived from H II regions and the C/O versus O/H evolution history of the solar vicinity obtained from stellar observations. In Figure 1 we present chemical evolution models by Carigi & Peimbert (2010) for the Y and O abundances of the Galactic disk for two sets of stellar yields where they have added the presolar values by Asplund et al. (2009) for comparison. These models are based on the same assumptions than those adopted by Carigi and Peimbert (2008). The only difference between the models in the left panel and those in the right one, is that for massive stars with $Z > 0.004$ the ones in the left use the yields by Maeder (1992) with high mass loss, while the ones on the right use the yields by Hirschi, Meynet, & Maeder (2005) with low mass loss. There are at least three conclusions that we can extract from the figure: (a) the fit for the presolar values is very good for the two sets of yields, (b) the fit for M17 for $t^2 = 0.036 \pm 0.013$ is good, but it can be improved by assuming a set of yields intermediate between the two sets used; a similar result in favor of an intermediate set of yields was obtained by Cescutti et al. (2009) based on C/O observations for stars in the bulge of the Galaxy, (c) the models do not fit M17 for $t^2 = 0.00$, this result is in agreement with those by Esteban et al. (2005, 2009) and Peimbert et al. (2007a) who find large t^2 values for Galactic and extragalactic H II regions. Moreover the O and Y abundances for the presolar material and for M17 are derived from independent methods, and they are fitted by the same chemical evolution model. This fit provides us with a consistency check on the gaseous nebulae helium and oxygen abundance determinations based on large t^2 values.

5. Conclusions

During the last 50 years the determination of Y_p has been very important for the study of cosmology, stellar evolution, and the chemical evolution of galaxies. To determine Y_p it is necessary to determine accurate atomic parameters and the physical conditions inside ionized gaseous nebulae.

During the last five decades the accuracy of the Y_p determination has increased considerably, and during the last two decades the differences among the best Y_p determinations have been due to systematic effects (*e. g.* Olive & Skillman 2004, Peimbert 2008). These systematic effects have been gradually understood, particularly during the last few years.

The best Y_p determination available, that by Peimbert et al. (2007a), is in agreement with the D_p determination and with the WMAP observations under the assumption of SBBN. The errors in the Y_p determination are still large and there is room for non-standard physics.

Similarly to improve the accuracy of the Y_p value derived under the assumption of SBBN and the $\Omega_b h^2$ derived from the background radiation, a new determination of the neutron lifetime is needed to sort out the difference between the τ_n obtained by Arzumanov et al. (2000) and the τ_n obtained by Serebrov et al. (2005, 2008).

To improve the accuracy of the Y_p determination based on metal poor H II regions, the following steps should be taken in the near future: (a) to obtain new observations of high spectral resolution of metal poor H II regions, those with $0.0005 < Z < 0.001$ to reduce the effect of the collisional excitation of the Balmer lines, which for the present day Y_p determinations is one of the two main sources of error; (b) to determine the temperature of the H II regions based on a large number of He I lines observed with high accuracy, and to try to avoid the use of $T(4363/5007)$ temperatures that weigh preferentially the regions of higher temperature than the average one, effect that artificially increases the Y_p determinations; (c) additional efforts should be made to understand the mechanisms

that produce temperature variations in giant H II regions and once they are understood they should be incorporated into photoionization models; (d) the He I recombination coefficients should be computed again with an accuracy higher than that of the last two determinations; (e) the computation of tailor-made photoionization models for extragalactic H II regions including the effect of case D on the intensity of the H I and He I lines should be carried out.

The observed $\Delta Y/\Delta O$ ratios provide us with strong constrains for models of galactic chemical evolution. The gaseous O abundances have to be corrected by the fraction of oxygen embedded in dust grains and by the effect of temperature variations, these two corrections together amount to about 0.2 to 0.4 dex. Chemical evolution models for the Galactic disk are able to reproduce the observed Y and O presolar values and the Y and O values derived for M17 based on H, He and O recombination lines, but not the M17 Y and O values derived from $T(4363/5007)$ and O collisionally excited lines under the assumption of $t^2 = 0.00$. This result provides a consistency check in favor of the presence of large temperature variations in H II regions and in favor of the Y_p determinations based on the T(He I) and t^2 values derived from He I recombination lines.

Acknowledgements

We wish to thank Gary Ferland, Evan Skillman and Gary Steigman for several fruitful discussions. We are grateful to the SOC for an outstanding meeting and to the LOC for their warm hospitality. We would also like to acknowledge partial support received from CONACyT grant 46904.

References

Allende-Prieto, C., Barklem, P. S., Lambert, D. L., & Kunha, K. 2004, *A&A*, 420, 183
Arzumanov, S., Bondarenko, L. Chernyavsky, S., et al. 2000, *Physics Letters B*, 483, 15
Asplund, M., Grevesse, N., Sauval, A. J., & Scott, P. 2009, *ARAA*, 47, 481
Bauman, R. P., Porter, R. L., Ferland, G. J., & MacAdam, K. B. 2005, *ApJ*, 628, 541
Benjamin, R. A., Skillman, E. D., & Smits, D. P. 1999, *ApJ*, 514, 307
Benjamin, R. A., Skillman, E. D., & Smits, D. P. 2002, *ApJ*, 569, 288
Bensby, T. & Feltzing, S. 2006, *MNRAS*, 367, 1181
Carigi, L. & Peimbert, M. 2008, *Rev. Mexicana AyA*, 44, 311
Carigi, L. & Peimbert, M. 2010, in preparation
Carigi, L., Peimbert, M., Esteban, C., & García-Rojas, J. 2005, *ApJ*, 623, 213
Casagrande, L., Flynn, C., Portinari, L., Girardi, L. & Jiménez, R. 2007, *MNRAS*, 382, 1516
Cescutti, G., Matteucci, F., McWilliam, A., & Chiappini, C. 2009, *A&A*, 505, 605
Dunkley, J., Komatsu, E., Nolta, M. R., et al. 2009, *ApJS*, 180, 306
Esteban, C., Bresolin, F., Peimbert, M., et al. 2009, *ApJ*, 700, 654
Esteban, C., García-Rojas, J., Peimbert, M., et al. 2005, *ApJ*, 618, L95
Esteban, C., Peimbert, M., Torres-Peimbert, S., & Escalante, V. 1998, *MNRAS*, 295, 401
Hirschi, R., Meynet, G., & Maeder, A. 2005, *A&A*, 433, 1013
Ichikawa, K., Sekiguchi, T., & Takahashi, T. 2008a, *Phys. Rev. D*, 78, 043509
Ichikawa, K., Sekiguchi, T., & Takahashi, T. 2008b, *Phys. Rev. D*, 78, 083526
Izotov, Y. I., Stasińska, G., Meynet, G., Guseva, N. G., & Thuan, T. X. 2006, *A&A*, 448, 955
Izotov, Y. I. & Thuan, T. X. 2004, *ApJ*, 602, 200
Izotov, Y. I., Thuan, T. X., & Stasińska, G. 2007, *ApJ*, 662, 15
Jiménez, R., Flynn, C., MacDonald, J., & Gibson, B. K. 2003, *Science*, 299, 1552
Luridiana, V., Simón-Díaz, S., Cerviño, M., et al. 2009, *ApJ*, 691, 1712
Maeder, A. 1992, *A&A*, 264, 105
Mangano, G., Miele, G., Pastor, S., & Peloso, M. 2002, *Physics Letters B*, 534, 8
Mathews, G. J., Kajino, T., & Shima, T. 2005, *Phys. Rev. D*, 71, 021302

Mesa-Delgado, A., Esteban, C., García-Rojas, J., et al. 2009, *MNRAS*, 395, 855
Olive, K. A. 2008, in: *Chemical Evolution Across Space & Time: From the Big Bang to Prebiotic Chemistry* L. Zaikowski & J. M. Friedrich, (eds.). ACS Symposium Series Vol. 981, 16
Olive, K. A. & Skillman, E. D. 2004, *ApJ*, 617, 290
O'Meara, J. M., Burles, S., Prochaska, J. X., & Prochter, G. E. 2006, *ApJ*, 649, L61
Pagel, B. E. J. 2009, *Nucleosynthesis and Chemical Evolution of Galaxies, Second Edition*, Cambridege University Press
Peimbert, A. 2003, *ApJ*, 584, 735
Peimbert, A. & Peimbert, M. 2010, in preparation
Peimbert, A., Peimbert, M., & Luridiana, V. 2002, *ApJ*, 565, 668
Peimbert, M. 1967, *ApJ*, 150, 825
Peimbert, M. 2008, *Current Science*, 95, 1165
Peimbert, M., Luridiana, V., & Peimbert, A. 2007a, *ApJ*, 666, 636
Peimbert, M., Luridiana, V., Peimbert, A., & Carigi, L. 2007b, in: *From Stars to Galaxies: Building the Pieces to Build Up the Universe* A. Vallenari, R. Tantalo, L. Portinari, & A. Moretti, (eds.), ASP Conference Series Vol. 374, 81
Peimbert, M., Peimbert, A., & Ruiz, M. T. 2000, *ApJ*, 541, 688
Peimbert, M. & Torres-Peimbert, S. 1999, *ApJ* (Centennial Issue), 525C, 1143
Porter, R. L., Bauman, R. P., Ferland, G. J., & MacAdam, K. B. 2005, *ApJ*, 622, L73
Porter, R. L., Ferland, G. J., & MacAdam, K. B. 2007, *ApJ*, 657, 327-337
Porter, R. L., Ferland, G. J., MacAdam, K. B., & Storey, P. J. 2009, *MNRAS*, 393, L36
Rodríguez, M. & Rubin, R. H. 2005, *ApJ*, 626, 900
Serebrov, A. P., Varlamov, V. E., Kharitonov, A. G., et al. 2005, *Physics Letters B*, 605, 72
Serebrov, A. P., Varlamov, V. E., Kharitonov, A. G., et al. 2008, *Phys. Rev. C*, 78, 035505
Stasińska, G. 1990, *A&AS*, 83, 501
Steigman, G. 2006, *Int. J. Mod. Phys. E*, 15, 1
Steigman, G. 2007, *Annu. Rev. Nucl. Part. Sci.*, 57, 463
Weinberg, S. 2008, *Cosmology*, Oxford University Press

Light elements in the Universe
Proceedings IAU Symposium No. 268, 2010
C. Charbonnel, M. Tosi, F. Primas & C. Chiappini, eds.

DOI: 00.0000/X000000000000000X

^{4}He abundances: Optical versus radio recombination line measurements

Dana S. Balser[1], Robert T. Rood[2] and T. M. Bania[3]

[1]National Radio Astronomy Observatory, 520 Edgemont Road, Charlottesville, VA 22903-2475 USA
email: dbalser@nrao.edu

[2] Astronomy Department, University of Virginia, P.O.Box 3818, Charlottesville VA 22903-0818, USA
email: rtr@virginia.edu

[3] Institute for Astrophysical Research, 725 Commonwealth Avenue, Boston University, Boston MA 02215, USA
email: bania@bu.edu

Abstract. Accurate measurements of the ^{4}He/H abundance ratio are important in constraining Big Bang nucleosynthesis, models of stellar and Galactic evolution, and H II region physics. We discuss observations of radio recombination lines using the Green Bank Telescope toward a small sample of H II regions and planetary nebulae. We report ^{4}He/H abundance ratio differences as high as $15-20\%$ between optical and ratio data that are difficult to reconcile. Using the H II regions S206 and M17 we determine ^{4}He production in the Galaxy to be $dY/dZ = 1.71 \pm 0.86$.

Keywords. Galaxy: abundances, ISM: planetary nebulae, H II regions, radio lines: ISM

1. Introduction

Observations of optical recombination lines (ORLs) are the primary diagnostics used to determine ^{4}He abundances in ionized nebulae such as H II regions and planetary nebulae (PNe). At optical wavelengths there are also many bright collisionally excited lines that can be used to probe the physical conditions in these objects and to derive their metallicity. Peimbert et al. (2010) discuss the main uncertainties in calculating accurate ^{4}He/H abundance ratios from ORLs. Much of the focus has been on deriving ^{4}He abundances in metal poor objects, such as blue compact galaxies, to deduce the primordial ^{4}He/H abundance (e.g., see Izotov 2010; Skillman 2010). Because there is no way to directly measure neutral helium within the H II region it is difficult to determine accurate ^{4}He/H abundance ratios for most Galactic H II regions due to the relatively soft ionizing radiation field for most objects. One exception is M17 which contains several O3 type stars and is estimated to contain little neutral helium (e.g., Carigi & Peimbert 2008).

Observations of recombination lines at other wavelengths (e.g., radio and infrared) give important checks to ORLs since deriving ^{4}He/H abundance ratios using these transitions will have different systematic uncertainties. Moreover, recombination lines at radio and infrared wavelengths are not obscured by dust and may be used to probe ^{4}He abundances throughout the Galactic disk.

Radio recombination lines (RRLs) are relatively weak when compared to ORLs and emission measures of $\int n_e^2 d\ell \sim 10^3$ cm^{-6} pc are required to detect these lines with current instrumentation compared with $\sim$ 1cm^{-6} pc at optical wavelengths. Recent improvements in radio spectrometers, however, now allow the simultaneous observation of

multiple RRLs. Adjacent RRLs have line intensities and widths that are different by only a few percent. Therefore, averaging adjacent RRLs can be used to increase the signal-to-noise ratio without significantly increasing the error in the line parameters.

Besides sensitivity, the main problem in making accurate ^{4}He measurements using RRLs has been poor spectral baselines. For single-dish telescopes reflections from the super-structure cause standing waves that are not easy to model and that do not integrate down with time. (Although the spectral baselines are much better for radio interferometers, until recently the spectral resolution and bandwidth were not sufficient to produce accurate line parameters in most cases.) The off-axis, clear aperture design of the Green Bank Telescope (GBT) has significantly improved the spectral baselines, and when combined with a flexible spectrometer provides a significant improvement over previous telescopes when measuring weak, wide spectral lines (e.g., Balser 2006; Bania et al. 2010).

One advantage to using RRLs over ORLs is that the high n states of hydrogen and helium should be altered by radiative and collisional effects in the same way so that the ratio of the line areas is equal to the ionic abundance ratio. At high n, where the levels are controlled by collisions and are in LTE, this should certainly be the case. H II region models indicate that near $n \sim 90$ (9 GHz) the RRLs are approximately in LTE (Shaver 1980; Balser et al. 1999). Early RRL observations of Galactic H II regions, however, produced $^4He^+/H^+$ abundance ratios that varied with n (Lockman & Brown 1982). Peimbert et al. (1992) studied α, β, and γ RRL transitions near 9 GHz with the same spatial resolution and derived $^4He^+/H^+$ abundance ratios consistent within the errors. These data had better sensitivity and improved spectral baselines over previous RRL measurements (Balser et al. 1994).

Ionization and density structure must be understood when using either optical or radio recombination lines to calculate ^{4}He/H abundance ratios. Since there is no transition of neutral helium other diagnostics must be used to determine if any neutral helium resides within the H II region. Therefore, corrections for ionization structure often contribute significantly to the uncertainty in calculating the ^{4}He/H abundance ratio (e.g., Baldwin et al. 1991). This is why H II regions with very hard radiation fields are often chosen for ^{4}He studies (e.g., blue compact galaxies). Nevertheless, a reverse ionization correction can result in these objects wherein neutral hydrogen exists within the He II region (Ballantyne et al. 2000; Gruenwald et al. 2002; Sauer & Jedamzik 2002). Moreover, when combined with density structures the ionization correction factor will change (Viegas et al. 2000). Also, density structure alone can alter the radiative transfer and thus effect ^{4}He analyses (Mathis & Wood 2005).

2. Observations

We made GBT RRL observations toward four PNe (NGC 3242, NGC 6826, NGC 6543, and NGC 7009) and two Galactic H II regions (M17 and S206). All observations were made at X-band ($8 - 10$ GHz) with a spatial resolution (beam) of 80 arcsec and a spectral resolution of 0.4 km s^{-1}. The PNe observations were part of the ^{3}He experiment wherein the 91α and 92α H and He RRLs were observed simultaneously with the $^3He^+$ hyperfine transition (see Bania et al. 2010). These PNe consist of multiple shells with large, extended halos. The RRL emission arises from the shell structure which is unresolved by the GBT beam. Because the hot central star produces a hard ionizing radiation field there should be little or no neutral helium in these nebulae.

The H II region observations were part of a Galactic H II survey measuring H, He and C RRL emission. Seven adjacent alpha RRLs were observed simultaneously ($87\alpha - 93\alpha$).

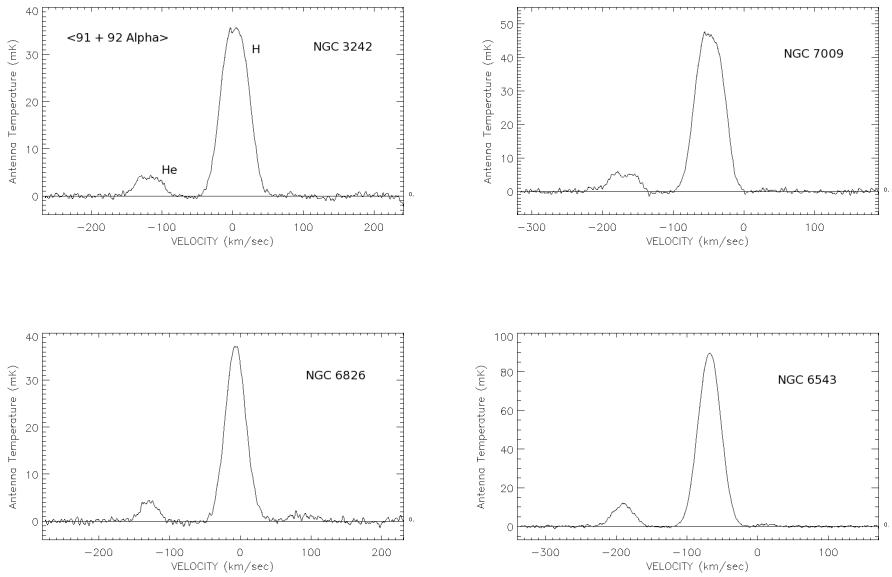

Figure 1. Planetary nebulae GBT RRL spectra. Plotted is the antenna temperature in mK versus the LSR velocity in km s^{-1}. The 91α and 92α RRLs have been averaged and the spectra smoothed to a velocity resolution of 2.0 km s^{-1}. The continuum emission has been subtracted.

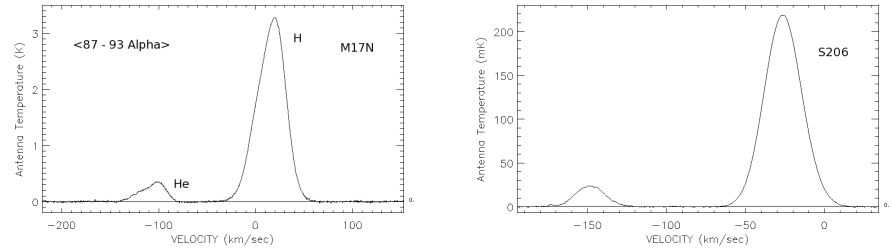

Figure 2. H II region GBT RRL spectra. Plotted is the antenna temperature in mK versus the LSR velocity in km s^{-1}. RRLs spanning 87α to 93α have been averaged. The continuum emission has been subtracted.

M17 and S206 are expected to have little neutral helium and therefore are good candidates for measuring ^{4}He/H (e.g., Deharveng et al. 2000; Carigi & Peimbert 2008). Both M17 and S206 are extended relative to the GBT beam and thus we are only probing part of these nebulae. Results for S206 have already been published (Balser 2006). The M17 data consist of observations toward a northern (M17N) and a southern (M17S) component. Since M17S is optically obscured, we discuss M17N here to make comparisons with ORLs. Our M17N J2000 position (RA=18:17:46.5, Dec=−16:10:33.1) overlaps with some optical positions.

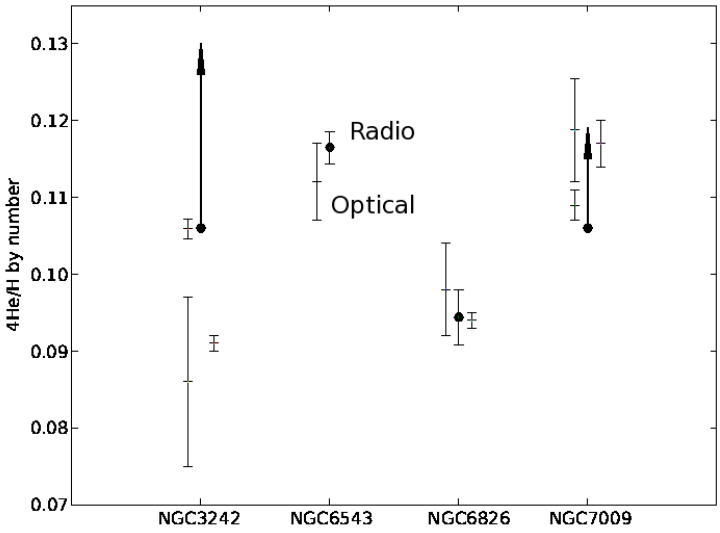

Figure 3. ^{4}He/H abundance ratios by number for the planetary nebulae sample. Filled circles are GBT results, while the plus sign symbols are from ORLs in the literature (Barker 1983,1985,1988; Perinotto et al. 2004; Krabbe & Copetti 2006).

The PNe spectra are summarized in Figure 1. The H and ^{4}He line profiles for NGC 3242 and NGC 7009 are square-shaped, consistent with an optically thin, unresolved, expanding nebulae. When the expansion velocity is small compared with the thermal and turbulent velocity dispersion then the line profiles will become Gaussian shaped. This appears to be the case for NGC 6826 and NGC 6543 since the line profiles for these objects are well modeled by a Gaussian function.

The H II region spectra are summarized in Figure 2. The line profiles are well fit by Gaussian components. M17N is best fit by two components and S206 by one component. In both nebulae carbon RRL emission is detected. The signal-to-noise ratio is excellent and the spectral baselines well behaved.

3. Results and discussion

The ^{4}He abundances for our PNe sample are shown in Figure 3. The GBT ^{4}He/H abundance ratios are calculated assuming $^4\mathrm{He/H} = {}^4\mathrm{He}^+/\mathrm{H}^+$. For NGC 3242 and NGC 7009 $^4\mathrm{He}^{++}$ has been detected and thus our abundance estimates are only limits as indicated by the arrows in Figure 3. The tip of the arrow is an estimate of ^{4}He/H using the $^4\mathrm{He}^{++}/{}^4\mathrm{He}^+$ ratios from Cahn et al. (1992) and assuming a uniform distribution of $^4\mathrm{He}^+$ and $^4\mathrm{He}^{++}$. The optical and radio data are in excellent agreement except for NGC 3242. This PN has significant amounts of $^4\mathrm{He}^{++}$, however, that may not be distributed uniformly. Therefore, the estimate of ^{4}He/H for the GBT data shown in Figure 3 may be smaller than indicated.

Figure 4 shows the derived abundance by mass, Y, plotted as a function of nebular metallicity, Z. Both Galactic and extragalactic H II region ^{4}He abundances are plotted

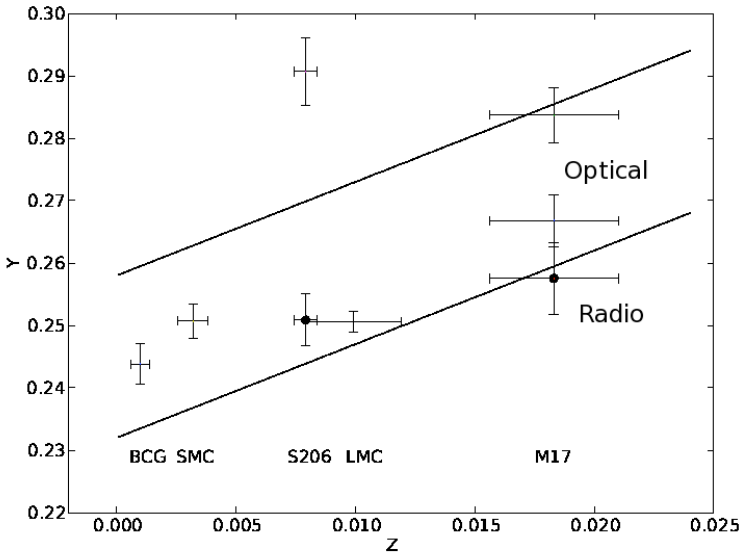

Figure 4. Evolution of ^{4}He/H. The helium abundance by mass, Y, is plotted against the metallicity, Z. GBT results are shown as filled circles for M17 and S206 while ORL results are plus signs for M17 (Carigi & Peimbert 2008; García-Rojas et al. 2007), the Small Magellanic Cloud (Peimbert et al. 2007), the Large Magellanic Cloud (Peimbert 2003), and a sample of blue compact galaxies (Izotov & Thuan 2004). The solid lines assume the range of primordial ^{4}He/H abundance ratios from Olive & Skillman (2004) and $dY/dZ = 1.5$ (Chiappini et al. 2002).

as symbols together with an estimate of ^{4}He processing, dY/dZ, shown by the solid lines. For the GBT H II region data we again assume $^4\mathrm{He/H} = {}^4\mathrm{He}^+/\mathrm{H}^+$. The optical data shown for M17 are based on two different positions: M17-14 and M17-123 (an average of M17-1, M17-2, and M17-3) (Peimbert et al. 1992). The high ^{4}He optical value shown in Figure 4 is from M17-123 and is expected to be a better estimate of ^{4}He/H since this region has a higher degree of ionization and therefore less neutral helium (Carigi & Peimbert 2008). Although the radio ^{4}He abundance is the same within the errors as the optical value for position M17-14, the GBT position overlaps with position M17-3 and not with M17-14. Yet the GBT ^{4}He/H abundance ratio is significantly smaller than the optical value for position M17-3. This discrepancy may result because the large GBT beam averages over regions with different properties.

The ^{4}He abundances for S206 are puzzling. Deharveng et al. (2000) measure no variation in ^{4}He/H across S206 and values of $\mathrm{O}^{++}/\mathrm{O}$ that range from 0.7 to 0.85; they conclude that there is no neutral helium in the nebula. S206 is ionized primarily by an O5 type star—the nebula structure is simple compared with M17 and contains less dust. Therefore, S206 should be an excellent candidate for measuring ^{4}He/H.

But the optical value for ^{4}He/H is 20% higher than the radio value. This discrepancy is difficult to reconcile and the optical result is not consistent with our understanding of Galactic chemical evolution. We expect there to be a net production of ^{4}He in stars and therefore $dY/dZ > 0$. This is illustrated by the two solid lines in Figure 4 where we have adopted the ^{4}He Galactic production of $dY/dZ = 1.5$ from Chiappini et al. (2002) and

the conservative range for the ^{4}He primordial abundance from Olive & Skillman (2004). For the Milky Way we derive $dY/dZ = 1.71 \pm 0.86$ by using only the radio ^{4}He/H value for S206, both the optical and radio ^{4}He/H values for M17, and the primordial ^{4}He/H abundance ratio from Steigman (2007).

References

Baldwin, J. A., Ferland, G. J., Martin, P. G., Corbin, M. R., Cota, S. A., Peterson, B. M., & Slettebak, A. 1991, *ApJ*, 374, 580

Ballantyne, D.R., Ferland, G.J., & Martin, P.G. 2000, *ApJ*, 536, 773

Balser, D.S. 2006, *AJ*, 132, 2326

Balser, D. S., Bania, T. M., Brockway, C. J., Rood, R. T., & Wilson, T. L. 1994, *ApJ*, 430, 667

Balser, D. S., Bania, T. M., Rood, R. T., & Wilson, T. L. 1999, *ApJ*, 510, 759

Bania, T.M., Rood, R.T., & Balser, D.S. 2010, in: *Light Elements in the Universe* C. Charbonnel, M. Tosi, F. Primas, & C. Chiappini (eds.), Proc. IAU Symposium No. 268, (Cambridge: CUP), p. XX

Barker, T. 1983, *ApJ*, 267, 630

Barker, T. 1985, *ApJ*, 294, 193

Barker, T. 1988, *ApJ*, 326, 164

Cahn, J.H., Kaler, J.B., & Stanghellini, L. 1992, *A&AS*, 94, 399

Carigi, L., & Peimbert, M. 2008, *Rev. Mexicana AyA*, 44, 311

Chiappini, C., Renda, A., & Matteucci, F. 2002, *A&A*, 395, 789

Deharveng, L., Peña, M., Caplan, J., & Costero, R. 2000, *MNRAS*, 311, 329

García-Rojas, J., Esteban, C., Peimbert, A., Rodríguez, M., Peimbert, M., & Ruiz, M.T. 2007, *Rev. Mexicana AyA*, 43, 3

Gruenwald, R., Steigman, G., & Viegas, S.M. 2002, *ApJ*, 567, 931

Izotov, Y.I. 2010, in: *Light Elements in the Universe* C. Charbonnel, M. Tosi, F. Primas, & C. Chiappini (eds.), Proc. IAU Symposium No. 268, (Cambridge: CUP), p. XX

Izotov, Y.I., & Thuan, T.X. 2004, *ApJ*, 602, 200

Krabbe, A.C., & Copetti, M.V.F. 2006, *A&A*, 450, 159

Lockman, F. J., & Brown, R. L. 1982, *ApJ*, 259, 595

Mathis, J. S., & Wood, K. 2005, *MNRAS*, 360, 227

Peimbert, A. 2003, *ApJ*, 584, 735

Peimbert, M., Luridiana, V., & Peimbert, A. 2007, *ApJ*, 666, 636

Peimbert, P., Peimbert, A., Carigi, L., & Luridiana, V. 2010, in: *Light Elements in the Universe* C. Charbonnel, M. Tosi, F. Primas, & C. Chiappini (eds.), Proc. IAU Symposium No. 268, (Cambridge: CUP), p. XX volume

Peimbert, M., Rodríguez, L.F., Bania, T.M., Rood, R.T., & Wilson, T.L. 1992a, *ApJ*, 395, 484

Peimbert, M., Torres-Peimbert, S., & Ruiz, M.T. 1992b, *Rev. Mexicana AyA*, 24, 155

Perinotto, M., Morbidelli, L., & Scatarzi, A. 2004, *MNRAS*, 349, 793

Olive, K.A., & Skillman, E.D. 2004, *ApJ*, 617, 29

Sauer, D., & Jedamizik, K. 2002, *A&A*, 381, 361

Shaver, P. A. 1980, *A&A*, 91, 279

Skillman, E. 2010, in: *Light Elements in the Universe* C. Charbonnel, M. Tosi, F. Primas, & C. Chiappini (eds.), Proc. IAU Symposium No. 268, (Cambridge: CUP), p. XX

Steigman, G. 2007, *Ann. Rev. Nucl. Part. Sci.*, 57, 463

Viegas, S.M., Gruenwald, R., & Steigman, G. 2002, *ApJ*, 531, 813

Light elements in the Universe
Proceedings IAU Symposium No. 268, 2010
C. Charbonnel, M. Tosi, F. Primas & C. Chiappini, eds.

DOI: 00.0000/X000000000000000X

The primordial abundance of ^{4}He from a large sample of low-metallicity H II regions

Yuri I. Izotov

Main Astronomical Observatory,
Ukrainian National Academy of Sciences,
Zabolotnoho 27, Kyiv 03680, Ukraine
email: izotov@mao.kiev.ua

Abstract. We determine the primordial helium mass fraction Y_p using 1700 spectra of low-metallicity extragalactic H II regions. This sample is selected from the Data Release 7 of the Sloan Digital Sky Survey, from European Southern Observatory archival data and from our own observations. We have considered known systematic effects which may affect the ^{4}He abundance determination. They include collisional and fluorescent enhancements of He I recombination lines, underlying He I and hydrogen stellar absorption lines, collisional excitation of hydrogen lines, temperature and ionization structure of the H II region. Monte Carlo methods are used to solve simultaneously the above systematic effects. We find a primordial helium mass fraction Y_p = 0.2512 ± 0.0006(stat.) ± 0.0020 (syst.). This value is higher than the value given by Standard Big Bang Nucleosynthesis (SBBN) theory. If confirmed, it would imply slight deviations from SBBN.

Keywords. galaxies: abundances; galaxies: irregular; galaxies: ISM; ISM: H II regions; ISM: abundances

1. Introduction

The determination of the primordial ^{4}He (hereafter He) abundance and some other light elements (D, ^{3}He, ^{7}Li) plays an important role in testing cosmological models. In the standard theory of big bang nucleosynthesis (SBBN), given the number of light neutrino species, the abundances of these light elements depend only on one cosmological parameter, the baryon-to-photon number ratio η.

While a single good baryometer like D is sufficient to derive the baryonic mass density from BBN, accurate measurements of the primordial abundance of He are required to check the consistency of SBBN. The primordial abundance of He, can in principle be derived accurately from observations of the helium and hydrogen emission lines from low-metallicity H II regions. Several groups have used this technique to derive the primordial He mass fraction Y_p, with somewhat different results. In the most recent study Izotov et al. (2007) based on a large sample of 93 H II regions derived $Y_p = 0.2472 \pm 0.0012$ and $Y_p = 0.2516 \pm 0.0011$, using Benjamin et al. (1999,2002) and Porter et al. (2005) He I emissivities, respectively. On the other hand, Peimbert et al. (2007) obtained $Y_p = 0.2477 \pm 0.0029$ based on the sample of 5 H II regions, Porter et al. (2005) He I emissivities, and adopting non-zero temperature fluctuations. Fukugita & Kawasaki (2006) derived $Y_p = 0.250 \pm 0.004$ for a sample of 31 H II regions by Izotov & Thuan (2004), adopting Benjamin et al. (1999,2002) He I emissivities.

Although He is not a sensitive baryometer (Y_p depends only logarithmically on the baryon density), its primordial abundance depends much more sensitively on the expansion rate of the Universe and is very sensitive to any small deviation from SBBN. However, to detect small deviations from SBBN and make cosmological inferences, Y_p

has to be determined to a level of accuracy of less than one percent. In particular, many known systematic effects need to be taken into account to transform the observed He I line intensities into a He abundance. These effects are: (1) reddening, (2) underlying stellar absorption in the He I lines, (3) collisional excitation of the He I lines which make their intensities deviate from their recombination values, (4) fluorescence of the He I lines which also make their intensities deviate from their recombination values, (5) collisional excitation of the hydrogen lines (hydrogen enters because the helium abundance is calculated relative to that of hydrogen), (6) possible departures from case B in the emissivities of H and He I lines, (7) the temperature structure of the H II region and (8) its ionization structure. All these corrections are at a level of a few percent except for effect (3) that can be much higher, exceeding 10% in the case of the He I λ5876 emission line in hot and dense H II regions. All these effects were analyzed and taken into account by Izotov et al. (2007) for a sample of 93 H II regions from Izotov & Thuan (2004) (hereafter HeBCD sample).

In this contribution we are aiming to significantly increase the sample of H II regions for the analysis of the systematic effects and determine the primordial He abundance with more accuracy. For this we select spectra of bright H II regions from the Data Release 7 (DR7) of the Sloan Digital Sky Survey (hereafter SDSS sample) (Abazajian et al. 2009). In addition, we use available spectroscopic data from the ESO archive. The use of these additional data greatly increases the sample of objects suitable for the primordial He determination by a factor up to ~ 20 compared to the HeBCD sample of H II regions.

In the present determination of the primordial He abundance, we take into account all eight effects discussed above. The method has been detailed in Izotov et al. (2007) and is more concisely discussed in this paper.

2. The sample

We determine Y_p for the sample which includes three different subsamples, HeBCD, VLT, and SDSS. The HeBCD subsample, composed of 93 spectra has been discussed by Izotov et al. (2007). The SDSS subsample was selected from the SDSS DR7 and consists of 1534 spectra of H II regions with the Hβ line flux greater than 4×10^{-15} erg s^{-1} cm^{-2}. Finally, we selected 73 spectra of H II regions from the ESO archive which were obtained with the spectrographs UVES, FORS1 and FORS2 mounted on the VLT. The majority of objects in the HeBCD, VLT and SDSS subsamples are low-metallicity H II regions in dwarf emission-line galaxies.

3. The method

3.1. *Linear regressions*

As in our previous work (see Izotov et al. 2007 and references therein), we determine the primordial He mass fraction Y_p by fitting the data points in the Y – O/H plane with linear regression line of the form (Peimbert & Torres-Peimbert 1974,1976)

$$Y = Y_p + \frac{\mathrm{d}Y}{\mathrm{d(O/H)}}(\mathrm{O/H}), \tag{3.1}$$

where

$$Y = \frac{4y(1-Z)}{1+4y} \tag{3.2}$$

is the He mass fraction, Z is the heavy element mass fraction, $y = (y^+ + y^{2+}) \times ICF(\mathrm{He^+}+\mathrm{He^{2+}})$ is the He abundance, $y^+ \equiv \mathrm{He^+/H^+}$ and $y^{2+} \equiv \mathrm{He^{2+}/H^+}$ are re-

spectively the abundances of singly and doubly ionized He, and $ICF(\mathrm{He^+}+\mathrm{He^{2+}})$ is the ionization correction factor for He.

We also take into account depletion of oxygen on dust grains. Izotov et al. (2006) demonstrated that the Ne/O abundance ratio for low-metallicity BCDs is not constant but is increased with increasing oxygen abundance. This effect is small, with ΔlogNe/O = 0.1 when the oxygen abundance is changed from 12+logO/H = 7.0 to 8.6, and it is attributed to oxygen depletion. We correct oxygen abundance for such depletion, using regression log Ne/O versus oxygen abundance found by Izotov et al. (2006) and assuming that depletion is absent in galaxies with 12+logO/H = 7.0.

To derive the parameters of the linear regressions, we use the maximum-likelihood method (Press et al. 1992) which takes into account the errors in Y, and O/H for each object.

The derived y^+ abundances depend on the He I emissivities, the fraction $\Delta I(\mathrm{H}\alpha)/I(\mathrm{H}\alpha)$ of the Hα emission line flux due to collisional excitation, the electron number density $N_e(\mathrm{He^+})$, the electron temperature $T_e(\mathrm{He^+})$, the equivalent widths $\mathrm{EW}_{abs}(\lambda3889)$, $\mathrm{EW}_{abs}(\lambda4471)$, $\mathrm{EW}_{abs}(\lambda5876)$, EW_{abs} ($\lambda6678$) and $\mathrm{EW}_{abs}(\lambda7065)$ of He I stellar absorption lines, and the optical depth $\tau(\lambda3889)$ of the He I $\lambda3889$ emission line. To determine the best weighted mean value of y^+_{wm} , we use the Monte Carlo procedure described in Izotov & Thuan (2004) and Izotov et al. (2007), randomly varying each of the above parameters within a specified range, excluding He I which are not varied.

In those cases when the nebular He II $\lambda4686$ emission line was detected, we have added the abundance of doubly ionized helium $y^{2+} \equiv \mathrm{He^{2+}/H^+}$ to y^+.

3.2. *Set of parameters for the He abundance determination*

For the determination of He abundance we adopt Porter et al. (2005) He I emissivities and take into account the following systematic effects: 1) reddening; 2) the temperature structure of the H II region, i.e. the temperature difference between $T_e(\mathrm{He^+})$ and T_e(O III); 4) underlying stellar He I absorption; 4) collisional and fluorescent excitation of He I lines; 5) collisional excitation of hydrogen lines; and 6) the ionization structure of the H II region.

The set of parameters, which vary in the range of physically reasonable values and is the same as that considered by Izotov et al. (2007), is defined in the following way:

1. We adopted the reddening law by Whitford (1958). Izotov et al. (2007) have shown that He abundances are not sensitive to the adopted reddening law. In particular, the use of the Cardelli et al. (1989) reddening curve is resulted in He and other element abundances, which are similar to those obtained with the Whitford (1958) reddening law. The extinction coefficient $C(\mathrm{H}\beta)$ is derived from the observed hydrogen Balmer decrement after subtraction of the contribution due to the collisional excitation from the the Hα and Hβ line fluxes. Finally, all emission lines are corrected for reddening adopting the derived $C(\mathrm{H}\beta)$.

2. The electron temperature of the $\mathrm{He^+}$ zone is varied in the range $T_e(\mathrm{He^+})$ = (0.95 – 1.0)$\times T_e$(O III). This assumption is adopted following Guseva et al. (2006,2007) who derived the electron temperature in the $\mathrm{H^+}$ zone from the Balmer and Paschen discontinuities in spectra of more than 100 H II regions and showed that $T_e(\mathrm{H^+})$ differs from T_e(O III) by not more than 5%.

3. Oxygen abundances are calculated adopting an electron temperature equal to T_e(O III) and $T_e(\mathrm{He^+})$.

4. $N_e(\mathrm{He^+})$ and $\tau(\lambda3889)$ vary respectively in the ranges 10 – 450 cm^{-3} and 0 – 5, typical for extragalactic H II regions.

5. The fraction of Hα emission due to collisional excitation is varied in the range 0%

– 5%, in accordance with Stasińska & Izotov (2001). The fraction of Hβ emission due to the collisional excitation is assumed to be 1/3 that of Hα emission.

6. The equivalent width of the He I λ4471 absorption line is fixed to EW$_{abs}(\lambda4471)$ = 0.4Å. The equivalent widths of the other absorption lines are fixed according to the ratios EW$_{abs}(\lambda3889)$ / EW$_{abs}(\lambda4471)$ = 1.0, EW$_{abs}(\lambda5876)$ / EW$_{abs}(\lambda4471)$ = 0.3, EW$_{abs}(\lambda6678)$ / EW$_{abs}(\lambda4471)$ = 0.1 and EW$_{abs}(\lambda7065)$ / EW$_{abs}(\lambda4471)$ = 0.1. This set of the EWs is justified by Izotov et al. (2007) as the most likely one.

7. He I emissivities from Porter et al. (2005) are adopted.

8. The He ionization correction factor $ICF(\mathrm{He^+}+\mathrm{He^{++}})$ is adopted from Izotov et al. (2007).

4. The primordial He mass fraction Y_p

Our sample constitues the largest sample for the primordial He determination and thus greatly reduces the uncertainties caused by the statistical errors in He abundances. This allows us to study systematic effects on firm statistical grounds.

Linear regressions Y – O/H for the total sample of 1700 spectra with the basic set of parameters are shown in Figs. 1a and 1b. The difference between these two regressions is that the oxygen abundance in Fig. 1a is derived adopting the temperature of the O^{++} zone equal to $T_e(\mathrm{He^+})$, while the temperature T_e(O III) derived from the [O III] $\lambda4363/(\lambda4959+\lambda5007)$ line flux ratio is used in Fig. 1b to obtain the oxygen abundance. The primordial value obtained from the regression in Fig. 1a of $Y_p = 0.2512 \pm 0.0006$ is very close to the value of $Y_p = 0.2516 \pm 0.0011$ obtained for HeBCD sample by Izotov et al. (2007) for the same set of parameters. It is seen from this comparison that the use of the large sample reduces statistical errors in Y_p by a factor of two. The value of Y_p derived here is by 1.3% greater than the SBBN value obtained from the WMAP data.

The variation of the parameter ranges, similar to that done by Izotov et al. (2007), shows that the primordial He abundance is always larger than the standard one and varies in the range $\sim 0.249 - 0.252$. Finally, we adopt as the best the regression in Fig. 1a with Y_p= 0.2512 ± 0.0006. This regression is obtained with the basic set of parameters and the temperature $T_e(\mathrm{He^+})$ for the oxygen abundance determination. Adding a systematic error caused by the uncertainties in He I emissivities (Porter et al. 2009) we obtain Y_p= 0.2512 ± 0.0006(stat.) ± 0.0020(syst.).

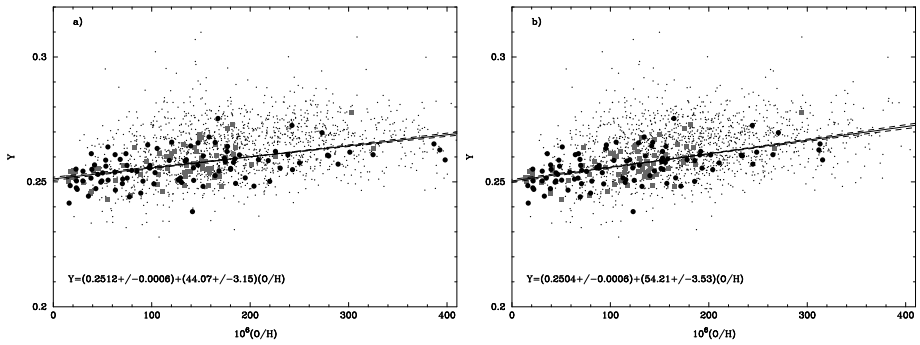

Figure 1. Linear regressions helium mass fraction Y vs. oxygen abundance O/H. The HeBCD H II regions are shown by filled circles, the archival VLT data by grey squares and the SDSS objects by dots. The oxygen abundance O/H is derived adopting (a) $T_e(\mathrm{He^+})$ and (b) T_e(O III).

5. Cosmological implications

We now investigate whether our derived values of Y_p are consistent with the predictions of SBBN and whether the baryonic mass density corresponding to Y_p agrees with the one derived from measurements of the CMB. We follow here the analysis by Izotov et al. (2007) with our new value $Y_p = 0.2512 \pm 0.0006$. With this value, and with an equivalent number of light neutrino species equal to 3, the SBBN model gives $\eta_{10} = 10^{10}\eta = 8.7 \pm 0.5$, where the error bars denote 1σ errors. This value corresponds to a baryonic mass fraction $\Omega_b h^2 = 0.032\pm 0.002$ and is significantly higher than $\Omega_b h^2 = 0.02273\pm0.00062$ derived from measurements of the fluctuations of the microwave background radiation by WMAP (Dunkley et al. 2009). Thus, the deviations from the SBBN are likely present. However, if the systematic error of 0.0020 in Y_p is taken into account because of uncertainties in the He I emissivities, then our value within 2σ is consistent with the SBBN value $Y_p = 0.2482^{+0.0003}_{-0.0004} \pm 0.0006$ (syst.) inferred by Spergel et al. (2007).

Deviations from the standard rate of Hubble expansion in the early Universe can be caused by an extra contribution to the total energy density (for example by additional flavors of active or sterile neutrinos) which can conveniently be parameterized by an equivalent number of neutrino flavors N_ν. Combining $\Omega_b h^2 = 0.002273 \pm 0.00062$ obtained by WMAP (Dunkley et al. 2009) with $Y_p = 0.2512 \pm 0.0006$, we obtain $N_\nu \sim 3.25$ (Steigman 2005,2007).

6. Summary

We present the determination of the primordial helium mass fraction Y_p by linear regressions of a large sample of low-metallicity extragalactic H II regions.

In the determination of Y_p, we have considered several known systematic effects. We have used Monte Carlo methods to take into account the effects of collisional and fluorescent enhancements of He I recombination lines, of collisional excitation of hydrogen emission lines, of underlying stellar He I absorption, of the difference between the temperature $T_e(\mathrm{He}^+)$ in the He^+ zone and the temperature T_e(O III) derived from the [O III]$\lambda4363/(\lambda4959+\lambda5007)$ flux ratio, and of the ionization correction factor $ICF(\mathrm{He}^+ + \mathrm{He}^{2+})$.

We have obtained the following results:

1. For the determination of the primordial He abundance we construct a sample of 1700 spectra of low-metallicity extragalactic H II regions which includes the HeBCD sample Izotov et al. (2007), archival VLT spectra and spectra from the Data Release 7 (DR7) of the Sloan Digital Sky Survey (SDSS). This sample is the largest data sets in existence for the determination of Y_p.

2. We obtain $Y_p = 0.2512 \pm 0.0006$(stat.) $\pm$ 0.0020(syst.), corresponding to $\Omega_b h^2 = 0.032 \pm 0.002$(stat.), significanly larger than the $\Omega_b h^2$ values derived from the deuterium abundance and microwave background radiation fluctuation measurements. If we take the higher value of Y_p at its face value, then this would imply the existence of small deviations from SBBN. In order to bring the high value of Y_p into agreement with the deuterium and WMAP measurements, we would need an equivalent number of neutrino flavors equal to 3.25 instead of the canonical 3.

References

Abazajian, K., et al. 2009, *ApJS*, 182, 543
Benjamin, R. A., Skillman, E. D., & Smits, D. P. 1999, *ApJ*, 514, 307

Benjamin, R. A., Skillman, E. D., & Smits, D. P. 2002, *ApJ*, 569, 288
Cardelli, J. A., Clayton, G. C., & Mathis, J. S. 1989, *ApJ*, 345, 245
Dunkley, J., et al. 2009, *ApJS*, 180, 306
Fukugita, M., & Kawasaki, M. 2006, *ApJ*, 646, 691
Guseva, N. G., Izotov, Y. I., & Thuan, T. X. 2006, *ApJ*, 644, 890
Guseva, N. G., Izotov, Y. I., Papaderos, P., & Fricke, K. J. 2007, *A&A*, 464, 885
Izotov, Y. I., & Thuan, T. X. 2004, *ApJ*, 602, 200 (IT04)
Izotov, Y. I., Thuan, T. X., & Lipovetsky, V. A. 1994, *ApJ*, 435, 647
Izotov, Y. I., Thuan, T. X., & Lipovetsky, V. A. 1997, *ApJS*, 108, 1
Izotov, Y. I., Stasińska, G., Meynet, G., Guseva, N. G., & Thuan, T. X. 2006, *A&A*, 448, 955
Izotov, Y. I., Thuan, T. X., & Stasińska, G. 2007, *ApJ*, 662, 15
Peimbert, M., & Torres-Peimbert, S. 1974, *ApJ*, 193, 327
Peimbert, M., & Torres-Peimbert, S. 1976, *ApJ*, 203, 581
Peimbert, M., Luridiana, V., & Peimbert, A. 2007, *ApJ*, 666, 636
Porter, R. L., Bauman, R. P., Ferland, G. J., & MacAdam, K. B. 2005, *ApJ*, 622, L73
Porter, R. L., Ferland, G. J., MacAdam, K. B., & Storey, P. J. 2009, *MNRAS*, 393, L36
Press, W. H., Teukolsky, S. A., Vetterling, W. T.,& Flannery, B. P. 1992, *Numerical Recipes in C, The Art of Scientific Computing /Second Edition/*, Cambridge University Press
Spergel, D. N., Bean, R., Doré, O., et al. 2007, *ApJS*, 170, 377
Stasińska, G., & Izotov, Y. I. 2001, *A&A*, 378, 817
Steigman, G. 2005, *Physica Scripta*, T121, 142
Steigman, G. 2007, *Annual Review of Nuclear and Particle Science*, 57, 463
Whitford, A. E. 1958, *AJ*, 63, 201

Light elements in the Universe
Proceedings IAU Symposium No. 268, 2010
C. Charbonnel, M. Tosi, F. Primas & C. Chiappini, eds.

DOI: 00.0000/X000000000000000X

Uncertainties in nebular helium abundances

Evan D. Skillman[1]

[1]Astronomy Department, University of Minnesota,
116 Church St. SE, Minneapolis, MN, USA
email: skillman@astro.umn.edu

Abstract. Efforts to determine the primordial helium abundance via observations of metal poor HII regions have been limited by significant uncertainties. Because of a degeneracy between the solutions for density and temperature, the precision of the helium abundance determinations is limited. Spectra from the literature are used to show the effects of new atomic data and to demonstrate the challenges of determining precise He abundances. Several suggestions are made for meeting these challenges.

Keywords. nucleosynthesis, abundances, cosmological parameters, early universe, ISM: HII regions

1. Introduction: In defense of Olive & Skillman (2004)

Fig. 1 shows the historical evolution of the observational determinations of the primordial helium abundance compared to the present day value inferred from WMAP observations and BBN calculations. One well known effect shown in the plot is the small error bars relative to the differences between determinations and relative to the currently favored value. In 2004, Keith Olive and I (Olive & Skillman 2004, hereafter OS04) attempted to account for most of the important statistical and systematic uncertainties, and, in a reanalysis of data from the literature (Izotov & Thuan 1998; Peimbert, Peimbert, & Ruiz 2000), found significantly larger uncertainties for helium abundance determinations for individual objects and a resulting larger uncertainty in the primordial helium abundance. In the plot, this result appears as a giant step backwards as the uncertainty in the primordial helium abundance is comparable to uncertainties associated with determinations from the 1980's. Part of the large uncertainty is due to concentrating on a small sample of "high quality" spectra of the lowest metallicity objects. This was to avoid two statistical effects which we felt were unsound. Including a large number of objects will reduce the error in the primordial helium abundance, even if some of those objects have relatively lower quality spectra. Additionally, including objects at higher metallicity will reduce the error on the primordial helium abundance because the extrapolation to zero metallicity will have a smaller error. However, this increases the dependence on the assumption of a linear relationship between the helium abundance and the oxygen (or nitrogen) abundance. By avoiding these two effects, we felt that the derived uncertainty in the primordial helium abundance better characterized the true uncertainty. Notably, a significant factor in the increased uncertainty of OS04 was simply larger uncertainties on the helium abundances of individual objects due to including neglected terms and running Monte Carlo analyses to account for degeneracies in minimization solutions.

An important result of the Monte Carlo analysis was the discovery of degeneracies in the sense that the physical conditions in the HII regions were not always independently constrained (Olive & Skillman 2001; Olive & Skillman 2004). In particular, the temperature and density exhibited a trade-off whereby increasing the temperature while decreasing the density would leave the χ^2 relatively unchanged. The main reason for this

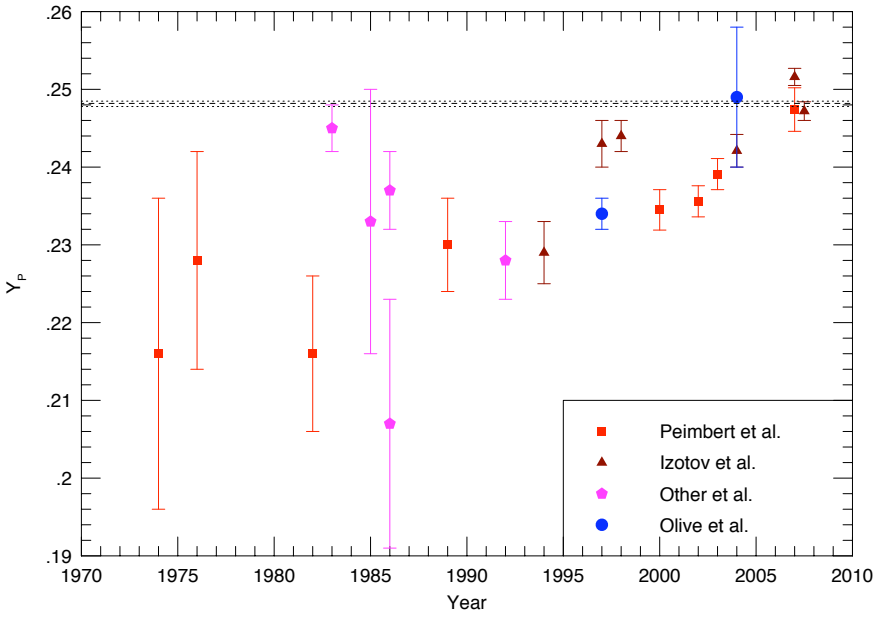

Figure 1. Historical evolution of the observational determinations of the primordial helium abundance. The solid horizontal line with dashes shows the value inferred from WMAP observations and BBN calculations.

is that four of the HeI emission lines used to derive the helium abundance show similar exponential dependencies on temperature and density.

We demonstrate the importance of the degeneracy between temperature and density in Figure 2. Here, we have generated a synthetic spectrum using typical physical conditions and a helium abundance. Values of the helium abundance and a corresponding χ^2 were then derived from this spectrum keeping all parameters fixed, but varying the density and temperature. The impact of trading the density against the temperature can be clearly seen in Figure 2 which illustrates a well constrained quotient of density and temperature but a $\triangle\chi^2 = 2.3$ boundary spanning a temperature range of 5500 K, a density range of 275 cm^{-3}, and an abundance variation of 10%. The shallow, extended minimum results in a large range of best fit parameters for the density and temperature upon the Monte Carlo perturbation, and the abundance gains a much larger uncertainty (see Figure 3). Only by solving for these two parameters simultaneously can this degeneracy be discovered.

2. New advances in helium abundance analysis

With University of Minnesota graduate student Erik Aver, Keith Olive and I have investigated improvements to the code that we used in 2004. This was, in part, in response to recent improvements to the atomic data (Porter, Ferland, & MacAdam 2007) which have resulted in significant changes to the derived helium abundances of HII regions (Izotov et al. 2007; Peimbert, Luridiana, & Peimbert 2007). Additionally, we have investigated combining the minimizations, previously based on the hydrogen lines and the helium lines separately, into a single minimization, which is inherently self-consistent. The single minimization allows us to investigate the correction for the collisional emission

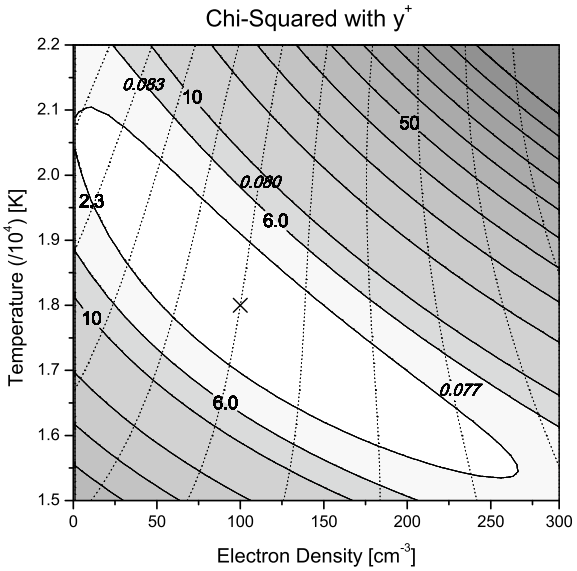

Figure 2. A plot of the derived helium abundance as a function of the temperature and density for a synthetically generated spectrum. Impressed on this diagram is a contour plot of χ^2 versus density and temperature for the same spectrum. The extension of the $\chi^2 = 2.3$ contour with a strong negative correlation highlights the degeneracy between density and temperature. That the χ^2 and abundance contours are nearly perpendicular demonstrates the impact of the degeneracy on the abundance determination ($\pm$5%). From Aver, Olive, & Skillman (2010).

of a small population of neutral hydrogen (e.g., Davidson & Kinman 1985; Skillman & Kennicutt 1993; Stasińska & Izotov 2001; Luridiana et al. 2003). Finally, the wavelength dependence in underlying stellar absorption can be included (initial previous work assumed identical values of equivalent width of underlying absorption for all H I or He I emission lines, regardless of wavelength) as has been investigated previously by Izotov et al. (2007). Detailing the incorporation of these four effects and investigation of their impact is the primary aim of a forthcoming paper (Aver, Olive, & Skillman 2010), and here I will provide a summary of the main results.

The updated emissivities, including the collisional corrections, in general raise the calculated abundance of helium (in agreement with Izotov et al. 2007; Peimbert, Luridiana, & Peimbert 2007). However, because the changes in different lines are qualitatively different, the update does not categorically raise the abundance. For λ4471, 5876, and 6678, the Hβ to He emissivity is increased rather uniformly (2-3%) across the relevant temperature range, and all three lines exhibit a gradual increase with temperature. The behavior of λ4026 is similar except that the new emissivity is shifted to lower values. λ3889 is more complicated in that the emissivity is reduced at low temperatures but is enhanced at $T \geqslant$ 16,000 K. λ7065 is similar though the enhancement begins at 13,000 K. Broadly though, both λ3889 and λ7065 as well as λ4471 track the BSS emissivities more closely (within $\sim$ 2%) than the other three lines. The three strongest lines with the smallest relative errors will produce a larger abundance, thus raising the average abundance. However, the changes to $\lambda\lambda$3889, 7065, and 4471 affect the derived physical

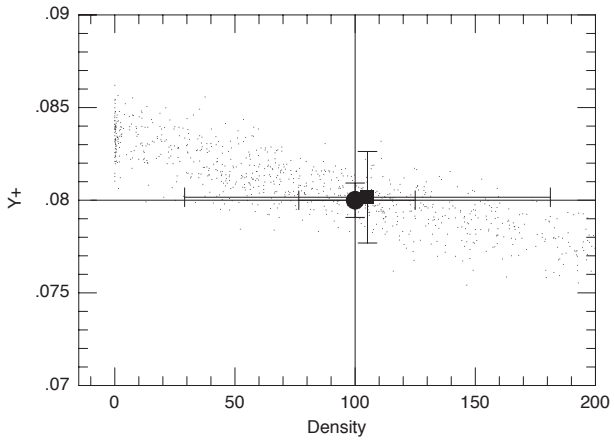

Figure 3. Plot of 1000 Monte Carlo solutions based upon a synthetic spectrum. The solid circle with error bars marks the original (direct) solution; while the solid square with error bars marks the average of the Monte Carlo solutions. Upon performing the Monte Carlo, the large range in density solutions (and correspondingly temperature solutions), gives a much larger density uncertainty, resulting in a marked increase in the abundance uncertainty (from 1% to 3%). From Olive, & Skillman (2001).

conditions in the nebula, and, in some cases, drive the derived abundance to lower values, opposite to the trend for the three strongest lines.

The changes to the atomic data for helium emissivities were much larger than ever accounted for in previous work. In most cases these uncertainties were regarded as insignificant when compared with the other uncertainties. Benjamin, Skillman, & Smits (1999) estimated a minimum uncertainty of 1.5% and this value is comparable to the changes due to the use of the new emissivities. This change alone validates the main conclusion of Olive & Skillman (2004) that the uncertainties in the derived helium abundances of individual objects were underestimated.

The combining of both the helium and hydrogen lines into a single minimization program has only small impact *as long as collisional excitation of neutral hydrogen is not included*. This is because the relative fluxes of the hydrogen emission from recombination has very low dependencies on density and temperature, so the hydrogen lines do not play into the density/temperature degeneracy. However, once collisional excitation of neutral hydrogen is included, then the strengths of the hydrogen lines gain a new temperature dependence, and it is crucial to include them in the minimization. A three way degeneracy between electron density, temperature, and the neutral hydrogen fraction emerges. These degeneracies are shown in Figure 4 which shows the Monte Carlo results for NGC 346. Plotted are the individual results for density, temperature, and neutral hydrogen fraction for 1000 MC realizations. As one can see, the solutions map out a wide range for these parameter values. The neutral hydrogen fraction can be increased to compensate for a decrease in the collisional to recombination rate which is itself only temperature dependent. Furthermore, the neutral hydrogen collisional emission correction can have a surprisingly significant effect in raising the abundance. Since the collisional correction for Hβ multiplies each helium line abundance, it multiplicatively raises the abundance but does not change the value of the corresponding χ^2. As a result, the helium abundances of all the objects that we studied increased.

The uncertainty in the choice of correction for underlying absorption is chiefly miti-

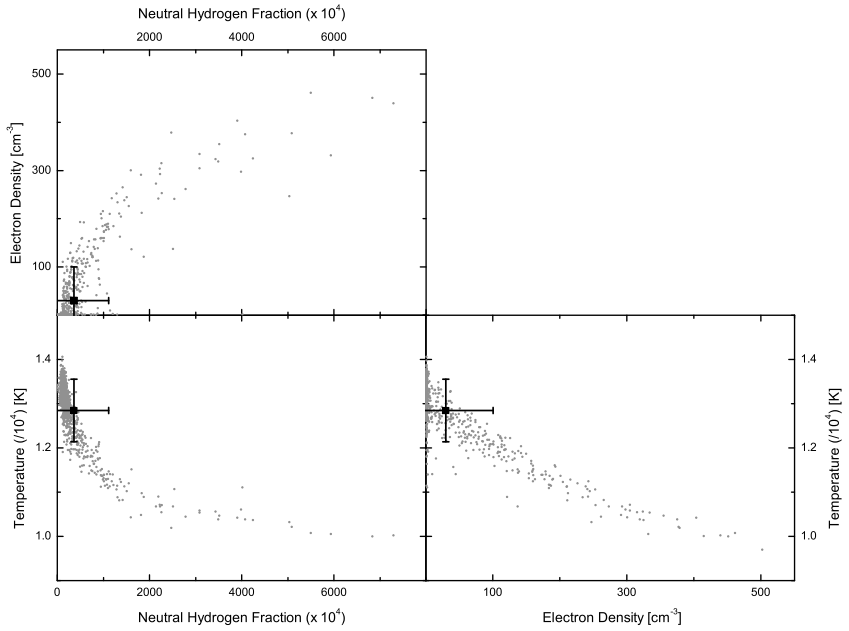

Figure 4. Plots of Monte Carlo results (1000 points) of density, temperature, and neutral hydrogen fraction for NGC 346. The strong correlation between the three parameters demonstrates the difficulty in solving for them independently. From Aver, Olive, & Skillman (2010).

gated by selecting only spectra with very high emission line equivalent widths. The main problems regarding underlying absorption arise when corrections are not included at all (cf. Skillman, Terlevich, & Terlevich 1998). Even in the case of NGC 346, where a filament with no obvious exciting stars was observed (Peimbert, Peimbert, & Ruiz 2000), Olive & Skillman (2004) found evidence for significant underlying absorption. This was confirmed by Peimbert, Luridiana, & Peimbert (2007). Once again, this underlines the importance of obtaining high quality spectra of the most promising targets.

Extending the previous work to allow for self-consistent analysis reflecting the common temperature and reddening parameters between the hydrogen and helium lines does not diminish the importance of the systematic uncertainties or the case for the larger errors determined via Monte Carlo. In fact, the addition of the neutral hydrogen collisional emission, introduced with a new physical parameter, the neutral hydrogen fraction, highlights that abundance errors may be even larger than previously thought. In addition to the need for observations to constrain systematic uncertainty as much as possible, we have found that relatively small systematic errors in the observed fluxes, even of the weakest lines, can have a significant impact on the derived value of y^+. Clearly the highest quality spectra are critical for a meaningful analysis.

Ultimately, the sensitivity of the determination of the primordial helium abundance demands that analysis be self-consistent and comprehensive; unfortunately efforts in providing such an analysis yield calculated uncertainties that limit the utility of that determination. Nevertheless, fully understanding the terrain of potential obstacles is necessary to direct further measurement efforts so as to provide a reliable calculation

of the primordial helium abundance. Apart from improving the quality of the spectra, the neutral hydrogen collisional correction for the weaker hydrogen lines can be easily improved from extended principal quantum number collisional strengths. Furthermore the use of an additional hydrogen line would benefit the neutral hydrogen fraction and hydrogen absorption since those two parameters are determined exclusively through the three hydrogen lines. The next Balmer line, H7 (λ3971) is blended with Ne III (λ3967), and H8, blended with HeI λ3889, would not be independent for analysis. This leaves the very weak H9 and H10 as the best candidates. The use of other emission lines may also be useful in lifting the error increasing degeneracy between density and temperature. However, this requires accurate metal line fluxes whose ratio is sensitive to the electron density or temperature in the applicable range. Most candidates are impaired by the weakness of their emission lines and ionization populations that are not characteristic of the majority of the HII region.

References

Benjamin, R. A., Skillman, E. D., & Smits, D. P., 1999, *ApJ*, 514, 307
Davidson, K., & Kinman, T. D. 1985, *ApJS*, 58, 321
Izotov, Y. I., & Thuan, T. X. 1998, *ApJ*, 500, 188
Izotov, Y. I., Thuan, T. X., & Stasinska, G. 2007, *ApJ*, 662, 15 (ITS07)
Luridiana, V., Peimbert, A., Peimbert, M., & Cerviño, M. 2003, *ApJ*, 592, 846
Olive, K. A., & Skillman, E. D. 2001, *New Astronomy*, 6, 119
Olive, K. A., & Skillman, E. D. 2004, *ApJ*, 617, 29
Peimbert, M., Luridiana, V., & Peimbert, A. 2007, *ApJ*, 666, 636 (PLP07)
Peimbert, M., Peimbert, A., & Ruiz, M. T. 2000, *ApJ*, 541, 688
Porter, R. L., Ferland, G. J., & MacAdam, K. B. 2007, *ApJ*, 657, 327 (PFM)
Skillman, E. D. & Kennicutt, R. C. 1993, *ApJ*, 411, 655
Skillman, E. D., Terlevich, E., & Terlevich, R. 1998, *Spa. Sci. Rev.*, 84, 105
Stasińska, G., & Izotov, Y. I. 2001, *A& A*, 378, 817

Light elements in the Universe
Proceedings IAU Symposium No. 268, 2010
C. Charbonnel, M. Tosi, F. Primas & C. Chiappini, eds.

DOI: 00.0000/X000000000000000X

The quite complex "Simple Stellar Populations" of globular clusters

Angela Bragaglia[1]

[1]INAF-Osservatorio Astronomico di Bologna,
via Ranzani 1, 40127 Bologna, Italy
email: angela.bragaglia@oabo.inaf.it

Abstract. There is compelling observational evidence that globular clusters (GCs) are quite complex objects. A growing body of photometric results indicate that the evolutionary sequences are not simply isochrones in the observational plane -as believed until a few years ago- from the main sequence, to the subgiant, giant, and horizontal branches. The strongest indication of complexity comes however from the chemistry, from internal dispersion in iron abundance in a few cases, and in light elements (C, N, O, Na, Mg, Al, etc.) in *all* GCs. This universality means that the complexity is *intrinsic* to the GCs and is most probably related to their formation mechanisms. The extent of the variations in light elements abundances is dependent on the GC mass, but mass is not the only modulating factor; metallicity, age, and possibly orbit can play a role. Finally, one of the many consequences of this new way of looking at GCs is that their stars may show different He contents.

Keywords. Stars: abundances, Population II – Galaxy: globular clusters

1. It's not so simple

Globular Clusters (GCs) have long been considered the best approximations of a *Simple Stellar Population* (Renzini & Buzzoni 1986), and this may still be valid for some purposes. However, they are not truly simple. We know that GCs contain a fraction of binaries (e.g., Meylan & Heggie 1987). But now we also know that their stars are not strictly coeval; for old clusters, like the Galactic globulars, the age differences are so small to be hardly detectable, but the same is not true for the Magellanic Clouds ones. And we also know that the initial chemical composition of the stars we presently observe was not the same.

There is a growing body of observational evidence of the complexity of GCs, both from photometry (with multiple, or split, or wide sequences) and from spectroscopy (with large differences in light elements and even, in a few cases, with spreads in metallicity).

Of course, ω Cen is the first example that comes to mind, even if for its characteristics (or better, because of its characteristics) it has often been labelled as the nucleus of an ancient dwarf spheroidal galaxy. However, ω Cen is only the tip of the iceberg and there are many other interesting cases, like M54, which lies in the nucleus of the Sagittarius dwarf galaxy (Ibata et al. 1994, Bellazzini et al. 2008a), and which resembles ω Cen in several aspects. But also more "normal", lower mass clusters show peculiarities, like NGC 2808 which, among many other oddities, presents three well separated main sequences (Bedin et al. 2004, Sollima et al. 2007). I will come back to these three objects later.

Among other evident examples we find for instance M22 (NGC 6656) which had long been suspected to have a dispersion in metallicity (from photometry, e.g. Hesser et al. 1977 or spectroscopy, e.g. Brown & Wallerstein 1992, but see also Ivans et al. 2004)

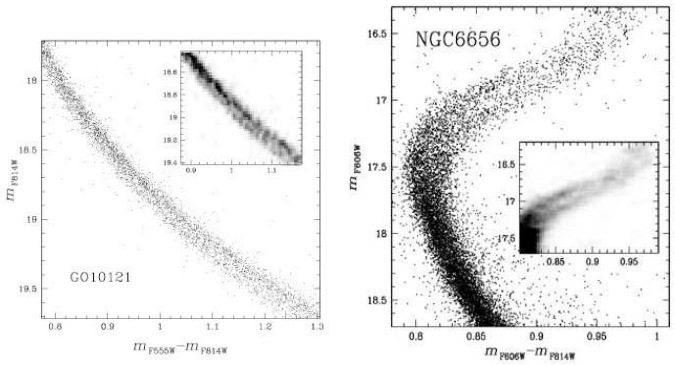

Figure 1. Examples of split main sequences or subgiant branches recently found in Galactic GCs using the high precision photometry of ACS@HST: NGC 6752 (Milone et al. 2009), and M22 (courtesy of A. Milone).

and that also displays a split in the SGB and RGB (see Fig. 1), or NGC 1851 with its split SGB (Milone et al. 2008) and RGB (Han et al. 2009), and its anomalous chemical abundances (e.g. Yong et al. 2009).

Interestingly, thanks to the exquisite precision of the ACS camera on HST (whose photometry can reach the depth and precision to detect even small colour and magnitude differences), more clusters were found to show wide or even split evolutionary sequences, from the main sequence and up to the SGB and RGB. The newest entries are 47 Tuc, where Anderson et al. (2009) find both a split SGB and a wide faint main sequence, and NGC 6752, unsuspected until now, which shows a split main sequence (Milone et al. 2009); for both, see Fig. 1. It seems that more and more GCs are beginning to unveil their complex photometric sequences; for a more extended discussion, see the earlier reviews by Piotto (2008, 2009).

Even if the evidence from photometry is the easiest to see, even for non-specialists, the strongest proof that GCs harbour at least two stellar generations comes from spectroscopy. Not only we may see stars with the same evolutionary status but with very different chemical composition in GCs, at least for some light elements, but also this situation is not limited to a few "freaks", as ω Cen or M22† were considered for a long time. The chemical signatures we used to call "anomalies" are widespread and show up in *all* clusters studied. Bimodality -and anticorrelation- in CN and CH strengths, or anticorrelations between other light elements, like Na and O, or Mg and Al, have long been observed in evolved stars, where they could be explained, although with some difficulties, considering extra-mixing episodes (see e.g. the reviews by Smith 1987 and Kraft 1994 where the extra-mixing *vs* the primordial-enrichment hypotheses are discussed).

However, these same so-called chemical anomalies were later found also in non evolved, main sequence stars (e.g., Cannon et al. 1998 found a bimodality in CN, CH in 47 Tuc, and other authors in many other GCs, see the review by Gratton et al. 2004).

Once established that the Na-O anticorrelation was present also in unevolved stars

† Recently, the claim of a dispersion in metallicity in M22 has gained substance, and two papers appeared. One is based on a sample of 17 stars studied with high resolution spectra (Marino et al. 2009), and indicates differences both in metallicity and heavy elements. The second paper, by Da Costa et al. (2009), presents a larger sample, but metallicity is derived from the Calcium triplet. Both show a bimodality in metallicity.

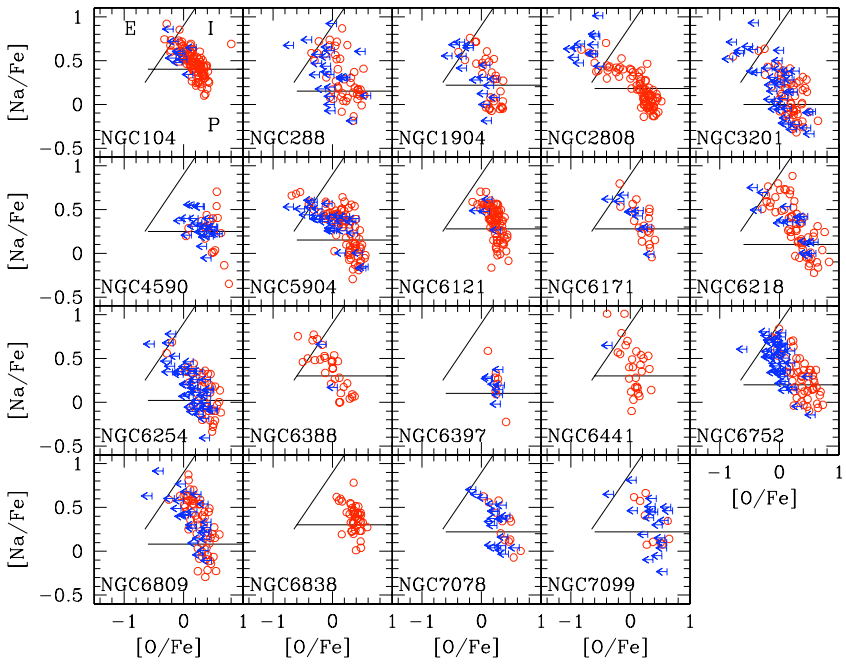

Figure 2. Na-O anticorrelations in 19 GCs observed with FLAMES@VLT, with separation among Primordial, Intermediate, and Extreme populations (see Carretta et al. 2009a for details).

(Gratton et al. 2001 found it for the first time in NGC 6752 and NGC 6397, followed by Ramirez & Cohen 2002 in M71, and by Carretta et al. 2004 in 47 Tuc), it became clear that another explanation was required. These chemical signatures are the result of H-burning at high temperature (ON, NeNa, MgAl cycles: see Denisenkov & Denisenkova 1989, Langer et al. 1993); the resulting chemical patterns cannot be produced in low mass, main sequence stars like those we are presently seeing in GCs. So the typical chemical signature of high N, Na, Al, and low C, O, Mg *must have originated in a previous generation of more massive stars, that polluted the gas from which part of the GC stars formed later.*

Perhaps the most famous pair of elements showing such variations, anti-correlated with each other, are O and Na. This Na-O anticorrelation was first found among cluster giants, mainly by the Lick-Texas group, by Kraft, Sneden, and many collaborators. They studied two-three tens of targets per cluster, observing stars one by one; for a review of their work, see Kraft (1994) and Gratton et al. (2004). The availability of efficient spectrographs at 8-10m telescopes, and their multi-object capabilities have permitted to extend this kind of study both to faint, unevolved stars and to much larger samples. About three years ago, there were about 200 giants studied in literature, and about 50 unevolved stars, as shown in Carretta et al. (2006) in their presentation of the Na-O anticorrelation in about 100 stars in NGC 2808, studied with FLAMES@VLT.

The work by Carretta and collaborators (e.g. Carretta et al. 2009a) has further demonstrated the universality of the Na-O anticorrelation; all GCs studied show it, as evident in the 19 GCs displayed in Fig. 2. However, this anticorrelation is not the same in all

clusters; the shape and the extension vary from cluster-to-cluster. On the basis of the Na and O abundances, Carretta and collaborators separated the cluster stars in first-generation and second-generation ones. The first are the ones with Na and O similar to field stars of the same metallicity, the second show varying degrees of O depletion and Na enhancement. Na and O are not the only light elements involved. Also Mg, Al (and even Si and F, Yong et al. 2005, Smith et al. 2005) are altered. In particular, Al is a powerful probe of the nature of first-generation polluters, due to the very high temperatures required for its production.The modification from the primordial value varies a lot from cluster to cluster (Carretta et al. 2009b: in some clusters Al changes a lot, in other much less or not at all). This is an indication that different polluters were at work. The chemical changes come all from H-burning, but at very different temperatures, and this indicates that polluters† of different mass were at work in different GCs.

2. The iceberg tip

A few clusters show the characteristics described above in a extreme way and have been the footholds, if one may say so, to convince even the distracted astronomer that something did not fit the notion of GCs being simple, old, boring systems.

2.1. ω *Centauri*

When talking of the complexity of GCs, the first example that comes to mind is of course ω Cen. It had long been suspected that it could host stars of different metallicity, given the width of the sequences (e.g., Cannon & Stobie 1973, Alcaino & Liller 1987) and also demonstrated by pioneering spectroscopic work (see Butler et al. 1978, Cohen 1981). Given the huge amount of papers dedicated to ω Cen, I can only touch upon a tiny fraction of the works on this cluster, concentrating on the very recent results, which show not only dispersion in colour or metallicity, but actual discrete separation in different sub-samples of the total cluster population. Initially the clear indication of multiple populations came from the RGB (Lee et al. 1999, Pancino et al. 2000, Ferraro et al. 2004), see Fig. 3. Several metallicities, and perhaps different ages were deduced for the different RGB sequences, in particular for the very metal-rich "anomalous RGB", see for instance the high resolution spectroscopic study of 40 giants by Norris & Da Costa (1995), the work on Ca abundances of about 500 giants observed at low spectroscopic resolution by Norris et al (1996), the Strömgren photometry by Hilker & Richtler (2000), the high resolution analysis of 6 stars on the "anomalous" RGB by Pancino et al. (2002), the near-IR spectroscopy of about 20 giants by Origlia et al. (2003), the study of main sequence stars by Stanford et al. (2007), the large survey at intermediate spectroscopic resolution by Johnson et al. (2009).

However, the differences go deeper, and with data obtained with HST, it was possible to detect also separate main sequences (Bedin et al. 2004, see Fig. 3), to which I will come back later.

2.2. *NGC 2808*

Even more "normal", less massive clusters show striking features. NGC 2808, among many other marked peculiarities, presents three well separated main sequences (Piotto et al. 2005). It also has a very complex Horizontal Branch (HB), with three main groups of

† While no definitive consensus has been reached on the actual nature of the polluters, the most promising candidates are fast rotating massive stars (e.g. Decressin et al. 2007), and asymptotic giant branch stars (e.g., Ventura et al. 2001). Since they are discussed in other contributions, I will not say more on the subject.

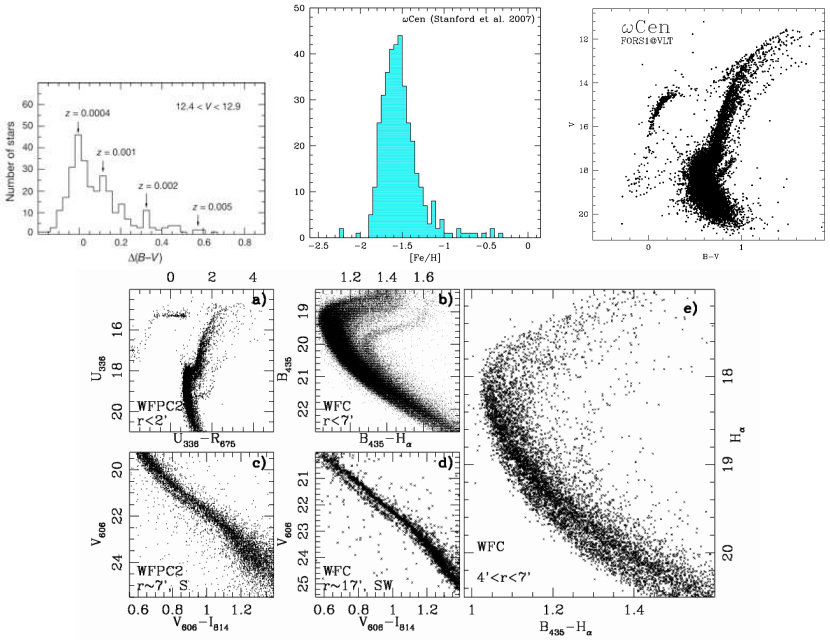

Figure 3. Evidence of multiple populations in ω Cen: Upper left panel: distribution in colour of RGB stars from Lee et al. (1999). Central upper panel: distribution in [Fe/H] of main sequence stars, adapted from Stanford et al. (2007). Upper right panel: distinct RGBs, from Ferraro et al. (2004). Lower panel: collection of CMDs showing the various populations, both for evolved and main sequence stars, from Bedin et al. (2004).

stars, that cannot be explained under standard assumptions. Both these features seem to require He enhancement in part of its stars (see next Section), which would also naturally agree very well with the observed Na-O anticorrelation (the third most extended one, after ω Cen and M54), since Na-rich and O-poor stars should also be He-rich (the main outcome of H-burning is, of course, He). Fig. 4 shows the three main sequences, a plausible interpretation of its HB (D'Antona et al. 2005), and the Na-O anticorrelation (Carretta et al. 2006).

2.3. *M54*

M54 is the second most massive cluster of the Galaxy, and lies at the center of the disrupting Sgr dwarf galaxy. It has been suspected to have a dispersion in metallicity since the observations by Sarajedini & Layden (1995), whose CMD shows a wide RGB, compatible with a dispersion of 0.16 dex in [Fe/H], see Fig. 5. This has been recently confirmed by low resolution spectroscopy of a very large sample of M54 and Sgr stars (Bellazzini et al. 2008a, see Fig. 5). The very recent results obtained by Carretta et al. (2010) using FLAMES spectra of about 80 RGB stars further confirm this: M54 has a dispersion in metallicity of the order of about 0.2 dex, well above the errors (see Fig. 5). Furthermore, it has a very extendend Na-O anticorrelation, more extended for the metal-rich than for the metal-poor stars. Carretta et al. (2010) also noticed that the same happens in ω Cen. M54 deserves more study, but it's clear that it resembles ω Cen; maybe, as it has been suggested (Bellazzini et al. 2008a, Carretta et al. 2010), we see it now as ω Cen was a long time ago, before the dwarf galaxy around it dispersed.

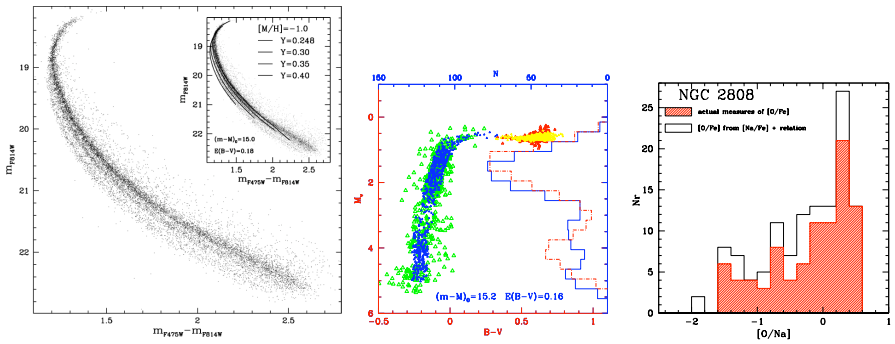

Figure 4. Evidence of multiple populations in NGC 2808. Left panel: the three separate main sequences found by Piotto et al. (2007). Central panel: the complex HB, and the interpretation assuming three different He contents, made by D'Antona et al. (2005). Right panel: the distribution of Na and O abundances, with three peaks, as found in Carretta et al. (2006).

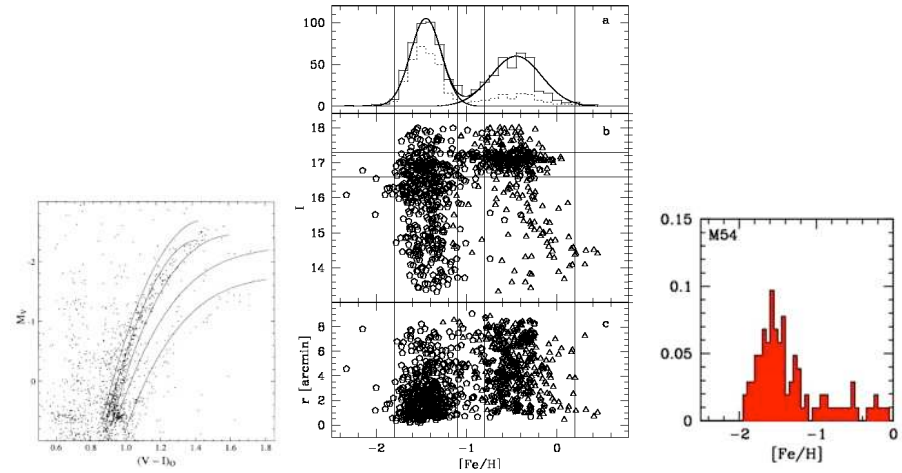

Figure 5. Dispersion in metallicity in M54. Left panel: Sarajedini & Layden (1995) found a colour dispersion in the RGB. Central panel: Separation of M54 from the Sgr population in Bellazzini et al. (2008a), based on Calcium triplet observations of several hundreds of stars; notice that both M54 and Sgr show a noticeable dispersion in [Fe/H]. Right panel: results obtained by Carretta et al. (2010) from 76 star in M54 (peaked at [Fe/H]~ -1.6) and 25 stars in Sgr (extending in [Fe/H] from about -1 to solar) observed with FLAMES@VLT.

3. Are there different He abundances in GCs ?

The main problem for establishing if He is variable in GCs it that it is difficult to see the effect of small variations in the CMDs, apart from the HB, which is a sort of "amplifier". HBs suffer from the notorious "second-parameter" problem: metallicity is of course the first parameter explaining their structure, age is most probably the second, but their combination cannot explain all HBs, in particular at the bluer, hotter extremes.

A solution is to bring also He into the problem, since an higher He content means brighter and bluer HBs. As shown in Fig. 4, D'Antona et al. (2005) were able to reproduce the observed distribution of HB stars in NGC 2808 assuming three different He contents (from a "primordial" value of Y=0.25 for the red HB, to Y=0.40 for the extreme blue

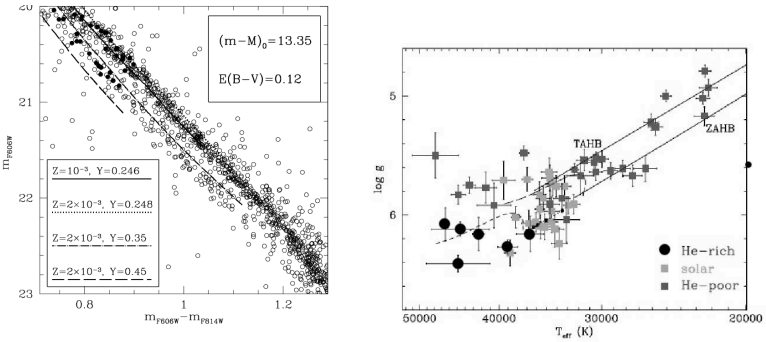

Figure 6. He abundances in ω Cen. Left panel: the two main sequences in Piotto et al. (2005), with star observed with FLAMES indicated by filled red and blue circles. The isochrones shown have been computed for Z=1 × 10^{-3}, Y=0.25 and Z=2 × 10^{-3}, Y=0.35. Right panel (adapted from Moehler et al. (2007)): blue and extreme HB stars for which Moehler et al. obtained low resolution spectra and for which determined temperatures, gravities, and He abundances; part of the extreme HB stars are He-enhanced.

HB). A similar exercise has been done by Busso et al. (2007) and D'Antona & Caloi (2008) for NGC 6388, producing similar results. This is a strong indication that GC stars are not so homogeneous in He as we thought: in the same cluster we may have stars with "normal" He and stars with different levels of He-enhancement, even if perhaps this doesn't happen in all clusters, or at least not at this high level.

It could be very interesting to directly measure He abundances in GC stars; however, this is possible only on the HB, and with many limitations. There is a small range in temperature (9500-11500 K) where He lines can be observed (even if they are tiny, at a few percent of the continuum level) and He abundances are not altered by dilution and mixing. Recently, Villanova et al. (2009) have obtained high resolution, high S/N of a few HB stars in NGC 6752, but their results are not decisive: they could measure He only in four stars, all of them Na-poor, O-rich (hence expected to be He-"normal", that is what they found), while they could not do so for the only Na-rich, O-poor star (expected to be He-enhanced). On the other hand, He has been found to be enhanced in some very blue HB stars in NGC 2808 and ω Cen (see Moehler et al. 2007 and Fig. 3), even if the cause of He-enhancement could also be mixing following a late He-flash (Castellani & Castellani 2003) for these extreme HB stars.

In the present volume there is also a discussion (see Bragaglia et al. 2010 for a lengthier presentation) on how to determine differences in He abundances from RGB stars using colours, metallicities, and magnitude of the RGB bump.

Finally, maybe the strongest case for He-enhancement of part of GC stars comes from two massive objects. The first one is again ω Cen, with its two separate main sequences (see Fig. 3). Piotto et al. (2005) obtained spectra of moderate resolution for 17 stars on the blue and 17 stars on the red sequences; surprisingly, the blue sequence turned out to be more metal-rich by about 0.3 dex. This could be explained only if we assume that the blue sequence is also much more He-rich than the red one (Y∼0.35-0.38 *vs* 0.25) as seen from isochrone fit. Of course we have to remember that the different metallicities are actually measured, while the He-enhancement is only inferred.

The split main sequence is even more spectacular in NGC 2808 (Fig. 4), and again the three sequences can be well fit assuming the same age but three different He levels (i.e., Y∼ 0.25, 0.30, and 0.38, see Piotto et al. 2007).

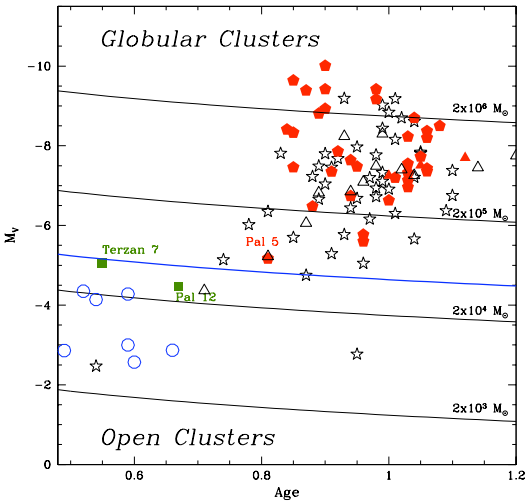

Figure 7. Relative Age parameter vs absolute magnitude M_V for globular and old open clusters. Red filled pentagons and triangles are GCs where Na-O anticorrelation has been observed, in the Milky Way or the LMC respectively; green squares are clusters which do not show (yet?) evidence for O-Na anticorrelation (Terzan 7 and Pal 12, both in the Sgr dwarf galaxy). Open stars and triangles mark clusters for which not enough data is available. Finally, open circles are old open clusters (data from Lata et al. 2002). Superimposed are lines of constant mass (light solid lines, see Bellazzini et al. 2008b). The heavy blue solid line (at a mass of 4×10^4 $M_\odot$) is the proposed separation between globular and open clusters. This figure is taken from Carretta et al., submitted

4. Summary and perspectives

We have seen that there is photometric evidence of multiple populations in many GCs. This generally happens among the most massive ones in our Galaxy, but not exclusively (see the cases of NGC 6752, M4). Mass is an important factor. It has been shown that many properties correlate with cluster mass, for instance, the maximum temperature reached on the HB (Recio-Blanco et al. 2006)

However, mass is not all the story. We have seen that all GCs display the Na-O anticorrelation, but if we quantify its extension (using e.g., the Interquartile range, see Carretta 2006) and plot it against total cluster mass, or integrated magnitude, we see that, preferentially, only high-mass clusters have an extended anticorrelation. This is, however, only a necessary condition; a notable counterexample is the massive GC 47 Tuc, which has a short anticorrelation. Some other factor, maybe metallicity, or age, or cluster orbit have to be involved.

Finally, I recall that the Na-O (and similar) anticorrelations seem to represent an intrinsic property of GCs: each time Na and O have been measured, they anti-correlate, while this does not happen in open clusters (see Fig. 7) or for field stars. So maybe we have an operative definition of the separation between globular and open clusters: GCs are those aggregates massive enough to sustain self-pollution, hence able to host at least two stellar generations and to develop a Na-O anticorrelation. This has of course to be related to the mechanism of cluster formation.

The financial support from the IAU and the Swiss National Science Foundation is

gratefully acknowledged. Many thanks to Eugenio Carretta, Raffaele Gratton, Valentina D'Orazi, Sara Lucatello, and Antonino Milone for their help and suggestions.

References

Alcaino, G., Liller, W. 1981, *AJ*, 94, 1585
Anderson, J., Piotto, G., King, I. R., Bedin, L. R., Guhathakurta, P. 2009, *ApJ*, 697, L58
Bedin, L. R., Piotto, G., Anderson, J., Cassisi, S., King, I. R., Momany, Y., Carraro, G. 2004, *ApJ*, 605, L125
Bellazzini, M., et al. 2008a, *AJ*, 136. 1147
Bellazzini, et al. 2008b, *Memorie della Societa Astronomica Italiana*, 79, 663
Bragaglia, A., Carretta, E., Gratton, R., D'Orazi, V., Cassisi, S., Lucatello, S. 2010, *A&A*, subm.
Brown, J. A. Wallerstein, G. 1992, *AJ*, 104, 1818
Busso, G., et al. 2007, *A&A*, 474, 105
Butler, D., Dickens, R. J., Epps, E. 1978, *ApJ*, 225, 148
Cannon, R.D., Stobie, R.S. 1987, *MNRAS*, 162, 207
Carretta, E. 2006, *AJ*, 131, 1766
Carretta, E., Carretta, E., Gratton, R. G., Bragaglia, A., Bonifacio, P., Pasquini, L. 2004, *A&A*, 416, 925
Carretta, E., Bragaglia, A., Gratton, R. G., Leone, F., Recio-Blanco, A., Lucatello, S. 2006, *A&A*, 450, 523
Carretta, E., et al. 2009a, *A&A*, 505, 117
Carretta, E., Bragaglia, A., Gratton, R. G., Lucatello, S. 2009b, *A&A*, 505, 139
Carretta, E., et al. 2010, *ApJ*, subm.
Castellani, M., Castellani, V. 1993, *ApJ*, 407, 649
Cohen, J.G. 1981, *ApJ*, 247, 869
D'Antona, F., Caloi, V. 2008, *MNRAS*, 390, 693
D'Antona, F., Bellazzini, M., Caloi, V., Pecci, F. F., Galleti, S., Rood, R. T. 2005, *ApJ*, 631, 868
Da Costa, G.S., Held, E.V., Saviane, I., Gullieuszik, M. 2009, *ApJ*, 705, 1481
Denisenkov, P. A., Denisenkova, S. N. 1989, *A.Tsir.*, 1538, 11
Decressin, T., Meynet, G., Charbonnel C. Prantzos, N., Ekstrom, S. 2007, *A&A*, 464, 1029
Ferraro, F. R., Sollima, A., Pancino, E., Bellazzini, M., Straniero, O., Origlia, L., Cool, A. M. 2004, *ApJ*, 603, L81
Gratton, R., Sneden, C., Carretta, E. 2004, *ARAA*, 42, 385
Gratton, R., et al. 2001, *A&A*, 369, 87
Gratton, R.G., Carretta, E., Bragaglia, A., Lucatello, S., D'Orazi, V. 2010, *A&A*, subm.
Han, S.-I., Lee, Y.-W., Joo, S.-J., Sohn, S. T., Yoon, S.-J., Kim, H.-S., Lee, J.-W. 2009, *ApJ*, 707, L190
Hesser, J. E., Hartwick, F. D. A., McClure,R. D. 1977, *ApJS*, 33, 471
Hilker, M., Richtler, T. 2000, *A&A*, 326, 895
Ibata, R. A., Gilmore, G., Irwin, M. J. 1994, *Nature*, 370, 194
Ivans, I. I., Sneden, C., Wallerstein, G., Kraft, R. P., Norris, J. E., Fulbright, J. P., Gonzalez, G. 2004, *Memorie della Societa Astronomica Italiana*, 75, 286
Johnson, C.J., Pilachowski, C.A., Rich, M.R., Fulbright, J.P 2009, *ApJ*, 698, 2048
Kraft, R. 1994, *PASP*, 106, 553
Langer, G. E., Hoffman, R., Sneden, C. 1993, *PASP*, 105, 301
Lata, S., Pandey, A.K., Sagar, R., Mohan, V. 2002, *A&A*, 388, 158
Lee, Y.-W., Joo, J.-M., Sohn, Y.-J., Rey, S.-C., Lee, H.-C., Walker, A. R. 1999, *Nature*, 402, 55
Marino, A. F., Milone, A. P., Piotto, G., Villanova, S., Bedin, L. R., Bellini, A., Renzini, A. 2009, *A&A*, 505, 1099
Meylan, G., Heggie, D.C. 1987, *A&ARv*, 8, 1
Milone, A. P., et al. 2008, *ApJ*, 673, 241
Milone, A. P., et al. 2009, *ApJ*, in press (arXiv:0912.2055)

Moehler, S., Dreizler, S., Lanz, T., Bono, G., Sweigart, A. V., Calamida, A., Monelli, M., Nonino, M. 2007, *A&A*, 475, L5
Norris, J. E., Freeman, K. C., Mighell, K. J. 1996, *ApJ*, 462, 241
Norris, J.E., Da Costa, G.S. 1995, *ApJ*, 447, 680
Origlia, L., Ferraro, F.R., Bellazzini, M., Pancino, E., 2003, *ApJ*, 591, 916
Pancino, E., Ferraro, F. R., Bellazzini, M., Piotto, G., Zoccali, M. 2000, *ApJ*, 534, L83
Pancino, E., Pasquini, L., Hill, V., Ferraro, F., Bellazzini, M. 2002, *ApJ* (Letters), 568, L101
Piotto, G. 2008, *IAU Symposium*, 246, 141
Piotto, G. 2009, *IAU Symposium*, 258, 233
Piotto, G., et al. 2005, *ApJ*, 621, 777
Piotto, G., et al. 2007, *ApJ*, 61, L53
Ramirez, S.V., Cohen, J.G. 2002, *AJ*, 123, 3277
Recio-Blanco, A., Aparicio, A., Piotto, G., de Angeli, F., Djorgovski, S. G. 2006, *A&A*, 452, 875
Renzini, A., Buzzoni, A. 1986, *Spectral Evolution of Galaxies*, 122, 195
Sarajedini, A. & Layden, A.C. 1995, *AJ*, 109, 1112
Smith, G. H. 1987, *PASP*, 99, 67
Smith, V. V., Cunha, K., Ivans, I. I., Lattanzio, J. C., Campbell, S., Hinkle, K. H. 2005, *ApJ*, 633, 392
Sollima, A., Ferraro, F. R., Bellazzini, M., Origlia, L., Straniero, O., Pancino, E. 2007, *ApJ*, 654, 915
Stanford, L.M., Da Costa, G.S., Norris, J.E., Cannon, R.D. 2007, *ApJ*, 667. 911
Ventura, P., D'Antona, F., Mazzitelli, I., Gratton, R.. 2001, *ApJ*, 550, L65
Villanova, S., Piotto, G., Gratton, R. G. 2009, *A&A*, 499, 755
Yong, D., Grundahl, F., Nissen, P. E., Jensen, H. R., Lambert, D. L. 2005, *A&A*, 438, 875
Yong, D., Grundahl, F., D'Antona, F., Karakas, A. I., Lattanzio, J. C., Norris, J. E. 2009, *ApJ*, 695, L62

Light elements in the Universe
Proceedings IAU Symposium No. 268, 2010
C. Charbonnel, M. Tosi, F. Primas & C. Chiappini, eds.

DOI: 00.0000/X000000000000000X

Revisiting the helium abundance in globular clusters with multiple main sequences

Luca Casagrande[1], Laura Portinari[2] and Chris Flynn[2]

[1]Max Planck Institue for Astrophysics, Karl Schwartzschild Straße 1, Garching, Germany
email: luca@mpa-garching.mpg.de

[2]Tuorla Observatory, Department of Physics and Astronomy, University of Turku, Finland
email: lporti@utu.fi,cflynn@utu.fi

Abstract. For nearby K dwarfs, the broadening of the observed Main Sequence at low metallicities is much narrower than expected from isochrones with the standard helium–to–metal enrichment ratio $\Delta Y/\Delta Z \sim 2$. A much higher value, of order 10, is formally needed to reproduce the observed broadening, but it returns helium abundances in awkward contrast with Big Bang Nucleosynthesis. This steep enrichment ratio resembles, on a milder scale, the very high $\Delta Y/\Delta Z$ estimated from the multiple Main Sequences observed in some metal-poor Globular Clusters. We argue that a revision of low Main Sequence stellar models, suggested from nearby stars, could help to reduce the overwhelmingly high $\Delta Y/\Delta Z$ deduced so far for those clusters. Under the most favourable assumptions, the estimated helium content for the enriched populations may decrease from $Y \simeq 0.4$ to as low as $Y \simeq 0.3$, with intermediate values being plausible.

Keywords. Stars: fundamental parameters, late-type – subdwarfs – globular clusters: individual (ωCen, NGC 2808, 47 Tuc)

1. Introduction

Helium (Y) is the second most abundant element in the Universe, having been produced by Big Bang Nucleosynthesis (BBN) with a universal mass fraction $Y_P = 0.24 - 0.25$ and topped up by successive stellar generations which also synthesize metals (Z). In spite of its large abundance, it is an elusive element. It can be measured directly, from spectroscopic lines, only for $T_{\rm eff} \gtrsim 8000$ K: young, massive stars or blue Horizontal Branch stars though, apart from a small temperature range, their surface abundance may not trace the original one, due to helium sedimentation and metal levitation (e.g. Villanova, Piotto & Gratton 2009). Only indirect methods can be used for stars of low mass and cooler temperatures, which constitute the bulk of the Galaxy's stellar population. One such method relies on the broadening of the low Main Sequence (MS), where evolutionary effects do not need to be taken into account. At a fixed metallicity Z, an increase of Y makes a given mass on the isochrone hotter and brighter, so that the net effect of varying $\Delta Y/\Delta Z$ is to affect the broadening of the lower MS (e.g. Faulkner 1967; Fernandes et al. 1996).

Previous studies based on Hipparcos parallaxes concluded $\Delta Y/\Delta Z = 2 - 3$ (Pagel & Portinari 1998; Jimenez et al. 2003). More recently, Casagrande et al. (2006, 2007) further improved the analysis by compiling a much larger sample of K dwarfs with bolometric magnitudes and effective temperatures derived via InfraRed Flux Method (IRFM). The implementation adopted for the IRFM resorted to homogeneous multi–band photometry to determine in a fully self-consistent, (almost) model independent way $T_{\rm eff}$ and $M_{\rm Bol}$. The study of the broadening of the lower MS could thus be performed in the theoretical

HR diagram where the effects of $\Delta Y/\Delta Z$ are more prominent, also bypassing uncertainties related to synthetic colour-temperature transformations†.

Around solar metallicities this analysis yielded $\Delta Y/\Delta Z \sim 2$ but at lower Z, Casagrande et al. (2007) found that the observed MS is narrower than expected from stellar models computed under this standard $\Delta Y/\Delta Z$ (i.e. the stars are cooler than the isochrones), rather implying a much steeper value of ~ 10. This change in slope is at odds with Galactic chemical evolution models, which predict a ratio substantially constant with Z (Carigi & Peimbert 2008; Casagrande 2008); a constant $\Delta Y/\Delta Z \sim 2$ is also found from HII regions (e.g. Peimbert et al. 2007). More importantly, $\Delta Y/\Delta Z \sim 10$ at low metallicities implies a helium content for nearby subdwarfs much lower than Y_P, in awkward contrast with the cosmological floor set by standard BBN.

This result points toward inadequacies in MS stellar models of low metallicity (see also Lebreton et al. 1999), an issue which is worth investigating since it may lead to reconsider the problem of the helium enrichment in Globular Clusters (GCs). In fact, at magnitudes comparable to those of the local stars studied in Casagrande et al. (2007, $M_V \sim 5.5-7.5$), multiple MSs have been discovered in some Globular Clusters and interpreted as evidence for huge helium enhancement in a sub-population (Piotto 2009 and references therein). The required $\Delta Y/\Delta Z \gtrsim 100$ is extremely difficult to explain for stellar nucleosynthesis and chemical evolution models (Yi 2009 and references therein). While it is likely that a significant helium enhancement is present in those stellar populations, our purpose is to show that the revision of low metallicity MS stellar models, needed to cure the problem of the high $\Delta Y/\Delta Z$ and sub-primordial Y deduced in nearby K dwarfs, may significantly reduce current estimates of $\Delta Y/\Delta Z$ in Globular Clusters with multiple MS, easing their theoretical interpretation. Full details on the work presented here are given in Portinari, Casagrande & Flynn (2010).

2. Homology relations

Homology relations, holding for largely radiative structures (Cox & Giuli 1968) such as MS stars of $M \lesssim 1\ M_\odot$, express the distance, in the theoretical HR diagram of a Zero Age Main Sequence (ZAMS) of composition (Y, Z) with respect to another reference ZAMS of composition (Y_r, Z_r):

$$\begin{aligned}\Delta \log T_{\rm eff} = \quad & -0.0935 \log\left[1 - \tfrac{\delta}{X_r}(Z - Z_r)\right] \\ & -0.196 \log\left[1 - \tfrac{5\delta+1}{(3+5X_r-Z_r)}(Z - Z_r)\right] \\ & -0.051 \log\left[1 - \tfrac{\delta}{(1+X_r)}(Z - Z_r)\right] \\ & -0.051 \log\left(\tfrac{100Z+1}{100Z_r+1}\right)\end{aligned} \tag{2.1}$$

where $\delta = 1 + \frac{\Delta Y}{\Delta Z}$ and $X_r = 1 - Y_r - Z_r$. Notice that the same relation holds also for a generic combination of (Y, Z) replacing $\delta\,(Z - Z_r) \rightarrow (Y - Y_r) + (Z - Z_r)$.

† It is worth recalling that the adopted $T_{\rm eff}$ scale has been recently validated by interferometric angular diameters and HST spectrophotometry (Casagrande et al. 2010). Without entering into further details, suffice here to say that this scale is hotter than other IRFM renditions, and hotter than or close to various spectroscopic scales. Therefore, any other $T_{\rm eff}$ scale will just worsen the comparison with the isochrones discussed in this paper, with real stars even cooler than the models.

2.1. *Application to Globular Clusters*

In recent years, thanks to deep photometric observations, multiple, distinct MSs have been detected in ωCen and NGC 2808 (Piotto 2009 and references therein). Recent observations also seem to support a MS broadening in 47 Tuc (Anderson et al. 2009). Since helium crucially affects the morphology of the HR diagram, it is very tempting to interpret multiple stellar populations in terms of different helium contents (Catelan, Valcarce & Sweigart 2009 and references therein).

For ωCen, detailed isochrone analysis indicates that a helium enrichment of $\Delta Y \simeq 0.15$ is needed to reproduce the observed split between the blue (bMS, [Fe/H] $= -1.3$) and red (rMS, [Fe/H] $= -1.6$, $Y_{\rm rMS} = 0.246$) main sequence. Homology relations (Eq. 2.1) indeed yield a similar result: using the colour–temperature–metallicity scale of Casagrande et al. (2006) to translate the dereddened maximum observed colour split between the bMS and rMS returns $\Delta \log T_{\rm eff} = 0.0185$ implying $\Delta Y = 0.144$ and $Y_{\rm bMS} = 0.39$ (Fig. 2). These values are in excellent agreement with the results obtained by Norris (2004), Piotto et al. (2005), Lee et al. (2005) and Sollima et al. (2007) by means of isochrone analysis.

Another striking example of multiple populations is NGC 2808, where three MSs are found at virtually the same metallicity [Fe/H] $= -1.1 \pm 0.03$ dex (Carretta et al. 2006) and helium abundances of $Y = 0.248$ (the value assumed for the red MS, which includes the bulk of the population), $Y = 0.30$ (middle MS) and $Y = 0.37$ (blue MS; D'Antona et al. 2005; Lee et al. 2005; Piotto et al. 2007). In this case $\Delta Z \to 0$, and one should just focus on ΔY. Translating the dereddened maximum split of the bMS and rMS with respect to the mMS and using the $T_{\rm eff}$ scale of Casagrande et al. (2006) returns $\Delta \log T_{\rm eff} = \pm 0.009$. For an assumed $Y_{\rm rMS} = 0.248$, homology relations return $Y_{\rm mMS} = 0.31$ and $Y_{\rm bMS} = 0.37$ again in excellent agreement with isochrone analysis (Piotto et al. 2007).

Finally, if the observed broadening of the MS in 47 Tuc is interpreted in terms of helium variation, homology relations reproduce the measured $\Delta \log T_{\rm eff} = 0.003$ with $\Delta Y = 0.023$, again close to the conclusion based on isochrones (Anderson et al. 2009).

2.2. *Application to isochrones*

We have shown that theoretical homology relations, applied to the multiple (or broadened) MSs of Globular Clusters, provide a similar interpretation of the data in terms of ΔY and $\Delta Y/\Delta Z$ as detailed isochrone analysis. We now compare directly homology relations to current stellar models by fitting isochrones with a homology–like relation.

An interpolation formula for isochrones directly inspired by Eq. (2.1) involves at least 4 independent parameters, but for fitting purposes, a simplified form of Eq. (2.1) is more suitable. We verified that the result is still a very good approximation of the rigorous homology relations, especially for metallicities $Z \leqslant Z_\odot$ and even for extremely high $\Delta Y/\Delta Z > 100$, which are of interest for Globular Clusters. Therefore we seek a three–parameters fitting formula for isochrones (and, later below, for real stars) of the kind:

$$\begin{aligned} \Delta \log T_{\rm eff} = \quad & -P_1 \log \left[1 - \tfrac{\delta}{(0.6+X_r)} (Z - Z_r) \right] \\ & -P_2 \log \left(\tfrac{P_3 Z + 1}{P_3 Z_r + 1} \right) \end{aligned} \tag{2.2}$$

where P_i are 3 free fitting parameters. It is our experience that this formula provides an adequate fit to isochrones, as good as (and more robust than) other homology-like fitting formulæ with 4 or more parameters. This simplified formulation condenses together the first three (helium dependent) terms of the original relation and has a clearcut separation between the helium– and metallicity–dependent part, which proves to be handy for the empirical calibration discussed in Section 3.

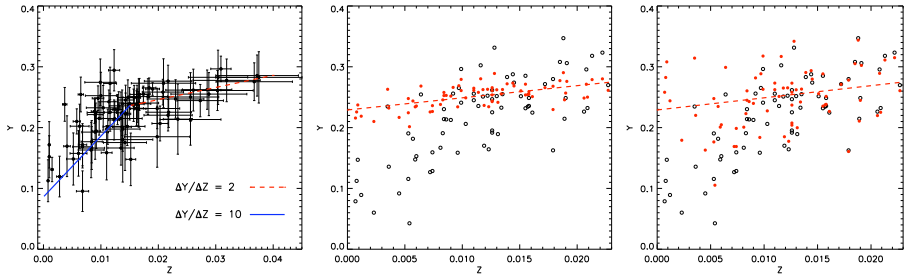

Figure 1. *Left panel:* metal versus helium mass fraction for nearby field dwarfs obtained from Casagrande et al. (2007). Lines with two values of $\Delta Y/\Delta Z$ (break at $Z = 0.015$) are plotted to guide the eye. *Central panel:* zooming on metallicities around and below solar. Open circles are derived applying *numerical homology relations* and look remarkably similar to those in the left panel. Full circles are obtained using *empirical homology relations* with $P_1 = 1.5$. *Right panel:* same as central panel, but using *empirical homology relations* with $P_3 \sim 150$.

We consider both the Padova isochrones computed specifically for the analysis in Casagrande et al. (2007), and the more recent release by Bertelli et al. (2008) with varying $\Delta Y/\Delta Z$ and $0.0001 \leqslant Z \leqslant 0.04$, which fully brackets the metallicity range relevant for the present study. In Casagrande et al. (2007) we had checked that other sets of isochrones (Yonsei–Yale, Teramo, McDonald) were very similar in the lower MS.

We find that the behaviour of isochrones, at least in the range $M_{\rm Bol} = 5.4 - 7.0$ (where the effect of $\Delta Y/\Delta Z$ is expected to be maximal) is well described by homology–like relations with the following set of parameters: $P_1 = 0.50 \pm 0.03$, $P_2 = 0.064 \pm 0.005$ and $P_3 = 670 \pm 200$. When using these parameters we will speak of *numerical homology relations*. In Casagrande et al. (2007) the metal and helium mass fraction of the stars were computed iteratively, with a star–by–star isochrone fitting: despite the less sophisticated approach provided by homology relations, with the aforementioned parameters nearly identical results are obtained, including the change in slope above and below $Z \sim 0.015$ (Fig. 1).

3. Empirical homology relations and Globular Clusters

In the previous section we have shown that theoretical homology relations agree very well with the isochrone–based interpretation of the MS splits observed in ωCen and NGC 2808, and adequately reproduce the behaviour of isochrones in general, as a function of $\Delta Y/\Delta Z$. However, isochrones are known to fail the interpretation of the HR diagram of nearby low–Z MS stars: while for $Z \gtrsim 0.015$ the broadening of the main sequence is well reproduced with the standard $\Delta Y/\Delta Z \sim 2$, with current isochrones a much higher $\Delta Y/\Delta Z \sim 10$ is needed to fit lower metallicities. While in principle $\Delta Y/\Delta Z$ may not necessarily be constant, taken at face value, this result implies a helium content in local metal poor stars as low as $Y = 0.1$. Such a striking contrast with BBN is to be ascribed to inadequacies of low metallicity MS stellar models.

While awaiting for a solution to this problem by improved stellar physics, we now define *empirical homology relations*, calibrated to reproduce the broadening of the local MS, and extrapolate the consequences for the interpretation of Globular Clusters. Here we adopt a very pragmatic approach: we *assume* $\Delta Y/\Delta Z \sim 2$ also for $Z < Z_{\odot}$, and empirically calibrate homology relations to fulfill this constraint for nearby stars. Our assumption is very reasonable, since HII region measurements and chemical evolution models support a constant $\Delta Y/\Delta Z \sim 2$ at all Z, as does the following simple argument: taking the solar

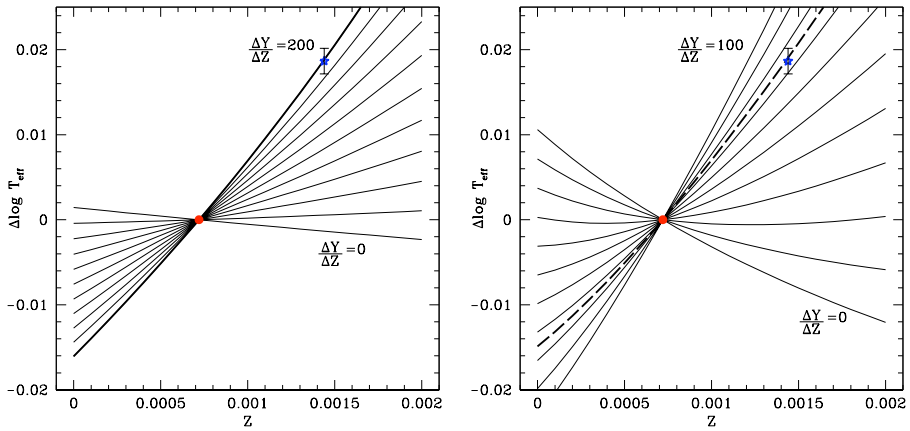

Figure 2. *Left panel:* $\Delta Y/\Delta Z$ obtained applying homology relations to the measured $\Delta \log T_{\rm eff}$ between the rMS (dot) and bMS (star) in ωCen. *Right panel:* same as left, but using *empirical homology relations* with maximized effect on helium (i.e. $P_1 = 1.5$)

bulk abundances (Asplund et al. 2009) and the primordial Y_P, one derives $\Delta Y/\Delta Z \sim 2$ for $Z < Z_\odot$.

To define *empirical homology relations*, one can act on either terms of Eq. (2.2). The first one includes the effects of the helium content, while the second term (stemming essentially from the metallicity dependence of opacity) is independent of $\Delta Y/\Delta Z$. The second term is therefore irrelevant for the multiple MSs in GCs, where metallicity differences are small or vanishing. Therefore, if we calibrate our empirical homology relations onto nearby stars acting only on the first term (via the parameter P_1), we maximize the change in the role of helium, and the consequences for the interpretation of GC's.

Keeping P_2 and P_3 fixed and optimizing P_1 so that the inferred helium content of nearby K dwarfs with $Z < Z_\odot$ follows $\Delta Y/\Delta Z = 2$ (Fig. 1, central panel) yields $P_1 = 1.5$ and the helium abundances required to describe the multiple MSs decrease to $Y_{\rm bMS} = 0.30$ (ωCen, Fig. 2), $Y_{\rm mMS} = 0.265$ and $Y_{\rm bMS} = 0.283$ (NGC 2808) and $\Delta Y = 0.006$ (47 Tuc).

Acting instead on the second term of the homology relations has no impact on the interpretation of the multiple MS of Globular Clusters. But for nearby K dwarfs and subdwarfs, the metallicity range is significant and exploring the effects of this second term is worthwhile. The parameters P_2 and P_3 are degenerate, in the sense that a given change in the second term can be obtained by modifying either of the two parameters. Therefore, we choose to discuss the role of the second term by optimizing P_3. Keeping P_1 and P_2 fixed we find that $P_3 \sim 150$ is the optimal value to obtain $\Delta Y/\Delta Z = 2$ for nearby low–Z stars. However, while we do obtain $\Delta Y/\Delta Z = 2$ on average, this solution has considerable scatter and many stars remain with uncomfortably low helium abundances (Fig. 1, right panel).

4. Conclusions

The purpose of the present exercise has been to draw attention on the possible connection between the HR diagram of Globular Clusters with multiple MSs and the broadening of the low MS defined by nearby stars. We estimate the possible extent of the required

revision of low MS stellar models on the base of homology relations. First we show that theoretical homology relations properly reproduce the response of stellar models to the helium content. Then, since both isochrones and theoretical homology relations fail the interpretation of the nearby low–Z MS, we calibrate empirical homology relations to yield $\Delta Y/\Delta Z \sim 2$ for nearby stars of all metallicities, and inspect the consequences for the MS splits in Globular Clusters.

If we entirely impute the failure of the low MS stellar models to a wrong response to the helium abundance (and correspondingly re-calibrate the helium–sensitive term of the homology relations), the consequences for Globular Clusters are highly significant: the helium content of the blue sub-populations is reduced from 40% to 30%, which is far easier to explain with chemical evolution models (e.g. Yi 2009; Romano et al. 2009).

Alternatively, if stellar models for the lower MS are assumed to fail in their metallicity dependence (i.e. we re-calibrate only the homology term expressing the metallicity dependence of opacity) the consequences for Globular Clusters are negligible — as the metallicity differences between the subpopulations are minimal or vanishing.

As the solution for K dwarf models can be intermediate between these two extreme assumptions, we suggest that the helium rich populations in Globular Clusters are likely to have a helium content Y in the range 0.3–0.4; but altogether, there is room to decrease their estimated helium content from the extreme $Y = 0.4$ that is the commonly quoted value. Improvements in the physics of low MS stellar models are thus potentially important also for the riddle of the helium self-enrichment in Globular Clusters.

References

Anderson J., Piotto G., King I.R., Bedin L.R., Guhathakurta P., 2009, *ApJ*, 697, L58
Asplund M., Grevesse N., Sauval A.J., Scott P., 2009, ARA&A, 47, 481
Bertelli G., Girardi L., Marigo P., Nasi E., 2008, *A&A*, 484, 815
Carigi L., Peimbert M., 2008, *RMxAA*, 44, 341
Carretta E., Bragaglia A., Gratton R.G., et al. 2006, *A&A*, 450, 523
Casagrande L., 2008, *PhD Thesis*, Annales Universitatis Turkuensis, Ser. A1 t., 382
Casagrande L., Portinari L., Flynn C., 2006, *MNRAS*, 373, 13
Casagrande L., Flynn C., Portinari L., Girardi L., Jimenez J., 2007, *MNRAS*, 382, 1516
Casagrande L., Ramírez I., Meléndez J., Bessell M., Asplund M., 2010, *A&A*, in press
Catelan M., Valcarce A.A.R., Sweigart A.V., 2009, *IAU Symp.* 266, (arXiv:0910.1367)
Cox J.P., Giuli R.T., 1968, *Principles of Stellar Structure*, Gordon & Breach, New York
D'Antona F., Bellazzini M., Caloi V., Pecci F.F., Galleti S., Rood R.T., 2005, *ApJ*, 631, 868
Faulkner J., 1967, ApJ 147, 617
Fernandes J., Lebreton Y., Baglin A., 1996, *A&A*, 311, 127
Jimenez R., Flynn C., McDonald J., Gibson B., 2003, *Science*, 299, 1552
Lebreton Y., Perrin M.-N.,, Cayrel R., Baglin A., Fernandes J., 1999, *A&A*, 350, 587
Lee Y.-W., Joo S.-J., Han S.-I., et al. 2005, *ApJ*, 621, L57
Norris J.E., 2004, *ApJ*, 612, 25
Pagel B.E.J., Portinari L., 1998, *MNRAS*, 298, 747
Peimbert M., Luridiana V., Peimbert A., 2007, *ApJ*, 666, 636
Piotto G., 2009, in The Ages of Stars *IAU Symp.* 258, 233
Piotto G., Villanova S., Bedin L.R., Gratton R., Cassisi S., et al. 2005, *ApJ*, 621, 777
Piotto G., Bedin L.R., Anderson J., King I.R., Cassisi S., et al. 2007, *ApJ*, 661, L53
Portinari L., Casagrande L., Flynn C., 2010, submitted
Romano D., Tosi M., Cignoni M., et al. 2009, *MNRAS*, in press (arXiv:0910.1299)
Sollima A., Ferraro F.R., Bellazzini M., et al. 2007, *ApJ*, 654, 915
Villanova S., Piotto G., Gratton R.G., 2009, *A&A*, 499, 755
Yi S.-K., 2009, in The Ages of Stars *IAU Symp.* 258, 253

Light elements in the Universe
Proceedings IAU Symposium No. 268, 2010
C. Charbonnel, M. Tosi, F. Primas & C. Chiappini, eds.

DOI: 00.0000/X000000000000000X

Helium-rich stars in globular clusters: constraints for self-enrichment by massive stars

Thibaut Decressin[1], G. Meynet[2] and C. Charbonnel[2,3]

[1]Argelander Institute for Astronomy (AIfA), Auf dem Hügel 71, D-53121 Bonn, Germany
email: decressin@astro.uni-bonn.de

[2]Geneva Observatory, University of Geneva, 51 ch. des Maillettes, 1290 Versoix, Switzerland
email: georges.meynet@unige.ch

[3]Laboratoire d'Astrophysique de Toulouse-Tarbes, CNRS UMR 5572, Université de Toulouse, 14 Av. E. Belin, 31400 Toulouse, France
email: corinne.charbonnel@unige.ch

Abstract. Globular clusters exhibit peculiar chemical patterns where Fe and heavy elements are constant inside a given cluster while light elements (Li to Al) show strong star-to-star variations. This pattern can be explained by self-pollution of the intracluster gas by the slow winds of fast rotating massive stars. Besides, several main sequences have been observed in several globular clusters which can be understood only with different stellar populations with distinct He content. Here we explore how these He abundances can constrain the self-enrichment in globular clusters.

Keywords. stars: abundances, evolution, horizontal-branch, mass loss – globular clusters: general

1. Chemical enrichment of globular clusters

Globular clusters are self-gravitating aggregates of tens of thousands to millions of stars that have survived over a Hubble time. Many observations show that these objects are composed of (at least) two distinct stellar populations. The first evidence rests on the chemical analysis that reveals large star-to-star abundance variations in light elements in all individual clusters studied so far, while the iron abundance stays constant (for a review see Gratton et al. 2004). These variations include the well-documented anticorrelations between C-N, O-Na, Mg-Al, Li-Na and F-Na (Kraft 1994; Carretta et al. 2007; Gratton et al. 2007; Carretta et al. 2006; Pasquini et al. 2007; Bonifacio et al. 2007; Lind et al. 2009). This global chemical pattern requires H-burning at high temperature around 75×10^6 K (Arnould et al. 1999; Prantzos et al. 2007). As the observed chemical pattern is present in low-mass stars both on the red giant branch (RGB) and at the turn-off that do not reach such high internal temperatures, the abundance anomalies must have been inherited at the time of formation of these stars.

Further indications for multiple populations in individual GCs come from deep photometric studies that have revealed multiple giant branches or main sequences. In ω Cen a blue main sequence has been discovered (Bedin et al. 2004) that is presumably related to a high content in He (Piotto et al. 2005; Villanova et al. 2007). A triple main sequence has been discovered in NGC 2808 (Piotto et al. 2007). The additional blue sequences are explainable by a higher He content of the corresponding stars which shifts the effective temperatures towards hotter values. He-rich stars have also been proposed to explain the morphology of extended horizontal branch (hereafter HB) seen in many globular clusters

(see e.g., Caloi & D'Antona 2005). Whereas no direct observational link between abundance anomalies and He-rich sequences has been found, this link is easily understood theoretically as abundance anomalies are the main result of H burning to He.

These observed properties lead to the conclusion that globular clusters born from giant gas clouds first form a generation of stars with the same abundance pattern as field stars. Then a polluting source enriches the intracluster-medium with H-burning material out of which a chemically-different second stellar generation forms. This scheme can explain at the same time the abundance anomalies in light elements and He-enrichment.

Two main candidates that reach the right temperature for H-burning have been proposed to be at the origin of the abundance anomalies (Prantzos & Charbonnel 2006): (a) intermediate mass stars evolving on the thermal pulses along the asymptotic giant branch (hereafter TP-AGB), and (b) main sequence massive stars. After being first proposed by Cottrell & Da Costa (1981) the AGB scenario has been extensively studied (see e.g., Ventura & D'Antona 2008b,a, 2009, see Ventura, this volume) and has been seriously challenged by rotating AGB models that predict unobserved CNO enrichment in low-metallicity globular clusters (Decressin et al. 2009).

On the other hand, as being suggested by Brown & Wallerstein (1993) and Wallerstein et al. (1987), massive stars can also pollute the interstellar medium (ISM) of a forming cluster (see Smith 2006; Prantzos & Charbonnel 2006). In particular Decressin et al. (2007b) show that fast rotating massive stars (with a mass higher than ~ 25 $M_{\odot}$) are good candidates for the self-enrichment of globular clusters. In this wind of fast rotating massive stars (WFRMS) scenario, rotationally-induced mixing transports H-burning products (and hence matter with correct abundance signatures) from the convective core to the stellar surface, and, providing initial rotation is high enough, the stars reach the break-up on the main sequence evolution. As a result a mechanical wind is launched from the equator that generates a disk around the star similar to that of Be stars (e.g. Townsend et al. 2004). Later, when He-burning products are brought to the surface, the star has already lost a high fraction of its initial mass and angular momentum, so that it no longer rotates at the break-up velocity. Matter is then ejected through a classical fast isotropic radiative wind. From the matter ejected in the disk, a second generation of stars may be created with chemical pattern in agreement with observations.

2. He-rich stars evolution

As explained in Decressin et al. (2007a), matter stored in the discs around massive stars is heavily enriched with He. If the second generation stars form locally around each massive star from a mixture of matter stored in the slow winds and the ISM, we expect the following distribution: a main peak is present at normal He-abundance (Y = 0.245, in mass fraction) and it extends up to 0.4. However a long tail toward higher Y-values is also present with around 12% of the stars with initial He value between 0.4 and 0.72. Here we want to explore in more details the consequence of the super He-rich stars for the properties of globular clusters.

To assert these implications we have computed a grid of low-mass stellar models from 0.2 to 0.9 $M_{\odot}$ at a metallicity of $Z = 0.0005$ (similar to the metal-poor globular cluster NGC 6752) for initial He mass fraction between 0.245 and 0.72 with the stellar evolution code STAREVOL V2.92 (see Siess et al. 2000; Siess 2006, for more details). These models have been computed without any kind of mixing except for an instantaneous mixing in convection zones. All models have been computed from the pre-main sequence to the end of the central He-burning phase.

The mass-loss rate is the only physical parameter that can change the evolution of

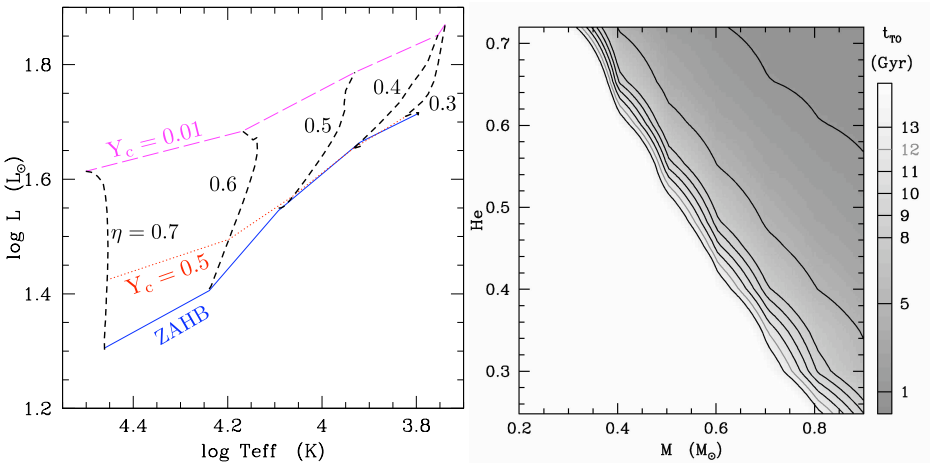

Figure 1. *Left:* Location of central He-burning stars with initial mass of 0.83 $M_\odot$ reaching the TO after 13 Gyr. with various mass loss parameters on the RGB (η_R = 0.3 to 0.7). Full, dotted, and long-dashed lines indicate respectively places where the stars arrive on the HB and where the central He abundance is 0.5, and 0.01. *Right:* Age at the turn-off for low-mass stars as a function of their initial mass (0.2–0.9 $M_\odot$) and initial He value (0.245-0.72, mass fraction). White area indicates stars still on the main sequence after 15 Gyr of evolution.

standard stellar models. This is of peculiar importance in globular clusters as both mass-loss and He-enrichment can produce blue HB. Here we adopt the mass-loss rate following Reimers (1975) prescription (without metallicity dependence). In Fig. 1 (left panel) we present the location of the stars on the HB used to calibrate the mass-loss. Models with He-normal composition (Y_{ini} = 0.245) are computed with different values, from 0.3 to 0.7, for the η parameter in Reimers (1975) prescription. A high value for η (i.e., a high mass-loss rate on the RGB) gives bluer stars on the HB. Below $\eta = 0.5$ the stars stay near the ZAHB in the first part of central He-burning phase. As time passes the luminosity of the H-burning shell (hereafter HBS) decreases while the luminosity of the He-burning core increases, leaving almost no variation of surface luminosity. On the other hand stars with high mass loss have a weak HBS on the ZAHB and the increase of surface luminosity reflects the one in the He-core.

From the observational point of view only few studies have been able to assess the He abundance for HB stars. In the GC M 3, Catelan et al. (2009) show that for stars with effective temperature below 10 000 K, only normal He abundance agreed with the surface gravity. Besides in NGC 6752, Villanova et al. (2009) find through spectroscopic measurements that stars with effective temperature in the range 9 000–8 500 K have a He composition compatible with normal He abundance. From Fig. 1 (left panel) we see that a value of η around 0.4 implies HB stars with standard He abundance and effective temperature below 10 000 K. If we assume the same mass-loss rate for He-rich stars, they will have a smaller mass on the HB and hence will only have hotter temperature. Therefore, higher η values than 0.4 will produce too hot HB stars without stars in the red part of the HB. On the other hand, lower η values will require high He abundance HB stars with effective temperature below 10 000 K in contradiction with the observations. In our computation we use $\eta = 0.4$ for the parameter of Reimers (1975) law for all models independently of the initial He content.

For a given stellar mass, He-rich stars evolve faster on the main-sequence due to their

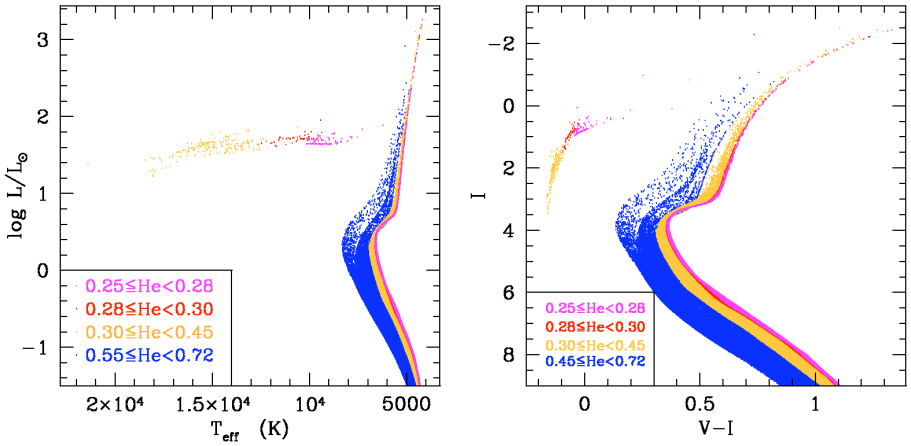

Figure 2. Synthetic diagram of a 13 Gyr old globular cluster in HR diagram (right) and CMD (left). Magenta, red, orange and blue colours (from right to left) indicate the initial abundance of He. He-rich stars are present on the blue part of the MS, RGB and HB, while super-He rich stars are only seen on the MS and RGB.

lower initial H-content and to their higher luminosity. Figure 1 (right panel) illustrates this point showing the turn-off age as a function of the initial mass and He mass fraction of stars. After 12 Gyr, stars of 0.85 $M_\odot$ with standard helium (Y = 0.245) as well as He-rich stars of 0.4 $M_\odot$ (Y = 0.6) are leaving the main sequence. Thus the distribution of the initial He abundance will be reflected by a distribution of stellar mass for stars at the same evolutionary stage.

3. Effects on colour-magnitude diagram of GCs

Figure 2 shows synthetic colour-magnitude diagrams (in the $T_{\rm eff}$ vs. $\log L$ and I vs. V-I planes) of a 13 Gyr old globular cluster with the initial spread in He following the distribution obtained by Decressin et al. (2007a) for a cluster enriched by fast rotating massive stars. The age is chosen to be of 13 Gyr, in agreement with that determined for NGC 6752 (13.8 ± 1.1 Gyr, Gratton et al. 2003). This CMD has been computed with a modified version of the program used by Meynet (1993) to investigate supergiant populations. We use the colours transformation from VandenBerg & Clem (2003) which considered only He-normal abundance. This adds another uncertainty to the position of He-rich stars in right panel of Fig. 2.

The spread in He converts into a spread in mass at the turn-off. The luminosity increase of He-rich stars is mainly compensated by their shorter lifetime so that the turn-off luminosity is almost constant. Besides due to their differences in opacity and to their compactness they are also hotter. Thus the He-rich main-sequence and RGB stars are shifted to the left side of the CMD.

While being present on blue side of MS and RGB, super He-rich stars are not laying in the blue part of the HB. This is due to the combined effects of mass-loss during the RGB phase with a smaller initial mass which produce a He-core too light to be able to start He-burning. Thus stars with He content higher than ~ 0.45–0.5 will end as He-WD instead of blue HB stars and CO-WD.

Recently Milone et al. (2009) analyse deep photometry of NGC 6752, revealing a

broadening of the main sequence which could be attributed neither to binaries nor to photometric errors. If we compare our theoretical CMD with the one observed by those authors we note some discrepancies. In particular the theoretical width of the main sequence at the turn-off is too large compared to that observed for this cluster. Let us stress however that we use calibration relations for normal He content while stars of different He content are present. This might artificially distort the MS. Interestingly the extended blue loop of NGC 6752 can be reproduced by our theoretical CMD with different He-value ranging from 0.245 to 0.45.

A possibility to avoid super He-rich stars is to consider stronger dilution factors. For instance, if we assume a global dilution to produce a mean value we will have Y$\sim$0.37, which is quite consistent with the blue main sequence in ω Cen and the triple main sequences detected in NGC 2808. However this situation is not completely satisfactory as it leads to a reduction of the amplitude of star-to-star variations of light elements that may then disagree with the observations.

Another way to solve the discrepancy comes from the stellar evolution models of fast rotating massive stars. As already explained, during the main sequence the star reaches the break-up velocity and we assume that the matter is ejected through a slow equatorial wind. However the matter with a very high He-abundance is released only at the end of the main-sequence and the beginning of the central-He burning phase. During these phases, the stars is still at the break-up velocity but this time the radiation pressure contribute significantly to it. This is the so-called $\Omega\Lambda$ limit (Maeder & Meynet 2000). In previous studies we have assumed that the matter released has still a small velocity and will be stored also in the disc to maximise the amount of H-burning processed matter released by fast rotating massive stars. However if the radiation starts to dominate we can instead expect faster winds that will escape the cluster potential well so that this super He-rich matter is lost for the self-enrichment of globular clusters. In this case it would be possible to produce both large abundance variations in light elements along with a moderate increase in He abundance.

Acknowledgements

We acknowledge support from the Swiss National Science Foundation (FNS) and from the "Programme National de Physique Stellaire" of CNRS/INSU, France.

References

Arnould, M., Goriely, S., & Jorissen, A. 1999, *A&A*, 347, 572
Bedin, L. R., Piotto, G., Anderson, J., et al. 2004, *ApJ* (Letters), 605, L125
Bonifacio, P., Pasquini, L., Molaro, P., et al. 2007, *A&A*, 470, 153
Brown, J. A. & Wallerstein, G. 1993, *AJ*, 106, 133
Caloi, V. & D'Antona, F. 2005, *A&A*, 435, 987
Carretta, E., Bragaglia, A., Gratton, R. G., et al. 2006, *A&A*, 450, 523
Carretta, E., Bragaglia, A., Gratton, R. G., Lucatello, S., & Momany, Y. 2007, *A&A*, 464, 927
Catelan, M., Grundahl, F., Sweigart, A. V., Valcarce, A. A. R., & Cortés, C. 2009, *ApJ* (Letters), 695, L97
Cottrell, P. L. & Da Costa, G. S. 1981, *ApJ* (Letters), 245, L79
Decressin, T., Charbonnel, C., & Meynet, G. 2007a, *A&A*, 475, 859
Decressin, T., Charbonnel, C., Siess, L., et al. 2009, *A&A*, 505, 727
Decressin, T., Meynet, G., Charbonnel, C., Prantzos, N., & Ekström, S. 2007b, *A&A*, 464, 1029
Gratton, R., Sneden, C., & Carretta, E. 2004, *ARAA*, 42, 385
Gratton, R. G., Bragaglia, A., Carretta, E., et al. 2003, *A&A*, 408, 529
Gratton, R. G., Lucatello, S., Bragaglia, A., et al. 2007, *A&A*, 464, 953

Kraft, R. P. 1994, *PASP*, 106, 553
Lind, K., Primas, F., Charbonnel, C., Grundahl, F., & Asplund, M. 2009, *A&A*, 503, 545
Maeder, A. & Meynet, G. 2000, *A&A*, 361, 159
Meynet, G. 1993, in The Feedback of Chemical Evolution on the Stellar Content of Galaxies, ed. D. Alloin & G. Stasińska, 40–+
Milone, A. P., Piotto, G., King, I. R., et al. 2009, ArXiv e-prints
Pasquini, L., Bonifacio, P., Randich, S., et al. 2007, *A&A*, 464, 601
Piotto, G., Bedin, L. R., Anderson, J., et al. 2007, *ApJ* (Letters), 661, L53
Piotto, G., Villanova, S., Bedin, L. R., et al. 2005, *ApJ*, 621, 777
Prantzos, N. & Charbonnel, C. 2006, *A&A*, 458, 135
Prantzos, N., Charbonnel, C., & Iliadis, C. 2007, *A&A*, 470, 179
Reimers, D. 1975, Circumstellar envelopes and mass loss of red giant stars (Problems in stellar atmospheres and envelopes.), 229–256
Siess, L. 2006, *A&A*, 448, 717
Siess, L., Dufour, E., & Forestini, M. 2000, *A&A*, 358, 593
Smith, G. H. 2006, *PASP*, 118, 1225
Townsend, R. H. D., Owocki, S. P., & Howarth, I. D. 2004, *MNRAS*, 350, 189
VandenBerg, D. A. & Clem, J. L. 2003, *AJ*, 126, 778
Ventura, P. & D'Antona, F. 2008a, *MNRAS*, 385, 2034
Ventura, P. & D'Antona, F. 2008b, *A&A*, 479, 805
Ventura, P. & D'Antona, F. 2009, *A&A*, 499, 835
Villanova, S., Piotto, G., & Gratton, R. G. 2009, *A&A*, 499, 755
Villanova, S., Piotto, G., King, I. R., et al. 2007, *ApJ*, 663, 296
Wallerstein, G., Leep, E. M., & Oke, J. B. 1987, *AJ*, 93, 1137

Light elements in the Universe
Proceedings IAU Symposium No. 268, 2010
C. Charbonnel, M. Tosi, F. Primas, C. Chiappini, eds.

DOI: 00.0000/X000000000000000X

What helium and lithium can tell us about CEMP stars?

Georges Meynet[1], Raphael Hirschi[2,3], Sylvia Ekstrom[1], André Maeder[1], Cyril Georgy[1], Patrick Eggenberger[1], and Cristina Chiappini[1]

[1]Geneva Observatory, Geneva University,
CH–1290 Sauverny, Switzerland
email: georges.meynet@unige.ch

[2]Astrophysics group, Keele University,
Lennard-Jones Lab., Keele, ST5 5BG, UK

[3]IPMU, University of Tokyo,
Kashiwa, Chiba 277-8582, Japan

Abstract. We show that the peculiar surface abundance patterns of Carbon Enhanced Metal Poor (CEMP) stars has been inherited from material having been processed by H- and He-burning phases in a previous generation of stars (hereafter called the "Source Stars"). In this previous generation, some mixing must have occurred between the He- and the H-burning regions in order to explain the high observed abundances of nitrogen. In addition, it is necessary to postulate that a very small fraction of the carbon-oxygen core has been expelled (either by winds or by the supernova explosion). Therefore only the outermost layers should have been released by the Source Stars. Some of the CEMP stars may be He-rich if the matter from the Source Star is not too much diluted with the InterStellar Medium (ISM). Those stars formed from nearly pure ejecta would also be Li-poor.

Keywords. stars: AGB, early-type, evolution – supernovae: general – Galaxy: halo – nucleosynthesis

1. Introduction

Observations have revealed in these last years a galactic halo much more complex than previously thought. The existence of two halos, an inner one and an outer one (Carollo et al. 2008) showed that, both from the point of view of kinematics and chemical composition, the galactic halo cannot be viewed as a single entity. At the smaller scale of the globular clusters, there are now ample evidences for the succession of at least two and maybe more stellar generations in clusters, each leaving a very peculiar imprint on the chemical composition of stars (see the talks by Bragaglia and Decressin in the present volume and references therein). In that respect it is striking to note that stellar populations in clusters and in the field have each their own "anomalous" counterpart. In globular clusters the "anomalous" component is made up of stars essentially made from material processed by only H-burning reactions. In the field, the "anomalous" component is made up of stars presenting the nucleosynthetic signature of both H- and He-burning processes. In this paper, we focus our attention on the "anomalous" population observed in the field of the halo. In that population, we find the most iron poor star known today, HE 1327-2326, with a [Fe/H] as low as -5.96 (Frebel et al. 2008). In this star, one counts 72 000 atoms of carbon for one atom of iron, while in the Sun, there is only 9 atoms of carbon per atom of iron! Hence the name of Carbon Enhanced Metal Poor Stars

(CEMPs). The CEMP stars represent about 1 in 5 stars at metallicity below [Fe/H] < -2.5 (Lucatello et al. 2006). In HE 1327-2326, the numbers of nitrogen and oxygen atoms with respect to the number of iron atoms are respectively 20 000 times and 2500 times greater than in the Sun. Thus this star could have also been named a N(itrogen)EMP or an Ox(ygen)EMP star! This star is either at the end of the Main-Sequence phase or just after the Main-Sequence (a subgiant), thus these abundances cannot have been produced in the star itself but must have been mainly inherited from the interstellar cloud from which it formed about 13 billion years ago† or be acquired through a mass transfer episode in a close binary system. Whatever the scenario chosen, the main question is what was the nature of the "Source Stars" which either enriched the natal cloud in such a peculiar way or transferred its envelope to its less massive companion conferring it its status of CEMP star? Was it a massive star? An intermediate mass star? Can we deduce some of its properties? This is the point we want to discuss in the present paper.

2. Constraints from nucleosynthesis

There are a few deductions that can be done without reference to any peculiar stellar models. These are the following:

• The CEMP stars present a great scatter in the abundances of the CNO elements (see the hatched zones in the left panel of Fig. 1). This is an indication that the chemical characteristics of the material from which these stars inherited their peculiar composition were different from case to case. This can be understood if the peculiar abundances reflect the chemical abundance of one or at a most a very small number of nucleosynthetic events.

• The very high overabundances with respect to iron of carbon, nitrogen and oxygen imply that the material responsible for these enhancements was mainly processed by the nuclear reactions involving nuclear reaction chains typical of H- (enhancement of N) and He-burnings (increases of C and O). In both nuclear phases, iron is not synthesized. Thus either iron has been produced in stars belonging to generations having occurred before the "Source Stars", or it has been produced, in part or in totality, by the "Source Stars" themselves in advanced nuclear phases. In that case, the "Source Stars" should produce much smaller quantities than those predicted by type II supernova explosions which are expected to produce [O/Fe] around 0.50 or less (see for instance table 1 in Tominaga et al. 2007), while the Frebel star, for instance, show [O/Fe] of the order of 3.4!

• The mixing of material having been processed by H-burning and of material processed by He-burning is however not a sufficient condition to reproduce the observed surface abundances of CEMP stars. To see what would be obtained by simple addition of material having been processed by these two nuclear phases *without allowing any mixing between them in the "Source Star"*, we can look at the dotted, short and long dashed curves plotted in the left panel of Fig. 1. These curves show the chemical composition of the mixed outer envelope of a non-rotating 7 $M_\odot$ at $Z=10^{-5}$ at the early-AGB phase. Only the CNO elements are shown because these models were computed without the Ne-Na, Mg-Al chains. When only the envelope above 1.1 $M_\odot$ is ejected, we see matter processed only by H-burning mixed with some unaltered material in the outer envelope. In case the initial metallicity of the model would have been chosen equal to $Z=10^{-6}$ (maximum metallicity of stars which could have participated to the production of the material from which HE 1327-2326 could form), the whole curve would have been shifted downward by 1 dex. We see that material enriched in H-burning material cannot account

† Microscopic diffusion may have altered the surface abundances however (Korn et al. 2009), but this process cannot be responsible for the huge excesses in CNO elements.

for the observed abundances in CEMP stars. When matter above 0.9 $M_\odot$ is ejected, some material processed by the He-burning reactions is added into the mixture. The abundance of nitrogen is not much changed, while those of carbon and oxygen increase a lot despite the fact that only 0.2 $M_\odot$ has been added with respect to previous case! The trend is reinforced in case a still lower mass cut is considered. Considering a lower initial metal content, would in those cases, shift downward the nitrogen abundances without much changing the positions of the carbon and oxygen abundances. We see thus that such models have no chance to reproduce the observed patterns. Similar conclusions can be reached looking at other initial mass models. In order to achieve high abundances for all the three main CNO isotopes, nitrogen must also be produced from helium as carbon and oxygen. This is possible if some carbon and oxygen produced in the helium core diffuse in the H-burning shell and are transformed there in nitrogen. *Thus the simultaneous large increases of the three CNO elements are an indication that some mixing occurred between the He- and the H-burning regions.*

• Let us suppose that such a mixing occurred. The increase of nitrogen in the H-burning shell cannot be as high as the one of carbon and oxygen in the He-burning core. Diffusion is indeed not as efficient as convection and will never allow to homogenize carbon and oxygen between the He- and the H-burning regions. To see what happens when such a mixing occurs let us consider the left panel of Fig. 1. The upper continuous and long-short dashed curves show the abundances in the mixed outer envelope of a rotating 7 $M_\odot$ stellar model with an initial value of Ω/Ω_c equal to ~ 0.8 where Ω is the surface angular velocity and Ω_c the critical angular velocity at the surface†. The model is in the early AGB phase. In such a model, during the whole core He-burning phase, carbon and oxygen diffuse from the He-core into the H-burning shell. We see that the envelope above the CO core (the CO core mass is about 1.3 $M_\odot$) is strongly enriched in CNO elements. Interestingly it would also be strongly enriched in fluorine, neon (actually ^{22}Ne), in ^{23}Na, in magnesium (mainly ^{26}Mg), and ^{27}Al. Mixing one part of this envelope material from the "Source Star" with 100 parts of ISM would shift the curve downward by 2 dex providing a very good fit to the mean values of the observed patterns shown in that figure. Since all these elements are formed either directly or indirectly from transformation of helium, the overabundances shown here are not so much dependant on the metallicity and would occur in a similar way in more metal poor stars. Also similar conclusions can be obtained from different initial mass models (Meynet et al. 2006; Hirschi 2007). However, depending on the initial mass of the model considered for the "Source Star", the degree of dilution required to fit the observed values can be different.

3. The spinstar scenario

In the "spinstar scenario" (Meynet et al. 2006; Hirschi 2007; Meynet et al. 2009), the required mixing is induced by the instabilities triggered by axial rotation of stars. Rotation can indeed induce mixing in radiative zones and thus allow for instance carbon and oxygen to diffuse from the He core into the H-burning zone. This produces important amounts of nitrogen (primary nitrogen since it is produced from carbon and oxygen synthesized by the star itself) and of primary ^{13}C. It is interesting to note that observations of the surface abundances of "normal" metal poor halo field stars (i.e. non CEMP stars) indicate that actually important amounts of primary nitrogen need to be

† The critical velocity is such that when this velocity is reached, the centrifugal acceleration at the equator compensates for the gravity there.

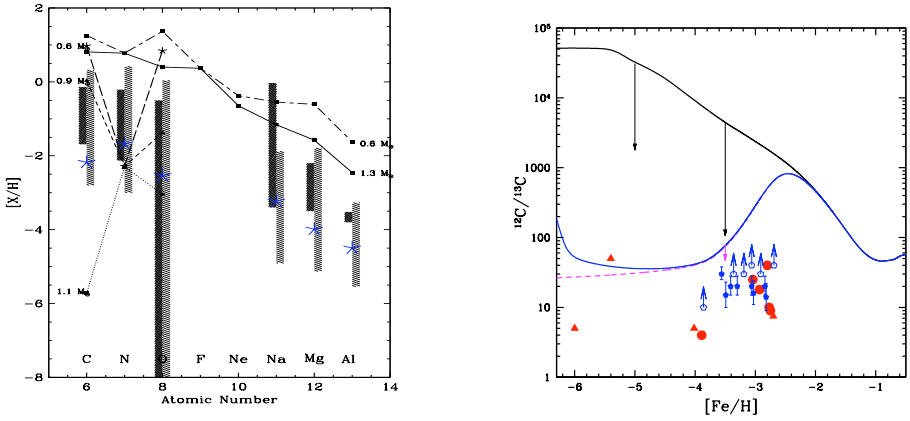

Figure 1. *Left panel :*The continuous and long-short dashed curves with filled squares show the composition obtained by mixing the outer envelope above the langrangian mass coordinate 1.3 $M_\odot$ and 0.6 $M_\odot$ at the E-AGB phase of our Z=10^{-5} rotating 7 $M_\odot$ stellar model. The dotted, short and long-dashed lines correspond to the composition of the envelope above the langrangian mass coordinate 1.1, 0.9 and 0.6 $M_\odot$ respectively at the E-AGB phase of our non-rotating 7 $M_\odot$ stellar model. The CO core in the rotating and non rotating models have masses around 1.3 and 0.9 $M_\odot$ respectively. The star symbols show the observed values for the most iron poor star known today (Frebel et al. 2008). The vertical hatched zones show the range of observed values for CEMP-no stars (i.e. those with no evidence of s-process element enhancements, see references in Masseron et al. 2009). The dark left hatched zone corresponds to non-evolved stars, the right light grey zone to giants. *Right panel :*Predicted evolution of the $^{12}C/^{13}C$ ratio according to chemical evolution models (CEM) for the halo computed with different stellar models for metallicities below Z=10^{-5}. The upper solid line corresponds to CEM models without fast rotators, the dashed and lower solid lines correspond to CEM models with fast rotators. The data are the unmixed stars of Spite et al. (2006). The open symbols represent lower limits. The descending arrows indicate the final $^{12}C/^{13}C$ ratio obtained after the first dredge-up in giants starting from the initial values given by the CEM models (see details in Chiappini et al. 2008). The filled triangles (lower limits) and circles correspond to CEMP stars showing no s-process element enhancements and to the Frebel star (most iron poor star at [Fe/H] =-5.96).

produced in very metal poor massive stars. Chiappini et al. (2006, 2008) showed that rotating massive star models can reproduce the amount of primary nitrogen required by observation provided they began their life with an initial angular momentum content of the same magnitude as the one in solar metallicity massive stars showing an averaged surface rotation rate during the MS of 200 km s^{-1}. In this model, the "normal" halo field stars are formed from a well mixed reservoir enriched by stars of different initial masses and of different initial metallicities. A consequence of this model is that low ratios of the $^{12}C/^{13}C$ should be observed at the surface of non-evolved metal poor halo field stars (see the right panel of Fig. 1).

If now, instead of considering stars formed from material taken from a well mixed reservoir, as above, we consider stars formed from material ejected by one single source, which kind of composition can we expect? This is shown in the left panel of Fig. 1 and was already discussed in the previous section. A good fit is obtained with the CEMP abundance patterns. Thus we see that, in the frame of this model, the main difference between the "normal" and the "anomalous" population is not the nature of the "Source Stars" which in both cases are rotating stars, but the fact that the normal populations are born from a well mixed reservoir, while the CEMP-stars are formed from a much more localized and specifically enriched reservoir.

An interesting feature of the present scenario is that rotational mixing can not only help in producing interesting abundance patterns, it can also be responsible for the loss through winds of the outermost layers. Indeed, due to rotational mixing, the radiative envelope is enriched in CNO elements, its global opacity is increased and this may trigger line driven stellar winds, both in the case of massive stars in the supergiant phase and in the case of intermediate mass stars along the AGB. Such an opacity increase only occurs when the stars have evolved beyond the Main-Sequence. Only at that time, can the surface be CNO enriched with values well above the initial metallicity. This will only occur at very low metallicity, let's say at metallicities below about 10^{-5} . Why? For two reasons, first when the metallicity decreases rotational mixing is more efficient (Maeder & Meynet 2001), second the mass losses, both due to line radiation winds and to mechanical winds due to the reaching of the critical velocity are very weak at these low metallicities (see Meynet et al. 2009), preventing the H-burning shell to disappear when the He-burning core is in activity. Thus only at low metallicities can we expect to have winds enriched in both H- and He-burning products. At higher metallicities ($10^{-5} < Z < 10^{-3}$) , fast rotating models lose important amounts of matter through mechanical equatorial winds during the Main-Sequence (Decressin et al. 2007, see also the contribution of Decressin in the present volume). This mechanical wind is enriched only in H-burning products. This may contribute to explain the origin of the different anomalous populations observed in the field and in the clusters of the halo: the clusters being more metal rich would be enriched by mechanical winds rich in H-burning products, while field halo stars may be enriched by line driven winds rich in both H- and He-burning products.

A prediction of the present scenario is that a very low $^{12}C/^{13}C$ ratio can be obtained in CEMP stars. In the present models both isotopes are produced as primary elements, the ratio is thus not much sensitive to the dilution factor (unless we consider so large dilution factors that it would also erase any strong overabundances in the CNO elements!). Very low ratios are obtained in case the "Source Star" is a massive star having lost its outer envelope (below about 10). Higher ratios are obtained in the envelope of early AGB models (of the order of 100, see Table 2 in Meynet et al. 2009). Thus this ratio may be useful both for providing clues supporting the present "spinstar" scenario and also for disentangling between massive and intermediate mass stars (early AGB) as the possible "Source Stars". In the right panel of Fig. 1, we have plotted the $^{12}C/^{13}C$ ratios observed at the surface of the CEMP-no stars. We see that even with some CEMP stars being dwarf stars (as for instance the filled circle at [Fe/H] equal to -4.015), the CEMP stars are in general below the $^{12}C/^{13}C$ ratio observed in giants (which should have lower $^{12}C/^{13}C$ ratios than dwarf stars since they went through the dredge-up episode). Moreover these CEMP stars are also below the predictions of the chemical evolution model which describes the evolution of the composition of stars made up from the well mixed reservoir. These two points support the view of a different origin of the CEMP star with respect to the normal halo stars based only from the $^{12}C/^{13}C$ ratio, second it shows that very low $^{12}C/^{13}C$ ratios are observed in some dwarf CEMP star supporting, in view of the large ^{12}C overabundances, a primary origin for ^{13}C as predicted by the rotating models.

4. Constraints from Li and He

Let us now come to the question asked in the title, namely how measures of the Li and He abundances in CEMP stars can be used to constrain the above scenario? The material of the "Source Stars" are Li-poor (actually Li is completely destroyed) and He-rich (see Table 2 in Meynet et al. 2009). Thus CEMP stars made of pure "Source Star" material

would be Li-poor and He-rich. Note that the same line of reasoning implies that stars presenting enhancements of Na and depletion of O in globular clusters should also be He-rich. Both in globular clusters and in the field, the actual level of He overabundance depends on the degree of dilution with interstellar medium (see the contribution by Decressin in the present volume and references therein, see also Maeder & Meynet 2006).

Some Li observations exist for CEMP stars. Many of the CEMP-no stars show very low Li or even only upper limits compatible with no Li at all. Of course these very low Li abundances can be due to depletion having occurred in the CEMP star itself and thus may not be the signature of a formation process from Li-depleted material. A high helium abundance in the whole star (and not only at the surface) would be a much stronger constraint pointing towards a small dilution factor. The finding of such a star would indeed be extremely interesting since in that case one would have an object providing a nearly direct insight into the chemical composition of the ejecta of the first stars. Of course the difficulty here resides in how to measure helium abundance in a cool star. Although this is a real challenge, the situation may not be completely desperate. A high helium abundance would imply a different initial mass associated to a given observed position in the HR diagram than the one obtained assuming a normal (here a cosmological helium) abundance (see the contribution by Decressin in the present volume). The discovery of eclipsing binaries whose components would be CEMP stars would be a way to associate observationnally determined masses to given positions in the HR diagram and thus to test the He-rich hypothesis. Asteroseismology would also be an interesting way to address that question. Finally, helium lines may be observable in cool stars, whose strength might be related to the He abundance (Moehler et al. 2000). While these possibilities appear quite exciting and will probably be explored in the future, it is however important to mention that the absence of He-rich stars among the CEMP stars would not be an argument against the present spinstar scenario. High helium abundances imply small dilution factors (a factor of a few), while normal helium abundances imply larger dilution factors (greater than an order of magnitude as in the case shown in the left panel of Fig. 1), but in both cases spinstars are required to explain the high CNO elements! It is also interesting to mention that the observed amounts of Li, Be and B produced by spallation reactions at very low metallicities give also some support to the present "spinstar" scenario (see the review by Prantzos in this volume).

References

Carollo, D., Beers, T. C., Lee, Y. S., et al. 2008, Nature, 451, 216
Chiappini, C., Ekström, S., Meynet, G., et al. 2008, A&A, 479, L9
Chiappini, C., Hirschi, R., Meynet, G., et al. 2006, A&A, 449, L27
Decressin, T., Meynet, G., Charbonnel, C., Prantzos, N., & Ekström, S. 2007, A&A, 464, 1029
Frebel, A., Collet, R., Eriksson, K., Christlieb, N., & Aoki, W. 2008, ApJ, 684, 588
Hirschi, R. 2007, A&A, 461, 571
Korn, A. J., Richard, O., Mashonkina, L., et al. 2009, ApJ, 698, 410
Lucatello, S., Beers, T. C., Christlieb, N., et al. 2006, ApJ, 652, L37
Maeder, A. & Meynet, G. 2001, A&A, 373, 555
Maeder, A. & Meynet, G. 2006, A&A, 448, L37
Masseron, T., Johnson, J. A., Plez, B., et al. 2009, ArXiv e-prints 0901.4737
Meynet, G., Ekström, S., & Maeder, A. 2006, A&A, 447, 623
Meynet, G., Hirschi, R., Ekstrom, S., et al. 2009, ArXiv e-prints 0910.3856
Moehler, S., Sweigart, A. V., Landsman, W. B., & Heber, U. 2000, A&A, 360, 120
Spite, M., Cayrel, R., Hill, V., et al. 2006, A&A, 455, 291
Tominaga, N., Umeda, H., & Nomoto, K. 2007, ApJ, 660, 516

Light elements in the Universe
Proceedings IAU Symposium No. 268, 2010
C. Charbonnel, M. Tosi, F. Primas & C. Chiappini, eds.

DOI: 00.0000/X000000000000000X

The Helium contribution from massive AGBs

Paolo Ventura

INAF - Observatory of Rome, 00040, Monte Porzio Catone (RM), Italy
email: ventura@oa-roma.inaf.it

Abstract. The helium produced by AGB and super-AGB stars is a key quantity to understand whether these objects may have been the main polluters of the interstellar medium within globular clusters, and originate a second generation of stars with a chemistry showing the imprinting of their ejecta. Helium is the most important element for this topic, as any difference in the original helium between the two populations would determine clearly distinguishable features both in the morphology of the Horizontal Branches and in the Main Sequences. We present the helium yields from massive AGB stars, and show that the results are rather robust, being approximately independent of the various uncertainties that affect the description of the evolution of these stars. The implications for the self-enrichment scenario are discussed and commented.

Keywords. Stars: abundances, AGB and post-AGB

1. Introduction

The traditional paradigma that stars in globular clusters (GC) are a classic example of a single stellar population, with the same age and chemistry, has been challenged in the last decades by spectroscopic evidences, showing that star-to-star differences exist in their surface chemistry, involving all the "light elements", i.e. all those species lighter than aluminium (Kraft 1994). The original idea (Denissenkov & Weiss 2001) that these differences were due to some "in-situ" mechanism, associated to non-canonical extra-mixing from the bottom of the convective envelope, was disregarded by the discovery that the same patterns were also present in main sequence stars (Gratton et al. 2001), for which no active advanced nucleosynthesis could be invoked.

This opened the way to studies focused on the understanding of whether these chemical anomalies, that were surely present in the gas from which these stars formed, could be generated by the winds of intermediate-mass stars during their Asymptotic Giant Branch (AGB) phase (Ventura et al. 2001): in fact, the most massive of these objects are known to experience Hot Bottom Burning (HBB), i.e. the base of their external mantle becomes hot enough to ignite an advanced nucleosynthesis, whose products would be almost instantaneously transported to the surface, due to the rapidity of convective motions (Blöcker & Schönberner 1991). The formation of new stellar generations in GC from the gas expelled by rapidly evolving stars belonging to the original population is commonly referred to as the "self-enrichment" scenario.

One predictions of these investigations is that massive AGB stars are helium producers, thus the gas from which the new generations of stars form is expected to be helium-rich (Ventura et al. 2001).

Based on this expectation, the stellar evolution group in Rome suggested in a series of papers that differences in the original helium content was the natural explanation of the so called "second parameter" in the interpretation of the different morphologies of the Horizontal Branches (HB) of GC, the bluest and less luminous clumps being populated by stars helium enhanced (Caloi & D'Antona 2005, Caloi & D'Antona 2007, D'Antona & Caloi 2004, D'Antona & Caloi 2008).

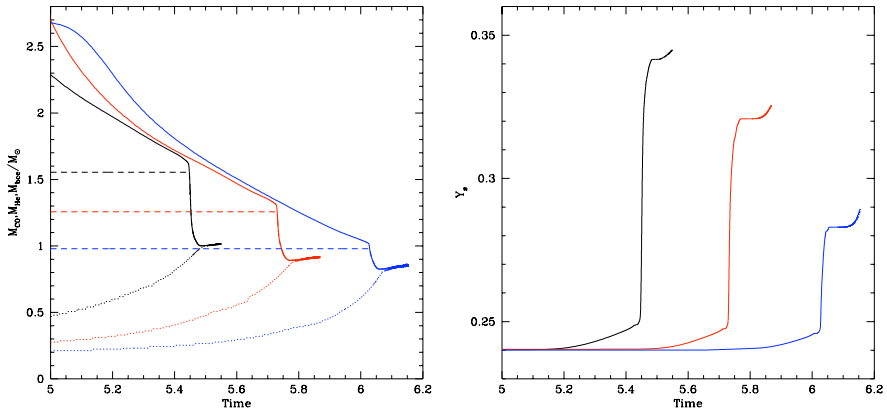

Figure 1. Left: Variation with time (in logarithmic scale, and counted from the helium exhaustion in the core) of the bottom of the convective envelope (solid), the H/He interface (dashed), and the external border of the CO core (dotted) in models with initial masses 4 (right), 5 (middle), and 6$M_{\odot}$ (left). Right: The helium increase following the second dredge-up for the models shown in the right panel.

This idea received a robust confirmation by the most recent photometric analysis, showing the presence of multiple main sequences in many massive GC, that can be understood only by assuming the existence of a stellar population enriched in helium (Piotto et al. 2007).

In this contribution we present the helium yields from massive AGBs, i.e. stars with mass in the range $3 - 6.5 M_{\odot}$, that never reach temperatures sufficiently high to burn carbon in the core. We discuss the major sources of uncertainty, and the physical processes most relevant for this particular issue. We compare these findings with the helium content of the ejecta of super-AGB stars, and find a trend monotonically increasing with the core mass.

We eventually discuss how these results may be used in the interpretation of the extendend blue tails in the HB of many GC and the presence of blue main sequences, in the context of the self-enrichment scenario for the formation and evolution of GC.

2. The enrichment of the surface helium in intermediate-mass stars

In stars of intermediate mass, helium burning is activated in the core in conditions of non-degeneracy; the relic of this phase is a core, made up of carbon and oxygen, evolving to conditions of progressively more enhanced degeneracy, and a helium burning buffer just above it. The ignition of this shell favours the expansion of the outer layers, with the consequent temporary extinction of the CNO burning region. During this phase the external convection sinks inwards, penetrating to layers previously touched by CNO burning, in what is commonly called "the second dredge-up" (SDU).

The left panel of Fig. 1 refers to models with masses 4, 5, and $6 M_{\odot}$; times are counted from the exhaustion of central helium. The chemistry is typical of GC with intermediate metallicity, i.e. Z=0.001, Y=0.24. The evolution of the bottom the convective envelope (solid), the border of the H-rich region (dashed), and the external border of the CO core (dotted) are shown. The H/He interface is initially unchanged with time, because the CNO shell is not active. The base of the external mantle eventually reaches such interface,

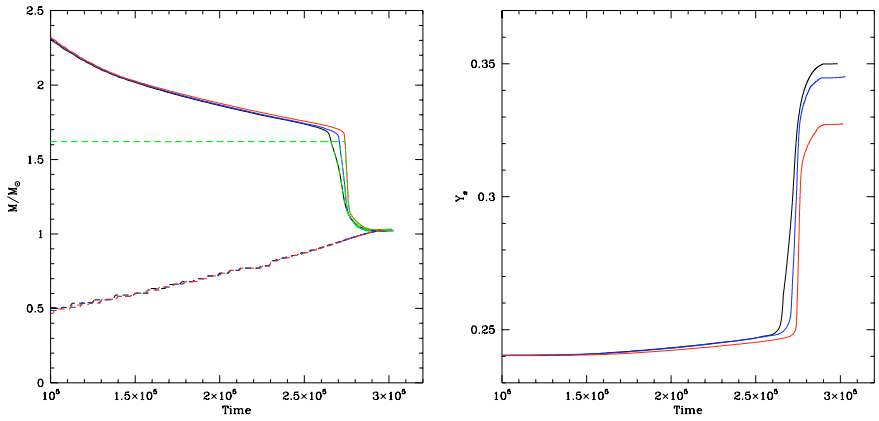

Figure 2. Left: Inwards penetration of the external envelope in a $5M_{\odot}$ models calculated with different extent of the overshooting region, i.e. with a choice of the free parameter $\zeta = 0.01$ (right), 0.02 (middle), 0.05 (right). Right: The increase in the surface helium in the same models presented in the left panel.

and penetrates inwards, down to the He-burning shell. This episode is accompanied by a sudden increase in the surface helium content (see the right panel of Fig. 1), which is higher in the $6M_{\odot}$ model, due to the largest width of the He-rich buffer.

We will see that the increase in the surface helium achieved during this phase will be crucial to determine the overall helium content of the ejecta of these stars. We therefore discuss how these results may depend on the way with which the convective/radiative interface is treated.

Modelling the AGB phase demands a diffusive approach, in which nuclear burning and mixing of chemical are coupled self-consistently (Cloutman & Eoll 1976). The reason for this is that a non-negligible percentage of the overall nuclear energy is generated within the convective envelope, due to a partial overlapping of the external mantle with the CNO burning shell (Mazzitelli et al. 1999). Within the diffusive context, overshooting from any convective border, fixed via the Schwartzschild criterion, is modelled by an exponential decay of convective velocities within the stable region, with an e-folding distance that is commonly parametrized as ζH_p: ζ is therefore the free parameter entering the description, and providing the extent of the extra-mixing region.

The ζ adopted in this investigation is $\zeta = 0.02$, in agreement with a calibration based on the observed main sequences of open clusters, given in Ventura et al. (1998). To study the sensitivity of the helium enhancement on the details of the overshooting description, we calculated three models with initial mass $5M_{\odot}$ with $\zeta = 0.01, 0.02$ and 0.05. The results of these simulations are shown in Fig. 2. We see in the left panel, showing the same quantities reported in the left panel of Fig. 1, that a greater extent of the extra-mixed region favours a faster inwards penetration of the convective envelope, though the innermost point reached, corresponding to the location of the He-burning shell, is approximately unchanged. The final surface helium reached at the end of this phase is thus only mildly dependent on ζ, showing an increase of $\delta Y \sim 0.01$ for ζ exceeding by more than 100% the value expected on the basis of empirical calibrations.

The surface helium reached after the second dredge-up by intermediate-mass stars will be the starting point for the following phase, during which these stars experience a series

of thermal pulses, provoked by the periodic ignition of a helium-rich buffer in conditions of thermal instability. Fig. 3 shows the evolution of the surface helium during the whole AGB phase, calculated up to the almost complete consumption of the whole external mantle. We show the mass as abscissa, to have a better feeling of the yields expected. We see in Fig. 3 that there is little space for further changes in the surface helium, that remains almost unchanged with respect to the mass fraction reached during the second dredge-up.

We conclude that the helium yield is one of the most robust results concerning the evolution of massive AGBs. Compared to the yields of other species, e.g. the CNO elements, that were shown to depend critically on the assumptions concerning the treatments of convection and mass loss (Ventura & D'Antona 2005), the helium content of the ejecta is only modestly touched by these indeterminations, the final Y depending only on the abundance achieved during the second dregde-up. The conclusion from previous investigations, that suggest a maximum helium yield of $Y \sim 0.35$ expected from these stars (see, e.g., Ventura & D'Antona 2008), is thus highly reliable.

3. The self-enrichment scenario

We showed that massive AGBs are expected to be efficient helium producers, providing ejecta with an average helium content up to $Y \sim 0.35$. These results confirm the speculation by Pumo et al. (2008), that the helium yields of the most massive AGBs are extremely close to the corresponding yields from the less massive super-AGBs, i.e. those stars that undergo an off-centre, degenerate, carbon ignition (Siess 2006). This fixes an increasing trend of Y with mass (or, more precisely, with core mass), the largest helium predicted being $Y \sim 0.40$ (see Fig.1 in Pumo et al. 2008).

We note that this is the helium invoked by D'Antona & Caloi (2004) to explain the presence of a detached clump of low-luminosity, blue stars, populating the HB of NGC 2808, and it is also the same quantity required to interpret the bluest main sequence observed in the same cluster (Piotto et al. 2007).

These results open the way to new tests of the self-enrichment scenario framework. It will be possible to explain any peculiar morphology of the HBs of GC or any intrinsic width of the observed main sequences as the overlapping of an original stellar component, with the helium coming from the Big Bang, and an additional generation, born from gas that was contaminated by the winds of AGB and super-AGB stars. The degree of dilution of this gas with a pristine component is the relevant quantity to determine the helium content of the second generation, hence the features expected on the HB and the spread of the MS. The total mass and the degree of concentration of the cluster is expected to determine the extent of such a dilution process (D'Ercole et al. 2008).

4. Conclusions

We presented a detailed investigation of the helium yields expected from intermediate-mass stars during their evolutionary history. We find that it is mainly during the second dredge-up that most of the helium enrichment is produced, with little increase in the following phase during which the stars experience a series of thermal pulses.

The helium yields show up to be scarcely sensitive to the uncertainties associated to convective overshooting, since the innermost point reached by the penetration of the convective envelope during the second dredge-up, i.e. the location of the helium-burning-shell, is almost independent of the overshooting assumed. Even the impact of mass loss is negligible, because most of the mass is lost after the major phase of helium enhancement.

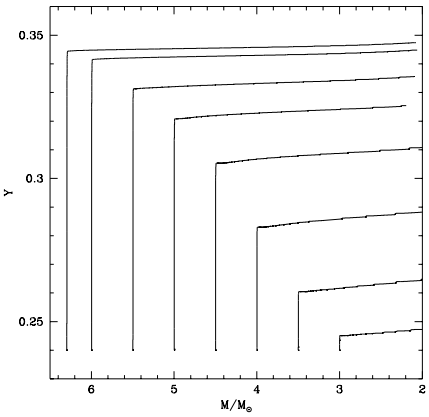

Figure 3. Evolution of the surface helium content within intermediate-mass models. Mass was chosen as abscissa, to have an idea of the chemical content of the ejecta. We note a sudden increase in the surface helium, associated to the second dredge-up, and little change in the following phase of thermal pulses

These results indicate that helium is produced during the evolution of stars of intermediate mass, the highest abundances, $Y \sim 0.35$, being reached by the highest masses not achieving carbon-burning, i.e. $\sim 6M_{\odot}$, this limit depending on the overshooting from the core during the H-burning phase. A higher helium enhancement is found in slightly higher mass models, the super-AGB stars, that undergo carbon ignition in a degenerate layer out of the centre.

The combination of AGB + super-AGB models produce yields with a helium content gradually increasing with mass, with a maximum of $Y \sim 0.4$. This is the value that was invoked to interpret the existence of extended blue tails in the HBs of some GC, and, more recently, the presence of a blue main sequence in NGC 2808, that is supposed to be populated by stars with a high helium content.

This result indirectly supports the self-enrichment scenario hypothesis, i.e. that in GC we observe the overlapping of more that an individual generation of stars, because new stars were born from the ashes left by the evolution of stars of intermediate mass.

References

Blöcker, T. & Schönberner, D. 1991, *A&A* (Letters), 244, 43
Caloi, V., & D'Antona, F. 2005, *A&A*, 435, 987
Caloi, V., & D'Antona, F. 2007, *A&A*, 463, 949
Cloutman, L., & Eoll, J.G. 1976, *ApJ*, 206, 548
D'Antona, F., & Caloi, V. 2004, *ApJ*, 611, 871
D'Antona, F., & Caloi, V. 2008, *MNRAS*, 390, 693
Denissenkov, P., & Weiss, A. 2001, *ApJ* (Letters), 559, 115
D'Ercole, A., Vesperini, E., D'Antona, F., McMillan, S.L.W., & Recchi, S. 2008, *MNRAS*, 391, 825
Gratton, R., Bonifacio, P., Bragaglia, A., Carretta, E., Castellani, V., et al. 2001, *A&A*, 369, 87
Kraft, R.P. 1994, *PASP*, 106, 553
Mazzitelli, I., D'Antona, F., & Ventura, P. 1999, *A&A*, 348, 846
Piotto, G., Bedin, L.R., Anderson, J.,King, I.R., Cassisi, S., et al. 2007, *ApJ* (Letters), 661, 53
Pumo, M.L.P., D'Antona, F., & Ventura, P. 2008, *ApJ* (Letters), 672, 25

Siess, L. 2006, *A&A*, 448, 717
Ventura, P., D'Antona, F., Mazzitelli, I., & Gratton, R. 2001, *ApJ* (Letters), 550, 65
Ventura, P., & D'Antona, F. 2005, *A&A*, 279, 288
Ventura, P., & D'Antona, F. 2008, *A&A*, 479, 805
Ventura, P., Zeppieri, A., Mazzitelli, I., & D'Antona, F. 1998, *A&A*, 334, 953

Light elements in the Universe
Proceedings IAU Symposium No. 268, 2010
C. Charbonnel, M. Tosi, F. Primas & C. Chiappini, eds.

DOI: 00.0000/X000000000000000X

Discussion A: On the abundance of deuterium in the local interstellar medium and in high-redshift systems

Monica Tosi

INAF - Osservatorio Astronomico di Bologna
Via Ranzani 1, I-40127, Bologna, Italy
email: monica.tosi@oabo.inaf.it

Abstract. The first discussion session held at the IAU Symposium 268 focussed on the deuterium content in the local interstellar medium (LISM) and in high-redshift systems. There were two key questions proposed to the audience: 1) what should be taken as representative abundance of D in the LISM, and 2) how can we explain the dispersion of the D abundance measured in high-redshift, very low metallicity environments ? While on the latter point people seem to agree that observational and data analyses uncertainties are the most likely explanation, on the former question no consensus was reached. The historical and observational background at the basis of these questions and the discussion are schematically reported here.

Keywords. ISM: abundances; Galaxy: evolution; cosmology: observations; quasars: absorption lines

1. Introduction

Four discussion sessions were held at the IAU Symposium 268 on the most debated issues related to the light elements. The first of these special sessions was devoted to our current understanding of the deuterium abundance in the local interstellar medium (LISM) and in high-redshift systems. Two key questions were selected by the SOC as the current hottest topics on deuterium and opened to discussion: 1) what should be taken as representative abundance of D in the LISM, and 2) how can we explain the dispersion of the D abundance measured in high-redshift, very low metallicity environments. In the recent literature there have been quite interesting debates on both instances and the lively discussion which took place at the meeting reflected the deep involvement of the community.

The very circumstance that these questions need to be asked is the positive result of the efforts and achievements of scientists exploiting modern, high-performance instruments, such as ground-based high-resolution spectrographs at 10 m class telescopes and those on the HST and FUSE satellites. On the high-redshift side, the data currently available on D have been summarized in the recent papers by O'Meara et al. (2006) and Pettini et al. (2008). On the Galactic side, Geiss, Hébrard, Linsky and Sembach have comprehensively described here (this volume) the available measurements. From their presentations, it is apparent that the increasing number of accurate measures has led to a much larger coverage of different environments. As summarized by Savage et al. (2007), we now have D measured in the solar system, in the LISM, in a couple of fields in the Galactic disk and halo, in a high-velocity cloud (Complex C) and in several Damped Lyman-α systems (DLAs). Yet, we have reached neither a clear understanding of the deuterium distribution in different environments, nor a consensus on its most representative values.

Ten years ago the situation looked much simpler and stable. At the IAU Symposium

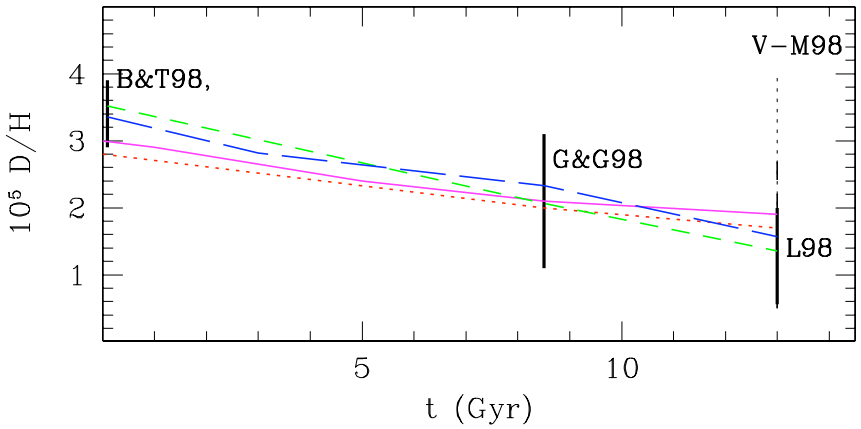

Figure 1. What we knew of the deuterium abundances by number ten years ago (see Tosi 2000). The coloured curves show the abundance variation with time as predicted by chemical evolution models for the solar neighbourhood. These curves refer to models by different groups, all able to reproduce the majority of the Galaxy observational constraints (see for references Tosi 2000). The vertical bars show at 2σ the abundances estimated by Burles & Tytler (1998) for high redshift absorbers, by Geiss & Gloeckler (1998) for the pre-solar cloud and by Linsky (1998) (solid bar) and Vidal-Madjar et al. (1998) (dashed and dotted bars) for the LISM.

198 on the Light Elements, held in Natal (Brasil) in 1999, the main players in the D measurement game showed D/H values with rather small dispersions, almost undistinguishable from those presented two years earlier at the meeting on the same topic organized by the International Space Science Institute (ISSI) in Bern (Switzerland). These values are schematically plotted in Fig.1 (showed at the IAU Symp.198) and display a steady and moderate decrease from the close-to-primordial D/H of high-z absorbers (Burles & Tytler 1998), to the proto-solar cloud (PSC) value inferred from solar-system data (Geiss & Gloeckler 1998), to the abundance (Linsky 1998) in the Local Interstellar Cloud (LIC). Assuming the high-z values as typical of proto-galactic clouds 13 Gyr ago, the PSC value as typical of the LISM at the time of the Sun formation 4.5 Gyr ago, and the LIC value as typical of the LISM at the present epoch, the plotted trend traces the evolution of D in the solar neighbourhood during the Galaxy lifetime.

Ten years ago, Tytler and collaborators had just demonstrated that the cases of high-z absorbers where D/H ratios almost an order of magnitude higher had been claimed to exist (e.g. Songaila et al. 1994) were actually misinterpretations of interloopers or of the continuum level in the observed spectra. Chemical evolution models able to reproduce the vast majority of the Galaxy observed properties were nicely consistent with these D/H data (coloured lines in Fig.1), including the value 9 times lower than the local ones measured by Lubowich et al. (2000) in the Galactic center, $(D/H)_{GC} = 1.7\pm 0.3$ ppm. People felt reassured and satisfied.

There were actually voices of warning (Vidal-Madjar et al. 1998), arguing that D/H in the LISM appeared to vary significantly from one line-of-sight (LOS) to the other, but the establishment tended to disclaim those arguments, although admitting that the constant values were actually confined within the quite small region (100 pc radius) of the Local Bubble (LB). The dashed and dotted vertical bars in Fig.1 show respectively the likely range of LISM values and the less likely one including the maximum, possibly wrong, D/H=4 ppm ever estimated (see Vidal-Madjar et al. 1998 for references).

2. What do we currently know of the local D abundance ?

In ancient Greece mythology Cassandra's profecies were never believed either by the Trojans or by the Achaeans, but she was always right. So were the skeptics about the homogeneity of LISM deuterium. If we look at the distribution of D/H with column density N(HI) (which can be considered a proxy for distance), as resulting now from years of analyses of both old and new data (see Fig.2, taken from Linsky et al. 2006), it is apparent that D/H varies significantly. Only the data within the LB are tight to the D/H value which was attributed to the LISM ten years ago. Regions with log N(HI) $\geqslant$ 20.7 seem to have much lower D/H (lower D or higher H ?) and regions with intermediate column densities show an impressive spread, which is now convincingly explained in terms of spatially varying D depletion onto dust grains (Jura 1982, Draine 2004, Linsky et al. 2006). So, what value, if any, could actually be taken as the current "average" LISM deuterium ? Is it the upper undepleted value 23±2.4 ppm of the intermediate region, or a lower value (say 20±1 ppm) allowing for observational errors, or the very low value 9.8±1.9 ppm of the highest column density regions ? Different authors (Linsky et al 2006, Prodanovich et al. 2009, Hébrard et al. 2005, respectively) have suggested each of these possibilities and the question is still open.

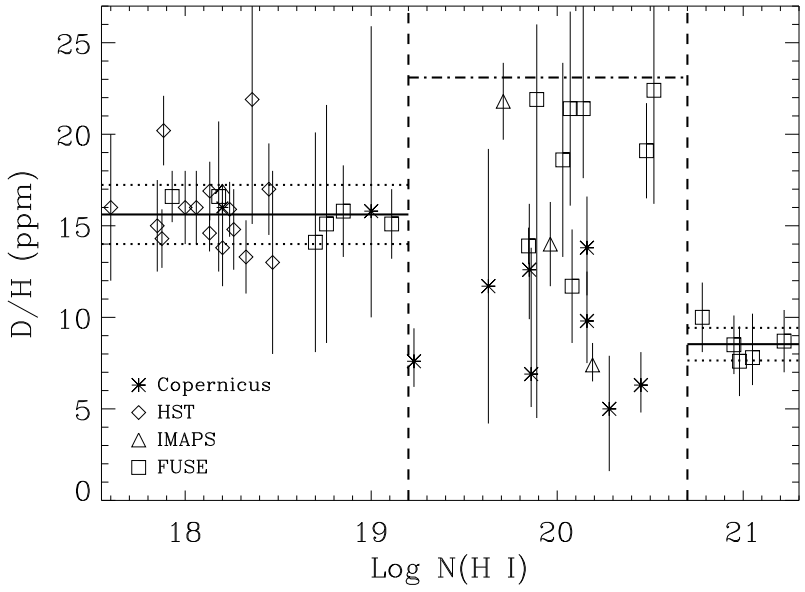

Figure 2. From Linsky et al. (2006): deuterium abundance vs hydrogen column density measured along several LOS in the LISM.

Each of these possibilities also has side effects on our understanding of the chemical evolution of the Galaxy. If the LISM D/H is as high as 23±2.4 ppm, at face value it is higher than in the PSC (21±5 ppm, Geiss & Gloeckler 1998) and implies either a way to enhance D in the last 4.5 Gyr (quite unlikely) or the need to consider the Sun not representative of the local medium at the time of its formation (a fairly recurrent theme, never settled with satisfactory arguments). Moreover, if the primordial D/H is

$(D/H)_P$=26.1±3 ppm as implied by the first modelling of the WMAP data (Spergel et al. 2003) the total deuterium astration factor from the Big Bang to a present LISM D/H=23 ppm would be 1.13, quite low even for chemical evolution models allowing for the continuous accretion of large amounts of primordial extragalactic gas, but still consistent with the Galaxy properties (Steigman et al. 2007). Once we consider that the infalling gas is probably not primordial and more likely with a D content similar to that of high velocity clouds (Sembach et al. 2004 estimated a D/H=22±7 ppm in Complex C), it becomes clear that no viable model can account for such values. If $(D/H)_P$=28.2 as recently suggested by Pettini et al. (2008), the astration factor to D/H=23 ppm would be 1.22, still challenging, but not impossible to achieve. Models consistent with the various Galactic constraints predict astration factors larger than 1.3 (e.g. Romano et al. 2006, Steigman et al. 2007) and can reproduce a LISM D/H of 19–20 ppm or lower with standard assumptions on metal poor infall. Most likely one should consider spatial variations of depleting dust grains and of the accreted metal-poor gas to account for the empirical inhomogeneity of the D abundances.

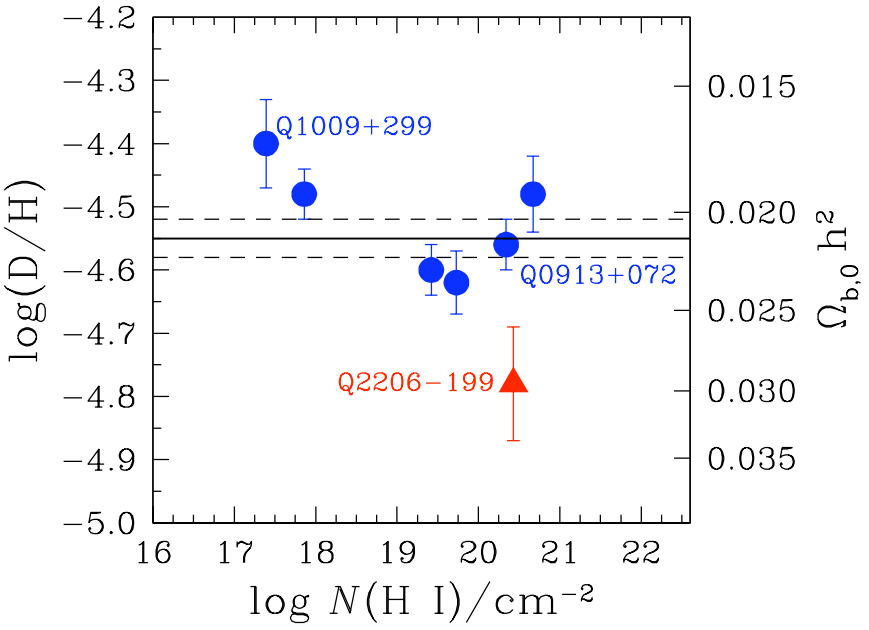

Figure 3. From Pettini et al. (2008): The deuterium abundance measured in high-redshift DLAs. The horizontal lines show their mean value (solid) ±1σ (dashed). On this scale the primordial D inferred from WMAP is -4.59.

3. What do we currently understand of high-redshift deuterium ?

Outside our Galaxy deuterium is measured in the absorption lines of gas systems falling on the LOS of QSOs with redshift lower than 4. Fig.3 (taken from Pettini et al. 2008) illustrates these data and the corresponding mean deuterium value, 28.2 ppm. All measurements are consistent at 1σ with this mean, except two values, which happen

however to be the most uncertain ones, one because of the lower S/N of its spectra (the red triangle in Fig.3) and the other because D is detected only in the Ly-α line.

Should this mean value of 28.2 ppm be taken as the best estimate of the primordial D/H ? At face value, it is slightly larger than – although consistent with – the values $(D/H)_P$=26.1±3 ppm, or $(D/H)_P$=25.7±1.5 ppm estimated from WMAP after the first year and the third year data release (Spergel et al. 2003 and Spergel et al. 2007, respectively). If real, this difference would be unexplainable, because DLAs have very low but non zero metals. Since metals are produced by stars, and stars always destroy D, DLAs are supposed to have D somewhat lower than primordial. If the DLA measurements can be considered sufficiently robust, Pettini's heuristical and backward approach of using the observed high-z D/H as a prior in the analysis of WMAP data appears very reasonable. Can we follow his arguments and conclude that $(D/H)_P$ is more likely 28.2 ppm ?

If we consider both the deuterium and oxygen abundances of these systems, we find that DLAs with higher O may also have higher D, contrary to basic nucleosynthesis principles. Is this also due to observational issues or should we worry ? And, more generally, are the apparent differences in D/H from one absorption system to the other real ? If so, what is the physical meaning of the high-z values different from the average value ?

4. Discussion

First of all, during the discussion session the participants, sollicited by Ken Sembach and me, agreed that one cannot assume the LISM D value as representative of the value for the Galaxy as a whole, or even for the local spiral arm. It is not clear whether we can actually identify a mean LISM value, but it is evident that such value could not be representative of other Galactic regions with different conditions and evolution.

The quest for the actual D abundances here and now (LISM), and there and then (high-z absorbers) was then debated at length.

Jeff Linsky noticed that in many papers authors implicitly assume that a measurement of D/H in the gas phase is a measure of the total D/H ratio, and urged authors to make a clear distinction between the gas phase D/H and the total D/H that include D in dust grains. Following up on this point, Donatella Romano asked if, on the other hand, there could be undetected molecular hydrogen along some FUSE LOS. If so, could the contribution from this unaccounted H_2 help to bring the highest observed values of D/H in the local ISM in agreement with the predictions on D evolution from standard chemical evolution models ? Linsky answered that all H_2 was included in the estimate of log N(H) and that, in any case, it provides only a negligible fraction of the total H column density.

Gary Steigman described in some detail his and Tijana Prodanovic' attempts on using both D and Fe to try to find the "true" (i.e., gas plus dust) ISM D abundance. Based on $\log(y_D)$ vs. $\log(y_{Fe})$ plots [where $y_D = 10^5$(D/H) and $y_{Fe} = 10^6$(Fe/H)], he argued that the LB D abundance shows no evidence for any variation, in contrast to the LB Fe abundance, suggesting that D may not be depleted in there (i.e., no correlation between D and Fe). Most of the non-LB LOS have lower Fe abundances than in the LB, and for most of them there is an apparent correlation between D and Fe. However, there are 6 remaining non-LB LOS which have D abundances in excess of the LB value, and he suggested that these high D and (mostly) low Fe abundances might have resulted from incompletely mixed infall, so that the "true" ISM D abundance might be the LB value $y_{D,LB} = 1.5$, corresponding to a D astration factor of 1.8. An alternative interpretation of the data is that the "true" ISM D abundance is the value ($y_{D,ISM} = 2.0$) found by Prodanovic et al. (2009) from Bayesian analysis. The potential problem with this choice is that the LB D abundance is uniform but depleted compared to the ISM value by a

factor of 2.0/1.5=1.3. In response to this speculation that the high D abundances might be due to infall, Guillaume Hébrard remarked however that the oxygen abundance along these LOS is "normal", and not low as would be expected for metal-poor gas.

Sembach asked what future observations of D or other species might help resolve the issue of deuterium depletion onto dust, but no encouraging answer was provided by the audience, either in terms of currently usable instrumentation or of tracing D through other elements. He himself did not see many future prospects for FUV DI absorption measures for gas within the Milky Way for two reasons. First, there is no obvious follow-on to FUSE in NASA's strategic plan (HST/COS could make some breakthroughs in the low-reshift IGM arena, however, with very interesting output). Second, within the Milky Way these types of measurements are confusion limited. Thus, it may be that nature simply doesn't provide a simple enough velocity structure along the vast majority of extended sight lines to be able to infer D/H or D/O much beyond a kiloparsec from the Sun. Higher resolution (R$\geqslant$50,000) observations might help in understanding this limitation better and may help push the distance envelope a factor of two or three.

Tom Bania replied reporting on the first solid detection of the D hyperfine transition at 327 MHz in the Milky Way ISM (Rogers et al. 2005, Rogers et al. 2007). Unfortunately, the array is now dismissed and there are no plans to either repeat or extend these measurements. In contrast to all other D/H abundance determinations these measurements are not made toward specific targets but rather probe specific Galactic directions. The three fields are all in the Galactic anticenter direction and latitude 0 deg. The average D/H abundance derived for these three fields is <D/H> = 21$\pm$7 ppm, where the error is $\pm 3\sigma$ and contains an estimate for the uncertainty in the HI excitation temperature. In one direction, D/H = 24 ppm is found at a SNR of 8.2 with a total integration time of 17.5 years. No one is going to supersede these 92 cm measurements any time soon. Bania and coworkers estimate that D is distributed over $\sim$5 kpc in these Galactic anticenter directions, with no significant difference between the three. This makes this path length as long as any of the measured optical paths for D LOS in the Milky Way. For this $\sim$5 kpc path the HI column density is $3 \times 10^{21}\mathrm{cm}^{-2}$. Sembach commented that, while the FUSE results apply over a very limited range of distances, the measures of the DI 92 cm emission might have more applicability in defining an "average" Galactic value, since those types of measurements can potentially sample large volumes of the Galaxy.

With reference to the two questions raised before, (1) how much molecular hydrogen is likely to be found in these LOS, and (2) is this a gas phase measurement only, Bania argued that each of these LOS probes DI emission from an enormous volume of the ISM, unlike the pencil beams absorbing the continuum radiation from a background target object. At a distance of 5 kpc the beam extends to $\pm$610 pc from the Galactic plane. This is $\sim$15 times the 40 pc scale-height of the molecular gas disk of the Milky Way. Thus most of the volume probed by the DI measurements should be devoid of molecular gas. There should be, on average, very little molecular hydrogen contamination on the corresponding D/H abundance derivation. The possibility that significant amounts of D has frozen out onto grains cannot be discounted, but Bania believes that their LOS may actually be the cleanest available in this regard, because most of their probed lies far above the dense, cold material in the Galactic plane. Most of their observed volume contains warm neutral medium (WNM) gas at temperatures between 1,000 and 4,000 K. Grains mixed into this environment are unlikely to be cold enough to freeze out D. Hence, the fraction of observed volume wherein D can freeze out onto grains is too small to significanly skew their D/H abundance determination.

Given the uncertainties in accurately deriving D/H, Guillaume Hébrard argued that a comparison of D with O may be more reliable. He pointed out that the D/O ratio appears

much more homogeneous than D/H. He thus suggested that the distant low D/O and D/H ratios are more likely representative of the local current values, whereas the high D/H for which no high D/O are measured could be due to systematics. Linsky agreed that it is important to estimate D/H by different techniques, but believes that estimating D/H through another element like oxygen (D/H = D/O×O/H) introduces a whole new set of poorly understood problems in addition to the problems in understanding D/H. One needs to know the ionization equilibrium, depletion, and perhaps also the distribution of the element along the LOS which will be different than for D and H. Also, chemical evolution, depletion, and mixing could be different for this element than for H and D.

Chris Howk mentioned that for Galactic measurements, there is almost certainly some bias due to the manner in which sight lines were chosen for analysis from the FUSE database. Given the work required for each individual sight line, there is a tendency to choose sight lines with visible deuterium absorption. This means the DI is separated from the HI absorption, but it potentially also biases the results against low D sight lines. How large a bias this represents is unknown. Sembach confirmed that the sight lines sampled by FUSE for both D/H and D/O measurements have strong selection effects. These are kinematically simple sight lines that probe the warm diffuse ISM in which there is little molecular hydrogen. Dust grains in these types of regions show no evidence of icy mantles. These types of regions tend to have mantles that are highly processed by shocks. These regions are not representative of the types of regions where grains mantles are built. Rather, they are regions grains inhabit after they leave darker cloud environments. He wondered if anyone has done (or will do) a systematic assessment of the FUSE archive to determine if there are any sight lines for which DI absorption could have been detected but wasn't. In other words, are there any "D-free" sight lines that might be telling us something interesting ? Nobody seemed able to answer this question.

Sembach also pointed out that a correlation between the inferred depletion of deuterium and heavier elements such as Fe and Ti is not surprising, but one should be puzzled by how little variation there is about the trend. Given that Fe or Ti are depleted by factors of 100-1000, compared to at most a factor of 2 for D, even a small change in the mantle properties should produce a large change in the gas-phase abundance of Fe or Ti. In other words, one could double the gas-phase abundance of Ti or Fe easily by releasing only 1 part in 100 or 1000 of the Fe or Ti back into the gas, whereas a doubling of the D abundance would require essentially all of the D to be released back into the gas phase. The observed data seem at odds with there being a simple distribution of D and the heavier elements within dust grains if this is indeed the explanation for the variations in the D/H ratio. These arguments made him skeptical, as they suggest there could still be considerable unknown (systematic) uncertainties associated with the values of the HI column densities along some of these sight lines.

Finally, Sembach recalled that, although difficult to test observationally, some of the LOS to LOS variation in D/H could be due to local sources of the type discussed during the conference. These sources are insufficient to produce cosmological quantities of D, but he saw no particular reason they couldn't add to the variation in deuterium abundances seen in different directions. The importance of such sources remains indeed to be determined.

To summarize, it is apparent that there is no consensus on which is the actual deuterium abundance of the LISM, or even on whether a representative value can exist. Clearly further studies are necessary to better understand this issue, but adequate instruments are currently missing. As pointed out by Linsky, we need a new spectrograph for the 912-1200 A spectral range, with higher sensitivity and spectral resolution than FUSE. This would allow a deeper insight on the local abundance distribution as well as

D/H measurements beyond 1 kpc providing information on the dependence of D/H with radial position in the disk and halo of the Galaxy and in neighboring galaxies like the Magellenic Clouds. Radio arrays able to measure the ground-state spin-flip transition of D at 327 MHz (92 cm) in several Galactic longitudes, to add to those described by Rogers et al. (2007) could be useful too.

Concerning high-z absorbers, Joanna Dunkley argued that, when comparing results for the deuterium abundance from WMAP and the Pettini et al. (2008) measurements, it is worth noting that there is a less than 2σ difference between the two. Since they are statistically consistent, at this stage it may not be worth investing much time in choosing one or the other. However, to try to compare the two measurements, one should consider how robust the WMAP result is. WMAP has very low systematics, leading to a precise measurement of the angular power spectrum. Inferring the baryon density from the power spectrum also relies on linear physics that we understand. We can numerically compute the expected spectrum for a given cosmological model to high precision, so the estimated density should not include additional uncertainties. There is a small dependence of the estimated baryon density on the cosmological model assumed; for example, the estimate moves by about 1σ if we extend the standard ΛCDM cosmological model to marginalize over a running spectral index, or a varying equation of state of dark energy (Komatsu et al. 2009). However, there is currently no evidence that these extended models are favored over ΛCDM. The final step, i.e. inferring the D abundance from the baryon density, assumes the standard Big Bang model. While this is consistent with the CMB observations, there could be extensions to this model to be invoked to explain the apparent discrepancy in the lithium abundance (discussed in Jedamzik's talk, this volume), that could modify this inference.

Finally, Paolo Molaro remarked that after almost two decades of 10m telescope efforts we remain with only 8 measurements. Moreover, these measurements show a dispersion which exceeds the reported errors, thus suggesting either the presence of a scatter in the D/H or an underestimate of the errors. He recalled two aspects to consider. First, the measurements are obtained towards absorbers with neutral hydrogen column densities differing by more than two orders of magnitude, which normally are referred to different classes of objects. Given that the major source of error is the estimate of the hydrogen column density, he would regard the determination obtained towards damped wings of the hydrogen lines in the DLAs somewhat more reliable than in the other systems. A second aspect is that these systems show low metallicities but within a quite large range $-3 \leqslant [\mathrm{Si/H}] \leqslant -1$. At these metallicities he believes that no significant astration can have occurred and there is no hint of correlation between D/H and metallicities. However, considering that the measurements in the Galaxy show a correlation with the Fe abundances, suggesting a depletion of D into dust grains, it would be important to check if any correlation exists between the D/H abundance and the gas depletion factor. Unfortunately, a robust estimate of depletion can be obtained only from Zn abundances, which are not available for the observed systems: certainly a check to be done in more detail in future observations.

Acknowledgements The Swiss National Science Foundation and IAU are gratefully acknowledged for financial support. Partial support comes also from the Italian PRIN-MIUR-2007. I'm grateful to Max Pettini for useful and updated information, and to Tom Bania, Joanna Dunkley, Guillaume Hébrard, Chris Howk, Jeff Linsky, Paolo Molaro, Donatella Romano, Ken Sembach, and Gary Steigman for their active participation to the discussion and for their contribution to this report. Fruitful and pleasant meetings and discussions on this topic held at ISSI in Bern are also acknowledged.

References

Burles, S., & Tytler, D. 1998, *in Primordial Nuclei and their Galactic evolution*, N.Prantzos, M.Tosi, R. von Steiger eds, *Space Science Reviews* 84, 65

Draine, B.T. 2004, *in Origin and evolution of the elements*, A. McWilliams, M. Rauch eds, CUP, p.317

Geiss, J., & Gloeckler, G. 1998, *in Primordial Nuclei and their Galactic evolution*, N.Prantzos, M.Tosi, R. von Steiger eds, *Space Science Reviews* 84, 239

Hébrard, G., Tripp, T.M., Chayer, P., Friedman, S.D., Dupuis, J., Sonnetrucker, P., Williger, G.M., & Moos, H.W. 2005, *ApJ*, 65, 1136

Jura, M. 1982, *in Advances in UV astronomy*, Y. Kondo, J. Mead, R.D. Chapman eds, NASA, p.54

Komatsu, E., Dunkley, J., et al. 2009, *ApJS*, 180, 330

Linsky, J.L. 1998, *in Primordial Nuclei and their Galactic evolution*, N.Prantzos, M.Tosi, R. von Steiger eds, *Space Science Reviews* 84, 285

Linsky, J.L., Draine, B.T., Moos, H.W., Jenkins, E.B. et al. 2006, *ApJ* 647, 1106

Lubowich, D. A., Pasachoff, J. M., Balonek, T. J., Millar, T. J., Tremonti, C., Roberts, H., & Galloway, R. P. 2000, *Nature*, 405, 1025

O'Meara, J.M., Burles, S., Prochaska, J.X., Prochter, G.E., Bernstein, R.A., & Burgess, K.M. 2006 *ApJ*, 649, L61

Pettini, M., Zych, B.J., Murphy, M.T., Lewis, A., & Steidel, C.C. 2008, *MNRAS*, 391, 1499

Prodanovic, T., Steigman, G., & Fields, B.D. 2009, arXiv:0910.4961

Rogers, A. E. E., Dudevoir, K. A., Carter, J. C., Fanous, B. J., Kratzenberg, E., & Bania, T. M. 2005, *ApJ*, 630, L41

Rogers, A. E. E., Dudevoir, K. A., & Bania, T. M. 2007, *AJ*, 133, 1625

Romano, D., Tosi, M., Chiappini, C., Matteucci, F. 2006, *MNRAS*, 369, 295

Savage, B.D., Lehner, N., Fox, A., Wakker, B., & Sembach, K. 2007, *ApJ*, 659, 1222

Sembach, K. et al. 2004, *ApJS*, 150, 387

Songaila, A., Cowie, L.L., Hogan, C.J., & Rugers, M. 1994, *Nature*, 368, 599

Spergel, D.N. et al. 2003, *ApJS*, 148, 175

Spergel, D.N. et al. 2007,*ApJS*, 170, 377

Steigman, G., Romano, D., & Tosi, M. 2007, *MNRAS*, 378, 576

Tosi, M. 2000, *in The light elements and their evolution*, IAU Symp.198, *ASP Conf.Ser.*, L.DaSilva, M.Spite, J.R. do Medeiros eds, p. 525

Vidal-Madjar, A., Ferlet, R., & Lemoine, M. 1998, *in Primordial Nuclei and their Galactic evolution*, N.Prantzos, M.Tosi, R. von Steiger eds, *Space Science Reviews* 84, 297

Monica Tosi & Angela Bragaglia

Georges Meynet & Urs Frischknecht

Light elements in the Universe
Proceedings IAU Symposium No. 268, 2010
C. Charbonnel, M. Tosi, F. Primas & C. Chiappini, eds.

DOI: 00.0000/X000000000000000X

What is ^{4}He from H II regions? What needs to be done to better understand the systematic errors?

Gary J. Ferland[1], Yuri Izotov[2], Antonio Peimbert[3], Manuel Peimbert[3], Ryan L. Porter[4], Evan Skillman[5] and Gary Steigman[6]

[1]Physics, University of Kentucky, Lexington KY 40506, USA,
email: gary@pa.uky.edu

[2]Main Astronomical Observatory, 27 Acad. Zabolotnoho St, UA Kyiv 03680 Ukraine
email: izotov@mao.kiev.ua

[3]Instituto de Astronomia, UNAM Apartado Postal 70-264 Mexico 04510, D.F., Mexico,
email: antonio@astroscu.unam.mx peimbert@astroscu.unam.mx

[4]Astronomy, University of Michigan, Ann Arbor, MI USA
email: ryanlporter@gmail.com

[5]Dept. of Astronomy, U of Minnesota, 116 Church St. SE, Minneapolis, MN 55455
email: skillman@astro.umn.edu

[6]Depts. of Physics and Astronomy, The Ohio State University, Columbus, OH 43210. USA
email: steigman.1@osu.edu

Abstract. Here we summarize the discussion that took place after the presentation of papers discussing measurement of abundances from emission lines in H II regions. A cosmological test using ^{4}He is harder than those using the other light elements due to the small dynamic range over which He/H varies for cosmologically interesting parameters. A precision of much better than 1% is needed. This precision challenges both observations and theory. Several of the major uncertainties were identified and methods of improving the accuracy were described.

Keywords. ISM: abundances, HII regions, Galaxy: abundances

1. Introduction

Ferland began the discussion with Don Osterbrock's reminder of how hard this problem is. Don's 1961 PASP paper (Osterbrock & Rogerson 1961) was the first to suggest that much of the current helium originated in the creation of the universe. He recounts the events leading to that paper in *The Helium Content of the Universe* (Osterbrock 2009). He concludes with the statement

> I have heard lectures, and seen cosmological papers, in which values of X and Y derived from nebular spectrophotometry are quoted and used to three significant figures. But all the available calculations of the H I and He I emission-line intensities that I know are based on simplified models. . . . The "mean" values may not represent these conditions to high accuracy . . .

From my own personal knowledge, Don thought that there was roughly a 10% error on He/H determinations from emission lines. I also fear that I was the one who gave the talk Don mentions in his review.

We need to identify the error sources that affect He/H determinations in H II regions, quantify their size, and establish priorities for reducing them to the level needed for pre-

cision cosmology. There are five broad sources of error – observing methods, correcting for stellar absorption beneath the emission lines, converting emission-line intensities into ionic abundances, converting ionic abundances into total abundances, and, finally, correcting for stellar contributions to the current helium content. These are enumerated in Davidson & Kinman (1985) and Peimbert et al. (2003). Unfortunately many of the errors are systematic rather than statistical and so are hard to quantify.

The discussion was organized into small presentations by active researchers. Each discussed what they saw as the major problems and the way to make progress. The session was then opened to the audience. The following summarizes this discussion.

2. Comments by Gary Ferland

Ryan Porter and I have worked on aspects of the physics of helium emission-line formation on the microscopic level. This includes the atomic physics of the line formation and the physical properties of the ionized gas where He I and H I lines form.

Porter et al. (2005) revisited the formation of He I lines under the Case B approximation (Osterbrock & Ferland 2006, hereafter AGN3) conditions. We found emissivities that differ by, in some cases, several percent from the previous high-accuracy calculation by Benjamin et al. (1999). These were mainly due to the treatment of non-hydrogenic small-l levels where improved atomic data or methods had become available since the publication of Benjamin et al. The critical atomic rates, which have significant remaining uncertainties, are the photoionization cross sections (used to get the radiative recombination coefficient from the Milne relation, AGN3) and l-changing collisions for small-l levels.

Porter et al. (2009) did an analysis of the error sources that enter into the calculation of the theoretical emissivities. We found that the photoionization cross sections and l-changing collisions for small-l levels introduce a significant uncertainty. Paradoxically, because of how the lines form, the stronger lines, like λ5876, can have the greater uncertainty. An abundance analysis which relies on only a handful of the stronger lines will have a significant error, as much as several percent, introduced by these uncertainties. It must be stressed that this will be a systematic error that will introduce spurious conclusions if the uncertainties in the atomic physics are not taken into account.

The best way to quantify the uncertainties is to carefully examine a bright H II region where many He I lines can be measured. We did this in Porter et al. (2007), using one of the deepest published spectra of the Orion Nebula ever obtained. We found that the observational errors, as indicated by line ratios that were set by the atomic physics, were much larger than was given in the original paper. The intensities of 22 of the highest quality He I lines are consistent with an optimized model of the Orion environment and an observational error of 3.8% percent. The strongest He I line, λ5876, a line with one of the larger theoretical uncertainties in the emissivity, was matched to within 6.6%. The conclusion was that the uncertainties were substantially larger than originally estimated.

What to make of this? Don's guess of a 10% uncertainty in He/H may be realistic. My opinion is that we should understand Orion first. This is the brightest and simplest H II region we know of, close to the Earth and predominantly ionized by a single star. The giant H II region 30 Dor should come next. It is the nearest and brightest object that is a close kin to the galaxies used to derive the primordial helium abundance. It would be good if independent data sets could be obtained and compared to form an impartial estimate of the observational errors. Finally high-precision photoionization cross sections and collisional rates are needed to improve the accuracy of the theoretical emissivities.

3. Comments by Yuri Izotov

Underlying stellar absorption is one of the most important systematic effects that should be taken into account for the primordial ^{4}He determination. Recently, Gonzalez Delgado et al. (2005) produced evolutionary stellar population synthesis models at high resolution for single stellar populations. These data allows one to take into account properly the underlying hydrogen and helium line absorption in spectra of H II regions. Another important source of systematic errors are collisional and fluorescent enhancements of He I emission lines. Recently, Porter et al. (2005) calculated new He I emissivities in the case B approximation using improved radiative and collisional data. However, for the practical use, simple fits of the emissivities including the contribution of the collisional and fluorescent excitation would be very useful.

I think that one or a few bright H II regions are not enough to derive the primordial ^{4}He abundance. The sample should be large enough to reduce the observational uncertainties. In particular, the spectrum of the bright H II region NGC 346 in the Small Magellanic Cloud mentioned by G.Steigman was obtained with a high signal-to-noise ratio. However, this object is extended and serious problems arise with the subtraction of the night sky foreground. Therefore, it is unlikely to reach very good accuracy in the determination of Y for this object. Bright compact sources are more preferable.

Evan Skillman presented a non-parametric method for corrections of the systematics using HeI lines themselves. Potentially, this method could be one of the best for estimation of the systematic errors. However, I am not very happy to see large error bars in Y values, the large spread of points and the absence of a correlation between helium mass fraction and oxygen abundance. Perhaps, some other constraints should be considered to reduce the large error in Y_p. In particular, the electron temperature and electron number density could be derived from the Balmer jump. Furthermore, larger samples could be considered in order to reduce statistical errors.

4. Comments by Antonio & Manuel Peimbert

By considering that the temperature structure of a gaseous nebula can be represented by the average temperature, T_0, and the mean square temperature variation, t^2, it is possible to a second approximation to determine observationally the temperature structure of a gaseous nebula.

For the 5 metal poor extragalactic H II regions, used by Peimbert, Luridiana, & Peimbert (2007) to derive Y_p, they obtained an average $< t^2 >$ of 0.026. With this value they derive $Y_p = 0.2477$, while by adopting $t^2 = 0.00$ they obtain $Y_p = 0.2523$, a difference of 0.0046. This difference is critical for deriving an accurate Y_p value.

What is the evidence in favor of $< t^2 > = 0.026$? The typical t^2 values derived from photoionization models like CLOUDY are in the 0.003 to 0.010 range. Many astronomers, mainly based on photoionization models and the simplicity of the equations for abundance determinations for constant temperature, adopt $t^2 = 0.000$ to derive chemical abundances. We consider that the observations of high quality that provide t^2 values higher than 0.020 are reliable and that the presence of temperature variations has to be considered in the abundance determinations.

To determine T_0 and t^2 you need to combine line intensities that have a different dependence on the electron temperature. There are at least seven methods that have been used in the literature to determine T_0 and t^2. The four most commonly used are: (a) the combination of [O III] collisionally excited lines with O II recombination lines, (b) the combination of [C III] collisionally excited lines with C II recombination lines,

(c) the combination of collisionally excited lines of [O II] and [O III] with the ratio of the Balmer continuum to a Balmer recombination line, and (d) the combination of about 10 He I lines with [O II] and [O III] collisionally excited lines to obtain t^2, N(He I), $\tau(3889)$, and Y simultaneously.

There are four well-observed objects where the four methods mentioned above have been used simultaneously, two H II regions and two planetary nebulae: the Orion nebula, 30 Doradus, NGC 5315, and NGC 6543; the derived $< t^2 >$, values for each object are 0.022 ± 0.002, 0.033 ± 0.005, 0.051 ± 0.004, and 0.028 ± 0.005, respectively. For any given object each of the four methods gives a t^2 in agreement with the average value. This result gives a very strong support to each of the methods, and to the existence of large temperature variations in each of these objects.

The presentation by Peimbert, Peimbert, Carigi, and Luridiana, in these proceedings, includes some observational evidence supporting the large t^2 value (0.036) derived for the galactic H II region M17.

5. Comments by Evan Skillman

My main comment was that the current work on He abundances in extragalactic H II regions indicates that the mean temperature (as indicated by the fluxes of the He I emission lines) is significantly lower than the temperature derived from the [O III] lines. This result is significant beyond the determination of the primordial He abundance, as a lower temperature implies higher abundances of the heavy elements in these regions. Since the uncertainty in the temperature in these H II regions is a dominant source of uncertainty, due to the degeneracy between temperature and density in the minimization, it is very important to sort this out.

Izotov et al. (2007) justify the assumption of low temperature fluctuations (and thus the suitability of the [O III] temperature) based on agreement between [O III] temperatures and temperatures derived from the Balmer decrement in a sample of blue compact dwarfs. However, deriving electron temperatures from the Balmer decrement is intrinsically difficult and the history of this technique in the literature is not consistent. I consider this question to be the major uncertainty in the determination of helium abundances in individual nebular objects.

6. Comments by Gary Steigman

In my opinion the dominant sources of uncertainty in the helium abundance determinations are systematic, not statistical. Neither the statistical error nor the uncertain extrapolation to zero metallicity limit the accuracy of our current estimate of the primordial helium abundance and the cosmological constraints that follow from it. To illustrate the significance of a concerted observational (and theoretical) effort to limit the systematic errors, I pointed out the value of a few (one!) good helium abundance determinations.

In my invited review talk I noted that if the value of the baryon density parameter inferred from the inferred primordial deuterium abundance is combined with that derived from the WMAP CMB observations, the estimate of the effective number of neutrinos is $N_{\rm eff} = 4.0 \pm 0.7$, which is within 1.4σ of the standard model value of 3. In contrast, if we simply adopt as an **upper limit** to the primordial helium abundance the Peimbert, Luridiana, Peimbert (2007) estimate of the helium abundance (and its uncertainty) for the SMC H II region NGC 346, $Y_{\rm SMC} = 0.2507 \pm 0.0042$ (where their statistical and systematic errors have been added linearly), and combine this with the observationally inferred primordial deuterium abundance, we would find an **upper bound** to the effective

number of neutrinos, $N_{\rm eff\ max} \leqslant 3.2 \pm 0.3$. The key point of this example is to illustrate that if the PLP error estimate is realistic, the **uncertainty** in $N_{\rm eff}$ may be reduced by more than a factor of two. A few more carefully observed and analysed H II regions like NGC 346 could go a long way in pinning down the value of the primordial helium abundance and tightening the constraints that follow from it.

7. Conclusions

The discussion illuminated several sources of uncertainty in the precision analysis of emission lines emitted by H II regions. A variety of approaches were suggested as ways to improve the accuracy of the derived abundances. It would be productive if all were attempted. Gary Steigman's comment that even a very few high-precision measurements would be cosmologically significant established a realizable goal. Clearly much work, both observational and theoretical, remains to be done.

References

Benjamin, Robert A.; Skillman, Evan D.; Smits, Derck P. 1999, *ApJ*, 514, 307

Davidson, K. & Kinman, T.D. 1985, *ApJS*, 58, 321

Gonzalez Delgado, R. M.; Cervio, M.; Martins, L. P.; Leitherer, C.; Hauschildt, P. H. 2005, *MNRAS*, 357, 945

Izotov, Y., Thuan, T., & Stasinska, G. 2007, *ApJ*, 662, 15

Osterbrock, D.E. & Ferland, G.J. 2006 *The Astrophysics of Gaseous Nebulae and Active Galactic Nuclei*, 2^{nd} Edition (Mill Valley; University Science Press) (ANG3)

Osterbrock,D.E. & Rogerson, J.B. 1961, *PASP*, 73, 129

Osterbrock, D.E., 2009, in *Finding the Big Bang*, P.J.E. Peebles, L.A. Page & R.B. Partridge eds (Cambridge; Cambridge University Press), p.86

Peimbert, Manuel, Luridiana, Valentina & Peimbert, Antonio 2007, *ApJ*, 666, 636

Peimbert, Manuel, Peimbert, Antonio, Luridiana, Valentina, & Ruiz, Maria Teresa 2003, *ASPC*, 297, 81

Porter, R. L., Bauman, R. P., Ferland, G. J., & MacAdam, K. B. 2005, *ApJ*, 622, L73

Porter, R. L., Ferland, G. J., MacAdam, K. B. 2007, *ApJ*, 657, 327

Porter, R. L., Ferland, G. J., MacAdam, K. B., Storey, P. J. 2009, *MNRAS*, 393L, 36

Roberto Costa

Piercarlo Bonifacio

Light elements in the Universe
Proceedings IAU Symposium No. 268, 2010
C. Charbonnel, M. Tosi, F. Primas & C. Chiappini, eds.

DOI: 00.0000/X000000000000000X

He-rich and He-poor populations in RGB stars. Results on a sample of 19 globular clusters

Angela Bragaglia[1], Valentina D'Orazi[2], Raffaele Gratton[2], Eugenio Carretta[1], Santi Cassisi[3] and Sara Lucatello[2]

[1]INAF-Osservatorio Astronomico di Bologna,
via Ranzani 1, 40127 Bologna, Italy
email: angela.bragaglia@oabo.inaf.it, eugenio.carretta@oabo.inaf.it

[2]INAF-Osservatorio Astronomico di Padova,
vicolo Osservatorio 5, 35122 Padova, Italy
email: valentina.dorazi@oapd.inaf.it, raffaele.gratton@oapd.inaf.it,
sara.lucatello@oapd.inaf.it

[3]INAF-Osservatorio Astronomico di Collurania,
via M. Maggini, I-64100, Teramo, Italy
emal: cassisi@oa-teramo.inaf.it

Abstract. We use about 1400 red giant branch stars observed in 19 Galactic Globular Clusters (GCs) to compare colours, metallicities, and RGB bump luminosities of stars assigned to first and second generations. We find subtle differences which we attribute to the different He content. In general these differences are visible only when we consider the extreme second generation stars, with the exception of NGC 2808. When using various indicators, the implied helium enhancements are similar, but the absolute calibration is still uncertain.

Keywords. Stars: abundances, Population II – Galaxy: globular clusters

1. He differences from globular clusters red giant stars

We exploit the unprecedented database of about 1400 stars on the Red Giant Branch (RGB) observed with FLAMES@VLT in 19 Galactic Globular Clusters (GCs) in the course of our project on the Na-O anticorrelation. For a description of our survey and for results see Carretta et al. (2009a), Carretta e al. (2009b); for a description of the influence of He, see Gratton et al. (2010) and Bragaglia et al. (2010).

Stars with different He are expected to have different temperatures (i.e., different colours), slightly different [Fe/H] values, and different magnitudes of the RGB bump. All these differences are small, but our study has the necessary precision, statistics, and homogeneity to detect them.

We derive the differences in colours, metallicities and RGB bump magnitudes in the Primordial (P), Intermediate (I) and Extreme (E) population (Carretta et al. 2009a), which are associated with different levels of pollution and correspond to different He enhancements, as is expected in a scenario of intra-cluster pollution by material processed through hot H-burning (e.g. CNO cycle) in a previous generation of stars. We find that P stars show significant differences in colour and metallicity only compared to E stars (see Fig. 1, left panels). If we interpret this as an effect of He, these differences imply a ΔY$\sim$0.05-0.10. NGC 2808 is an exception, since differences are visible both between P and I stars and between P and E stars (indicating a $\Delta Y \gtrapprox 0.10$-0.12).

We find that the level of the RGB bump defined by first-generation P stars is fainter

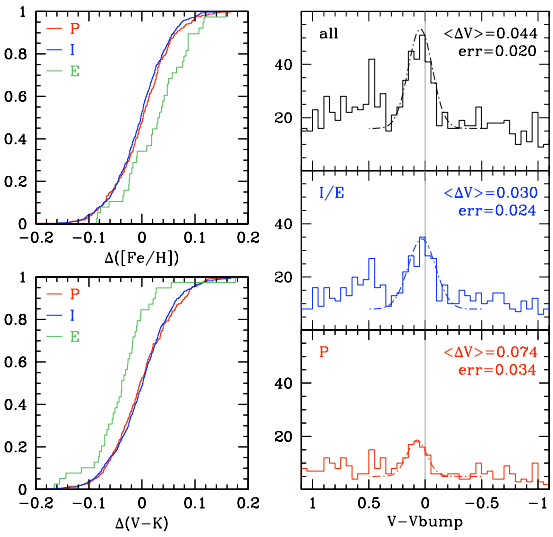

Figure 1. Left panels: Cumulative distributions of the differences in metallicity (upper panel) and in colour (lower panel) for the three populations: the P and I ones are similar, while the P and E ones are significantly different. Right panels: Histograms of the difference in magnitude between individual V values and V_{bump} (for each cluster), zoomed near the RGB bump. We show for al stars (upper panel), second-generation I and E, and first-generation P stars (middle and lower panel, respectively), with gaussians fitting each bump. In each panel the peak of the bump and the associated error are indicated.

than the one defined by second-generation I and E stars (see Fig. 1, right panels). The interpretation in terms of different He is complex. We explore two cases with different mixtures of heavy elements: one with "normal" α-enhancement (Pietrinferni et al. 2006) and one that takes into account the observed anticorrelations in the chemical abundances observed in GCs (Pietrinferni et al. 2009). We obtain results in fair agreement with those obtained with the other methods.

We conclude that *i*) RGB stars in GCs show indication of different He levels, *ii*) that different methods produce similar results, but that *iii*) the absolute calibration of the derived ΔY is still uncertain.

AB is grateful to the IAU and the Swiss National Science Foundation for financial support. SL acknowledges the DFG cluster of excellence "Origin and Structure of the Universe" for support.

References

Bragaglia, A., Carretta, E., Gratton, R., D'Orazi, V., Cassisi, S., Lucatello, S. 2010, *A&A*, subm.
Carretta, E., Bragaglia, A., Gratton R.G., Leone, F., Recio-Blanco, A., Lucatello, S. 2006, *A&A*, 450, 523
Carretta, E., et al. 2009a, *A&A*, 505, 117
Gratton, R.G., Carretta, E., Bragaglia, A., Lucatello, S., D'Orazi, V. 2010, *A&A*, subm.
Pietrinferni, A., Cassisi, S., Salaris, M., Castelli, F. 2006, *ApJ*, 642, 797
Pietrinferni, A., Cassisi, S., Salaris, M., Percival, S., Ferguson, J.W. 2009, *ApJ*, 697, 275

Light elements in the Universe
Proceedings IAU Symposium No. 268, 2010
C. Charbonnel, M. Tosi, F. Primas & C. Chiappini, eds.

DOI: 00.0000/X000000000000000X

Helium abundances in inner Galaxy planetary nebulae

Oscar Cavichia[1,2], Roberto D. D. Costa[1], and Walter J. Maciel[1]

[1]IAG, University of São Paulo, 05508-900, São Paulo-SP, Brazil.
[2] email: cavichia@astro.iag.usp.br

Abstract. New helium abundances of planetary nebulae located towards the bulge of the Galaxy were derived, based on observations made at OPD (Brazil). We present accurate helium abundances for 56 PNe located towards the galactic bulge. The data show good agreement with other results in the literature, in the sense that the distribution of the abundances is similar to previous works. Furthermore, the radial helium gradient is extended towards the galactic center. The results show that no trend can be identified when comparing the internal gradient ($R \leqslant 4$ kpc) to the whole galactic disk.

Keywords. ISM: planetary nebulae: general; Galaxy: abundances, evolution

1. Introduction

Planetary nebulae (PNe) are an important tool to study the chemical abundances in the Galaxy. As an offspring of intermediate mass stars, their helium abundances suffer from contamination from the evolution of the progenitor star. Even when the contamination of the progenitor star is considered, the existence of a He/H gradient in the galactic disk is very uncertain (see Maciel 2000). The derived He/H gradients from PNe abundances are negligible, and can be written as $d(He/H)/dR = 0.0000 \pm 0.0004$ (Maciel 2000).

Since bulge and disk may have formed in different ways such as represented by the disk inside-out formation model (Chiappini et al. 2001), or the model of multiple infalls onto the bulge (Costa et al. 2008), we would expect that these differences should appear in the abundance distributions of these structures. This way, in the present work we have extended the radial He/H gradient of the disk ($R \geqslant 4$ kpc) towards the galactic center, in order to compare the He/H gradient of both regions. This was done by using a new set of helium abundances of PNe located towards the galactic bulge derived by our group.

2. Method

Spectrophotometry observations in the optical domain were made at OPD observatory (Brazil) for a sample of 56 planetary nebulae located in the direction of the galactic bulge. The data were reduced following standard reduction procedures with the IRAF software (see Escudero et al. 2004). Details of the observation and data reduction procedures are described by Cavichia et al. (2009). The disk sample consists of 73 PNe compiled from our group (see for example Costa et al. 2004 and references therein).

In order to study the He/H gradient, PNe distances were taken from Stanghellini et al. (2008). The heliocentric distances were converted to galactocentric distances adopting $R_\odot = 8$ kpc. Additionally, new distances were derived for 46 PNe using the statistical distance scale proposed by Stanghellini et al. (2008), and based on the 5 GHz radio flux and optical angular diameter. In a first approach, no correction was considered for the contamination of the progenitor star evolution on the original helium abundance.

3. Results and discussion

The He/H radial gradient is shown in Figure 1. For R $\leqslant$ 4 kpc we addopted two different binnings in order to minimize the effect of the bin selection on the radial gradient.

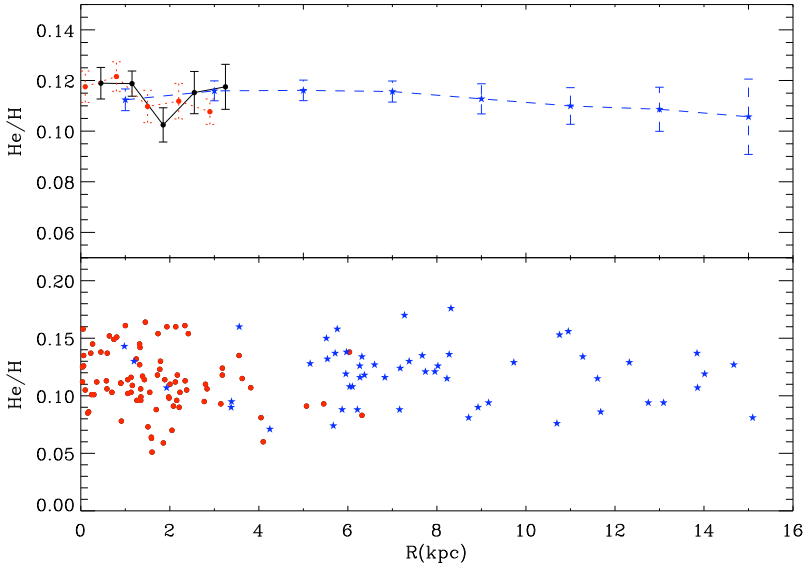

Figure 1. Top panel: the helium abundance as a function of the galactocentric distance for the bulge/inner disk sample (continuous and dotted lines represent the two different binnings) and for the disk sample (dashed line). For each bin the mean and the standard error of the mean (error bars) are given. Bottom panel: the radial distribution of helium abundances without considering mean abundances. Circles represent bulge/inner disk data and stars represent disk.

It can be seen in the figure that the He/H gradient for R $\leqslant$ 4 kpc is negligible, as it is in the outer part of the disk. As a conclusion, more reliable abundances and distances, especially in the inner region of the Galaxy, are necessary in order to investigate the radial dependence of the helium abundance.

References

Cavichia, O., Costa, R. D. D., & Maciel, W. J. 2009, *Rev. Mexicana AyA*, (Submitted)
Chiappini, C., Matteucci, F., & Romano, D. 2001, *ApJ*, 554, 1044
Costa, R. D. D., Uchida, M. M. M., & Maciel, W. J. 2004, *A&A*, 423, 199
Costa, R. D. D., Maciel, W. J., & Escudero, A. V. 2008, *Baltic Astronomy*, 17, 321
Escudero, A. V., Costa, R. D. D., & Maciel, W. J. 2004, *A&A*, 414, 211
Maciel, W. J. 2000, in: L. da Silva, R. de Medeiros, & M. Spite (eds.), *The Light Elements and their Evolution*, Proc. IAU Symposium No. 198, p. 204
Stanghellini, L., Shaw, R. A., & Villaver, E. 2008, *ApJ*, 689, 194

Light elements in the Universe
Proceedings IAU Symposium No. 268, 2010
C. Charbonnel, M. Tosi, F. Primas & C. Chiappini, eds.

DOI: 00.0000/X000000000000000X

Primordial helium abundance of the SMC: a view from intermediate mass stars

Roberto D.D. Costa[1], Walter J. Maciel[1] and Thais E.P. Idiart[1]

[1]IAG, University of São Paulo,
Rua do Matão 1226, 05508-090, São Paulo/SP, Brazil
email: roberto@astro.iag.usp.br, maciel@astro.iag.usp.br, thais@astro.iag.usp.br

Abstract. Helium abundances were derived for a sample of planetary nebulae of the Small Magellanic Cloud. These abundances were corrected from the chemical evolution of the galaxy as well as from stellar nucleosynthesis, and the primordial helium abundance then was estimated for the sample. Results indicate that the resulting average value for the sample is consistent with the expected values for primordial helium from SBBN and other values derived from HII regions in different stellar systems, even varying the enrichment ratio within its uncertainty range.

Keywords. ISM: planetary nebulae; stars: abundances; galaxies: Magellanic Clouds

1. Introduction

We derived the chemical composition for a sample of planetary nebulae of the Small Magellanic Cloud. Helium abundances were estimated as accurately as possible, including correction of collisional effects using collision-to-recombination correction factors. Based on luminosities and effective temperatures derived for the central star of each nebula, the masses, and then ages of the progenitor stars were estimated using isochrones and mass-age relationships. Using these results, helium abundance for each nebula was corrected for the contamination from the evolution of their progenitor star as well as from the chemical evolution of the interstellar medium, by using yields for intermediate mass stars and a helium-to-heavy elements abundance ratio. Therefore we determined the helium enrichment in the SMC and used these results to estimate the pregalactic helium abundance of this galaxy.

2. Results and discussion

The observational sample consisted in 49 PNe of the SMC. Observations were made at ESO/La Silla and OPD/Brazil. The observation and analysis procedures are described by Idiart *et al.* (2007). Primordial helium was estimated for each nebula using the expression

$$Y_P = Y - \frac{\Delta Y}{\Delta Z} Z - \Delta Y_S$$

where Y was derived from the helium abundance, Z was estimated from the chemical abundances, ΔY_S are the helium yields from van den Hoek & Groenewegen (1997) and $\Delta Y/\Delta Z = 2.0 \pm 0.6$ was taken from Peimbert *et al.* (2007).

The results are in Table 1, that shows the average values for primordial helium derived from the expression above, using the described PNe sample and excluding objects with neutral helium, without available yield and type-I PNe. The primordial abundances were calculated for $\Delta Y/\Delta Z = 2.0 \pm 0.6$. The error is mainly due to uncertainties in the mass determination of the progenitor stars, that were derived from their effective temperatures and luminosities using isochrones and mass-age relationships.

Table 1. Average values for the primordial helium abundance.

$\Delta Y/\Delta Z$	$\overline{Y_P}$	Error
2.0	0.234	0.009
2.6	0.234	0.009
1.4	0.241	0.008

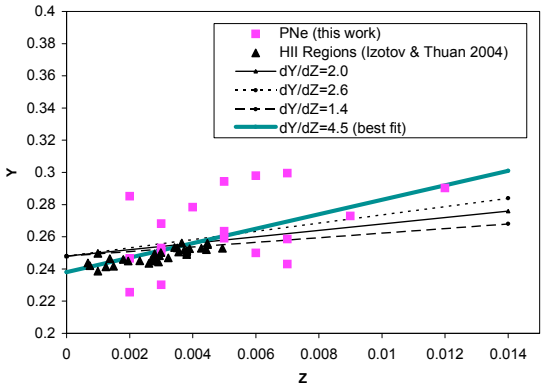

Figure 1. Y vs Z relation derived from our data, compared to a sample of HII regions in blue compact galaxies.

Figure 1 shows the Y vs Z relation derived from our data, compared to a sample of HII regions in blue compact galaxies, that are usually adopted to derive primordial helium abundances, taken from Izotov & Thuan (2004). It can be seen that, despite their larger dispersion, the data from PNe fit well the abundance distribution of HII regions. The thin lines correspond to $\Delta Y/\Delta Z = 2.0 \pm 0.6$, using the theoretical value of $Y_P = 0.248$ (Steigman 2007) as the $Z = 0$ value. The thick line corresponds to the best fit for both samples combined, which resulted in $\Delta Y/\Delta Z = 4.5$. It is important to note that this steeper value is consistent with that reported by Izotov & Thuan (2004): $\Delta Y/\Delta Z = 3.7 \pm 1.2$. The figure also shows that, despite their different Z ranges, enrichment ratios derived from HII regions and PNe are compatible.

From this result it is possible to see that He/H abundances derived from planetary nebulae can be used to study helium abundances throughout a stellar system like the SMC, and the resulting Y_P values calculated as described above are consistent with the expected values for primordial helium from SBBN and other values derived from HII regions in different stellar systems, even varying the enrichment ratio within its uncertainty range. Moreover, our results indicate that despite their metallicities are distributed in different Z ranges, enrichment ratios of HII regions and PNe are compatible, although a larger sample of PNe is required to improve these results.

References

Idiart, T.P., Maciel, W.J., & Costa, R.D.D. 2007, *A&A*, 472, 101
Izotov, Y.I., Thuan, T.X. 2004, *ApJ*, 602, 200
Peimbert, M., Luridiana, V., Peimbert, A., & Carigi, L. 2007, *ASPC*, 374, 81
Steigman, G. 2007, *Ann.Rev.Nuc.Part.Sci.* 57, 463
van den Hoek, L.B., & Groenewegen, M.A.T. 1997, *A&AS*, 123, 305

Light elements in the Universe
Proceedings IAU Symposium No. 268, 2010
C. Charbonnel, M. Tosi, F. Primas & C. Chiappini, eds.

DOI: 00.0000/X000000000000000X

The helium spread among the stars of 47Tuc

Marcella Di Criscienzo
INAF-Osservatorio Astronomico di Roma,
Monte Porzio Catone, Roma 00100, Italy
email: dicrisci@oa-roma.inaf.it

Abstract. We show that the current data of the HB branch of 47 Tuc show a particular feature that cannot be explained if a single population with an unique mechanism of mass loss is considered. We find that a spread in helium abundance among the stars is necessary, of ∼0.02. We indicate that the same variation in helium is present among the sub giant branch stars and suggest that is responsible of the spread in luminosity of the bright sub giant branch, while only a small part of the second generation is characterized by C+N+O increase and gives the faint sub giant branch.

Keywords. globular clusters: individual (47 Tuc); stars: horizontal-branch, evolution, abundances

1. Introduction

Spectroscopic data show chemical anomalies in most of 47 Tucanae stars consisting in bimodal CN band strengths (Briley 1997) and Na-O anticorrelations(Carretta et al. 2009).
These results indicate that the abundance spread in 47 Tuc is not due to an evolutionary effect, rather to the existence of an original stellar population (first generation, FG) and of a second generation (SG). Stars in the SG formed from material processed through the hot CNO cycle in the progenitors, belonging to the FG, but not enriched in the heavy elements expected in supernova ejecta, according to todays' new paradigm for the formation of galactic GCs (D'Ercole et al. 2008 and reference therein).
The recent photometric data by Anderson et al. (2009) seem to confirm the existence of multiple populations in 47 Tuc. In particular, they found a splitted sub giant branch (SGB) with at least two distinct components: a brighter one with a small and real spread in magnitude (∼0.06 mag) and a second one containing about 10% of star a little (∼0.05 mag) fainter.
Our idea is that CN-strong stars all belong to the SG, and were formed from gas showing the signature of CNO processing and a helium enrichment, but that only a small percentage of SG stars are increased in the overall CNO content.

2. The results

Following the suggestion of D'Antona & Caloi (2008) we decided to investigate this hypothesis using the morphology of the HB of 47 Tuc, where a population with a larger helium abundance should emerge. In Figure 1 we show a zoom of the CMD of 47 Tuc at the HB level (filled circle) based on images of 5 sec in F606W and F814W from ACS (GO-10775, PI Sarajedini).
In particular we note that at m_{F606W}-m_{F814W} ∼0.675 mag there is a particular feature in the data: a step in luminosity between the blue and brighter and red and dimmer part

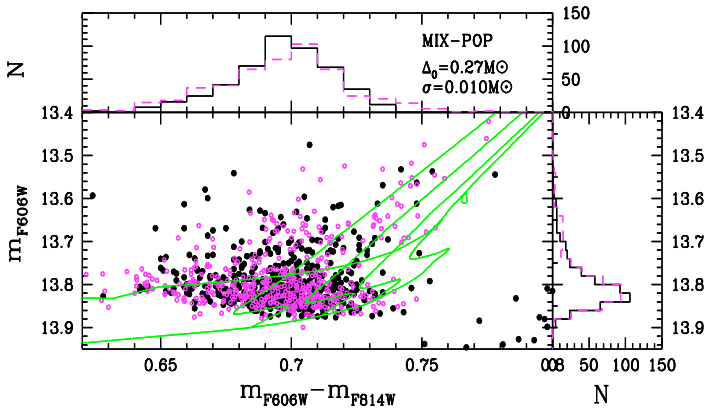

Figure 1. Comparison between observed (filled circle) and synthetic HB stars (open circle-magenta in the electronic version) calculate as described in the text considering an helium spread among stars of ΔY$\sim$0.02. The dashed histograms refer to synthetic populations while solid ones are those relative observations.

of HB. Our simulations show that a single mechanism mass loss can't reproduce this feature, while if we consider two different populations with two different helium contents it is possible to do a good job. The solid lines in the Figure are ZAHBs calculated from our models and reported in the observational plane using a reddening E(606-814)=0.038 mag. An apparent distance modulus $(m–M)_{F606W}$=13.09 mag was chosen in order to fit a ZAHB of pristine Y(=0.25) to the lower envelope. ZAHB for Y=0.28 is also reported together with HB evolutionary tracks of stars with masses M=0.63, 0.66, 0.70 and 0.80 solar masses.

Open circles are synthetic stars obtained using a gaussian mass loss around the central value ΔM_0=0.27$M_\odot$ and σ=0.010$M_\odot$. The synthetic population is built under the hypothesis that 70 % of stars have a N(Y) constant between Y=0.25 and Y=YUP=0.27. Other details of the model are reported in Di Criscienzo et al. (2010, in preparation). The two histograms for both magnitudes and colours show the comparison between the data and our simulations. The most interesting result is that the same variation in helium N(Y) can also explain the spread of the bright SGB observed by Anderson et al. 2009 while the faint SGB is made of stars with higher C+N+O (for details see Di Criscienzo et al. 2010).

We interpret these results as the confirmation that SG in 47 Tuc consist of about 70 % of stars, as suggested by spectroscopic studies.

References

Anderson, J.; Piotto, G.; King, I. R.; Bedin, L. R.; Guhathakurta, 2009, 2009, *ApJ*, 697, L58

Briley,M., 1997, *AJ*, 114, 1051

Carretta, E.; Bragaglia, A.; Gratton, R. G. et al., 2009, *A&A*, 505, 117

D'Antona, F., & Caloi, V. 2008, *MNRAS*, 390, 693

D'Ercole, A., Vesperini, E., D'Antona, F., McMillan, S. L. W., & Recchi, S. 2008, *MNRAS*, 391, 825

Light elements in the Universe
Proceedings IAU Symposium No. 268, 2010
C. Charbonnel, M. Tosi, F. Primas & C. Chiappini, eds.

DOI: 00.0000/X000000000000000X

Lithium and proton-capture elements in globular clusters: the case of 47 Tucanae

Valentina D'Orazi[1], Sara Lucatello[1,2], Raffaele Gratton[1], Angela Bragaglia[3], and Eugenio Carretta[3]

[1]INAF-Osservatorio Astronomico di Padova, vicolo dell'Osservatorio 5, I-35122, Padova;
email: valentina.dorazi@oapd.inaf.it, sara.lucatello@oapd.inaf.it, raffaele.gratton@oapd.inaf.it

[2] Excellence Cluster Universe, Boltzmannstr. 2, D-85748, Garching, Germany.
[3]INAF-Osservatorio Astronomico di Bologna, via Ranzani 1, I-40127, Bologna
email: angela.bragaglia@oabo.inaf.it; eugenio.carretta@oabo.inaf.it

Abstract. The determination of lithium (Li) abundances in Globular Clusters (GCs), along with proton-capture elements (Na, O, Mg, Al), offer a key tool to address the pollution scenario and its mechanisms, the dilution process acting within each star and the first phases in the lifetime of GCs. We present our results on Na, O and Li abundance determination in a large sample of dwarf stars in the GC 47 Tucanae (NGC 104). While we found a clear Na-O anti-correlation, in perfect agreement with giant members by Carretta et al. (2009a,b), Li abundance appears neither positively correlated with oxygen, nor anti-correlated with sodium. Our finding unveils an intrinsic scatter in Li content, independent of intra-cluster pollution by a first generation of more massive, faster evolving stars.

Keywords. Stars: abundances – Galaxy: globular clusters: individual: 47 Tuc

1. Introduction

The traditional assumption of GCs as simple stellar populations has been proven too simplistic. In the last years a lot of observational studies revealed the presence of anti-correlations between C, O, Mg and N, Na, Al, respectively, pointing out to self-enrichment processes within GCs, and to the existence of multiple stellar generations. In this context, Li abundances can provide very powerful tracers of cluster formation and evolution, because this element is easily destroyed in the stellar interiors. Regardless of the nature of the polluters (AGB stars -Ventura & D'Antona 2009- or fast rotating massive stars -Decressin et al. 2007), the Li content in polluting matter must be very close to zero (although in some cases AGB stars can also produce Li). The determination of Li variations in GCs allows us to uniquely constrain the nature and the extent of the dilution process between pristine and polluted material. Specifically two main issues can be addressed: (1) Do entirely polluted (Li$\simeq$0) stars exist? (2) Is the minimum detectable Li the same in all GCs or, otherwise, can it significantly vary from cluster-to-cluster? The latter point has also strong implications on the GC formation and early evolution. Here we present our results on the metal-rich ([Fe/H]=-0.76, Carretta et al. 2009c) GC 47 Tuc.

2. Sample and analysis

We retrieved from the ESO Archive (Programme 081.D-0287, PI P. Shen) FLAMES-GIRAFFE spectra of 109 unevolved, turnoff (TO) member stars of 47 Tuc. Gratings HR15n, HR18 and HR20a were employed to cover the Li I (6707 Å), O I (7771, 7773,

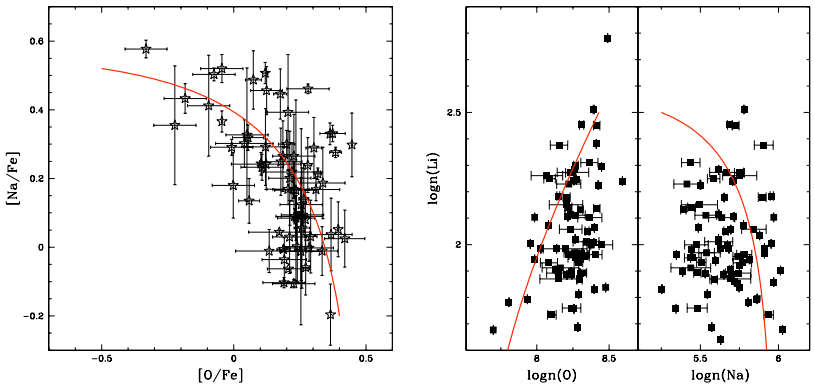

Figure 1. Na-O anticorrelation (left panel) and Li-Na-O distributions in dwarf stars of 47 Tuc (right panels).

7774 Å), and Na I (8183, 8194 Å) features, respectively. The analysis was carried out using the ROSA code (developed by R. Gratton) and Kurucz model atmospheres; for Na and O, we derived abundances from the equivalent widths, applying corrections due to NLTE effects; LTE Li abundances were instead obtained through spectral synthesis.

3. Results and discussion

As shown in Fig.1, the unevolved cluster stars reveal a very clear Na-O anti-correlation, confirming what has been obtained for giant members (Carretta et al. 2009a). The Na-O anti-correlation is well described by a simple dilution model (red solid line in Fig. 1), like the one proposed by Prantzos & Charbonnel (2006). On the other hand, Li abundances show a wide scatter, in both the Li-O and Li-Na planes, with values often well below those expected from a simple dilution model. Furthermore, the cluster behaviour seems different from that of NGC 6397 (Lind et al. 2009), a GC much more metal-poor than 47 Tuc ([Fe/H]=-1.99, Carretta et al. 2009c) and for which Lind et al. detected a significant Li-Na anti-correlation. Note that turnoff stars in 47 Tuc are cooler (T_{eff}∼5700-5800 K) than those in NGC 6397 (T_{eff}∼6100-6300 K) , being well below the limit usually considered for the Spite plateau. Finally, the large scatter observed in 47 Tuc seems reminiscent of the wide Li variations observed in the old open cluster M 67 (Randich et al. 2000) and, in general, in old thick disk stars with T_{eff}≈5800K (Ryan et al. 2001): this is the first time that this phenomenon is observed in GC stars.

References

Carretta, E., Bragaglia, A., Gratton, R., et al. 2009a, *A&A*, 505, 117
Carretta, E., Bragaglia, A., Gratton, R., Lucatello, S. 2009b, *A&A*, 505, 139
Carretta, E., Bragaglia, A., Gratton, R. , D'Orazi, V., Lucatello, S. 2009c, *A&A*, 508, 695
Decressin, T., Charbonnel C., Prantzos, N., Ekstrom, S. 2007, *A&A*, 464, 1029
Lind, K., Primas, F., Charbonnel, C., Grundahl, F., Asplund, M. 2009, *A&A*, 503, 545
Prantzos, N., Charbonnel, C. 2006, *A&A*, 458, 135
Randich, S., Pasquini, L., Pallavicini, R. 2000, *A&A*, 356, 25
Ryan, S., Kajino, T., Beers, T. 2001, *ApJ*, 549, 55
Ventura, P., D'Antona, F. 2009, *A&A*, 499, 835

Light elements in the Universe
Proceedings IAU Symposium No. 268, 2010
C. Charbonnel, M. Tosi, F. Primas & C. Chiappini, eds.

DOI: 00.0000/X000000000000000X

The Galactic deuterium gradient

Donald Lubowich[1] and Jay M. Pasachoff[2]

[1]Dept. of Physics and Astronomy, Hofstra University,
Hempstead, NY 11549
email: donald.lubowich@hofstra.edu

[2]Dept. of Astronomy, Williams College
Williamstown, MA 01267
email: jay.m.pasachoff@williams.edu

Abstract. The Galactic deuterium abundance gradient has been determined from observations of DCN in Galactic molecular clouds. This is the only way to observe D throughout the Galaxy because the molecular clouds are not limited to the 2 kpc region around the Sun observed with FUSE and from DI. We used an astrochemistry model and the DCN/HCN ratios to estimate the underlying D/H ratios in 16 molecular clouds including five in the Galactic Center. The resulting positive Galactic D gradient and reduced Galactic Center D/H ratio imply that there are no significant Galactic sources of D, there is continuous infall of low-metallicity gas into the Galaxy, and that deuterium is cosmological.

Keywords. Galaxy: abundances; ISM: molecules, abundances; radio lines: galaxies

1. Introduction

Deuterium has been extensively studied because it is not produced via stellar nucleosynthesis and is thought to be primarily produced in the big-bang so its abundance will decrease with time and metallicity unless there are any additional sources of D. The abundance of D depends on the temperature and baryonic density during the epoch of nucleosynthesis (first 3 min). Thus any Galactic source of D would undermine its use to estimate the baryonic density of the universe and place constraints on big-bang nucleosynthesis models. In homogeneous inflationary or other flat models, the D/H ratio gives the amount of dark matter and an upper limit to the number of ν families.

"Independently of the model for chemical evolution, it is predicted that the D abundance (D/H) increases with Z if D is produced in stars, but decreases as Z increases if it is primordial: these correlations hold as a function of time and for gradients of abundances at the present time. A firm observation of the correlation of D/H with Z (e.g., a gradient in the Galaxy) would therefore tell whether D is mostly made during galactic evolution before most metals were synthesized; this test could not distinguish between production in the Big-Bang and production in the first generation of stars." (Audouze & Tinsley 1976). If D is produced via any stellar or Galactic process, then the D/H ratio would be a maximum in the GC. Conversely, if there are no Galactic sources of D, then astration would reduce the D abundance in the GC to 3×10^{-12} (Audouze et al. 1976).

2. Observations and results

We observed DCN and $HC^{15}N$ in 16 Galactic molecular clouds (including five Galactic Center clouds). $HC^{15}N$ was observed because the HCN line is saturated. Thus DCN/HCN = $(DCN/HC^{15}N)(^{15}N/^{14}N)$. As in Lubowich et al.(2000) a model with 5300 chemical reactions was used to determine the underlying D/H ratios. Our results (a positive gradient

Table 1. D/H ratios in Galactic Molecular Clouds

Source	R (kpc)	D/H (ppm)
CND	0.002	< 1
Sgr A 20 km/s	0.01	2.4 0.7
Sgr A 50 km/s	0.01	2.3 0.6
GC Arc G0.13-0.13	0.035	2.5 0.5
Sgr B2	0.100	2.9 0.9
W33	4.2	9.82.4
G34.26	5.3	4.00.8
M17	5.9	2.81.1
DR21(OH)	8.1	7.10.7
Ori KL	8.2	8.72.2
NGC 2024	8.2	9.22.0
S140	8.3	143.5
NGC 2264	8.8	7.01.4
NGC 7538	9.4	173.9
W3(OH)	9.8	205.1
Edge 2 cloud	20	< 32

in the D/H ratio) are shown in Table 1 and Fig. 1 (compare to Pasachoff & Vidal-Madjar 1989). Our detection of DCN in GC molecular clouds shows D within 10-100 pc of the GC. The Sgr A clouds are 10^7 years old and contain reprocessed gas from recent star formation. Since fractionation enhances deuterated molecules, these results confirm our previous GC observations that there are no significant Galactic sources of D and that D is the result of infall of primordial gas. The low D/H ratios of 4 ppm and 2.8 ppm at 5.3 and 5.9 kpc may reflect astration in spiral arms. However, the D/H = 9.8 ppm in W33 at 4.2 kpc is not explained. At 10 kpc our results are in agreement with ISM FUSE (Linsky et al. 2006, 23 ppm), anticenter DI (Rogers, Dudevoir, & Bania 2007, 21 ppm, and low-metallicity halo-cloud (Sembach et al. 2004, 22 ppm,) D/H ratios. Better models of grain depletion, infall, astration, and astrochemistry are needed to explain the similar Galactic, quasar, and WMAP D/H ratios (26 ppm, Table 1, Linsky et al. 2006) while allowing large variation in the abundances of other elements. These observations are strong evidence that D is cosmological with no other significant sources of D.

References

Audouze, J., Lequeux, J., Reeves, H. and Vigroux, L. 1976, *ApJ* (Letters), 208, L51
Audouze, J. and Tinsley, B. M. 1976, *ARAA*, 14, 43
Linsky, J. L. et al. 2006, *ApJ* 647, 1106
Lubowich, D. A. and Pasachoff, J. M. et al. 2000, *Nature*, 405, 1025
Pasachoff, J. M. and Vidal-Madjar, A. 1989 *ComAp*, 14, 61
Rogers, A. E. E., Dudevoir, K. A., and Bania, T. M. 2007, *AJ* 133, 1625
Sembach, K. R. et al. 2004, *ApJS* 150, 387

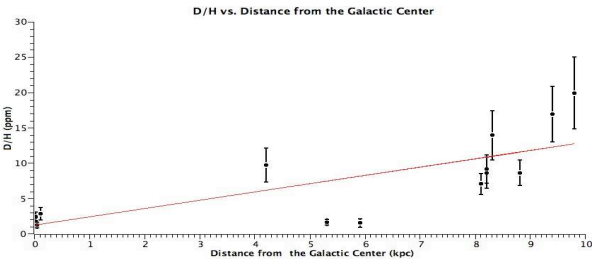

Figure 1. The Galactic Deuterium Abundance Gradient.

Light elements in the Universe
Proceedings IAU Symposium No. 268, 2010
C. Charbonnel, M. Tosi, F. Primas & C. Chiappini, eds.

DOI: 00.0000/X000000000000000X

Helium abundances in planetary nebulae: Nucleosynthesis and chemical evolution

W. J. Maciel, R. D. D. Costa and T. E. P. Idiart

University of São Paulo, Astronomy Department,
Rua do Matão 1226, Cidade Universitária, São Paulo SP, CEP 05509-0900, Brazil
email: maciel@astro.iag.usp.br, roberto@astro.iag.usp.br, thais@astro.iag.usp.br

Abstract.
We have obtained a large sample of PN with accurately determined helium abundances, as well as abundances of several heavy elements. The nebulae are located in the solar neighbourhood, in the galactic bulge, disk and anticentre, and in the Magellanic Clouds. The abundances are analyzed both in terms of the nucleosynthesis of intermediate mass stars and the chemical evolution of the host galaxies. In particular, correlations between the He/H ratio and the abundances of N and O are used as constraints of the nucleosynthetic processes occurring in the progenitor stars.

Keywords. ISM: planetary nebulae: general; Galaxy: abundances

1. Introduction

Helium abundances can be accurately measured in photoionized nebulae, comprising planetary nebulae (PN) and HII regions. The abundances measured in PN include the original helium content previous to the formation of the progenitor stars and the contamination during the nuclear processes in these objects. As a consequence, PN can be used to study the nucleosynthetic processes in intermediate mass stars and the chemical evolution of the host systems. In this work, we analyze the helium abundances of a large sample of PN in different systems, namely, the disk and bulge of the Milky Way (MW), and both the Small (SMC) and Large (LMC) Magellanic Clouds.

2. Average abundances and abundance distributions

We have analyzed several samples of PN with elemental abundances obtained in a homogeneous way. We have considered our own data, the IAG sample (see Maciel et al. 2009 and references therein, and Cavichia et al., in preparation), plus some recent data from the literature (Stasińska et al. 1998, SRM, Leisy & Dennefeld 2006, LD). Maciel et al. (2009) made a detailed comparison of these results concerning the heavy elements, and concluded that the merged sample maintains the homogeneity of the individual samples, in view of the similar methods employed. Average helium abundances are in the range $0.093 \leqslant \mathrm{He/H} \leqslant 0.119$. These averages are similar in all systems, within the uncertainties, but the SMC abundances are slightly lower than either the LMC and MW, being similar to the HII region value, as in the Orion nebula or 30 Dor. The MW disk seems slightly richer in He than the bulge, which may be due to a lack of intermediate mass stars near the upper mass limit in the latter. Concerning the He/H distributions, there is a general agreement among the different samples. The peaks of the distributions are in the range He/H = 0.080 to 0.100 (SMC) and He/H = 0.080 to 0.120 (LMC), while the MW data show a peak between He/H = 0.120 and 0.140 for the disk and He/H = 0.080 to 0.120 for the bulge.

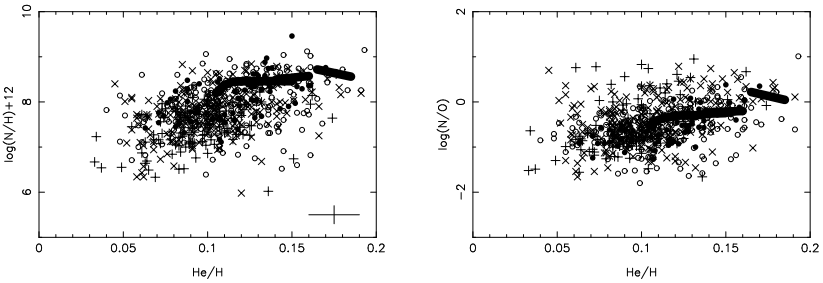

Figure 1. He and N abundances in PN in the Milky Way disk (dots), Bulge (empty circles), SMC (crosses) and LMC (x signs). Thick lines are models for TP-AGB stars with masses in the range 1.1 to 5 $M_{\odot}$ by Marigo et al. (2003).

3. Abundance correlations: Observations and theory

Fig. 1 shows the N/H vs He/H and N/O vs He/H plots for the merged sample. A few objects with He/H < 0.03 are not included, as some contribution from neutral helium is probably unaccounted for. It is apparent that all systems have a similar behaviour, with similar results for the N/O ratio, although the metallicity range may be different in these systems. For example, the MW shows a larger range in nitrogen abundances, as expected, since our galaxy is more metal rich than the Magellanic Clouds. However, the evolution of the abundances is consistent with a similar trend for all systems, since the slopes are similar. In Fig. 1 we have included the predictions of theoretical models by Marigo et al. (2003), as shown by the thick lines. These are synthetic evolutionary models for the thermally-pulsing Asymptotic Giant Branch stars (TP-AGB) with masses in the range 1.1 to 5 $M_{\odot}$. In these objects, up to three dredge-up episodes occur, apart from hot-bottom burning (HBB) for the most massive objects. All of these processes affect the He/H ratio, and in fact most objects present some enhancement compared to the solar values. According to Marigo et al. (2003), progenitors having 0.9 to 4 $M_{\odot}$ and solar composition can explain the "normal" abundances, He/H $\leqslant 0.15$, while for those objects with higher enhancements (He/H > 0.15) larger masses are needed, in the range 4 to 5 $M_{\odot}$, plus an efficient HBB. The latter are represented in Fig. 1 by the slanted black thick lines at the upper right corner of the figures. It can be seen that the agreement is very good, especially for the N/O ratio. For the N/H ratio the plot shows a better agreement for the Milky Way, as expected, since this galaxy is somewhat more metal rich than the Magellanic Clouds, so that we would expect the theoretical predictions to be located in the upper part of the plot, as is indeed the case. We found a continuous transition between the "normal" and He-richer nebulae, which is probably due to the fact that we have a much larger sample compared to Marigo et al. (2003). These results suggest that the nucleosynthetic processes occurring in these systems are similar, even though the global metallicity may be different and the chemical evolution may be affected by different star formation rates.

Acknowledgements. This work was partially supported by FAPESP and CNPq.

References

Leisy, P., Dennefeld, M. 2006, *A&A*, 456, 451
Maciel, W. J., Costa, R. D. D., Idiart, T. E. P. 2009, *Rev. Mexicana AyA*, 45, 127
Marigo, P., Bernard-Salas, J., Pottasch, S. R., et al., 2003, *A&A*, 409, 619
Stasińska, G., Richer, M. G., McCall, M. 1998, *A&A*, 336, 667

Light elements in the Universe
Proceedings IAU Symposium No. 268, 2010
C. Charbonnel, M. Tosi, F. Primas & C. Chiappini, eds.

DOI: 00.0000/X000000000000000X

Chemical composition of stellar populations in ω Centauri

A. F. Marino[1,2], G. Piotto[1], R. Gratton[3], A. P. Milone[1], M. Zoccali[2], L. R. Bedin[4], S. Villanova[5] and A. Bellini[1,4]

[1]Dept. of Astronomy, University of Padova, Vicolo dell'osservatorio 3, 35122, Padova, Italy
email: anna.marino@unipd.it

[2]P. Univ. Católica de Chile, Dept. de Astronomía y Astrofísica, Casilla 306, Santiago 22, Chile
[3]INAF-Osservatorio Astronomico di Padova, Vicolo dell'Osservatorio 5, 35122 Padova, Italy
[4]Space Telescope Science Institute, 3700 San Martin Drive, Baltimore, MD 21218, USA
[5] Dept. de Astronomia, Universidad de Concepcion, Casilla 160-C, Concepcion, Chile

Abstract. We derive abundances of Fe, Na, O, α and *s*-elements from GIRAFFE@VLT spectra for more than 200 red giant stars in the Milky Way satellite ω Centauri. Our preliminary results are that: (*i*) we confirm that ω Centauri exhibits large star-to-star metallicity variation ($\sim$ 1.4 dex); (*ii*) the metallicity distribution reveals the presence of at least five stellar populations with different [Fe/H]; (*iii*) a distinct Na-O anticorrelation is clearly observed for the metal-poor and metal-intermediate stellar populations while apparently the anticorrelation disappears for the most metal rich populations. Interestingly the Na level grows with iron.

Keywords. galaxy: stellar content, Globular clusters: individual (Omega Centauri)

1. Introduction

Omega Centauri (ω Cen) is among the most studied and enigmatic Milky Way satellites. It has always been considered a Globular Cluster (GC), but a number of peculiarities, like the mass, the kinematics, and the complexity of its numerous populations identified by both spectroscopic and photometric investigations (Cannon & Stobie 1973, Lee et al. 1999, Pancino et al. 2000, Bedin et al. 2004, Piotto et al. 2005, Villanova et al. 2007), suggest that it may be the remnant of a larger stellar system.

Recently, it has been shown that some peculiar features observed in ω Cen are shared with other GCs: A bimodality in s-elements is present in NGC 1851 (Yong et al. 2008) and M22 (Marino et al. 2009), and intrinsic variations in [Fe/H] were detected in M22 (Marino et al. 2009), and M54 (Sarajedini & Layden 1995; Bellazzini et al. 2008; Carretta et al. 2010). However ω Cen still remains a unique GC in the Milky Way as concerns the complexity of its stellar populations.

Here we present preliminary results of our project aimed to characterize the evolutionary connections of the sub-populations in ω Cen, by studying their chemical content.

2. Observations and data reduction

We analyzed FLAMES/GIRAFFE HR09 and HR13 spectra for a sample of more than 200 red giant stars. Iron abundances are obtained from an equivalent width analysis by using the Local Thermodynamical Equilibrium program MOOG (Sneden 1973), while the other elements are measured by comparing observed spectra with synthetic ones. More details on the abundance measurements can be found in Marino et al. (2008, 2009).

3. Results

We obtained that the [Fe/H] ranges from ~ -2.1 to ~ -0.7 dex, with at least five distinct stellar groups in the iron distribution as shown in Fig.1 (left panel). In the top right panels of Fig.1 we represent Na and O abundances for the five sub-populations, selected on the basis of different iron content and position on the color magnitude diagram (CMD). In the lower panels the position on the B-$(B-R)$ CMD from Bellini et al. (2009) for the different selected groups is shown, with the corresponding NaO anticorrelation in each upper panel. We superimposed to each Na-O plane, a fiducial traced by hand on the NaO anticorrelation for stars with $-1.80<$[Fe/H]< -1.34. We note that the NaO anticorrelation is well defined for stars belonging to the metal intermediate populations ($-1.80<$[Fe/H]< -1.34), and some hints of a probably less extended one are present for the more metal poor stars with [Fe/H]< -1.80. Apparently, the anticorrelation disappears for stars with [Fe/H]> -1.00. Note that the Na level grows with Fe.

From the analysis of the s-elements La and Ba we derive that the s element abundance grows with increasing iron, and interestingly enough, in each group defined as in Fig.1, apparently the s element abundance increases also with Na.

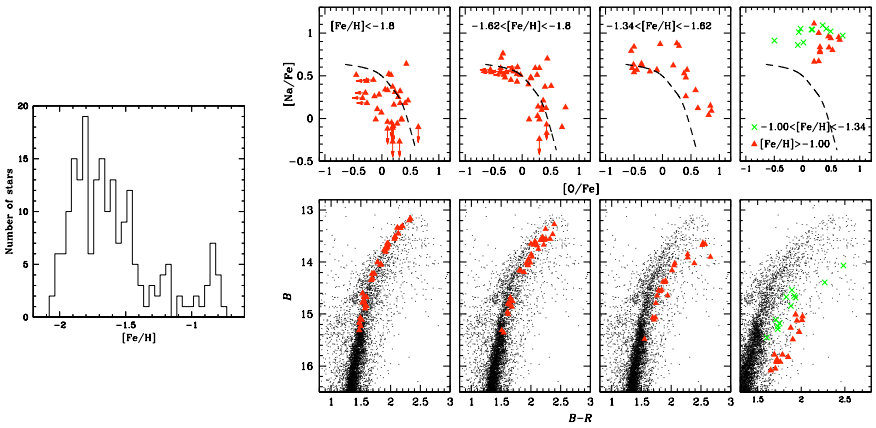

Figure 1. *Left panel*: Distribution of the iron content for our analyzed sample. *Right panels*: Na-O anticorrelation for the different groups of stars selected on the basis of the iron content and the position on the CMD represented in lower panels.

References

Bedin L. R., et al., 2004, *ApJ*, 605, L125
Bellazzini M., et al., 2008, *AJ*, 136, 1147
Bellini A., et al., 2009, *A&A*, 493, 959
Cannon R. D. & Stobie R. S., 1973, *MNRAS*, 162, 207
Carretta E., et al., 2010, *ApJL* in press
Marino A. F., et al., 2008, *A&A*, 490, 625
Marino A. F., et al., 2009, *A&A*, 505, 1099
Lee Y.-W., et al. 1999, *Nature*, 402, 55
Pancino E., et al., 2000, *ApJ*, 534, L83
Piotto G., et al., 2005, *ApJ*, 621, 777
Sarajedini, A. & Layden, A. C., 1995, *AJ*, 109, 1086
Sneden C. A., 1973, Ph.D. Thesis
Villanova, S. et al., 2007, *ApJ*, 663, 296

Light elements in the Universe
Proceedings IAU Symposium No. 268, 2010
C. Charbonnel, M. Tosi, F. Primas, & C. Chiappini, eds.

DOI: 00.0000/X000000000000000X

On the total O/H abundance ratio in Galactic and extragalactic H II regions

Antonio Peimbert[1] **and Manuel Peimbert**[1]

[1]Instituto de Astronomía, Universidad Nacional Autónoma de México, Apdo. postal 70-264, México D.F. 04510, Mexico
email: antonio@astroscu.unam.mx

Abstract. To determine the primordial helium abundance and to study the chemical evolution of galaxies it is necessary to derive the total O/H ratio in H II regions. To determine the total O/H ratio in H II regions it is necessary to add to the gas-phase component the dust-phase component of O atoms. Based on the Fe/O ratio and other considerations we estimate the dust-phase fraction as a function of O/H.

Keywords. ISM: abundances – H II regions – galaxies: abundances, evolution, irregular – Galaxy: disk – early universe

1. Introduction

In this note we present a preliminary discussion on the fraction of O trapped in dust grains, elsewhere we present a full discussion of this problem (Peimbert & Peimbert 2010a). Mesa-Delgado et al. (2009) based on three different methods have estimated that the fraction of O atoms trapped in dust in the Orion nebula amounts to 0.12 ± 0.03 dex.

2. The Fe/O ratio

In Figure 1 we present the Fe/O versus O/H ratio compiled from many sources in the literature. Part of the scatter in Figure 1 could be due to errors in the determinations of the gas-phase Fe/O ratios and part to the different star formation histories of the different galaxies. The closer in time to a recent burst of star formation the lower the total Fe/O ratio in the ISM. In the solar vicinity at present all the O abundance is due to core collapse supernovae, while about 40% of the Fe is due to core collapse supernovae and the other 60% to Type Ia supernovae (e. g. Pagel 2009). There is a time delay in the Fe formation relative to the O formation, and consequently the Fe/O ratio depends on: the star formation rate, the initial stellar mass function, and the gas flows from and into the intergalactic medium. There are two well established Fe/O ratios from observations: the one when the Sun was formed, called the protosolar ratio that amounts to -1.19 dex (Asplund et al. 2009), and the present value in the solar vicinity based on observations of B stars that amounts to -1.32 dex (Przybilla, Nieva, & Butler 2008). From the previous discussion we will adopt for the ISM of the objects in Figure 1 a total value of Fe/O = -1.3 dex.

From Figure 1, and assuming that the total Fe/O ratio amounts to -1.3 dex, we obtain that for the Galactic and extragalactic H II regions with abundances in the $8.35 < 12 + \log \mathrm{O/H} < 8.85$ range the average fraction of Fe in the gaseous-phase is about 4% . For the extragalactic H II regions with abundances in the $7.75 < 12 + \log \mathrm{O/H} < 8.35$ range the fraction of Fe in the gaseous-phase is about 20%. For the extragalactic H II regions

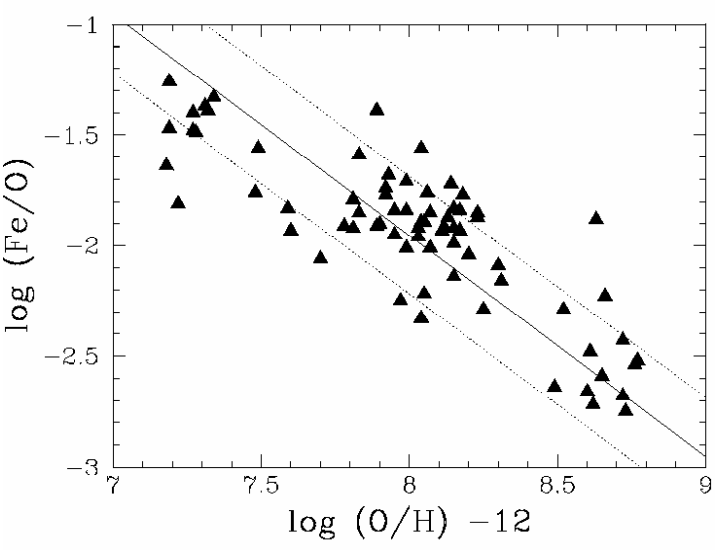

Figure 1. Log Fe/O versus 12 + log O/H gas-phase abundance ratios. The data comes from the literature. The straight line corresponds to 12 + log Fe/H = 6.05 ± 0.27.

in the $7.15 < 12 + \log O/H < 7.75$ range the fraction of Fe in the gaseous phase is about 40%.

3. Conclusions

We find that the gaseous 12 + log Fe/H ratio is typically in the 6.05 ± 0.27 range for H II regions with 12 + log O/H in the 7.35 to 8.85 range. The almost constancy of the gas-phase Fe/H ratio reflects the efficiency of the processes of dust formation and dust destruction. It probably implies that there is a minimum threshold for dust formation given by a gas-phase 12 + log Fe/H ratio of about 5.7.

We estimate that the dust-phase fraction of O in Galactic and extragalactic H II regions is in the 0.08 ± 0.03 to 0.12 ± 0.03 dex range. We also consider that the H II region abundances derived from the $T(4363)$ method underestimate the O/H ratio by about 0.2 to 0.4 dex (Peimbert & Peimbert 2010b, and references therein). These two effects taken together imply that to obtain the gas-phase plus the dust-phase O/H abundance ratio it is necessary to increase the O/H gas values derived from the $T(4363)$ method by about 0.25 to 0.50 dex.

References

Asplund, M., Grevesse, N., Sauval, A. J., & Scott, P. 2009, *A*RAA 47, 481
Mesa-Delgado, A., Esteban, C., García-Rojas, J., et al. 2009, *M*NRAS 395, 855
Pagel, B. E. J. 2009, *Nucleosynthesis and Chemical Evolution of Galaxies, Second Edition*, Cambridge University Press
Peimbert, A. & Peimbert, M. 2010a, in preparation
Peimbert, M. & Peimbert, A. 2010b, *R*ev. Mexicana AyA, arXiv: 0912.3781, in press
Przybilla, N., Nieva, M. F., & Butler, K. 2008, *A*pJ 688, L103

Light elements in the Universe
Proceedings IAU Symposium No. 268, 2010
C. Charbonnel, M. Tosi, F. Primas & C. Chiappini, eds.

DOI: 00.0000/X000000000000000X

On the origin of the helium-rich population in the peculiar globular cluster Omega Centauri

Donatella Romano[1,2], M. Tosi[2], M. Cignoni[1,2], F. Matteucci[3], E. Pancino[2] and M. Bellazzini[2]

[1]Dept. of Astronomy, Bologna University,
Via Ranzani 1, I-40127, Bologna, Italy
email: donatella.romano@oabo.inaf.it

[2]INAF-Bologna Observatory,
Via Ranzani 1, I-40127, Bologna, Italy

[3]Dept. of Physics, Trieste University,
Via Tiepolo 11, I-34143, Trieste, Italy

Abstract. In this contribution we discuss the origin of the extreme helium-rich stars which inhabit the blue main sequence (bMS) of the Galactic globular cluster Omega Centauri. In a scenario where the cluster is the surviving remnant of a dwarf galaxy ingested by the Milky Way many Gyr ago, the peculiar chemical composition of the bMS stars can be naturally explained by considering the effects of strong differential galactic winds, which develop owing to multiple supernova explosions in a shallow potential well.

Keywords. globular clusters: individual (Omega Centauri) – galaxies: dwarf, evolution – stars: abundances, chemically peculiar

1. A dwarf galaxy progenitor suffering strong galactic winds

It has been suggested – and it is now widely accepted – that the kinematical, dynamical and chemical properties of the most massive globular cluster of the Milky Way, Omega Centauri (ω Cen, NGC 5139), can all be understood if it is the surviving remnant of a larger system, captured and partially disrupted by the Milky Way many Gyrs ago (see, e.g., Romano et al. 2007, and references therein). However, the origin of the extreme He-rich stars hosted on its blue main sequence (bMS) still awaits a satisfactory explanation. Here we propose a possible solution, in the framework of a chemical evolution model which reproduces other major observed properties of the cluster, namely, its stellar metallicity distribution function (MDF), age-metallicity relation (AMR), trends of several abundance ratios with metallicity and Na-O anticorrelation (Fig. 1; see Romano et al. 2007, 2010).

In order to reproduce all the relevant observations, the parent galaxy must experience both infall of gas of primordial chemical composition and outflow of processed matter. The key assumption that allows the formation of extreme He-rich stars is that, while supernova (SN) ejecta are efficiently lost through the galactic outflow, elements restored to the interstellar medium (ISM) by gentle winds from both asymptotic giant branch (AGB) and fast rotating massive stars (FRMSs) are mostly retained in the cluster potential well (see Romano et al. 2010 and references therein for details).

He and Na are dispersed in the ISM through slow stellar winds by both AGBs and FRMSs. O, instead, as well as other heavy elements, is expelled by massive stars through fast polar winds. Hence, in the framework of our model, He and Na are preferentially

retained inside the cluster potential well, while O is mainly vented out through the galactic outflow. This naturally produces the Na-O anticorrelation and He-rich bMS population, as observed (Fig. 1, right-hand panels). The coexistence of populations with 'normal' and 'high' He content at [Fe/H] $\geqslant -1.4$ is expected if He is removed with different intensities from different regions of the proto-cluster.

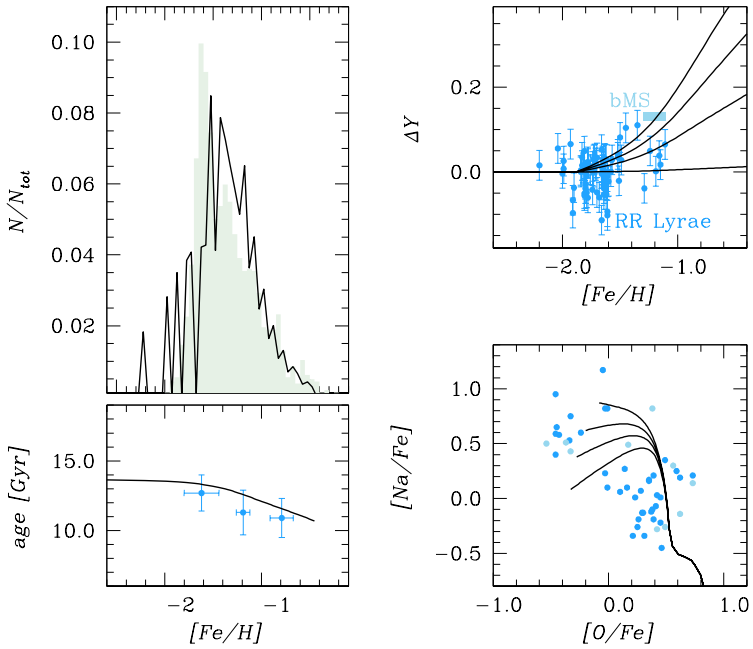

Figure 1. Predicted (thick solid lines) MDF (top left-hand panel), AMR (bottom left-hand panel), relative He enrichment (top right-hand panel) and Na-O anticorrelation (bottom right–hand panel) for ω Cen stars compared to observations from Sollima et al. (2005; shaded histogram, top left-hand panel), Hilker et al. (2004; dots with error bars, bottom left-hand panel), Sollima et al. (2006; dots, top right-hand panel), Norris (2004; box, top right-hand panel), Norris & Da Costa (1995) and Smith et al. (2000) (dots, bottom right-hand panel). The upper (lower) curves in the right-hand panels correspond to models computed with lower (higher) efficiencies of He and Na entrainment in the galactic outflow (see Romano et al. 2010).

References

Hilker, M., Kayser, A., Richtler, T., & Willemsen, P. 2004, *A&A*, 422, L9

Norris, J.E. 2004, *ApJ*, 612, L25

Norris, J.E., & Da Costa, G.S. 1995, *ApJ*, 447, 680

Romano, D., Matteucci, F., Tosi, M., Pancino, E., Bellazzini, M., Ferraro, F.R., Limongi, M., & Sollima, A. 2007, *MNRAS*, 376, 405

Romano, D., Tosi, M., Cignoni, M., Matteucci, F., Pancino, E., & Bellazzini, M. 2010, *MNRAS*, in press (arXiv:0910.1299)

Smith, V.V., Suntzeff, N.B., Cunha, K., Gallino, R., Busso, M., Lambert, D.L., & Straniero, O. 2000, *AJ*, 119, 1239

Sollima, A., Ferraro, F.R., Pancino, E., & Bellazzini, M. 2005, *MNRAS*, 357, 265

Sollima, A., Borissova, J., Catelan, M., Smith, H.A., Minniti, D., Cacciari, C., & Ferraro, F.R. 2006, *ApJ*, 640, L43